THE UNIVERSITY
of EDINBURGH

THE UNIVERSITY *of* EDINBURGH
Edinburgh Clinical Academic Track

The Role of Semaphorin3F in Neutrophilic Inflammation

Tracie M Plant
BMedSci MB ChB MRCP(UK)

Thesis submitted for the degree of Doctor of Philosophy
The University of Edinburgh
2018

Table of Contents

Figures

Abstract

Effective host responses to injury and infection require both rapid recruitment of neutrophils into tissues and timely inflammation resolution. Research efforts have primarily focused separately on the initiation and resolution phases of inflammation and on how neutrophil survival responses determine the duration and extent of the inflammatory response. Less focus has been placed on mechanisms retaining viable neutrophils at inflamed sites and thus contributing to ongoing inflammation. This may be of therapeutic importance given the numerical dominance of viable over apoptotic neutrophils in inflamed tissue, even during inflammation resolution.

Semaphorins were originally identified as chemo-repulsive molecules for axonal growth cones. They have since been implicated in cell motility in the context of vascular growth, tumour progression and in immune signalling and immune synapse formation. Recently the class 3 Semaphorin, Sema3A, was shown to act as an attractant for tumour-associated macrophages (TAM), regulating their localization and retention within hypoxic tumour areas. Previous unpublished work from our group found neutrophils express the class 3 Semaphorin, Sema3F, with differential expression observed in hypoxia. Whether neutrophil expression of Sema3F can directly regulate recruitment to inflamed sites is currently unknown. Semaphorins can interact both directly with Plexins and in complexes with Neuropilin co-receptors, leading to activation of protein kinase and (guanosine triphosphate-ase) GTPase signalling pathways. This affects actin cytoskeletal re-organisation following oxidation of actin filaments leading to modifications of neutrophil shape and migration. In light of emerging evidence that neutrophils also undergo a process of reverse migration away from inflamed tissue, I propose neutrophil expression of Sema3F regulates neutrophil retention within the tissues. Where autocrine production of neutrophil Sema3F induces neutrophil F-actin disassembly, acting as a cytoskeletal brake to cell movement and is thus a

determinant of both the magnitude and duration of the innate immune response. To investigate this, *in vivo* experiments were performed in murine models of acute lung injury, using both wild type and neutrophil specific Sema3F knockout mice. Complementary *in vitro* experiments were performed in human peripheral blood neutrophils.

Inflammatory neutrophils express sema3F. Sema3F protein expression is seen in the recruited neutrophils found in tissue from patients with chronic inflammatory lung disease (COPD). *In vivo* modelling showed Sema3F expression is regulated at a transcriptional level during inflammation, with induction of Sema3F mRNA in neutrophils recruited to the airways following Lipopolysaccharide (LPS) challenge and a parallel increase in Sema3F protein expression in Ly6G positive cells within the alveoli. Similarly, the surface expression of Neuropilin 2 (NRP2), the obligatory co-receptor to Sema3F, is increased in both human and murine neutrophils following an inflammatory stimulus. In a murine model of LPS-induced lung injury, intra-tracheal instillation of Sema3F at 24 hours increases retention of airway recruited neutrophils at 48 hours. Furthermore, neutrophil specific knockout of murine Sema3F in an LPS-induced lung injury model increases both recruitment and clearance of neutrophils found in the bronchoalveolar lavage but does not alter apoptotic responses. The Sema3F deficient neutrophils migrate, to and away from the site of tissue injury rapidly and are not retained within inflamed murine lung tissue. The retention phenotype seen in the Sema3F knockout mouse appears neutrophil specific as macrophage numbers were unchanged throughout the inflammatory response.

In human peripheral blood neutrophils Sema3F treatment inhibits neutrophil chemotaxis to the bacterial product N-Formyl-Met-Leu-Phe (fMLF). Using a microfluidic chip assay, neutrophils responded to Sema3F in a dose dependent manner. Following Sema3F treatment there was a reduction in neutrophil migration. This was observed in neutrophils migrating up an increasing Leukotriene B4 (LTB4) gradient (chemotaxis). After the neutrophils

had reached the chamber and the highest concentration of LTB4, the rate of neutrophil migration out of the chamber and against the gradient (retrotaxis) was reduced. Effectively the neutrophils were retained within the chamber for 90 minutes. Sema3F treated neutrophils have preserved functions including phagocytosis of opsonised Zymosan granules and fluorescently labelled *Escherichia coli* (*E. coli)* particles. Following Sema3F treatment neutrophils produce increased intra-cellular levels of radical oxygen species (ROS). Increased ROS has been shown to promote F-actin disassembly and result in cytoskeleton rearrangement. Sema3F not only inhibits neutrophil chemotaxis, but also affects neutrophil rounding and regulates exogenous myeloperoxidase and elastase activity. It is evident that Sema3F signalling could selectively modulate diverse neutrophil functions related to neutrophil cytoskeletal dynamics.

Using cultured murine lung slices and real-time confocal imaging neutrophils treated with Sema3F are slower than controls. On delivery of intra-tracheal (IT) Sema3F to the murine ALI model the retained neutrophils are found in the alveoli space and are not retained by a rate-limiting interaction with the barriers to neutrophil lung transmigration. Following IT Sema3F, these neutrophils retained in the murine airway are more spherical and undergo increased F-actin disassembly. These results for the first time identify a role for Sema3F as a neutrophil specific retention signal in acute lung injury. Thus, revealing a novel mechanism by which neutrophils are recruited to and maintained at the site of tissue injury. I therefore propose that Sema3F and the co-receptor NRP2 are potential therapeutic targets in acute lung injury and lung diseases caused by exaggerated and persistent neutrophilic inflammation.

Lay abstract

Neutrophils are a type of white blood cell and are essential for tissue healing after injury and protection against infection. Neutrophils contain toxic substances which they can release in a controlled way to kill bacteria. They can also eat debris, bacteria and foreign particles clearing the way for tissue repair and inflammation resolution when there is full recovery and the process is over. The number of neutrophils present at the injury site, in part, determines when the resolution of the injury and inflammation happens. However, in certain situations neutrophils overreact staying at the injury site too long or too many arrive in response to the injury. In these situations, the helpful infection-fighting responses of the neutrophils spill over and can begin to harm the patient's own tissues. In this way excessive neutrophil numbers, activity or neutrophil lifespan can cause diseases such as Chronic Obstructive Pulmonary Disease (COPD), asthma and acute lung injury (ALI). The extent of help, or harm, neutrophils cause is determined partly by how long these cells live within the site of injury. Neutrophils usually die in a controlled manner called "apoptosis" or programmed cell death and are eaten by another cell type found in the blood, macrophages. More recently there is evidence that the control over neutrophil driven inflammation is not only through apoptosis (organised neutrophil death), but even before this happens, there are signals that instruct neutrophils to "go" or "stay" at the injury site. One such potential signal is Sema3F, which is part of a family of proteins called Semaphorins, named after the flag signalling system used by ships to direct traffic. We know neutrophils make different levels of the signal Sema3F themselves and can respond to their own Sema3F signal, this is a process called "autocrine" signalling. We have shown in animal models that neutrophils without Sema3F move into the injury site faster than the neutrophils producing Sema3F and they also move away from the injury site quicker. In another animal model the opposite is true: giving excess Sema3F after a lung injury retains the neutrophils within the injury site. It is known that Semaphorins cause changes

in the cytoskeleton of cells, which is the scaffolding that allows cells to do many functions including change shape and move. It appears that Sema3F causes neutrophils to disassemble their scaffolding and therefore the neutrophils cannot move as well. Sema3F acts as a “brake” to neutrophil movement and “migration”. It may be that, in the future, we can harness Sema3F signalling to control neutrophil migration in the context of disease, to move neutrophils to the injury site when this would be helpful but away when they are responsible for damage and disease.

Declarations

I declare that this thesis presented for the degree of Doctor of Philosophy in Respiratory Medicine has been composed solely by myself except where stated otherwise by reference or acknowledgment. This thesis is entirely my own work and it has not been submitted, in whole or in part, in any previous application for other degrees or qualifications.

Signed:

Dr Tracie Plant

Acknowledgements

I would like to thank my supervisors, Professor Sarah Walmsley and Professor Moira Whyte for their ongoing support, advice and encouragement. I would like to thank Dr Roger Thompson for his excellent tuition in the finer points of neutrophil isolation and functional assays during my previous Academic Clinical Fellowship. I would also like to thank my current lab group, in particular Dr Patricia Coelho and Dr Emily Watts for their much-needed help with murine husbandry and colony maintenance. Also, Dr Ananda Mirchandani for her help with lung digests and flow cytometry. My thanks go to Dr Eoghan O'Duibhir for his supervision, advice and skill when using the Operetta imaging system. I would like to thank Dr Leo Carlin for his supervision and direct contribution to my thesis in terms of both experimental work and intellectual input. Also, to the Beatson Institute in Glasgow for allowing me access to their excellent resources. Furthermore, I would like to thank the larger scientific community in the Centre for Inflammation Research for their patience and resources, including the healthy volunteers who have donated blood samples. I would like to extend my thanks to ECAT and the ECAT directors for this fantastic opportunity, for the training and support provided in shaping my project, for the privilege of excellent resources and for the leave afforded me from my clinical duties. Finally, I wish to thank my husband Dr Pete Sanderson for unquestionably accepting and facilitating the move to Edinburgh and for his understanding while enduring his own PhD studies and clinical responsibilities.

1 Introduction

1.1 Neutrophils in the innate immune response: initiation and resolution

Neutrophils are the most abundant type of granulocyte forming 40-75% of the circulating population, the remaining cell types being basophils and eosinophils. They form a crucial component of the innate immune system. Neutrophils are recruited to the site of tissue damage or infection by chemoattractants these are released from damaged cells, activated macrophages or the early-recruited neutrophils themselves. They are able to transmigrate from the circulation, through the endothelial and epithelial layers, to reach the site of injury promptly. After developing from pluripotent hematopoietic cells within the bone marrow, they are very short-lived cells. Neutrophils mature within 1 week and are present in the circulation for a further 6-8 hours they usually they undergo constitutive apoptosis following transmigration.[1] They have efficient cytotoxic abilities including phagocytosis, the “respiratory burst” and the release of granules.[2-5] Neutrophil apoptosis (programmed cell death) is a series of highly regulated biological events that leads to cell changes and death. Apoptosis ensures neutrophils maintain membrane integrity and thus retain their cytotoxic granule contents; it also reduces chemotaxis, phagocytosis and the respiratory burst.[6] Apoptosis promotes the recognition and safe removal of neutrophils and their cytotoxic content by macrophages. It is a major route of neutrophil clearance which is vital in the resolution of inflammation and infection to maintain tissue homeostasis.[1] Typically, the survival of neutrophils is extended in the inflammatory environment found at site of tissue damage or infection. Neutrophils have an enhanced survival in response to bacteria and bacterial products, hypoxia and cytokines.[7-9] This unique robustness, in the face of inhospitable surroundings, allows these cells to defend the organism against pathogens and tissue injury.

1.2 Neutrophilic inflammation in lung disease

ARDS is a severe and common cause of respiratory failure. This clinical syndrome is defined by an acute onset of hypoxia (PaO_2:FiO_2 of < 40 kPa) associated with diffuse bilateral chest infiltrates seen on x-ray consistent with non-cardiogenic pulmonary oedema.[10] The dysregulation of the resolution phase leading to persistent neutrophilic inflammation is implicated in the pathogenesis of many lung diseases. In acute respiratory distress syndrome (ARDS) neutrophils predominate in the pulmonary oedema fluid and bronchoalveolar lavage fluid obtained from affected patients.[11] Histological findings include diffuse alveolar damage, disruption to the hyaline membranes and capillary injury. This results in a protein rich oedema fluid in the alveolar spaces and disruption of the alveolar epithelium.[12] ARDS has been observed in neutropenic patients, suggesting that in this minority of cases, neutrophilic inflammation is not responsible for the clinical findings. Yet, in the most part, it cannot be refuted that neutrophils have the both the proximity and ability to produce this distinctive pattern of cellular damage.[13]

There are a variety of injuries which can lead to the characteristic and deleterious excessive neutrophil recruitment and activity seen in ARDS. Moreover, the degree of neutrophil recruitment correlates with increasing disease severity and morbidity.[14-16] Mortality from this syndrome is high (> 40%) and following recovery survivors often endure significant and chronic sequalae.[17] As such ARDS can levy a considerable burden upon resources within both hospitals and the wider community. Neutrophil recruitment and migration are central in the generation of the harmful neutrophilic response seen following injury. BAL taken from patients with ARDS is highly chemotactic for neutrophils and contains many of the potent neutrophil chemoattractant signals including interleukin-8 (IL-8). There is further enhancement of neutrophil chemotaxis through synergy between signals.[14] The initial exudative phase is heralded by a deluge of recruited neutrophils and release of their histotoxic contents. These bactericidal agents (for example myeloperoxidase, elastase and free radicals) contribute to catastrophic diffuse alveolar damage

and loss of lung architecture and the ability to perform gaseous exchange resulting in organ failure and often death.[18,19] The instigating injury can occur at a distant site and these primed neutrophils may relocate to the lung and once there cause an acute lung injury without a clear or direct insult to the lung itself.[20-24]

1.2.1 Neutrophilic inflammation in chronic pulmonary disease

The destructive presence of inflammatory neutrophils is responsible for the chronic inflammatory changes seen in the airways of patients with Chronic Obstructive Pulmonary Disease (COPD). This is characterised by airway thickening and constriction, increased secretions and ultimately non-reversible airway obstruction with airflow limitation. Patients with COPD suffer from breathlessness, fatigue and respiratory failure.[25]

While ARDS and COPD are very different clinical entities they are both underpinned by neutrophilic inflammation. In the case of COPD, it is often a result of exposure to environmental factors such as cigarette smoke and coal fires. The inflammation leads to a largely non-reversible narrowing of the airways and airflow restriction. Symptomatically the patient will experience shortness of breath and as the disease progresses, respiratory failure associated cardiovascular complications. The disease progression is characterised by exacerbations, where the gradual decline and background inflammation is punctuated by acute periods of either infection or increased inflammation. Following resolution of an exacerbation there is often a progression of the background damage to the lung architecture and over time, worsening of the chronic symptoms. The neutrophil is central in the propagation of this pathological inflammation and is a dominant cell-type present in the lung BAL fluid, found in larger numbers in diseased than in healthy lung. This is attributed to the inflammatory signals produced in the COPD affected lung.[26]

The neutrophil is implicated in other respiratory diseases, it appears to be the dominant cell type in non-atopic and severe forms of asthma.[27] In addition, the generation of oxidative stress by activated neutrophils is proposed as a potential mechanism in the pathogenesis of lung fibrosis.[28] The ongoing release of neutrophil proteases, such as elastase, generate the bronchiectatic changes seen in patients with cystic fibrosis. These proteases may go on to dysregulate neutrophil cytotoxic abilities promoting infection, such that elastase is present early in the life of these patients and appears as a biomarker of progression throughout.[29]

1.3 Neutrophil recruitment

Tissue injury releases a variety of chemoattractants; neutrophils are able to sense these signals and navigate rapidly to the site of damage. The first neutrophils to arrive at the site of injury amplify the recruitment signal, thus ensuring a prompt delivery of neutrophils from the blood stream. Acutely, damage-associated molecular patterns (DAMPs) are released from injured or necrotic cells these include: DNA, proteins, *N*-formyl peptides, extracellular matrix components, ATP and uric acid.[30] Neutrophils detect early signals, such as DAMPs, by G protein-coupled receptors (GPCRs).[31] At the site of injury, the detection of DAMPs results in the local production of a hydrogen peroxide (H_2O_2). In larval zebrafish the release of H_2O_2 starts at 3 minutes post injury and the gradient peaks at 20mins.[32] This rapid signal is sensed by a proto-oncogene tyrosine-protein kinase Lyn a member of the Src family kinases (SFKs) which have been shown to produce chemotaxis of human and murine neutrophils in *vitro.* [33] SFK activation results in the activation of PI-3 Kinase, the Rac subfamily of the Rho family of GTPases and extracellular signal-regulated kinases (ERK) to mediate directed migration.[33,34] Locally DAMPs stimulate the release of CXC-chemokine ligands such as CXCL8 and CXCL2, interleukin 1 beta (IL-1β) and LTB4 from both immune cells and non-immune cells, such as epithelium and endothelium.[35,36]

Amplification of the chemoattractant signal is further augmented by the early-recruited neutrophil itself. The migrated neutrophils are activated and this promotes both directly, and indirectly, additional secretion of CXCL8 and LTB4.[37,38] The role of CXCL8 family–CXCR signalling in neutrophil migration has been confirmed in zebrafish, mice and humans.[39-41] Neutrophil chemotaxis and activation is also triggered by N-formyl peptides, such as fMLF. Whilst these N-formyl peptides can be derived from bacterial proteins, they are also released from mitochondria after tissue damage and activate human neutrophils by binding to the GPCRs fMLF receptor 1 (FPR1), FPR2 and FPR3.[42] In addition to early-recruited neutrophils, DAMPs attract pro-inflammatory monocytes and macrophages. Neutrophils also produce chemokines that directly recruit macrophages, and in response recruited macrophages release further stimuli that perpetuate this feed-forward loop. Thus exponentially more neutrophils are drawn into the inflammatory site often termed “neutrophil swarming” (figure 1.3-1).[36]

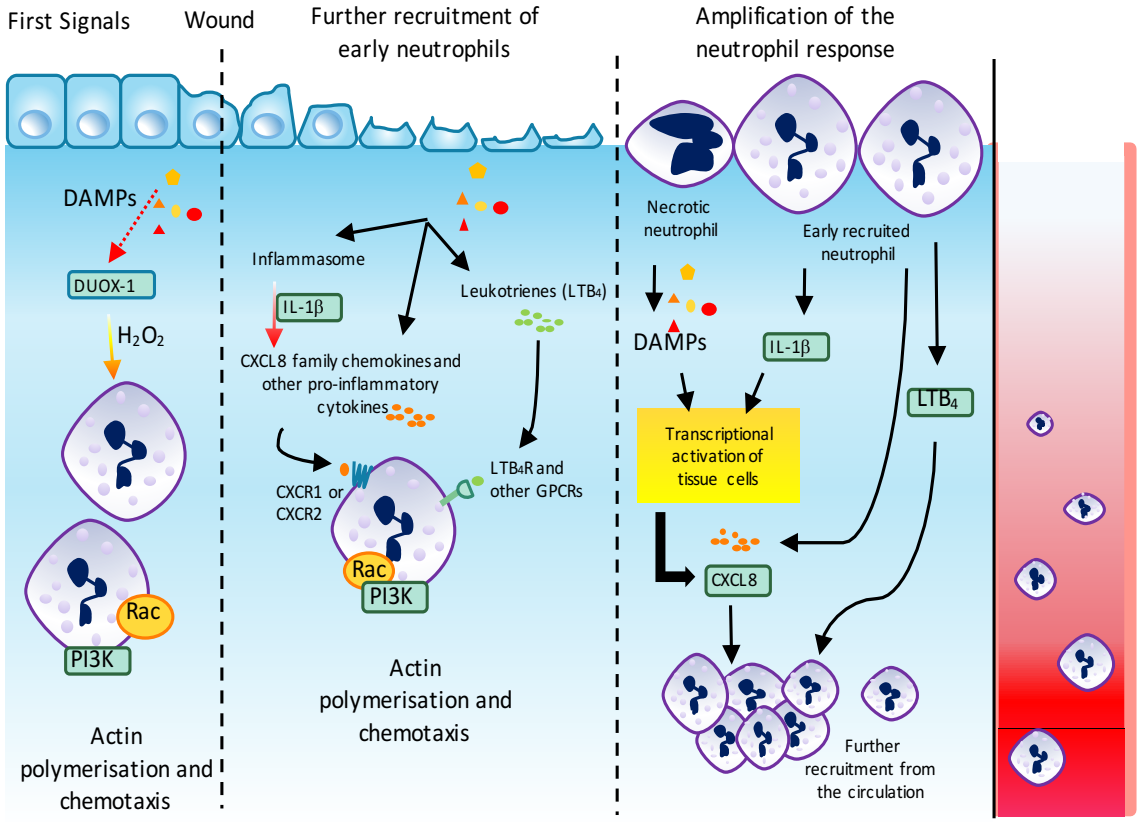

Figure 1.3-1 The phases of neutrophil recruitment leading to neutrophil swarming
Damage-associated molecular patterns (DAMPs) are released at a tissue injury site and promote the release of hydrogen peroxide (H_2O_2). Following detection of chemoattractant cues (DAMPs & H_2O_2) recruited neutrophils undergo actin polymerisation and chemotaxis. DAMPs also induce the production of CXC-chemokine ligand 8 (CXCL8) family chemokines and leukotrienes from surrounding tissue cells to further recruit neutrophils. Early-recruited neutrophils are then activated, which directly and indirectly promotes further secretion of CXCL8 family chemokines and leukotriene B4 (LTB4) to induce neutrophil recruitment from the circulation and amplification of the response.

1.4 Neutrophil Transmigration

For circulating neutrophils to gain access to the site of inflammation they must be notified of the insult, locate the damaged tissue and exit the vascular compartment, to arrive accurately and promptly. This is in part achieved through the leukocyte adhesion cascade. Capture and rolling of circulating leukocytes is mediated by L-selectin, P-selectin and E-selectin.[43] These interact with P-selectin glycoprotein ligand 1 (PSGL1). PSGL1 was first described as a receptor for P-selectin, however it does interact with all three selectins.[44] Most leukocytes express L-selectin where it mediates leukocyte to leukocyte interactions, whilst E- and P-selectins are found on damaged endothelial cells; the latter is also found on activated platelets. E-selectin can bind to both glycosylated CD44 and E-selectin ligand 1 (ESL1).[45] Leukocyte arrest occurs usually under conditions of high flow. Following the binding of selectins with their ligands, they work cooperatively with integrins to promote firm leukocyte adhesion. For example, the lymphocyte function-associated antigen 1 (LFA1), also known as α1β2-integrin, undergoes affinity change when interacting with E-selectin. This allows LFA1 to transiently bind to its substrate, the inter-cellular adhesion molecule 1 (ICAM).[46] Likewise, the rolling of human lymphocytes is enhanced and slowed when ICAM1 is co-expressed with L-selectin ligands in a human vascular endothelial cell line.[47] Chemokines and chemoattractants are produced by a variety of sources, leukocytes themselves, endothelial cells or by-standing cells such as platelets or mast cells. They trigger arrest of leukocytes through GPCRs receptors and are powerful mediators of integrin adhesion. Integrins most relevant to leukocyte arrest belong to the β1-integrin and β2-integrin subfamilies. The most studied of these are the β1-integrin, Very Late Antigen-4 (vLA4) and the β2-integrin, LFA1. The effect of chemoattractants on integrin binding appears to be cell and ligand specific. Chemoattractants affect integrin valency and affinity employing inside-out signalling pathways and generating internal signals. As a result, under physiological conditions, integrin binding can be an instantaneous event.[48,49] The current literature identifies 47 proteins that are

implicated in the regulation of integrin-mediated adhesion by chemoattractants.[50] The arrest of leukocytes depends on the balance between chemoattractants, integrin expression and selectins. This combination may define the subtype of leukocyte and its availability in certain environments.

Transmigrating neutrophils must traverse distinct barriers to gain access to the inflamed compartment. These are the endothelial cells, the endothelial-cell basement membrane, the interstitium, the epithelial layer and at times, the pericyte sheath. Transmigration is controlled, in part, by the ratio of these barriers which varies within the organism. The whole process can be completed within 15mins, with the basement membrane providing the greatest challenge. Initially neutrophils crawl inside the blood vessel in an ICAM1 dependent manner.[51] There the neutrophil may take either the paracellular or transcellular route. Inflamed endothelial cells can redistribute junctional molecules in a way that favours transendothelial cell migration.[52] Immunoglobulin superfamily members actively mediate leukocyte transendothelial migration. Examples include Platelet endothelial cell adhesion molecule (PECAM)1, ICAM1, ICAM2, Junction adhesion molecule (JAM)-A, JAM-B, JAM-C and endothelial cell-selective adhesion molecule (ESAM), as well as the non-immunoglobulin molecule CD99. In response to IL-1β, but not Tumour Necrosis Factor-α (TNF-α), PECAM1, ICAM2 and JAM-A mediate leukocyte transmigration.[53] Direct activation of leukocytes by TNF, fMLF or LTB4 appears to bypass the need for these molecules and actively mediates leukocyte transendothelial migration. The transcellular route is taken by the minority of emigrating leukocytes, largely seen within the central nervous system and during inflammation. Leukocyte transcellular migration starts with the extension of membrane protrusions into endothelial cells.[54,55] Ligation of ICAM1 triggers cytoplasmic signalling events that leads to the translocation of apical ICAM1 to regions high in caveolae (small lipid rafts 50-100nanometer) and rich in F-actin. This results in the eventual transport of the apical ICAM1 with caveolin-1 (a scaffolding protein) to the basal plasma membrane.[54,55]

These responses collectively result in the formation of channels through which leukocytes can transmigrate migrate.[55,56] Finally, leukocytes reach the endothelial-cell barrier, largely formed by the endothelial basement-membrane comprising vascular laminins, collagen IV and connecting molecules and intermittently the pericyte sheath.[57] Variations in the constituents of the basement membrane, in relation to the density of the pericyte population, may favour neutrophil transmigration.[58] Integrins are the main receptor for laminins and during transmigration there is a mobilization of internal stores. There appears to also be an interaction between integrins and cell surface proteases, for example there is evidence that α6β1-N integrin works synergistically with neutrophil elastase.[58,59]

Within the lung transmigrating neutrophils face specific challenges. Due to the small diameter of the capillary, transmigrating neutrophils must deform, referred to as margination, which increases transit time even under resting conditions.[60,61] Neutrophils may reside in the capillary bed for a time, pausing in intravascular pools, although the extent of this remains a controversial topic. In the venules, initially adhesion-molecule independent rolling can occur and in response to chemokines, neutrophils sequester to the capillary endothelium where they later adhere.[62,63] Alveolar macrophages and type II pneumocytes produce CXC chemokines, thus promoting transendothelial migration, neutrophils journey through the endothelium, interstitial space, and epithelium to reach the alveolar space. Compared with transendothelial migration, the molecular details of transepithelial migration into large or the small airways and the alveolar epithelia, remain mostly unknown. Only recently are proteins emerging that might be involved such as the receptor TREM-1. TREM-1 deficient neutrophils effectively migrate across primary endothelial cell monolayers but fail to migrate across primary airway epithelia.[64] This highlights that within the lung, neutrophil recruitment can by altered at multiple levels, including those less well described such as transepithelial migration. These

may not only provide new and interesting areas of study but give rise to novel mechanisms prime for therapeutic manipulation.

1.5 Neutrophil Chemotaxis

For the directional migration of neutrophils termed 'chemotaxis,' the polarisation of the cell is obligatory. This is achieved with formation of the leading edge by actin rich lamella and at the opposite pole, the uropod, a tail like projection.[65] Phosphatidylinositol-4,5-bisphosphate 3-kinases (PI-3 kinases) have been identified down stream of G-protein-coupled receptors and are stimulated by chemoattractants. PI-3k activity regulates the establishment of cell polarity, whilst inhibition of PI-3 kinase, results in defective formation of the leading edge and suppression of neutrophil chemotaxis.[66-68] PI-3 Kinase phosphorylates phosphatidylinositol 4,5-bisphosphate [PI{4,5}P_2] to generate PIP_3, which stimulates guanine nucleotide exchange factors (GEFs). GEFs are small GTPases; they act as a molecular switch promoting the activity of Rho-GTPases such as Rac and Cell division control protein 42 homolog (Cdc42). Rac and Cdc42 induce localised actin polymerisation through Actin-Related Proteins2/3 (Arp2/3) pathway amongst other mechanisms.

Rac and Cdc42 appear to have complementary but divergent roles. Rac participates in the feed-forward generation of PIP_3 at the leading edge of the migrating cell. This is perhaps to amplify subtle external chemoattractive gradients into larger internal signals. Whereas Cdc42 is responsible for maintaining the location of the leading edge, by signalling the 'backness' of the polarised cell, thus stabilising polarity.[69] Negative feed-back pathways are essential to produce effective chemotaxis. GTPase-activating proteins (GAPs) directly antagonise the action of GEFs as they catalyse the conversion of active (GTP-bound) Rac/Cdc42 to inactive (GDP-bound) Rac/Cdc42. Phosphatase and tensin homolog (PTEN) generates PI(4,5)P_2 a negative regulator of PI-3 kinase pathways and has a reciprocal location to the leading edge. In contrast, SH2-domain-containing inositol 5-phosphatase (SHIP), a 5′

inositol polyphosphatase, is active both at the leading edge and at the tail and is thought to terminate PI-3 kinase activity.[70] Whilst PTEN maintains PIP_3 accumulation at the anterior end, SHIP1 has been shown to inhibit integrin activated PIP_3 gradients. Loss of SHIP1 results in defective chemotaxis probably due to enhanced adhesion and loss of PIP_3 polarity.[71] The interplay of these complementary pathways regulate cell motility, such that cells can appropriately migrate in variety of environments, in a precise and rapid manner.

1.6 Reverse migration

At the site of injury neutrophils may undergo cell death by either apoptosis or necrosis, with clearance occurring through phagocytosis by macrophages.[72] Alternatively they transmigrate into the airway and are expectorated. Most recently there is evidence that they are also retained within the tissues, or may undergo reverse migration away from the injury site.[73,74] Reverse migration is a term to describe the phenomenon of leukocytes migrating in an unconventional direction within tissues and organs. [75] For example, leukocytes moving in the opposite direction from the net leukocyte population or moving away from a known chemotactic stimulus. Less is known regarding the underlying mechanisms of reverse migration or retention of neutrophils within inflamed tissue; despite this it is clear that they are important factors in controlling inflammation resolution.[76] Reverse migration has been observed in zebrafish models of inflammation.[77] These models of neutrophil inflammation have distinct advantages namely, larvae are transparent allowing excellent visualisation of fluorescent proteins in *vivo*. Zebrafish neutrophils (Heterophils) are identifiable early after fertilisation and the innate immune system remains separate from any adaptive immune system. There exists a wide range of tools for genetic manipulation of this model. Thus zebrafish provide a simplified, genetically tractable model, where fluorescent neutrophils can be used to track the immune response.[78] In one such a transgenic zebrafish model neutrophils express green fluorescent protein (GFP) under control of the myeloperoxidase

(MPO) promoter (zMPO:GFP). In this model, following recruitment to the site of tail fin injury fish neutrophils have been shown to later undergo retrograde chemotaxis away from the injury site. It is postulated this is an additional mechanism of inflammation resolution.[73,79] The pro-inflammatory compound Tanshinone 11A in a zebrafish model increased reverse migration.[79] The relevance of reverse migration to mammalian systems is controversial.[77]

In physiological conditions at resting state, neutrophils are seen to "patrol" vessels crawling along the luminal surface but do not transmigrate into tissue, termed abortive emigration.[80] As discussed, neutrophils are recruited by release of chemoattractants from activated macrophages, epithelial cells and bacteria and then transmigrate across capillary epithelium to enter the site of injury.[81,82] Hughes et al. (1997) demonstrated in a rat model of glomerulonephritis, that the majority of neutrophils recruited to the injured glomerular did not undergo apoptosis. Interestingly these neutrophils were observed to return to the circulation.[83] In this study radiolabelled neutrophils were obtained from an identical rat strain and were infused prior to glomerular injury. Histological analysis of apoptosis, cell counts and flow cytometry were used to delineate the magnitude of neutrophil migration from the site of injury into the circulation after 0, 4 and 24 hours. These data were then compared with the corresponding peripheral neutrophil counts and reverse migration of the radiolabelled neutrophils detected. It must be conceded that vascular leak in the injured glomerular may also play a part in neutrophils returning to the circulation following recruitment to the injury site.

Similar reverse migration has been shown in humans. Buckley et al. (2006) observed that in patients with rheumatoid arthritis 1-2% of their peripheral blood neutrophils had undergone retrograde transmigration or reverse migration. In healthy controls this is still seen but represents less than 0.25% of the total neutrophil population. Neutrophils that had returned to the circulation were identified by unique cell surface expression of CD54 with low levels of expression of the CXC chemokine receptor 1 ($CXCR1^{low}$). This

pattern is seen on neutrophils that have migrated through an endothelial layer. In these patients, this neutrophil subpopulation appeared phenotypically altered compared to other non-recruited circulating neutrophils.[74] The neutrophils that had undergone reverse migration demonstrated more resistant to apoptosis in subsequent assays.

To date reverse migration has been visualised in zebrafish,[79,84-86] mice[87,88] and humans.[77,89] Reverse transmigration of neutrophils has implications in both immune surveillance and dissemination of systemic inflammation as seen in ARDS.[87,90] The mechanisms behind reverse migration remain are not fully understood. Interactions between neutrophils and endothelial cells are key in controlling neutrophil migration and ultimately leukocyte transmigration. The signals involved are probably organ specific, for example neutrophil migration into the lung parenchyma can be both selectin- and β2-integrin-independent.[91] There is evidence that neutrophils can crawl along the walls of blood vessels against the direction of blood flow. This is termed reverse luminal crawling (rLC).[92] rLC of neutrophils contributes to trans-endothelial migration (TEM) sites in stimulated murine cremasteric venules. rLC has also been seen in natural killer (NK) cells and monocytes; it is thought to contribute to immune-surveillance in multiple murine models.[80,93,94] Reverse transmigration of the endothelial layer by leukocytes is decreased when either endothelial cell junctional molecule C (EC-JAM- C) or neutrophil elastase is genetically knocked down in murine models.[74,95,96] As part of the reverse transmigration of any tissue the leukocyte must undergo reverse interstitial migration. This may require the migrating cell to dynamically re-prioritise the ongoing chemoattractant cues. There may be distinctive repellent signals turned on during resolution and these could be released from other sources including neighboring cells such as macrophages. [97] Also, the concentration of the chemoattractant may change during the course of tissue injury. In this way the response of the neutrophil could changed over the time despite the injury persisting. For example, a high dose (verses lower dose) of CXCL8 changes

the nature of the signal from chemoattractant, to chemorepellent. A proposed mechanism for this, is the desensitization of the neutrophil to the ongoing stimulus.[98] The environment itself may alter the direction of neutrophil migration. Osmolarity differences between interstitial fluid and the external environment have been shown to mediate rapid leukocyte recruitment to sites of tissue damage.[99] Other environmental cues may regulate the migration of neutrophils, for example in injured and hypoxic tissue the subsequent activation of Hypoxia-inducible factor (HIF) pathway increases the number of neutrophils at the site of injury.[84,98]

Neutrophils can move away from an established chemoattractant gradient termed retrotaxis (can also be referred to fugetaxis); this is the specific ability of a neutrophil to move against a chemoattractant gradient for long distances and may form part of the process of reverse migration. [79,97,100] A microfluidic model of neutrophil chemotaxis revealed 90% of chemotaxed neutrophils subsequently underwent retrotaxis and this was enhanced by lipoxin A4, a known antioxidant.[101] There is evidence of crosstalk between macrophages and neutrophils, whereby macrophage autocrine redox-SFK signalling is an important step in the reverse migration of companion neutrophils.[86] The type of recruiting stimulus may alter the propensity for reverse migration, exposure of neutrophils to Zymosan yeast particles has been shown to reduce transmigration.[89,101] Lipid mediates such as LTB4, have been shown to increase reverse migration in an ischaemia-reperfusion model. [102] LTB4 induced proteolytic cleavage of JAM-C by neutrophil elastase, enables neutrophils to migrate back into the circulation.[96] It is also possible that the reverse migration of neutrophils is a passive process and is based on diffusion rather than active migration.[103]

Reverse migration is not simply chemoattraction followed by chemorepulsion; it is a far more complicated series of events which involve: multiple tissues layers, the comprising cells, cell receptors and signalling molecules. The recruited neutrophil is exposed to a plethora of contrasting and potentially

confusing signals which results in coordinated response. This could also represent a point of weakness that could generate dysregulation of the neutrophil response and subsequent disease. As per the definition of neutrophil reverse transmigration only a small proportion of the migrating neutrophil population undergoes reverse migration. This might suggest that this represents a pathological response rather than a novel form of neutrophil injury response. This evidence taken together suggests that accumulation of neutrophils at the inflammatory site is due to a balance between many factors. Neutrophil migration is determined by: chemotaxis, retrotaxis, the structure of the traversed cells and the environment at the site of injury. It is likely that there is an equally complex reverse migration cascade at play that is likely to include signals that retain neutrophils at the injury site. The lung has been shown to be a secondary site for neutrophils that have undergone reverse transendothelial migration (rTEM) as defined by the up regulation of ICAM 1 with a greater ability to generate ROS. After pancreatitis and ischaemic-reperfusion injuries rTEM neutrophils are found in the lung.[82-84] From this it could be concluded that the resolution of inflammation is determined, not only by apoptosis and necrosis, but by the balance and patterns of neutrophil migration including neutrophil retention.

Neutrophil migration could be manipulated to alleviate the damaging effect of neutrophilic inflammation. As such, neutrophil migration signals are a target for new therapies to prevent ischemic reperfusion injuries and to disrupt neutrophil migration to prevent disease.[104] For example, CXCR2 antagonists have been shown to reduce both neutrophil numbers and elastase activity in the sputum of health volunteers following an inhaled LPS lung challenge.[105] To date there is limited research on signals that specifically arrest neutrophil migration and maintain their presence and activity in areas of inflammation.

1.7 Cell motility and the actin cytoskeleton

Cooperatively divergent signalling pathways produce a distinct polarity within the migrating cell. [69] In response to external chemoattractant gradients, and by using internally manufactured gradients, neutrophils self-regulate the machinery required for polarisation and motility. [106] Small GTPases such as Rho, Rac and Cdc42 can trigger the nucleation of actin and determine specific patterns of actin polymerisation. [107] Actin polymerization occurs directly below the cell membrane taking two forms, either a branching structure termed filopodia, or lamellipodia composed by sheet like protrusions. [108] Arp2/3 complex is a member of the Wiskott-Aldrich Syndrome Protein (WASP) family of proteins. [109] This family of proteins detects signals and translates these into the nucleation of new actin branches, which are initiated from pre-existing filaments to construct lamellipodia.[110] Filopodia are produced in two ways, either by branches formed by the actin bundling protein fascin, or directly nucleated by formin.[111] Lipids and proteins within the plasma membrane may also direct actin dynamics. There are many actin binding proteins that modulate both form and function of the actin network. Actin polymerisation is the initiating step in a complicated and sophisticated network of pathways that produce orchestrated shape change and cell motility, through dynamic changes within the actin cytoskeleton.

Following nucleation by Arp2/3, the formation of an actin filament sees an actin monomer unit added to the barbed end of the structure, whilst units are detached from the rear. This process is intimately related to the hydrolysis of Adenosine triphosphate (ATP), where G-actin-ATP is preferentially added to the barbed end paired with simultaneous loss of F-actin-GDP. The hydrolysed phosphate group remains non-covalently attached to the actin unit, leading to possibly three types of actin within the filament: ATP, ATP+Pi or Adenosine diphosphate (ADP). The actin filament is in constant flux termed “treadmilling” and it is the proportions of these three types of actin monomer unit that determine the growth pattern of the filament. Two proteins control this process; actin depolymerizing factor ADF (Cofilin) and capping proteins. These are

examples of proteins that bias the treadmilling, for example Cofilin increases treadmilling while capping prevents barbed end growth and increases the addition of units at non-capped ends. Only when acting together can these proteins dramatically increase the growth at the barbed end. This is seen in the filaments facing the leading edge in a developing lamellipodia.[112]

1.8 The Resolution Phase

The induction of inflammation resolution is initiated relatively early in the inflammatory process and a myriad of signals begin the termination sequence. These signals largely pertain to the reduction in active neutrophils at the injury site. Initially, granulocyte cells switch the production of arachidonic prostaglandins and leukotrienes to lipoxins.[113] Neutrophils undergo apoptosis and are phagocytosed by accompanying macrophages, providing major route by which neutrophils cleared.[114]

Apoptosis is crucial for the removal of potentially harmful material in the inflammatory environment and fostering resolution. Apoptosis is precisely controlled and augmented, a small increment in the percentage of apoptosis can greatly increase the rate and ultimately the clearance of neutrophils and consequently resolution. [115] Classically apoptosis is triggered by either intrinsic or extrinsic pathways. Mitochondria are central in the intrinsic apoptotic pathway, where permeabilisation of the mitochondria causes release of cytochrome c into the cytoplasm. Cytochrome c then forms a multi-protein complex known as the 'apoptosome' and initiates activation of the caspase cascade through caspase 9.[116] Extrinsic signals include ligation of receptors by the (first apoptosis signal) Fas ligand (FasL), TNF-related apoptosis including ligand (TRAIL) and under certain conditions, TNF-α induce neutrophil apoptosis via generation of the death-induced signalling complex (DISC) and subsequent caspase 8 activation. The death-receptor ligand TRAIL has also been shown to accelerate neutrophil apoptosis.[78] Moreover, TRAIL deficient mice demonstrate an enhanced inflammatory response but normal constitutive

apoptosis.[117] The inflammatory microenvironment can further manipulate apoptosis, inflammatory cytokines present at the site of injury, such as IL-1β, interferon-gamma (IFN-γ), Granulocyte-colony stimulating factor (C-CSF) and Granulocyte-macrophage colony-stimulating factor (GM-CSF) can delay apoptosis.[118] Likewise, hypoxia found at sites of inflammation, has been shown to regulate apoptosis through the HIF oxygen-sensing pathway. This pathway has a major effect on the susceptibility of neutrophils to apoptosis. HIF expression and transcriptional activity are regulated by the oxygen-sensitive prolyl hydroxylases (PHD1-3); mice deficient in PHD3 had associated upregulation of the pro-apoptotic mediator Siva1 and loss of its binding target B-cell lymphoma-extra large (Bcl-xL).[119] This resulted in increased levels of neutrophil apoptosis and was protective in a mouse model of colitis. Other extrinsic signals modulate neutrophil apoptosis, for example cyclin-dependent kinase inhibitors have been shown to enhance the resolution of inflammation by promoting apoptosis.[115]

Extravasated neutrophils are also cleared mechanically for example though expectoration of sputum, or in faeces and urine. A family of lipid mediators, generated from omega-3 polyunsaturated fatty acid called resolvins (resolution-phase interaction products) and (pro-resolving mediators) protectins also regulate this phase.[120,121] More recently, it has been postulated that neutrophils from the inflammatory site might then re-enter the circulation through a process of reverse migration, which in turn may promote the resolution of inflammation.[75]

1.9 Semaphorins

Semaphorins are a family of secreted and transmembrane molecules that have well-described chemotropic roles essential for growth cone collapse and neuronal development.[122] They are also implicated in regulating cell motility in the context of vascular growth, tumour progression, immune signalling and immune synapse formation.[123,124] The first Semaphorin protein to be identified

was called Collapsin, to reflect its effect upon developing axonal growth cones.[125] This molecule was identified as a repulsive cue through a motility modulating ability. Collapsin (Semaphorin D) and Fasciclin (Semaphorin 1) led to the discovery of a larger family of related proteins.[126] Over 20 mammalian Semaphorin proteins are known: they are divided into eight subclasses according to their structural features. Semaphorins are either secreted or transmembrane glycoproteins, classes 1 & 2 represent the invertebrate classes, whilst 3-7 are vertebrate and class 8 contain viral Semaphorins.[123,127] Subclass 3 are secreted and can form steep tissue gradients. Individual proteins are designated by their class and an accompanying letter, for example Sema4D. All Semaphorins contain a highly conserved Sema domain formed of a 400 amino acid sequence. The central feature of this structure is a seven-blade β-propeller fold, with overall a degree of similarity to the β-propeller repeats of α integrins.[128] They can range in size between 400 and 1000 amino acids; their size depends on which domains are added to the prerequisite phenotypic Sema domain and PSI domain (Plexins, Semaphorin and integrins). In classes 2-4 and class 7 a single immunoglobulin (IG) like domain is found, whereas class 5 Semaphorins have 5 thrombospondin domains. The highly conserved Sema domain and the PSI domain share familiarity with other important cell proteins such as integrins. This shared structure suggests that Semaphorins like integrins, may have an important role throughout the organism.

1.9.1 Semaphorins and their receptors

Semaphorins largely signal through Plexins, grouped A-D coded with both a letter and number to signify an individual receptor, such as PlexinA3. They were first identified through a role in cell adhesion.[129] As with Semaphorins, a feature of the Plexin receptor is a Sema domain, extracellularly Plexins have three PSI domains and three multiple (Ig-like, Plexins and transcription factors). Interestingly they have GTPase- binding domain, this can interact Cdc42/ Rac, RhoD, RND1 and may also bind Ras proteins.[130]

Dimers of Sema4D and Sema6A have been shown to bind dimers of their Plexin receptors (B and A respectively). [131] Class 3 Semaphorins, with one exception, require Neuropilins as essential co-receptors to signal through class A Plexins (see figure 1.9.1-1).[132] Dimeric Sema3A, two copies of plexinA2 and two copies of Neuropilin 1 are arranged as a dimer of heterotrimers. [133] The co receptor Neuropilin 1 (NRP 1) stabilises this structure by cross bracing the connection between sema domains of the Sema3A and Plexin A2 subunits from two heterotrimers (see figure, 1.9.1-1). Neuropilins also act as co-receptors for the vascular endothelial growth factor (VEGF).[134]

Semaphorin binding relieves Plexin auto-inhibition. When the sema domain is lost from Plexin-A1 the receptor becomes constitutively active.[135] Most Plexin–Semaphorin interactions are mediated through the sema domains of both proteins. Plexin A1 ectodomains are autoinhibited through intermolecular cis-interactions prior to ligand binding. [136] Prior to ligand binding Plexin A1 may exist in a pre-formed cluster to facilitate rapid signalling. When Semaphorin dimers then bind, the cytoplasmic domains of the Plexin undergo a conformational change. This leads to a reduction in the intermolecular cis-interactions of the Plexin A ectodomains that impose pre-signaling autoinhibition and outside-in signalling occurs. [136]

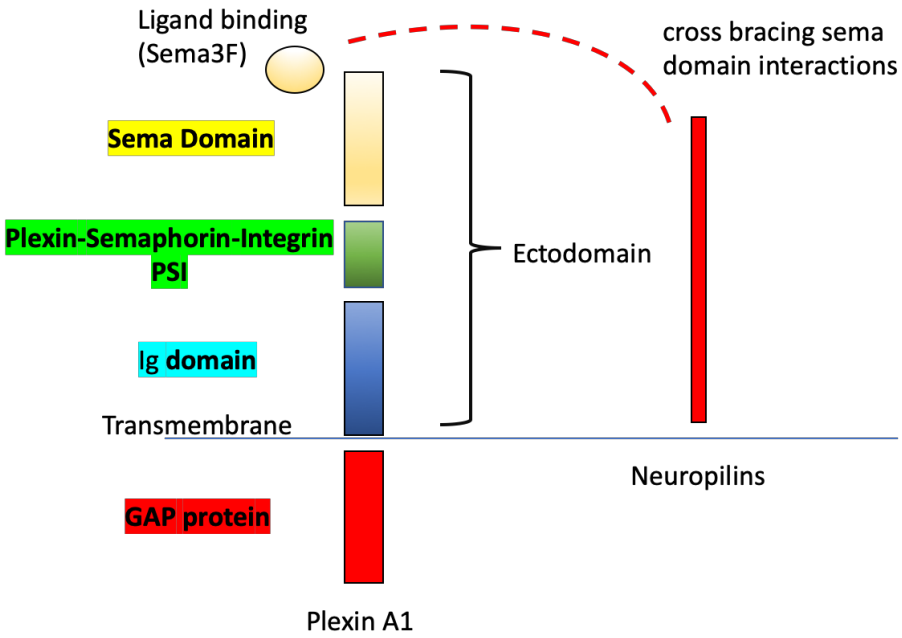

Figure 1.9.1-1 The Semaphorin-Plexin-Neuropilin complex
There are four classes of Plexin A-D, class 3 Semaphorins such as Sema3F require co-receptors Neuropilin 1 or 2 to bind the Semaphorin ligand forming a complex with the transmembrane Plexin receptor which has a large intracellular component formed of a GTPase activating protein (GAP). The crystalline structure of the Plexin ectodomain is a ring like and generates *cis*-interactions between neighboring plexins. This is thought to prevent dimerization and allow clustering. [131] The obligatory co-receptor Neuropilins 1 and 2 have no intracellular component and serve to stabilise the binding between the sema domains of adjacent Plexins and Sema ligands as part of a heterotrimeric receptor complex. [136]

1.10 Neuropilins

Neuropilins are a family of pleiotropic receptors with roles in the cardiovascular, nervous and immune systems.[137] Neuropilin (NRP) 1 and 2 are type 1 transmembrane proteins of ~ 900 amino acids with short intracellular domains that lack intrinsic enzymatic activity and share 44% homology.[138] Neuropilins are obligatory a co-receptors binding the exogenous class 3 Semaphorin ligand, with the larger Plexin transmembrane receptor then transducing this signal intracellularly.[138] Neuropilin 2 and the Plexin A family have been identified as receptors for Sema3F.[139] NRP2 is a high affinity receptor for Sema3F, both NRP1 and 2 are ligand-binding partners in co-receptor complexes for not only Plexins, but also vascular endothelial growth factor receptors (VEGFRs).[115,116] Soluble forms of NRPs are created by alternate splicing or by ectodomain shedding of the transmembrane proteins.[140,141]

NRP1 signalling is relevant to the immune system and has been shown to be involved in inhibitory T-cell activation, tumorigenesis and the regulation of tumour associated macrophages within the hypoxic niche.[142,143] Recently the class 3 Semaphorin, Sema3A, was shown to act as an attractant for tumour-associated macrophages (TAM) and its expression was found to be up regulated in hypoxic areas. NRP1 is essential for TAM attraction to hypoxic regions and unlike Sema3A, Neuropilin 1 was down regulated in hypoxia. This demonstrates how Neuropilins and Semaphorins can be individually and differently regulated by one stimulus (hypoxia) and this is turn regulates TAM localization and retention within hypoxic areas.[144] There would be many potential outcomes of a single stimulus depending on the unique combination of individually regulated co-receptor and ligand. Similarly, Plexin A3 was also down regulated in hypoxic conditions however both receptors' down-regulation appeared partially reversed when stimulated with TNF-α or IL-1β. Likewise, pro-inflammatory cytokines TNF-α and IL-1β also overcame observed hypoxic suppression of Sema3F seen in human neutrophils. Furthermore, surface

expression of NRP1 is down regulated on retinal neurons following Sema3A treatment through receptor mediated endocytosis.[145] Therefore, any effect Sema3F has on cell motility is likely to be manipulated by the cells' environment through both Sema3F and receptor expression.

NRP2 is expressed by thymocytes, macrophages and dendritic cells with a clear role in controlling cell migration.[146-148] Immormino et al. (2018) demonstrated in a murine model following LPS induced lung injury, myeloid specific ablation of NRP2 resulted in increased chemokine (C-C motif) ligand 2 (CCL2) and leukocyte infiltration into the lung.[149] Human alveolar macrophages were found to up regulate NRP2 in response to LPS dependent upon Myeloid differentiation primary response 88 (MyD88) signaling and nuclear factor kappa-light-chain-enhancer of activated B cells (NFκB). Whether neutrophils also upregulated NRP2 in the inflammatory niche remains unknown.

NRP2 is an obligatory co-receptor for Sema3F and forms the receptor complex with a plexin (A1-A4), through which class 3 Semaphorins signal. Sema3F has higher affinity for NRP2 over NRP1. Alterations in Neuropilin expression may determine the outcome of Sema3F signaling and account for a degree of the plasticity seen in Semaphorin signalling across contexts, times and locations. For example, Sema3F has been shown to promote cell detachment through loss of cell-to-cell attachments and lamellipodia. In the MC57 breast cancer cell line this occurs exclusively through NRP1, whereas in the C100 breast cancer cell line this is through NRP2 signaling.[150] NRP1 and NRP2 can be expressed on the same cell type and their stimulation by different class 3 semaphorins may work synergistically to regulate complex biological patterns of neuronal growth seen in gangliogenesis.[151]

1.10.1 Class A Plexins

Currently most research on Semaphorin-Plexin signalling focuses on class A Plexins mediating downstream effects such as growth cone collapse and the

regulation of cell motility. Class A Plexins regulate the kinases Fes and Fyn. The binding of Sema3A to PlexinA1 results in an association between PlexinA1 and Fes. Fes then phosphorylates both the Plexin receptor and a complex of collapse response mediator protein-2 (CRMP-2) and CRMP-associated molecule (CRAM).[152] Through this pathway, Fes has been shown to promote Sema3A-induced collapse of COS-7 cells [**C**V-1 (simian) in **O**rigin, and carrying the **S**V40 genetic material - cells], which contributes to the collapse of neuronal growth cones.[152] CRMP-2 is thought to be related to microtubule dynamics whereas Plexins regulate Rho GTPases including Rho, Rac and Cdc42.[153]

The involvement of Rac1 in class A Plexin signalling has been confirmed by various means.[154,155] Rac1 has recently been shown to interact directly with PlexinA1; Sema3A growth cone collapse requires Rac activity, yet a constitutively active form of PlexinA1 did not require Rac to affect growth cone collapse.[154] This is surprising on two counts, firstly Rac is usually involved in the generation of membrane protrusion and secondly this may identify a role of Rac upstream of Plexin signalling. Similarly, Rac1 not Cdc42 or Rho, mediated Sema3D induced growth cone collapse.[155] Within the developing nervous system Semaphorins and their co-receptors Neuropilins, have an established role as repulsive signals essential for the formation of the neuronal network.[156] PlexinA3 is required for the reduction of hippocampal mossy fibres and pyramidal axons needed to sculpt the pattern of neuronal connections; Sema3A and Sema3F appeared to be likely candidates triggering this function.[157] Sema3A inhibits branching of cortical neurons by de-polymerising actin filaments.[158] Sema3A was shown in culture to promote dendrite growth while reducing axonal growth thus determining early neuronal morphogenesis and polarising neurons. [159] PlexinA1 and other type A Plexins are expressed by endothelial cells, as are many of the class 3 Semaphorins. Semaphorin-mediated autocrine signalling facilitates vascular re-modelling, by reducing endothelial cell adhesion and promoting cell movement.[160] Semaphorins and

their receptors are not only involved in angiogenesis and vascular re-modelling, they also play a role in morphogenesis in the nervous system, the heart and skeleton.[161]

1.10.2 Other Plexins and direct Semaphorin signaling

PlexinB1 can function as a GAP for the Ras-family GTPase, R-Ras. Following Plexin-B1 interacting with RND1, a small GTP-binding protein of the Rho family, there is down regulation of R-Ras activity by the Plexin-B1-RND1 complex. This is essential for the Sema4D-induced growth cone collapse in hippocampal neurons.[162] Integrin inactivation has been shown to be an early event in Sema4D-induced COS cell collapse and is crucial in the cell movement that is regulated by Semaphorins.[160,163] It has therefore been proposed by Oinuma et al. (2004) that the GAP activity of Plexins decreases active R-Ras, leading to the detachment of cells from the extracellular matrix.[136,137] Whilst most Semaphorin signalling occurs through interactions with Plexins and Neuropilins, CD72 and T cell immunoglobulin and mucin domain containing protein-2 (Tim2) have been found to interact functionally with transmembrane Semaphorins in the immune system.[164] Sema7A binds directly to Plexin-C1 displaying Plexin-independent activity that is mediated by integrin-β1.[139,140] Class 3 Semaphorin, Sema3E, is unusual in its class as it does not require a NRP co-receptor for Plexin mediated signalling.[165]

1.10.3 Semaphorins in disease

Viral Semaphorins and Sema7A are found in the genome of pox viruses and the wildebeest herpes virus, *alcelaphine*. Sema7A is also expressed by activated T cells, the shared homology with the viral Semaphorin *Vaccina* virus semaphorin (A39R) is not surprising, as Sema7A binds to PlexinC1 to induce a pro-inflammatory response by monocytes.[166] It also suppresses the migration of dendritic cells and monocytes towards the virus infected cells and may interfere with phagocytosis.[167,168] This prevents the acquisition and processing of viral antigens by dendritic cells, a mechanism of immune evasion by the pox virus. A39R decreases integrin-mediated attachment of dendritic

cells and in PlexinC1$^{-/-}$ mice integrin inactivation by A39R is abrogated.[169] It is intriguing that a pox virus has evolved to utilise their signalling pathways to manipulate immunity and this probably reflects their prominence with the immune system.

The 3p21.3 homozygous deletion in small cell lung cancer was found to contain genes for Sema3B and Sema3F.[170] In lung tissue, a reduction in Sema3F seen in the epithelial layer, with a predominance of localisation to the cytoplasmic membrane, correlated with a higher stage of lung cancer.[171] When metastatic human melanoma cells were transfected with Sema3F and implanted into mice, the resultant tumors did not metastasize.[172] In this model tumour cells expressing Sema3F had diminished ability to adhere and migrate on fibronectin. They were chemorepulsive for vascular and lymphatic endothelial cells expressing NRP2 and the repulsive activity was abrogated by NRP2 RNA interference. Semaphorin signalling in the transfected tumour cells appears to be autocrine, this has also been observed in endothelial cell Semaphorin signalling.[160]

1.10.4 Sema3F regulates motility in a zebrafish model

Published work from my group found neutrophils express the class 3 Semaphorin, Sema3F, with differential expression observed in hypoxia.[119] This is interesting as neutrophils migrate to injury sites that are far more hypoxic than the circulatory system. Little is known about the role of Sema3F within the immune system. To investigate this further my group used a Sema3F knockout zebrafish model, where a Sema3F mutation was induced by TALENs genome editing. In this Sema3F knockout fish, whole body neutrophil counts remained unchanged compared to wild type, as was neutrophil recruitment to the site of injury (figure 1.10.4-1, graphs A-C) (unpublished work completed by Dr Suttida Eamsamarng, this work was supervised by Professor Moira Whyte, Dr Sarah Walmsley and Dr Andrew Furley). Intriguingly, accelerated neutrophil resolution was observed. In contrast, in a Sema3F whole-animal

overexpression model, neutrophil recruitment was reduced, and inflammation resolution delayed (graphs D & E). Sema3F modulates cell behaviour through both directly signalling with Plexins and also in complexes with NRP1 or NRP2. This leads to activation of protein kinases and GTPase signalling pathways, promoting actin cytoskeletal re-organisation following the oxidation of actin filaments.[123,124,173,174]

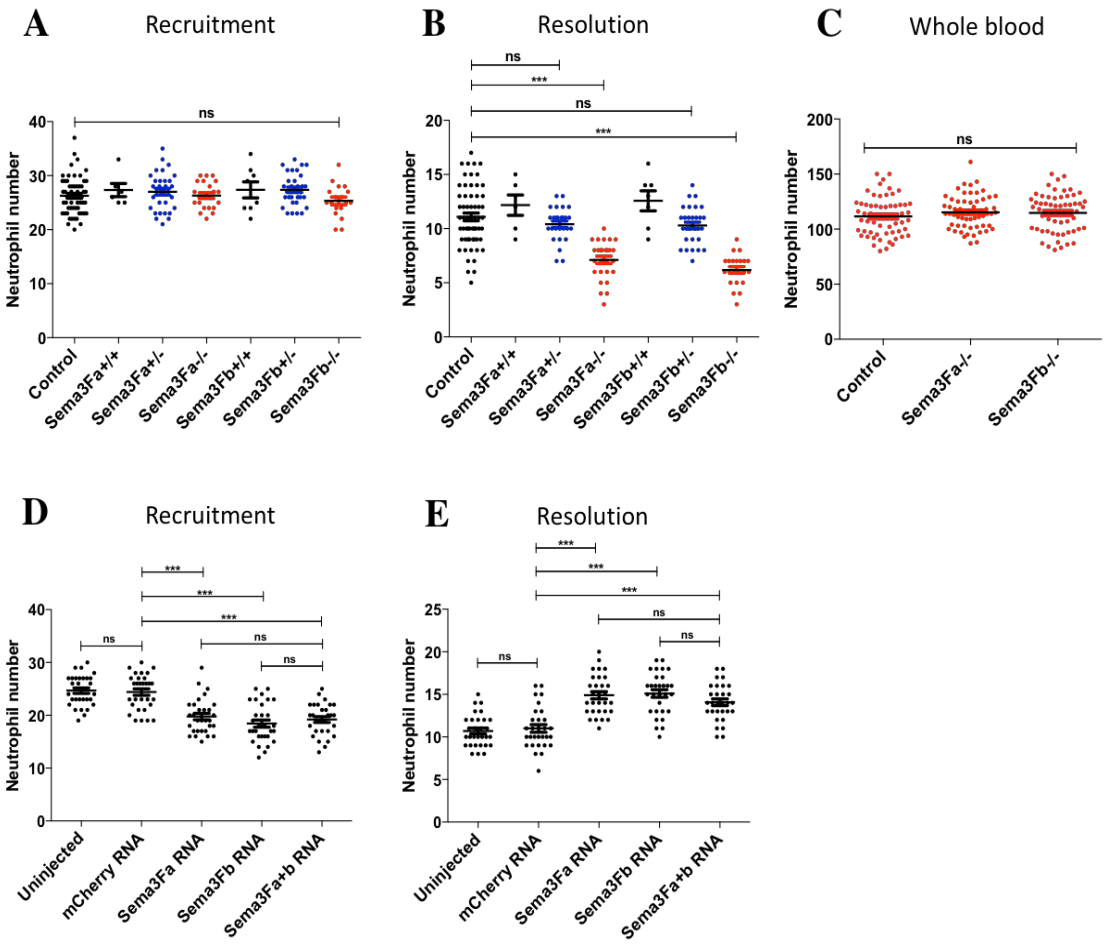

Figure 1.10.4-1 Sema3F expression in a transgenic Zebrafish model alters both recruitment and resolution in a tail fin injury model

Whole-fish Sema3F knockout was achieved using TALEN in situ genome editing, results are shown graphs (A-C). Semaphorin3Fa or semaphorin3Fb mutated F1 fish were incrossed and compared to myeloid-specific peroxidase (mpx): GFP fish. Tailfin transection was performed at 2 days post fertilisation (dpf), neutrophils were counted at 6 hours post injection (hpi) [recruitment phase] and 24 hpi [resolution phase]. (A) Neutrophils counted at 24 hpi. Data shown are mean ± SEM, n= 50 performed as 4 independent experiments, *P<0.01, ***P<0.001. (B) TALENs had no effect on the whole-body neutrophil numbers. Whole body total neutrophil numbers were counted at 3dpf, n= 50 performed as 4 independent experiments. (C) Neutrophils counted at 6 hpi. Data shown are mean + SEM, n= 50 performed as 4 independent experiments, *P<0.01, ***P<0.001. Semaphorin3Fa or Semaphorin3Fb RNA (50ng/µl) was injected into 1-cell stage zebrafish mpx: GFP embryos, with 50ng/µl mCherry RNA used as a negative control, to create a Sema3F whole-fish overexpression model. Tailfin transection was performed at 2dpf, and neutrophils counted at 6 and 24 hpi. (D) 6 hpi time point neutrophil counts (recruitment) and (E) 24 hpi time point neutrophil counts (resolution). Data shown are mean + SEM, n= 30 performed as 3 independent experiments, P values were calculated using one-way ANOVA, with a post-test correction for multiple comparisons (Bonferroni), ***P<0.001.

1.10.5 Semaphorin signaling and chemotaxis

During chemotaxis directional migration of neutrophils requires polarisation of the cell with formation of the leading edge formed by actin rich lamella and at the opposite pole the uropod a tail like projection.[65] PI-3 kinases have been identified down stream of G-protein-coupled receptors and are stimulated by chemoattractants, PI-3k activity regulates the establishment of cell polarity.[67] The cytoplasmic region of Plexin have been shown to interact with 20 different proteins, of which some are GEFs (Guanine nucleotide exchange factors). [175] One such GEF is FARP2, this is a Dbl-family guanine nucleotide exchange factor (GEF) that contains a 4.1, ezrin, radixin and moesin (FERM) domain, a Dbl-homology (DH) domain and two pleckstrin homology (PH) domains. [176] This may link Plexin signalling to the leading edge of a migrating cell. Recruitment of pleckstrin homology (PH) domain containing proteins bind to phosphoinositides (PIs) such as $P1(3,4,5)_3$ leading to pseudopodia production.[177] PH domain containing proteins are concentrated at the leading edge of neutrophils undergoing chemotaxis.[178] Production and regulation of $P1(3,4,5)_3$ is controlled by PI-3 kinases and PI-3 phosphatases. Inhibition of PI-3 Kinase activity results in defective formation of the leading edge and suppression of neutrophil chemotaxis.[66] In addition accumulation of a major lipid product of PI-3 kinase namely PIP_3 is a key event in in direct downstream cell signalling augmenting cell polarity and chemotaxis.[68] PI-3 Kinase activity determines the level of PIP_3, AKt binds directly to PIP_3 at the PH domain situated at the membrane, therefore levels of Akt indirectly reflects PI-3K activity.

My group measured dynamic PI-3 kinase activity using a transgenic zebrafish line: lyz/PHAkt-EGFP. Sema3F overexpression was induced by injection of Semaphorin3Fa or Semaphorin3Fb RNA and enhanced green fluorescent protein (EGFP). Fluorescence intensity was compared between the leading edge and the trailing edge of migrating neutrophils. Localisation of PHAkt-EGFP in neutrophils was observed during recruitment to a tail fin injury site.

Both the level and localisation of PHAkt-EGFP were similar between wild-type and in overexpression of Sema3F, there was clear formation of a distinct leading edge, polarity of the cell was maintained, but they appeared rounder. This suggests that Sema3F signalling is acting downstream of both Akt and PI-3K. This initial data suggests that Sema3F affects chemotaxis via changes in the neutrophil cytoskeleton. Furthermore they demonstrated that Semaphorin induced F-actin disassembly in the zebrafish line Tg(mpx:LifeActRuby). This is where LifeAct is 17 amino acid bioprobe originating from yeast bound to a Ruby fluorochrome which binds all F-actin. Following injection with Semaphorin3Fa and Semaphorin3Fb, neutrophils from this transgenic zebrafish appear “rounder” and the area of the F-actin detected was diminished in the Sema3F treated cells. Barberis et al. (2004) observed that Sema4D-PlexinB1 signalling caused cell rounding.[163] The PlexinB1 activation resulted in disassembly of integrin-based adhesion followed by F-actin depolymerisation. These results highlight the importance of Sema3F signalling in neutrophil actin dynamics. Sema3F unlike Sema3A, has no evident affect on heterophil polarisation but does result in cell rounding. Sema3F may signal downstream of the of Akt and PI-3K promoting actin depolymerisation leading to “cellular collapse”.

The pathway linking Plexin signalling and actin dynamics has not been fully described. Hung et al. (2010) demonstrated convincing evidence the multi-domain cytosolic protein MICAL1 (microtubule associated monooxygenase, calponin and LIM domain containing 1) provides the physical link between Semaphorin-Plexin signalling and cytoskeletal response. Associated with PlexinA4 these proteins have redox activity, which in turn is responsible for the destabilisation of F-actin directly.[173] Distinct temporal spatial activation of small GTPases of the Rho subfamily manifest in dynamic changes within the cytoskeleton and it is possible Sema3F signalling may interact with members of this pathway. Key effectors in this pathway include Rho GTPases (Rho, Rac, and Cdc42) which are prominent downstream targets of PI-3 Kinase and are

activated by rising PIP_3 levels. Semaphorin-induced cell rounding may demonstrate global actin depolymerisation. Certainly it been shown that Sema3A signalling results in loss of branched F-actin mesh works. [179] This may also be a result of altered or inhibited cross-talk between the front and back of a polarised neutrophil. It is known that RhoA and its downstream effector, myosin II, mediate the ‘‘back-ness’’ response, which locally inhibits the ‘‘front-ness’’ response and constrains its location to one part of the cell.[180] Roundness and cellular collapse may result from a lack of protrusions, achieved through inhibition of Rac signalling as this is essential for the protrusion of lamellipodia and forward movement. Other members of the Rho-family may be implicated in cell rounding such as: Cdc42. This maintains polarity through directing spatial orientation of lamellipodia and intracellular organs, or Rho which promotes adhesions during movement, or indeed Ras signalling as this regulates focal adhesions and dynamic stress fibre responses.[181] How Semaphorin-Plexin signalling mediates cell rounding and cell motility remains a challenging puzzle, certainly it appears redox signalling, the Rho-super family and actin dynamics are key players.

Sema3F evidently has an important role in controlling neutrophil migration to the injury site and as a consequence the magnitude of the inflammatory response. Neutrophils have differential expression of Sema3F in hypoxia, similarly the expression of Neuropilin 1 at hypoxic sites is reduced. Both in transfected tumour cells and endothelial cell Semaphorin signalling occurred in an autocrine manner.[160] Whether neutrophil autocrine expression of Sema3F can directly regulate neutrophil recruitment to inflamed sites is currently unknown. In light of emerging evidence that neutrophils also undergo processes of reverse migration away from inflamed tissue I propose neutrophil expression of Sema3F regulates neutrophil retention within the lung parenchyma and is thus a determinant of the intensity of the innate immune response. The varying response of cells to class 3 Semaphorins may in part be accounted for by the heterogeneity of receptor expression. Following signal

transduction, the mechanism by which Sema3F regulates cell motility is not through a disruption of cellular polarity, with preservation of a leading edge, it is downstream of this involving the signalling pathways and cross-talk that control dynamic cytoskeletal organisation within a neutrophil.

1.11 Hypothesis and aims

My specific hypothesis is that loss of neutrophil autocrine expression of Sema3F enhances neutrophil recruitment and resolution in acute lung injury through alterations in F-actin dynamics leading to reduced neutrophil retention.

Aims:

1. Characterise neutrophil specific expression of Sema3F and its co-receptors in both human and murine neutrophils in response to inflammation.
2. Investigate the role of Sema3F in neutrophil mediated acute lung injury through the study of whole animal and transgenic mice.
3. Define the mechanism by which Sema3F regulates neutrophil movement.

2 Materials and Methods

2.1 Ethical approval

The healthy human blood donation was obtained under the University of Edinburgh ethics protocol of the project entitled: The Role of inflammation in Human Immunity AMREC Reference number 15-HV-013. This has been reviewed and approved by:

1) The Blood Resource Management Committee, Medical Research Council (MRC) Centre for Inflammation Research (CIR), Queens Medical Research Institute, Little France, Edinburgh (appendix XIV);

2) The ACCORD medical research ethics committee, AMREC (ACCORD is the Academic and Clinical Central Office for Research and Development, a joint office of the University of Edinburgh and NHS Lothian).

Similarly, human lung tissue was obtained from biopsy through the Edinburgh tissue bank which has also been reviewed and approved by the Edinburgh Tissue Bank ethics committee and AMREC. The NHS Lothian Bio-resources provided lung tissue from non-tumour regions of lung following biopsy was used for immunohistochemistry in this project (application number: SR451).

2.2 Human neutrophil isolation

Neutrophils were isolated from peripheral blood using Dextran sedimentation with discontinuous plasma-Percoll gradients.[182] Initially, blood was drawn using a 21-gauge needle and then decanted into a 50ml polypropylene falcon (Corning B.V. Life Sciences, MA USA, 352098) and 4.4ml of 3.8% sodium citrate (Sigma-Aldrich, UK 00526) added to 35.6ml blood. The whole blood was then centrifuged at 350g for 20 minutes, at 20°C, with Brake 5, Acceleration 5. The platelet rich plasma (PRP) phase was aspirated into 10ml narrow neck glass vial (Fisher-Scientific, UK, 11563680) and 200µl of 1M CaCl2 added. Then the vial was incubated at 37°C for 1 hour to produce

autologous serum. Using the cell-rich lower layer remaining, leukocytes were then separated from erythrocytes by Dextran sedimentation using a 6% Dextran solution (Dextran T500, Pharmacosmos, Denmark 5510 0500 9006) and 0.9% saline to warm in 37°C incubator. When a clear interface was achieved the leukocyte, rich layer was aspirated into 50ml falcon and centrifuged at 350g for 6 minutes, at 20°C, with Brake 9, Acceleration 9. Discontinuous plasma-Percoll (GE Healthcare, UK, 17089102) gradients were prepared by overlaying 2 ml of 81% Percoll/9% phosphate buffered saline (PBS. Gibco, 14190250) onto 68% Percoll/32% PBS in a 15ml falcon tube. After spinning the leukocyte rich cell suspension, the cell pellet was re-suspended with a 1 ml of 55% Percoll/45% PBS and this carefully layered over the gradient. The gradients were then centrifuged at 700xg, for 20 minutes, at 20°C, with Brake 0, Acceleration 0. The erythrocytes pellet is formed at the bottom of the tube, between 68% and 81% Percoll layer are the neutrophils and eosinophils. A further band is seen above and lies the between the 81% layer and 55% cell suspension, these are the PBMCs and were removed before the PMCs using a Pasteur pipette. The neutrophil layer transferred to RPMI 1640 media (Thermo Fisher Scientific, UK, 11875-085) and counted using a haemocytometer (C-CHIP, Cambridge BioScience, UK, DHC-F01-50). Granulocytes were then centrifuged at 250g for 6 minutes, at 20°C, with Brake 9, Acceleration 5. Supernatant was discarded, and the cells were re-suspended to give $5x10^6$ neutrophils per ml in RPMI 1640 containing 1% penicillin, 1% streptomycin (Sigma-Aldrich, UK, P0781) and 10% autologous serum or 10% heat -inactivated foetal calf serum (FCS, Sigma-Aldrich, UK, N4762). Neutrophils were cultured 150 µl of $5x10^6$ neutrophils per well on a 96-well polypropylene plate (Corning Costar plates, Sigma-Aldrich, UK, 6551). Neutrophil purity was measured by examination of cytocentrifuge slides using freshly isolated cells and was routinely >95% with eosinophils as the main contaminant cell type.

2.3 Human Neutrophil Culture

Human neutrophils were cultured at a concentration of $5x10^6$ neutrophils per ml of media on a 96-well polypropylene plate at 37°C in a humidified incubator with 5% supplemental CO2 (BB15 incubator, ThermoScientific, UK). Neutrophils were cultured in RPMI 1640, with 10% heat-inactivated FCS in the presence or absence: of 10 ng/ml LPS from E coli, (Enzo Life Sciences New York, USA, ALX-581-010-L001) fMLF [10-100nM] (Sigma-Aldrich, UK, F3506), IL-1β[100nM] (AMS Biotechnology, Oxford, UK, 6460-10) IL-8 [100nM] (Life technologies, UK, 10098H01H2U25), human recombinant Sema3F protein[10-1000nM] and (R&D Systems Inc, UK, 3237-S3-05), TNF-α [100nM] (AMS Biotechnology, UK, 1050-10).[7]

2.4 Western Blotting

2.4.1 Preparation of human neutrophil lysates for protein separation

Following culture for the appropriate time period, neutrophils were gently harvested into 2ml Eppendorfs from the culture plates and spun at 300g for 2 minutes at 4°C.The cells were combined so that $1x10^6$ cells per condition were in each 1.5ml Eppendorf and washed in ice cold phosphate buffered saline (PBS, Gibco®, Invitrogen Ltd, UK 10010015). They underwent a second wash in 1ml of sonication lysis buffer (Appendix I). The supernatant was discarded, and cells re-suspended in 100 µl of sonication lysis buffer and incubated on ice for 10 minutes. Cells were then sonicated in a Bioruptor*PLUS*™ iced water bath (Diagenode Europe SA, Liège, Belgium) using 30 second on-off high power cycles for 10 minutes. The whole cell lysates were centrifuged at 12,000 g for 10 minutes at 4°C. The supernatant was removed into fresh 1.5ml tubes and an equal volume of 2X SDS lysis buffer was added to each aliquot (see appendix II). Samples were boiled for 5 minutes at 100°C then stored at -80°C.

2.4.2 Protein separation

Proteins were separated by sodium dodecyl sulphate polyacrylamide electrophoresis (SDSPAGE) using the Bio-Rad mini PROTEAN®II electrophoresis cell system (Bio-Rad laboratories, UK 1658000). Precast 7.5 % gels from (Bio-rad laboratories, 5671023) were loaded with preheated neutrophil cell lysates (100°C for 2-5 minutes) containing rainbow markers (Bio-Rad Laboratories). Proteins size ranged from 38-120 kDa therefore 7.5% gels were appropriate for all proteins studied. The gel was run at 180 volts (PowerPac 300, Bio-Rad Laboratories) in a tank containing running buffer (see appendix III) until the blue dye front reached the bottom of the gel.

2.4.3 Protein Transfer

Following separation by SDS-PAGE as described above, the gel apparatus was disassembled. A piece of PVDF Immobilon-FL transfer membrane (Life technologies, UK, 22860) was activated by soaking in methanol for 2 minutes and then placed in transfer buffer (see appendix IV). In a tray containing transfer buffer, a gel-holding transfer cassette was opened, and a fibre pad soaked in transfer buffer was placed on the black side of the cassette. Two pieces of blotting paper (Whatman®3mm chromatography paper, Whatman International, Maidstone, UK) were then placed on top of this followed by the resolving gel and then the activated membrane. Two further pieces of blotting paper and another fibre pad were applied on top before the gel holding cassette was closed and placed in a tank filled with ice-cold transfer buffer. Transfer of protein to the membrane was performed using a Bio-Rad Mini Trans-Blot® cell at 100 volts for 90 minutes.

2.4.4 Immunoblotting and Detection

After transfer, the membrane was blocked in blocking buffer (Odyssey buffer (PBS), Li-Cor, Lincoln, USA) for 1 hour on an orbital shaker. This minimised non-specific binding of antibodies to the membrane. The membrane was transferred to a 50 ml tube and the primary antibody, diluted in 2 ml of Li-cor Odyssey blocking buffer, was added. The dilutions at which the antibodies

were used are shown in appendix V. The membrane was incubated overnight at 4˚C on a rolling platform. After incubation with the primary antibody, the membrane was washed for 30 minutes in PBS with 0.1% Tween20 before being incubated for one hour at room temperature with the appropriate fluorophore-conjugated secondary antibody diluted in 2 ml of blocking buffer (IRDye® Donkey anti-Rabbit IgG, Li-cor Bio-sciences UK, 925-32213). The membrane was then washed again as before. Labelled proteins were detected using the Li-cor Fc-Odyssey System (Li-Cor, Lincoln, USA).

2.5 Immunohistochemistry

Immunohistochemistry was kindly performed by Lyndsey Boswell, Service Manager at the Shared University Research Facilities (*SuRF*) department of the Edinburgh University, Queen's Medical Research Institute. Following cull, lungs were instilled via a cannulated trachea with 10% formalin under 20 cm H_20 and lungs dissected *en bloc*. They were then submerged in 10% formalin for 1 hour at room temperature, then at 4˚C for 4 hours. After this they were placed in 70% ethanol until used. Tissue was paraffin-embedded and sections cut at 3-5 microns.

2.5.1 Staining of tissue sections

Slides were then loaded onto Leica Bond-Max automated immunostainer (Leica Microsystems GmbH, Ernst-Leitz-Straße, Wetzlar, Germany). Epitope retrieval was performed on board Bond-Max using DAKO Proteinase k solution (DAKO, Glostrup, Denmark). Primary antibodies used are listed in appendix VI alongside the matched isotype control (using a non-immune immunoglobulin of the same type at an identical concentration) and was applied to sections at room temperature for one hour. The presence of antigen was visualized with Bond Polymer refine detection kit (Leica Microsystems GmbH, Ernst-Leitz-Straße, Wetzlar, Germany). The nuclei of the tissue were

counterstained using the heamatoxylin from the refine detection kit. Slides were removed from bond max, dehydrated and mounted.

2.6 Assessment of neutrophil function

2.6.1 Neutrophil chemotaxis assay

Neutrophil chemotaxis was assessed using Neuro Probe ChemoTx® microplates with a 5µm filter (Neuro probe, Inc. Receptor Technologies Ltd., UK). Plates are molded from tissue culture grade transparent polystyrene. PVP Treatment –PCTE membranes are available pre-treated with the wetting agent polyvinylpyrrolidone (PVP) which makes the surface hydrophilic. Neutrophils do not adhere well to PVP treated membranes and drop off after migrating when quantifying cell numbers in the end well this is an key advantage. Microplate wells were filled in duplicate with 29µl of test solutions containing various concentrations of recombinant Sema3F[10-100nM] (R&D Systems, Abingdon, UK 3237-S3-025) and fMLF. A negative control (RPMI 1640) and a positive control (25µl of cells at a concentration of $2x10^6$/ml) were also added to the microplate. The framed filter was firmly applied to the microplate so that the fluid in the wells made contact with the filter and there were no air bubbles. Cells (25µl of cell suspension) were added to each site on the filter except for the positive control well and allowed to migrate for an hour. Chemokinesis controls were prepared, cells were suspended with either recombinant Sema3F or fMLF in the microplate and the same reagent added to the corresponding well below. After incubation, any remaining cells on the top of the filter were carefully removed and the cells in the microplate wells counted using a haemocytometer. The number of cells in the microplate wells is expressed as a percentage of the positive control and the chemokinesis controls shown for clarity and not deducted from the chemotaxis values. The percentage of neutrophil chemotaxis was calculated as follows:

(Average* number of neutrophils in well / Average* number of neutrophils in control well) x 100 = Percentage chemotaxis

***Average is calculated of mechanical repeats of condition**

2.6.2 Microfluidic chemotaxis assay

Transwell assays have significant limitations to assess neutrophil migration yet are relatively easy and therefore widely used. It gives an endpoint readout only and provides no further information on the pattern of cell migration. To investigate further the effect of Sema3F on neutrophil migration I collaborated with Dr Felix Ellett a Clinical Fellow at Harvard medical school. The chemoattractant LTB4 is loaded into the chamber and washed through the channels creating a stable gradient for up to eight hours.[89] The narrow 8μm diameter channels replicate the pulmonary capillaries. A drop of whole human blood is placed on the opposing pole and only the neutrophils population are able to migrate to the start of the channels through the first section of the chip assay (figure 2.6.2-1). Real-time light microscopy is used to monitor the neutrophil journey to the chamber and retrotaxis (against the preserved gradient, away from the chamber). Every ~5min the percentage of maximal recruitment to the chamber was calculated. The inflection point represents maximal recruitment; after this point declining percentages represent retrotaxis and not apoptosis as these cells can be viewed actively leaving the chamber against the maintained gradient.

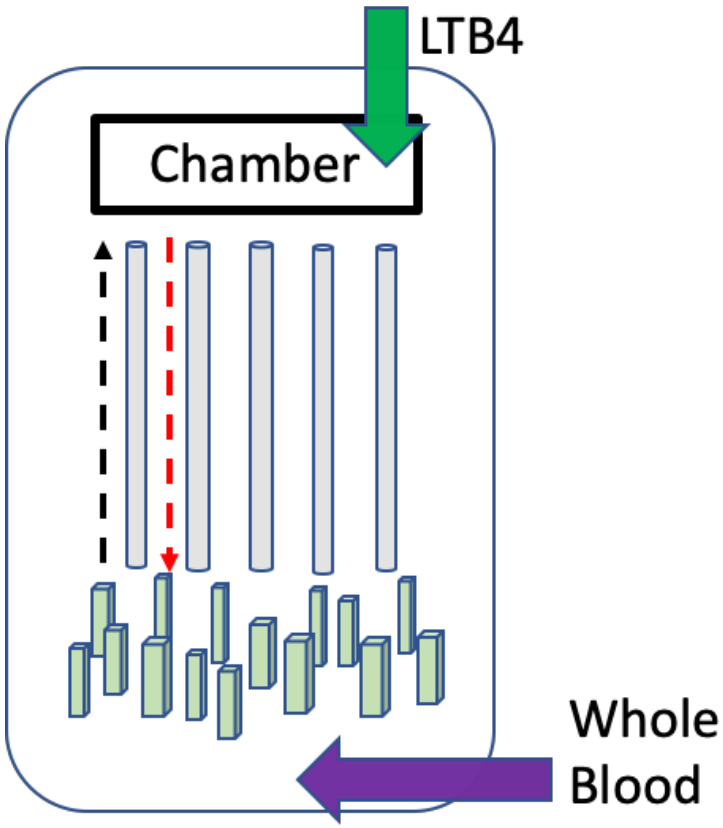

Figure 2.6.2-1 A microfluidic chip for the investigation of neutrophil migration
A chip assay was used to assay the migration of human neutrophils in response to LTB4 [100nM] shown in the diagram. Only neutrophils can exit the blood and progress to the migration channels. The neutrophils are then recorded in real-time as they migrate to the loading chamber and the maximal concentration of the chemotactic stimulus.

2.6.3 Neutrophil Phagocytosis

2.6.3.1 Phagocytosis of opsonized Zymosan A

Zymosan A is prepared from the cell wall of Saccharomyces cerevisiae (Sigma-Aldrich, 58856-93-2), initially 1g of Zymosan was boiled in 20ml of sterile PBS for 30 minutes then allowed to cool. Aliquots of this mixture were centrifuged (1200rpm for 10 minutes at 4°C) and washed three times with sterile PBS. The Zymosan was then pooled into a final volume of 20ml of sterile PBS and aliquots transferred into Eppendorf tubes. These aliquots were spun at 3000 rpm for 5 minutes and the supernatant discarded before storing at -20°C. On the day of use the Zymosan was opsonized by adding 1 ml of foetal bovine serum to 10mg of Zymosan and agitating for 1 hour at 37°C. Particles were then washed three times in PBS before re-suspending in PBS to give a stock suspension of particles of 50mg/ml. Prepared in this way Zymosan forms a fine suspension of particles around 3µm in diameter.

Neutrophils were incubated with 0.2mg/ml of opsonized Zymosan A particles for 15 minutes at 37°C. Cytocentrifuge slides were then prepared and uptake of the yeast particles assessed. In excess of 300 cells were counted and the phagocytic index was calculated as follows:

PI = (Mean number of particles per neutrophil) x (% of neutrophils containing particles)

2.6.3.2 Phagocytosis of Escherichia Coli

Neutrophils were incubated with heat-inactivated fluorescein isothiocyanate-conjugated *Escherichia Coli* O55:B5 (Sigma-Aldrich, 297-473-0) at a multiplicity of infection of 1 for 30 minutes at 37°C. The cells were then placed on ice to stop phagocytosis, washed in PBS and re-suspended in fluorescence-activated cell sorting buffer (FACS buffer: PBS without Ca2+/Mg2+, Bovine Serum Albumin 1% (BSA, Sigma-Aldrich, A8412), 2 mM

EDTA). Samples were processed using a flow cytometer (BD FACSCalibur™, BD Biosciences, Becton Dickinson Ltd., Oxford, UK). Results were analysed using FlowJo software (version 9.0, Tree Star Inc., Ashland, USA).

2.7 Operetta High Content Imaging System

Nunc™ MicroWell™ optical bottom 96 well plates (ThermoFisher, 265301) were pre-coated with Corning™ Cell-tak (Fisher Scientific Ltd., 354240). Isolated human neutrophils from healthy volunteers were incubated in media and autologous serum at the optimized density of $2x10^5$ cells per 100μl well with recombinant Sema3F [10nM, 100nM]. Each condition had 4-8 replicates on the plate. The plate was then centrifuged at 300g for 2 minutes and fMLF [100nM] added after 40 minutes of culture at 37°C The neutrophils were then fixed with 4% paraformaldehyde (ThermoFisher, UK, 28906) for 15 minutes at room temperature in a laminar flow cabinet. PBS was also added at the same volumes as fMLF for the vehicle control. The plate was then carefully washed twice with PBS and a 0.1% Triton® X-100 (Sigma-Aldrich, 9002-93-1) in PBS solution added to the well for 15 minutes at room temperature. Following two more washes with PBS the HCS CellMask™ Green stain (Thermofisher, H32714) was added for 30 mins at room temperature. Once removed, Alexa Fluor® 594 conjugated Phalloidin (Thermofisher, A12381) was added for 45 minutes. Finally, this was removed and DAPI (4',6-Diamidino-2-Phenylindole Dihydrochloride, ThermoFisher, D1306) added for 15 minutes. The plate was washed 2 more times in PBS and sealed with para-film and protected from light. Images of the neutrophils at x20 magnification were acquired using Operetta High-Content Imaging System; each well was analysed using a minimum of 20 fields. Analysis of cell roundness was performed by the Columbus image analysis software (PerkinElmer, UK). Nuclei were first identified in the DAPI channel. Nuclei were quality controlled for size (<70μm2) and DAPI intensity (<5000) with passing nuclei used to seed a cytoplasmic segmentation algorithm in the 488 channel (Cell Mask™). Intensity of pixels in the 594 channel (Phalloidin) and the shape distribution were then measured

inside the predefined cytoplasmic boundary region for each cell. All cells imaged were analysed individually and mean of each well calculated and reported.[183] Roundness was determined on a scale where 0 is a straight line and 1 a perfect circle. The pipeline used to measure neutrophil roundness is summarised in appendix VII.

2.8 Project and Personal Animal Work Licence

2.9 Murine Colonies

2.9.1 Wild type mice

Male and female C57BL/6 mice were purchased from Harlan (Oxon, UK) aged 6-8 weeks. They were then rested in standard housing for 1 week prior to commencing experiments.

2.9.2 Sema3F$^{flox/flox}$ MRP8Cre$^{-/-}$ and Sema3F$^{flox/flox}$ MRP8Cre$^{+/-}$ colonies

A tissue specific Cre-LoxP system was used to delete Sema3F. MRP8 driven Cre recombinase (MRP8Cre) was used to target Sema3F (Sema3F$^{flox/flox}$ MRP8Cre$^{+/-}$) in neutrophils (Sema3F KO). Sema3F^{floxflox} mice were generated via the MRC IMPC consortium and was crossed with MRP8 Cre heterozygous mice to generate neutrophil-specific knockouts.

Details can be found at http://www.informatics.jax.org/allele/MGI:5692585 [Sema3f_HEPD0570_6_A04, allele type Tm1c]. [184,185] Animals were backcrossed to a C57BL/6 background. C57BL/6 mice (Harlan, Oxon, UK) or littermate Sema3F$^{flox/flox}$MRP8Cre$^{-/-}$ mice were used as controls. All animal experiments were conducted in accordance with Home Office Animals (Scientific Procedures) Act of 1986 with local ethics approval. MRP8 (Myeloid-related protein 8) is a member of the family of S100 calcium binding proteins. [186] MRP8 driven Cre recombinase has been shown to delete the targeted gene in ~80% of neutrophils, with little deletion in macrophages/monocytes, dendritic cells, natural killer cells, mast cells, basophils or eosinophils.[187]

2.9.3 Catchup$^{IVM\text{-}RED;Lifeact\ GFP}$ transgenic mice

Catchup$^{IVM\text{-}RED;Lifeact\text{-}GFP}$ mice were provided by Dr Leo Carlin and generated by crossing lines available at the Beatson Institute animal facilities, for use during ex-*vivo* lung imaging experiments. Mice were culled, and tissue prepared within this facility under local licences. Ly6G is expressed exclusively by neutrophils in mice.[159,160] Mice were obtained where Cre recombinase and the fluorescent protein tdTomato were targeted to the Ly6G promotor sequence creating a murine model where neutrophils could be detected through expression of tdTomato termed "catchup mice".[161188]. While the neutrophils in the catchup mouse can be identified by flow cytometry the tdtomato in this construct is not bright enough for microscopy, therefore these mice were crossed with a transgenic mouse containing tdTomato under the control of the constitutively active promotor Rosa26 (Rosa26.LSL.tdTomato) producing Catchup$^{IVM\text{-}RED}$. Termed "IVM-Red" as these mice allow intravital microscopy of red-fluorescent endogenous neutrophils. [188] Catchup$^{IVM\text{-}RED}$ mice were then crossed with another transgenic animal where the peptide lifeact is used to report the dynamics of filamentous actin (F-actin) in a tissue specific manner ('floxed-lifeact). In this mouse the promotor is the X-linked Hprt gene and the peptide lifeact is attached to green fluorescent protein (GFP) for detection (Hprt.LSL.lifeact-GFP). The term Catchup$^{IVM\text{-}RED;Lifeact\text{-}GFP}$ will be used for these mice moving forward.

2.9.4 Genotyping for Murine Colonies

Genotyping of the mice during breeding of the Sema3F$^{flox/flox}$MRP8Cre$^{+/-}$ colony and cross was initially performed by Transnetyx (Tennessee, USA) using protocols provided to us by the MRC Harwell (MRC IMPC consortium). There three probes used LIL2-Bact-P MD (the promotor driver cassette), Sema3F-3 WT (Sema3F gene) and Cre recombinase. Once the lines Sema3F$^{flox/flox}$MRP8Cre$^{+/-}$ and Sema3F$^{flox/flox}$MRP8Cre$^{-/-}$ had been established in-house genotyping was performed based on the Cre-recombinase expression. This was performed by Dr Lauren Melrose (MRC Centre for

Inflammation Research, Queen's Medical Research Institute, UK) using primers, mastermix and cycling conditions detailed in Appendix VIII. An example of the genotyping results for animals from these colonies are shown in figure 2.9.4-1. Every 3 months samples would be sent to Transnetyx for more detailed genotyping to ensure the maintenance of the genotypes of the colony. For the Catchup$^{IVM\text{-}RED;Lifeact\text{-}GFP}$ mice samples were also sent to Transnetyx and propriety probes sets were used to confirm genotypes.

A

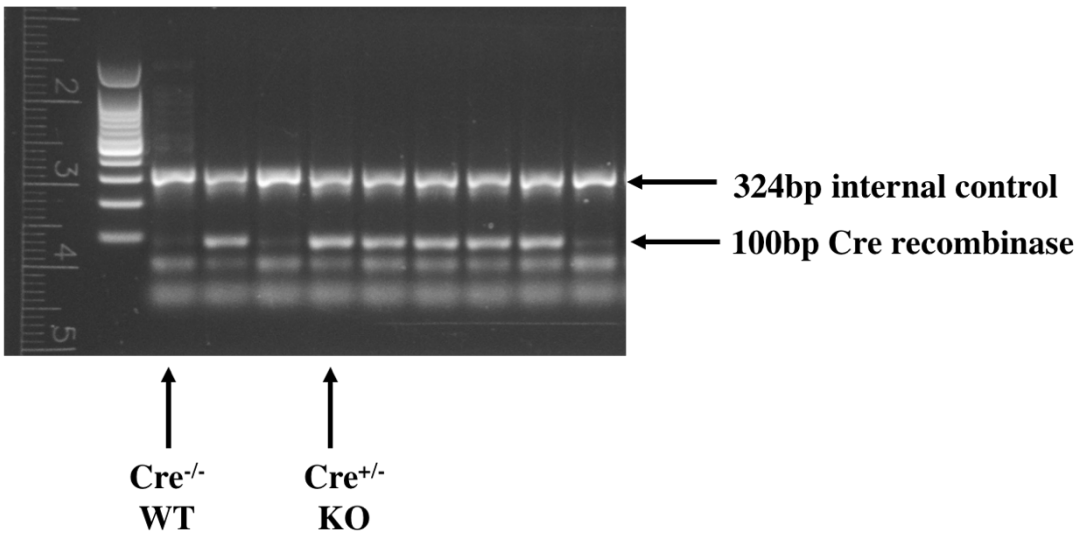

B

Protocol Primers

Primer	5' Label	Sequence 5' --> 3'	3' Label	Primer Type
oIMR1084		GCG GTC TGG CAG TAA AAA CTA TC		Transgene
oIMR1085		GTG AAA CAG CAT TGC TGT CAC TT		Transgene
oIMR7338		CTA GGC CAC AGA ATT GAA AGA TCT		Internal Positive Control Forward
oIMR7339		GTA GGT GGA AAT TCT AGC ATC ATC C		Internal Positive Control Reverse

Figure 2.9.4-1 Example of PCR gel used for murine colony genotyping
Representative images of a PCR gel (A) performed to detect murine genotypes extracted from ear clips of mice and amplified using primers to detect wild type Cre recombinase expression. Wild type and knock bands are labelled. (B) A table showing the primers used to identify Cre recombinase in this colony and the internal controls.

2.10 Acute lung injury model

Mice were placed into a plastic chamber and connected to an oxygen-driven nebuliser. Oxygen was delivered at 6 litres per minute through 3mg Lipopolysaccharide (LPS from *E. coli*, Sigma-Aldrich, L7018) suspended in sterile water creating a vapour that was delivered into the chamber. Once all LPS was vaporised (after approximately 20 minutes) the mice were then returned to their cages. In prior experimental work from my group and in the literature, it has been established that nebulised PBS does not result in lung injury but nebulised LPS induces a mild and predictable murine lung injury. This model has been is well characterised, widely used and publicised from in work from both my research group and others. [8,119,189,190]

2.11 Intratracheal instillation of exogenous Sema3F

Mice were anesthetised with an intra-peritoneal injection of medetomidine 1mg/kg and ketamine 76mg/kg. Then intratracheal instillation of phosphate buffered saline and Sema3F 1µM performed. Using a blunted metal hub needle (Harvard Apparatus, Cambridge) to cannulate the trachea under direct visualisation Sema3F 1µM in 50µl of PBS or PBS was then directly instilled. Following this, to induce recovery mice were given a subcutaneous injection of the reversal agent Atipamezole was used at 1mg/kg.

The chimeric fusion protein Sema3F used in these experiments was prepared in keeping with future production of Sema3F as a therapeutic. Recombinant fusion proteins consisting of the extracellular domain of immunoregulatory proteins and the constant (Fc) domain of immunoglobulin G (IgG) represent a growing class of human therapeutics leading to higher yields and potentially an increased half-life of the protein. The murine IgG-Fc protein was used as a control and did not yield any alteration in neutrophil behaviour or measured parameters during these experiments.

2.12 Bronchoalveolar lavage of mice

At specified time points mice were given an intraperitoneal injection of pentobarbital 100 µl of 40mg/ml. The chest wall was exposed by opening the skin in the midline from the initial neck wound down to the abdomen. Pneumothoraces were introduced by carefully puncturing the inferior surface of the diaphragm and then the thorax was opened by carefully cutting along the lateral margins of the rib cage on each side exposing the lungs and heart. The trachea was exposed, cannulated and secured in placed with suture before the lungs were instilled with 5 x 0.8ml of Phosphate Buffered Saline (PBS). The recovered lavage fluid was maintained on ice before haemocytometer counts were performed. Cytospins of cells were stained with Re-stain Quick-Diff for differential cell counts.

2.13 Histology sections from mice

The mouse trachea was cannulated under direct visualisation and lungs inflated with 10% formalin and then harvested.

2.14 Murine lung imaging

2.14.1 Harvesting of Lung Tissue

This work was done in collaboration with Dr Leo Carlin (Cancer Research UK, Beatson Institute, Glasgow), with animal work being done at the animal facilities at the University of Edinburgh and the final processing and imaging of the lung slices performed at the Beatson Institute. Mice were nebulised with 1mg/ml of LPS) from *E.Coli*. For mice treated with Sema3F (1µM) or PBS intra-tracheal instillation (IT) instillation was performed 24 hours post LPS. Mice were culled using a lethal injection of pentobarbital and then dissected to expose the thoracic cavity. Following this the trachea was cannulated and instilled with 2%(w/v) low melting point agarose gel (Life Technologies, UK16520050) maintained at 37°C. The cannula was secured with a drain-type suture, which was pulled closed once the lungs were fully inflated with the gel

to prevent leakage. The carcass was then cooled on ice allowing the agarose to set for >3mins. Lungs were then dissected *en bloc* and rinsed in PBS and placed in either 4% paraformaldehyde solution or RPMI media.

2.14.2 Preparation of fixed lung slices

Following harvesting lungs were rinsed in PBS and placed in 4% paraformaldehyde solution. To ensure total coverage of the tissue the attached suture was trapped in the lid of a universal container and the tube inverted ensuring total coverage of the air-filled lungs in the solution. The fixed lungs remained in the 4% Paraformaldehyde (PFA, 16% Paraformaldehyde (w/v) Methanol-free, Thermo Scientific Pierce, UK 28908) for 15mins at room temperature and then 1 hour and 45mins at 4°C. Lungs were then rinsed and re-submerged in a solution containing PBS, BSA 1% and Sodium Azide 0.05% (Scientific Laboratory Supplies Ltd, UK CHE3270). The left lower lobe was carefully isolated and attached to vibratome stage (Campden Instruments, UK 5100mz) using Vetbond tissue adhesive (VWR International Ltd, M1469SB). Using the highest oscillation amplitude and speed (1mm/sec advancing speed for fixed tissue, 0.5-1mm/sec for non-fixed) 300µm slices were made into a 4°C solution of PBS/BSA 1%/0.05% Sodium Azide.[191]

2.14.3 Staining protocol for fixed lung slices

All incubation steps and washes were performed on a rocker. In the well of standard 12 well culture plate individual fixed lung slices were blocked and permeabilised in 300 µl of PBS with10 % normal goat serum (NGS) (Sigma Aldrich G9023), 1% BSA, 0.3% Triton-X 100 (Sigma Aldrich, UK RES9690T-A101X) and 0.05% sodium Azide (PBS/10%NGS/1%BSA/0.03%TX-100/0.05%Azide) for 30 mins at room temperature. The lung was washed in a PBS/1%BSA/0.01% TX-100/0.05%Azide solution and transferred to 24 well culture plate. The slices were incubated with the primary antibodies unconjugated Anti-S100A9 (1:200 Hycult Biotech, Netherlands, HM1102) and unconjugated Anti-CD31 (1:250, Armenian hamster monoclonal [2H8] to CD31 monoclonal, Abcam ab119341) in 250 µl of PBS/10%NGS/1%BSA/0.01%/TX-

100/0.05% Azide for 2 hours at room temperature. One rinse and 3x2min washes were then performed using a PBS/1%BSA/0.01% TX-100/0.05%Azide solution. The slices were incubated on a rocker for a further 1 hour at room temperature with the secondary antibodies Cy™3 AffiniPure Donkey Anti-Rat IgG (1/250, Jackson ImmunoResearch Laboratories, Inc. USA, 712-165-150), Goat anti-Hamster IgG (H+L) Cross-Adsorbed Secondary Antibody, Alexa Fluor 488 (1/250 Thermofisher, A-21110) and DAPI 1:2000 in a PBS/10%NGS/1%BSA/0.01%/TX-100/0.05%Azide solution. Finally, 3x2minutes washes were performed using a PBS/1%BSA/0.01% TX-100/0.05%Azide solution, with a final rinse in PBS alone. They were then fixed in 2% PFA for 2 minutes at room temperature and washed twice with PBS.[191]

2.14.4 Mounting of fixed lung slices

Plastic gantries were attached to clean glass slides. To unfold the lung slices and for easy mounting, lung slices were placed in a beaker of distilled water and then wound around a small spatula they were then floated on the water droplet placed within the gantry. The water was then aspirated and replaced with Mowiol with 2.5% DABCO (1,4-diazabicyclo-[2,2,2]-octane; Sigma Aldrich, UK D27802) (Mowiol Hard set media see Appendix IX) using approximately 100-150 µl of Mowiol mounting media. Slices were then carefully covered with a glass slip and dried in the dark.

2.14.5 Preparation of lung slices for culture and ex-*vivo* imaging

Harvesting of lungs from Catchup$^{IVM_RED;Lifeact\text{-}GFP}$ mice were performed at the animal facility at the Beatson institute by Dr Leo Carlin. Sema3F WT and KO lung tissue was collected by myself from the University of Edinburgh animal facilities and transported on ice to the Beatson institute within 1.5 hours. Following *en bloc* dissection lungs were rinsed in PBS and placed in RPMI media. In an identical manner to the fixed lung the left lower lobe was carefully isolated and attached to vibratome stage (Campden Instruments, UK 5100mz) using Vetbond tissue adhesive (VWR International Ltd, M1469SB). Using the highest oscillation amplitude and speed (1mm/sec advancing speed for fixed

tissue, 0.5-1mm/sec for non-fixed) 300µm slices were made into a 4°C RPMI 1640 media with 1% FCS.

2.14.6 Mounting of cultured lung slices

The treated and control slices were placed into a double glass bottomed plastic chamber (Thermo Scientific™ Nunc™ Lab-Tek™ Chambered Coverglass, Thermofisher UK, 155361) with 800 µl RPMI 1640 media at room temperature. A metal tissue harp was placed over each slice and weighted down with a titanium washer overlaying a tissue harp (both from: Warner Instruments, UK). The chamber was then placed inside an environmentally controlled chamber on a Zeiss LSM 880 Airyscan (with Fast module). The temperature was maintained at 37°C with normal atmospheric oxygen and 5% CO_2. Temperature of the media and slice were allowed to equilibrate for up to 1 hour, this also allowed the slices to settle reducing movement artefact. At the beginning of this resting period Alexa Fluor® 647 anti-mouse CD31 Antibody (Biolegend, 102415) and Alexa Fluor® 488 anti-mouse S100A9 Antibody (47-8D3, Novus, NBP2-47980AF488) 10µl of each were directly added to the media surrounding each slice. At the appropriate timings the treatments were also added to the media. [191]

2.14.7 Lung slice Image acquisition and analysis

Laser scanning confocal microscopy was performed using an inverted LSM 880 Airyscan 'Fast' microscope (Carl Zeiss). The Airyscan Fast detector has advantages of increased resolution, increased signal-to-noise ratio, and faster image acquisition (the 'Fast' module essentially allows the microscope to obtain four image scanning 'lines' simultaneously). The latter was important in the cultured lung slices when imaging moving neutrophils. The Airyscan detector is comprised of 32 individual detectors arranged in concentric circles. With this detector arrangement, some of the unfocused signal usually rejected when using a standard confocal microscope, can be used to increase signal:noise without decreasing resolution. In fact, combining the signal detected by an array of sensitive sub-airy detectors allows a maximum

resolution that moderately improves what is normally possible in diffraction limited microscopy, i.e. 'super-resolution'. Acquisition for both cultured and fixed slices used a Zeiss 20x objective (0.8 N.A. Plan Apochromat Air). During live lung imaging pre-programmed automated time-lapse acquisition of cultured lung slices was used. Sequential alternating imaging of the control vs treated lung slice over the experiment approximated simultaneous recording. Z-stacks where acquired and projected using Imaris (Bitplane; Oxford Instruments) for analysis. Image stiching was performed using Zen 'black' or 'blue software (Carl Zeiss) and represented an area of 1mm x 1mm of tissue imaged at 1 time-point/position. Analysis of imaging using IMARIS V 9.1 software is detailed within the description of the corresponding data in results chapters 1 and 2.

2.15 Murine neutrophil isolation

Peripheral blood murine neutrophils were isolated by negative magnetic selection using commercially available kit from EasySep®. Once adequately anaesthetised, a laparotomy was performed, and the inferior vena cava was exposed by blunt dissection. Blood was collected using a 23G needle and 1ml syringe. The syringe and needle were heparinised (10% solution, StemCell Technologies, UK 07980). Between 0.5 and 1ml of blood was collected from each mouse and transferred to a 15ml falcon on ice. Mice were then culled by cervical dislocation following venesection. The red blood cells were then lysed using 9 parts of an ammonium chloride solution (StemCell technologies, 07800) to every 1part blood. This solution was then incubated in the dark for 10 minutes. The leukocytes were then pelleted at 300g for 10 minutes at 4°C and the supernatant removed. Pellets were re-suspended in 10ml of a PBS buffer solution containing 2% foetal bovine serum and 5nM EDTA (RoboSep™ buffer, StemCell Technologies, 20104) and spun again at 300g for 10 minutes at 4°C. Typically leukocytes from 2 or 3 mice were pooled to obtain sufficient numbers for neutrophil isolation.

Leukocyte pellets were re-suspended in 150μl of RoboSep™ buffer and transferred into a 96-well non-tissue treated U-bottom plate (Corning, 10739314). The EasySep® neutrophil enrichment antibody cocktail labels a maximum concentration of leukocytes of 100x106 per ml. Typically 3 mice were pooled to provide an optimal number of cells. Rat serum (7.5μl per 150μl sample) and neutrophil cocktail (7.5μl per 150μl sample) were added and the plate incubated at 4°C for 15 minutes. RoboSep™ buffer (100μl) was then added to each sample and the plates centrifuged at 300g for 7 minutes. The supernatant was aspirated, and the cell pellets re-suspended in 150μl of RoboSep™ buffer. A biotin selection cocktail was then added (7.5μl per 150μl sample) and plates were incubated for a further 15 minutes at 4°C. Magnetic dextran-coated iron particles (D particles) were added (20μl per 150μl sample) and plates incubated for 10 mins at 4°C. RoboSep™ buffer was added to each well to give a total volume of 250μl and the plate then placed on an EasyPlate™ EasySep® magnet (StemCell technologies) for 10 minutes at room temperature. The tetrameric antibody complexes bound to contaminating cells were attracted to the magnet and settled at the bottom of the wells leaving the unlabelled neutrophils in the supernatant. This supernatant was carefully transferred into 15ml falcon tubes and topped up with RoboSep™ buffer to a final volume of 500μl. A haemocytometer count was performed, and cells washed in excess PBS before being spun at 300g for 10 minutes. The cells were then ready to be suspended in media or the appropriate lysis solution.

2.16 Ultra-purification of murine BAL neutrophils

Following murine LPS nebulisation and bronchioalveolar lavage with PBS the extracted fluid samples were kept on ice at 4°C, then spun at 300g for 10 mins. Ultra-purification was achieved using Percoll gradients optimised by Dr Emily Watts, Clinical Fellow, Walmsley Lab Group. Using 10x PBS, a 90% Percoll solution was made and % gradients made as described in Appendix X. The gradients were layered, starting with the 3ml of 78% layer, then the 3ml of the

69% layer and finally the sample pellet reconstituted with 52% Percoll. The samples were then centrifuged at 1200rpm for 30 min with an acceleration setting of 1 and deacceleration setting of 0. The two layers of cells were aspirated with the first containing the monocyte/macrophage population and the second containing >95% purity of neutrophils. The samples were topped up with PBS and then centrifuged and counted using a haemocytometer. A representative image is shown in figure 2.16-1.

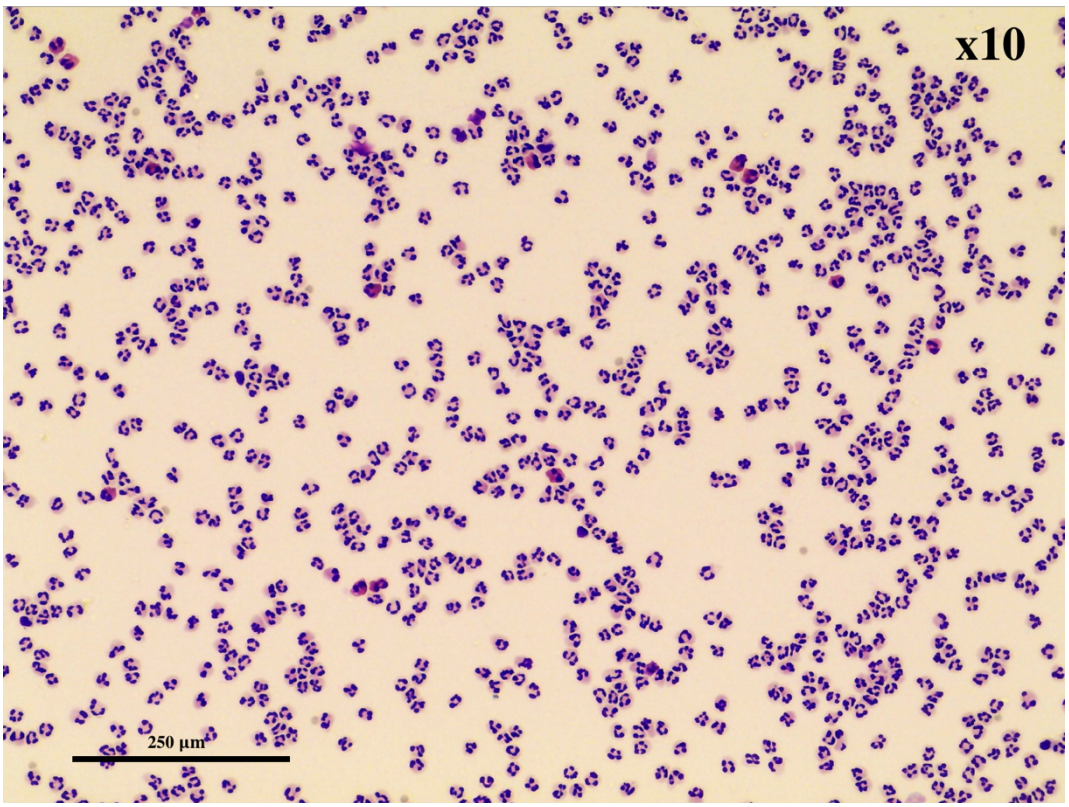

Figure 2.16-1 Example of ultra-purified neutrophils
Following bronchioalveolar lavage neutrophils obtained were subject to another discontinuous Percoll gradient to improve the purity of neutrophils in the sample. The image in this figure shows a pure sample of neutrophils. Original magnification x10.

2.17 Murine Neutrophil RNA extraction

Murine peripheral blood or bone marrow neutrophil RNA was extracted using the mirVana™ total RNA isolation protocol (Ambion, USA AM1560). Cells ($1x10^6$ per condition) were lysed in 300μl of mirVana lysis/binding buffer and stored at - 80°C if not being extracted immediately. To extract the RNA, miRNA homogenate (1/10th of the lysates volume) was added to the lysate to stabilize the RNA and inactivate the RNases. Samples were vortexed to mix and incubated on ice for 10 minutes. Volumes of Acid-Phenol Chloroform (Ambion AM9720) equivalent to that of the initial lysate was added, mixed using a vortex mixer and spun at 13400 rpm (Eppendorf Mini Spin Hamburg, Sigma Aldrich, Z605220) for 5 minutes at room temperature. The upper aqueous layer was carefully removed and transferred to clean RNase-free 1.5ml Eppendorf tubes. The volume removed was noted to enable 1.25 volumes of ethanol to be added. Samples were vortexed and a maximum of 700μl of this aqueous layer/ethanol mixture was transferred into a filter cartridge within a labelled mirVana kit collection tube. The tubes were spun for 15 seconds at room temperature at a 10000 rpm. The flow through was discarded and any remaining aqueous/ethanol mixture was added to the filter cartilage. Once all the aqueous/ethanol mixture had been spun over the cartridge, 700μl of miRNA wash solution 1 was added to the filter cartridge. Tubes were again spun for 15 seconds at room temperature at a 10000 rpm, the flow through discarded and washing of the filter cartridge was repeated a further two times using 500μl miRNA wash solution 2/3, discarding the flow through after each wash. After the final wash, the tubes were spun for a further 60 seconds to dry the cartridge. Cartridges were then placed into clean labelled collection tubes and 30-50μl of RNase free water pre-heated to 95°C was added to the filter cartridge. Tubes were spun again for 20-30 seconds at 13400rpm. The flow through containing the RNA was then used using the NanoDrop™ 1000 spectrophotometer (Fisher Scientific Ltd., UK).

2.18 cDNA Synthesis

Avian myeoblastosis virus (AMV) reverse transcriptase and random primers were used to generate cDNA from RNA aliquots. Every 1μg RNA was made to 12.4μl with RNase-free water and a cocktail of primers, enzyme and dNTP was added. Samples were run on a ³Prime Thermal Cycler (Teche Ltd., Staffordshire, UK) at 23°C for 5 minutes, then 42°C for 2 hours, followed by 99°C for 2 mins to heat inactivate the enzyme and stored at -20°C.

Regents were from Promega (Promega, Southampton, UK). The following master mix was added to 500ng of murine RNA in water: 8μl 5 x AMV RT Buffer, 16μl 10mM dNTPs, 1.2μl RNasin®, 1.2μl random primer and 1.2μl AMV reverse transcriptase.

For future use with customer designed Sema3F primer probe set from Primer Design, the Precision nanoScript2 Reverse Transcription Kit was used (Primer Design, UK). For the annealing step 0.5μl Oligo-DT and 0.5μl random primers were added to RNAse/DNAse free water along with up to 2μg of RNA template to a final volume of 10μg. Using ³Prime Thermal Cycler these samples were heated to 65°C for 5 min then immediately cooled in an ice water bath. The 10μl of the following solution added to each sample: 5μl nanoScript 4x buffer, 1μl dNTP mix 10mM, 3μl RNAse/DNAse free water and 1μl nanoScript2 enzyme. Samples were vortexed followed by a pulse spin and incubated at 25°C (room temperature) for 5 minutes and then at 42°C for 20 minutes. The reaction was heat inactivated at 75°C for 10 minutes and stored cDNA samples at -20°C until use

2.19 TaqMan® and PerfectProbe™ protocol

TaqMan® commercially available primer probe sets were obtained from Applied Biosystems for the target assay (Sema3F) and the endogenous control assay (β-actin) (Applied Biosystems, USA). To prove knockdown of the Sema3F gene at the mRNA level customised PerfectProbe™ primer sets were

obtained from Primer Design targeted to the deleted region containing the Sema3f Tm1d allele (critical region between the LoxP sites and validation of primer probes see Appendix XI). Each product contained sequence-specific primers and a 6-FAM dye labelled probe. β-actin was selected as the endogenous control as it is highly expressed, and expression is not altered by inflammation or hypoxia. This enables relative quantification following RT-PCR reactions. cDNA samples from wild type murine BAL or brain tissue were diluted to give standards in order to create a standard curve for each gene of interest. For TaqMan® primers the PCR mastermix consisted of 10μl 2 x qPCR MasterMix II with UNG, 8μl RNase free water, 1μl Primer probe set1μl of cDNA was added to 19μl of mastermix per reaction. On the same opaque 384-well plate cDNA was added to the master mix in duplicate or triplicate and covered with a sealed plate lid.

Standard thermal cycle conditions were used. 2 minutes at 50°C, 10 minutes at 95°C, then 40 cycles of 15 seconds at 95°C to denature and 1 minute at 60°C to anneal and extend.

In the case of PerfectProbe™ primers the PCR master mix consisted of: 10μl PrecisionPLUS qPCR Master Mix, 1μl primer probe mix, 5μl [25ng] of cDNA template, 4μl RNAse/DNAse free water. Thermal cycling conditions required a hot start with 10 min at 95°C, then 50 cycles of denaturation 15 seconds at 95°C and 60 seconds at 60°C.

Average threshold cycles were obtained for each sample using SDS2.4.1 software (Applied Biosystems). Standard curves were plotted using an arbitrary value of 10,000 for the top standard followed by the appropriate dilution series against average threshold cycle values. Samples were then quantified using the standard curve. The values obtained were normalised to β-actin expression in the same samples using the following equation: Normalised value=Gene-of-interest expression/β-actin expression. Alternatively, for the previously validated custom primer-probe sets (Appendix

XI) values were analysed using delta-delta Ct method to calculate the relative fold gene expression of samples.

2.20 Lung digest and analysis using flow cytometry

Knockout Sema3F$^{flox/flox}$ MRP8Cre$^{+/-}$ and wild type Sema3F$^{flox/flox}$ MRP8Cre$^{+/-}$ mice were nebulised with LPS at 2, 6 and 24 hours post nebulisation mice were culled and lungs were harvested in RPMI 1640 media at 4°C. A lung digest cocktail of: [all sigma] Collagenase V (C9263), Collagenase D (11088858001), DNase I (10104159001) and Dispase (Thermofisher, UK 17105-041) was made in RPMI 1640 media and warmed to 37°C. Once the cold media had been removed, 2mls of the cocktail was added to each lung in a 5ml bijou. Each lung was then sectioned in 1-2mm pieces using stainless steel scissors. The bijous were then placed on a heated (37°C) shaker for 40mins and vigorously agitated by hand every 10mins. Following this, digested cells were run through a 100μm cell strainer and excess of cold FACS buffer (~15mls) (PBS without Ca^{2+}/Mg^{2+}, 1 % bovine serum albumin, 2 mM EDTA) into a 50ml falcon and centrifuged at 300g for 5 minutes at 4°C. Cell pellets were then re-suspended in 2mls of red cell lysis buffer (Sigma-Aldrich, UK R7757) for 2-5 minutes at room temperature and excess of FACS buffer added to stop the reaction. Following this, cells were spun at 300g for 5 minutes at 4°C and re-suspended in in fluorescence-activated cell sorting (FACS) buffer and centrifuged at 300g for 5 minutes at 4°C. Following this the cell pellet was resuspended in 5mls FACS buffer and the suspension was passed through a 40μm cell strainer. Cell number was counted using the live/dead stain trypan blue (Sigma Aldrich, T8154) and a haemocytometer. A maximum of $2x10^6$ cells were placed in a V-bottom FACS 96-well staining plate (VWR, UK ANIC20.20.18EMV) for each lung and controls. The plate was then spun at 300g for 5 minutes at 4°C, re-suspended in PBS and spun again at 300g for 5 minutes at 4°C. Excess fluid was then removed and 25μl of fixable live/dead aqua dye (Applied Biosystems, USA L34957) 1:100 in PBS was added to each

well apart from the unstained and the plate incubated in the dark for 15 minutes at room temperature. The plate was blocked with Fc block (Biolegend, UK 101319) 1:100 in PBS with mouse serum 1:10, this was added to each well for a 15-minute incubation at 4°C. A master mix of the flow markers to be used was prepared in FACS buffer (as detailed in the table below) and 50μl added to each well except the unstained condition, the single aqua and the control FMOs (fluorescence minus one). FMOs for each Ab used were made. The plate was then incubated in the dark at 4°C for 30mins. All antibodies are listed in Appendix XII.

Comp beads (Thermofisher, UK 01-1111-41) were used for single controls for each fluorochrome at the same concentration as the master mix. Following staining, the plates were washed with FACs buffer and samples transferred, through a final 40μm cell strainer into glass flow tubes. Following this, samples were analysed using the LSR II 6 laser Fortessa (BD Biosciences, UK). The gating strategy is shown in figure 2.20-1.

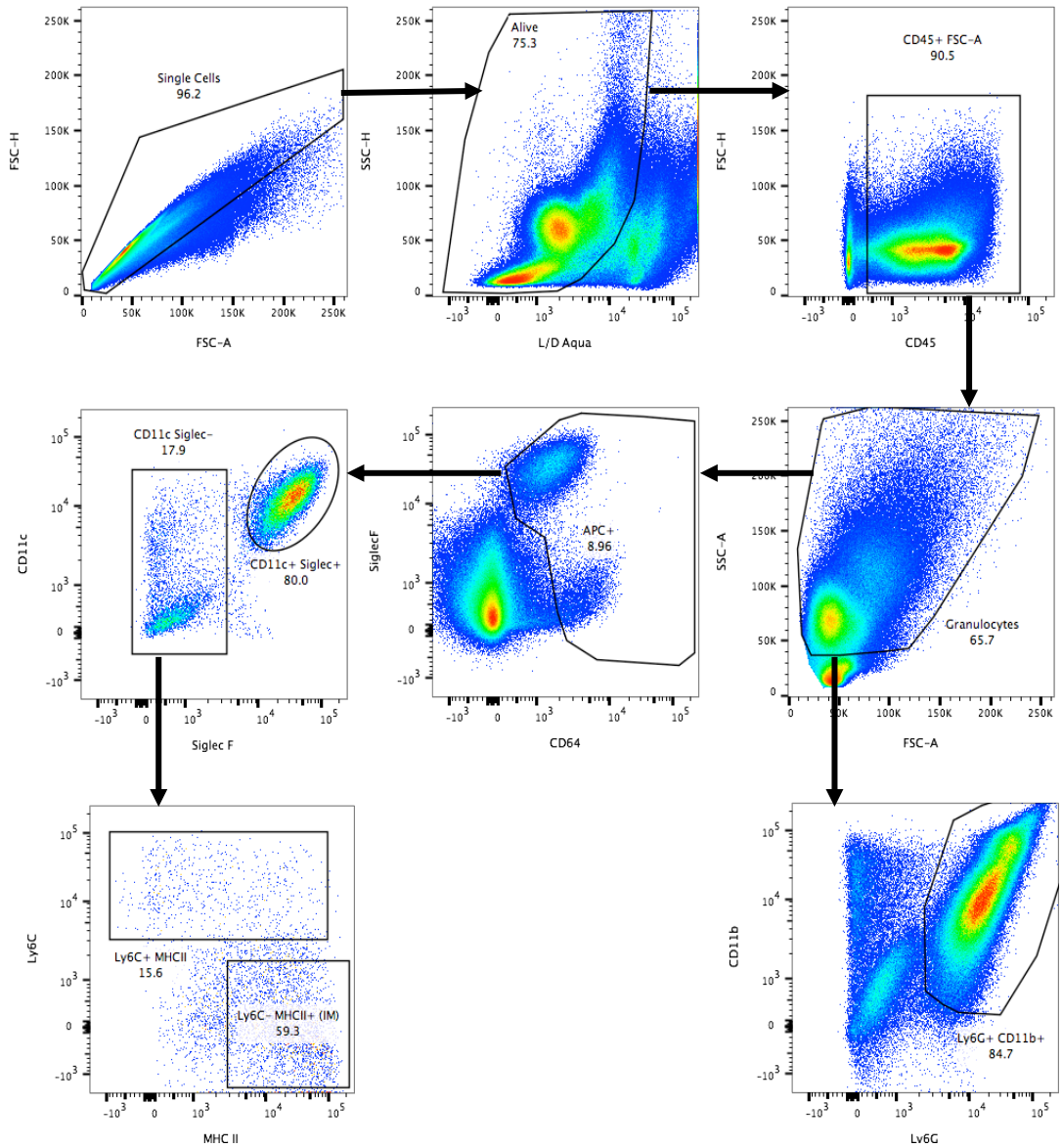

Figure 2.20-1 Gating strategy for lung neutrophils and macrophages
Doublets were excluded using FSC-H and FSC-A and the live population of cells selected as the aqua negative population. CD45 was used to highlight the leukocyte population. A granulocyte gate was applied, and macrophages were identified through their expression of CD64 and further subdivided into alveolar macrophages and interstitial macrophages based on their expression of Siglec F and CD11c. Interstitial macrophages were further subdivided into Ly6C+ or MHCII+ cells. Neutrophils were gated upon as Ly6G+ cells.

2.21 Flowcytometry analysis of neutrophil surface expression of Sema3F receptors

Blood was obtained from healthy controls recruited locally from the Centre for Inflammation Research (CIR) Blood Resource database (AMREC, 15/HV/013). Whole blood was immediately added to 3.8% sodium citrate (Sigma Aldrich, 1613859). The sample was prepared as described in section 2.1 Human neutrophil isolation, however after the dextran sedimentation the cells were removed and decanted into a 50ml falcon then pelleted. To induce red cell lysis the cell pellet was re-suspended in 1 ml of a 0.2% NaCl hypotonic solution and then a further 9 mls of 0.2%NaCl was added and the falcon inverted 10 times. Next, 10 mls of 1.6% NaCl hypertonic solution was added to achieve isotonicity and the falcon inverted once. The cells were centrifuged at 1500 rpm for 6 minutes and the pellet re-suspended in PBS and countered. A maximum of $3x10^5$ cells were placed in a well of a V-bottom FACS 96-well staining plate for each condition and for controls. The plate was then spun at 300g for 5 minutes at 4°C, re-suspended in PBS and spun again at 300g for 5 minutes at 4°C. Excess fluid was then removed and blocked with Fc block (1:100 in PBS) with mouse serum 1:10. This was added to each well for a 15 minute incubation at 4°C. A master mix of the flow markers to be used was prepared in FACS buffer (as detailed in Appendix XII) and 50μl added to each well except the unstained condition. FMOs for each Ab used were made. The plate was then incubated in the dark at 4°C for 30mins. The antibodies are listed below. Following this, samples were analysed using the LSR II 6 laser Fortessa (BD Biosciences, Oxford, UK). Results were processed using FlowJo software (version 10.0, Tree Star Inc., Ashland, US).

2.22 Neutrophil surface expression of L-Selectin and CD11b

Following 4 hours incubation with LPS, neutrophils were washed with ice-cold FACS buffer (PBS plus 0.5% BSA) and stained with anti-mouse antibodies at 4°C. Cells were single-stained with PE-anti-CD62L (-selectin) (8 μg/ml, BD

Pharmingen™) and PE-anti-CD11b (8 μg/ml, BD Pharmingen™). Isotype matched controls (PE-IgG2a and PE-IgG2b respectively) were used to set baselines. Antibody binding was detected using a BD FACS Calibur™ flow cytometer (BD Biosciences, Dickinson Ltd., Oxford, UK). During analysis specific geometric mean fluorescence was calculated by obtaining geometric mean fluorescence intensity values for each antibody and subtracting the geometric mean fluorescence of the isotype control.

2.23 Measurement of neutrophil respiratory burst

Human neutrophils were isolated using a discontinuous Percoll gradient and cultured in RPMI 1640 media with 1%FCS at a density of $5x10^6$ cells/ml in 96 well plate at 37°C in an incubator with 5% CO_2 as previously described. Those conditions requiring treatment with Sema3F, the recombinant Sema3F protein [10, 100nM] (R&D Systems), was added prior to re-suspension of the cell pellet. Following culture in media, or media with Sema3F for an hour, the general oxidative stress indicator CM-H2DCFDA (DCF) (Life Technologies, USA C6827) was added at concentration of 5 μM for 30 minutes at 37°C in an incubator with 5% CO_2. The stimulus N-formyl methionyl peptide, formyl-methionyl-leucyl phenylalanine (fMLF) [100nM] (Sigma Aldrich, 59880-97-6) was added for further 30 minutes returning the plate to the incubator. The entire plate was cooled in an ice bath and the conditions rapidly aspirated into cooled Eppendorfs which were centrifuged at 2000rpm for 5 minutes, rinsed once in cold FACS buffer and placed in glass flowcytometry tubes then analysed immediately on an LSR II 6 laser Fortessa (BD Biosciences, Oxford, UK).

2.24 Measurement of neutrophil myeloperoxidase activity

Neutrophils were cultured in RPMI 1640 with 1% FCS at a density of $1x10^6$ per well. At time 0, 100nM of Sema3F or 15μl PBS vehicle control was added to wells. Following a 1-hour incubation at 37°C with 5% C02 a further 10ng/ml

granulocyte-macrophage colony stimulating factor (GM-CSF, Pepro-Tech, UK 300-03-5) or 15μl of RPMI 1640 media was added to wells. The plate was returned to the incubator and the neutrophils were treated with 100nM of FMLF or PBS vehicle control after 30 minutes for another 10 minutes. The plate was centrifuged at 350g for 5mins at 4 and 10μl removed from each technical replicate and pipetted onto a 96 well ELISA assay plate (CoStar, Corning, USA, 3590). To each 10μl of sample 80μl of H_2O_2 0.75mM pipetted onto all wells using a multi-channel pipette in addition 110μl of 3,3',5,5'-Tetramethylbenzidine (TMB, Thermofisher, UK) substrate added to each well. The plate was covered to protect it from light and incubated for 5 mins at 37°C with 5% CO_2. Finally, 50ul of 0.16M sulfuric acid stop solution was pipetted into the wells and the plate read on plate reader at 450nm (Synergy HT, Biotek, UK).

2.25 Measurement of neutrophil elastase

Elastase activity in cultured neutrophil and BAL supernatant was measured using the Enzcheck kit procured from Life Technologies and the supplied protocol adhered to (Enzcheck elastase, Life technologies, E12056). Cell supernatant was prepared as described in methods section 2.24 and the measurement of neutrophil elastase activity in response to pre-treatment with Sema3F[100nM] determined. Standard curves were made from DQ Elastin with 1:2 serial dilutions in triplicate. Neat neutrophil supernatant was used; samples and standards were incubated at room temperature for 20-30 minutes with the reaction buffer and then analysed using a plate reader (excitation/emission 485/530, Synergy HT, Biotek, UK).

2.26 Statistical Analysis

Data were analysed using Prism 7.0 software (GraphPad Software Inc, San Diego, CA). For comparison of two sample means when cells from the same subject were used, paired *t*-tests were performed. Unpaired *t*-tests were used

for comparisons between control and patient or wild type and transgenic sample means. If multiple time points or concentrations were used, repeated measures ANOVA with the relevant post tests were performed. If many comparisons between genotypes or controls and patients were required in these experiments, two-way ANOVA. Bonferroni or Šídák post-hoc tests were used when a selected set of means was to be compared. The Šídák method was used when each comparison was independent of the others. If this assumption of independence could not be supported, the Bonferroni method was used. Statistical significance was accepted when $P < 0.05$.

3 Results chapter: Neutrophil Sema3F expression is upregulated following inflammation and regulates neutrophil migration in the injured lung

3.1 Introduction

3.1.1 Class 3 Semaphorins in disease

As previously shown by Walmsley et al. (2011), in hypoxic neutrophils deficient in the PHD3 (a regulator of HIF pathway), the transcript for Sema3F was highly up regulated.[192] This suggested that Sema3F has a role in the neutrophil response to hypoxia and inflammation. Certainly, it is known that Semaphorins have key roles in immune signalling and have been shown to act as a neutrophil chemorepellent in the context of chronic lung allergy by Movassagh et al. (2016).[193] More widely Semaphorins have been demonstrated as having a role in lung cancer as a tumour-suppressor gene.[194,195] Higher abundance of its co-receptor NRP2 is associated with increased metastasis in lung cancer.[194,196] Moreover class 3 Semaphorins appear to regulate cell behaviour in an autocrine manner.[160,197] Therefore neutrophil Sema3F could plausibly regulate neutrophil behaviour during the innate immune response in an autocrine manner.

3.1.2 Lipopolysaccharide induced lung injury

In order to investigate Sema3F in the context of acute lung injury a murine model of acute lung injury was used. This model is generated by the delivery of nebulised LPS to mice. LPS is a pathogen-associated molecular pattern (PAMP) which through interaction with TLR4 releases pro-inflammatory stimuli and recruits leukocytes to the injury site. LPS induced lung injury is an approximation of acute lung injury seen in humans, both produces a largely neutrophil-dependent response. The LPS-induced lung injury has a well characterised course and duration which is well tolerated by mice.[189]

3.1.3 Neutrophil responses to TNF-α and IL-1β

TNF-α and IL-1β have both been shown to be important signals in lung inflammation and elicit characteristic neutrophil responses. They are useful

experimentally, as part of a reductionist strategy, to stimulate neutrophils to aid understanding of neutrophil behaviour in the inflammatory niche. TNF-α has a key role in myriad of respiratory diseases ranging from ALI to asthma and lung cancer. It is also prominent in the pathophysiology of conditions affecting other systems, including rheumatoid arthritis and inflammatory bowel disease. Monoclonal antibodies against TNF-α are now used as therapeutic agents in some of these illnesses.[198-201] TNF-α has been shown to prime neutrophils and can enhance the respiratory burst through cytoskeletal rearrangements.[202] In terms of apoptosis a bimodal effect is observed whereby, following cell culture, TNF-α inhibits apoptosis in neutrophils aged 6-20 hours but after 20 hours it is pro-survival.[203] This is in contrast to most cytokines and chemokines which promote neutrophil survival in the inflammatory niche. TNF-α has also been shown to promote neutrophil adhesion alongside inhibiting neutrophil polarisation and migration thus retaining the neutrophil in situ.[204] The pleiotropic affect of TNF-α diverge at the level of its two receptors Tumour necrosis factor receptor (TNFR) 1 and 2. An inhibitor of TNFR1 was shown to reduce pro-inflammatory effects of TNF-α favouring the protective effect of TNFR2 signaling. This gives rise to the inhibition of neutrophil adhesion molecule expression and a reduction in lung inflammation and neutrophilia in non-human primates and healthy volunteers following an endotoxin lung challenge.[205]

IL-1β has also been shown to recruit neutrophils and has a role in ALI.[206] More generally IL-1β is involved in auto-immunity and is a target for emerging therapies in rheumatoid arthritis.[207] IL-1β deficient mice are hypersusceptible to group B streptococcal infection due to a reduction in neutrophil but not macrophage influx to the infective site. This occurs through a reduction in the neutrophil production of CXCL 1 & 2, which promotes neutrophil release from the bone marrow and is reflected in the neutropenia (defined as a neutrophil count of less than 0.5×10^9/l) found at baseline in these animals.[208]

3.1.4 Clearance of neutrophils in the resolution of inflammation

Following recruitment to the injured lungs neutrophils are either disposed of through apoptosis and subsequent phagocytosis by macrophages or a significant number of neutrophils and macrophages will be cleared through the mucociliary escalator after which they are either swallowed or expectorated.[25,114] These routes of clearance may not be mutually exclusive. It is highly improbable that neutrophils undergo reverse migration from the lung alveolus due to the complexity of the barriers to reverse transmigration. In effect this location represents loss to the external environment and therefore is final and to-date there is no evidence this can occur. However, there could be a degree of reverse migration from the pulmonary vasculature to the wider circulation.[75] For example the lung has been posited as a de-priming station for neutrophils and a repository of neutrophils ready for rapid response. Also, as a mid-way station for neutrophils as they relocate back to the bone marrow following up-regulation of C-X-C chemokine receptor type 4 (CXCR4). [20,21,23]

There is an interplay between signals which control neutrophil survival during resolution. The majority of inflammatory stimuli present during the inflammatory response potentiate neutrophil survival. [8] [7,209-211] For example, hypoxia, which is inextricability linked to the inflammatory niche, has been shown to promote neutrophil survival through neutrophil hypoxia-inducible factor (HIF)-1α.[8] Thus a reduction in inflammatory signals may herald resolution and neutrophil death. As described, some inflammatory stimuli have opposing effects on neutrophil apoptosis which is timing-dependent[203] Apoptosis is regulated through a complex network of signals which include anti-apoptotic protein myeloid cell leukemia 1 (Mcl-1), Bcl-2 family member Bax (bcl-2-like protein 4), and the caspase family of proteases.[212-214] Once apoptosis is engaged neutrophil functions are reduced but cell integrity is maintained and phagocytosis by macrophages clears the dying cells preventing their harmful contents being inappropriately released.[114] Not only is

the amount of neutrophil apoptosis important but the rate of apoptosis over time will in part determine resolution.[115]

More recently resolvins and protectins have been identified which further control the inflammatory response. These terminating signals are pre-emptive and begin prior to resolution.[215] Influx and efflux of neutrophils to the injury site, in addition to apoptosis, will facilitate the inflammatory response. Other molecules that control neutrophil recruitment such as LTB4, may modulate neutrophil swarming behaviours at the injury site itself.[36] Within this cacophony of signals there could be cues that instruct neutrophils to remain, and through antagonising opposing stimuli, maintain a helpful balance of neutrophil recruitment and loss working alongside established mechanisms of neutrophil clearance.

I propose that Sema3F is a neutrophil autocrine retention signal that controls neutrophil transit to the lung and can differently regulate the inflammatory response with wider implications for host defense response and tissue damage.

3.2 Sema3F expression

3.2.1 Human neutrophil expression of Sema3F is regulated by inflammatory mediators

To investigate the regulation of Sema3F expression in human neutrophils, western blot analysis of neutrophil lysates was performed following culture with pro-inflammatory cytokines. The Sema3F detected in human neutrophil lysates was seen at 60 kDa and not the predicted 120 kDa. Sema3F possesses an RXRR furin recognition site in its C-terminus and can be proteolytically processed. [216] To prove that the 60 kDa represented a cleaved portion of the Sema3F protein, a blocking peptide to the Sema3F antibody (LS-C135015-50 antibody) was used. When the blocking peptide was incubated (in excess) with the antibody only 120 kDa band was seen in the murine brain sample (figure 3.2.1-1 A & B). This shows that the antibody is specific for the Sema3F and detects the protein (or a portion of it) at 60 kDa in human neutrophil lysates. The signal seen in the murine brain sample may result from non-specific binding of the antibody. This antibody was then used to investigate Sema3F protein expression in human neutrophils. An example western blot is shown in figure 3.2.1-1 C and P^{38} was used as a loading control. Subsequently densitometry was performed, and protein expression is shown in (D), sample expression was adjusted according to the corresponding loading control. P38 MAPK (mitogen-activated protein kinases) was used in these experiments as it is detected at an ideal kDa for comparison with the protein of interest – Sema3F (60 kDa). P38 MAPK is both abundant and there is little variation in neutrophil expression overtime or with stimuli [190]. Tubulin and actin are unsuitable alternatives being detectable at 55 kDa. Neutrophil GAPDH is altered by hypoxia and therefore inflammation. [8] This demonstrates human neutrophils express the protein Sema3F at baseline (cultured for 4 hours without treatment). There is a significant increase in Sema3F protein expression following treatment (one-way ANVOA, **P=0.0019). When comparing individual treatments, stimulation with LPS results in a significant up-regulation of Sema3F protein expression after 4 hours (4 hours culture vs

LPS *P=0.0058, n=3). There is an increased trend in the level of Sema3F expression seen following TNF-α. Following IL-1β stimulation there is no difference in Sema3F expression compared to the control group.

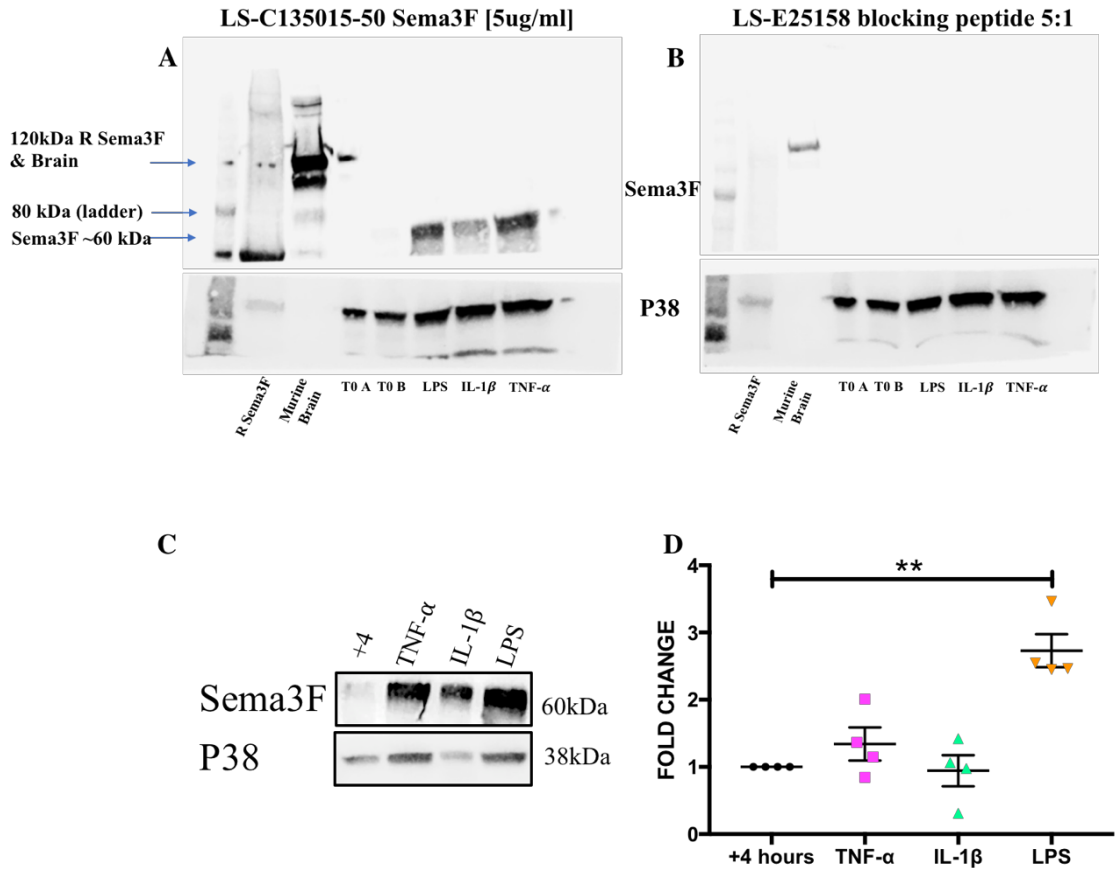

Figure 3.2.1-1 Sema3F differentially expressed in human neutrophils in response to inflammatory stimuli

The Western blots shown in A represent neutrophil lysate samples and the controls recombinant Sema3F (R Sema3F) and murine brain tissue. Sema3F expression was detected using the polyclonal rabbit antibody LS-C135015-50, an anti-P38 antibody was used to provide a loading control. The membrane was cut below 50 kDa prior to incubation with the primary antibodies. The bands shown in the right blot (image A) are specific to this antibody, whereby following the addition of a paired blocking peptide (image B) there is a loss of bands at approximately 60 kDa in both the neutrophil lysates and controls. Using this antibody, the amount of neutrophil expression of Sema3F following culture with TNF-α, IL-1β and LPS [all at 100nM] is shown in the representative blot (C). The densitometry is represented in graph D, this is shown as a fold change of the time-matched control. There is a significant treatment effect and increase following LPS stimulation in Sema3F protein expression. Data shown are mean ± SEM, n = 3 performed as 3 independent experiments. Analysed using a one-way ANOVA (**P<0.01) with post test analysis using Fisher's test to compare individual treatment groups (**P=0.0058).

3.2.2 Neutrophil Sema3F expression is seen in the inflamed airways of patients with COPD

To test the relevance of Sema3F expression in the context of human respiratory disease, patient samples were obtained from the NHS Research Scotland (NRS) biorepositories and Sema3F expression identified using immunohistochemistry. To test whether that Sema3F expression is seen in transmigrated human neutrophils, lung sections were taken from patients at the time of lung resection with concomitant COPD; tissue samples were used from non-tumour areas. The sections were stained for Sema3F (dark brown staining) which is present in the myeloid population found in the airspaces of the lung, as indicated by the black arrows seen in image B, figure 3.2.2-1.

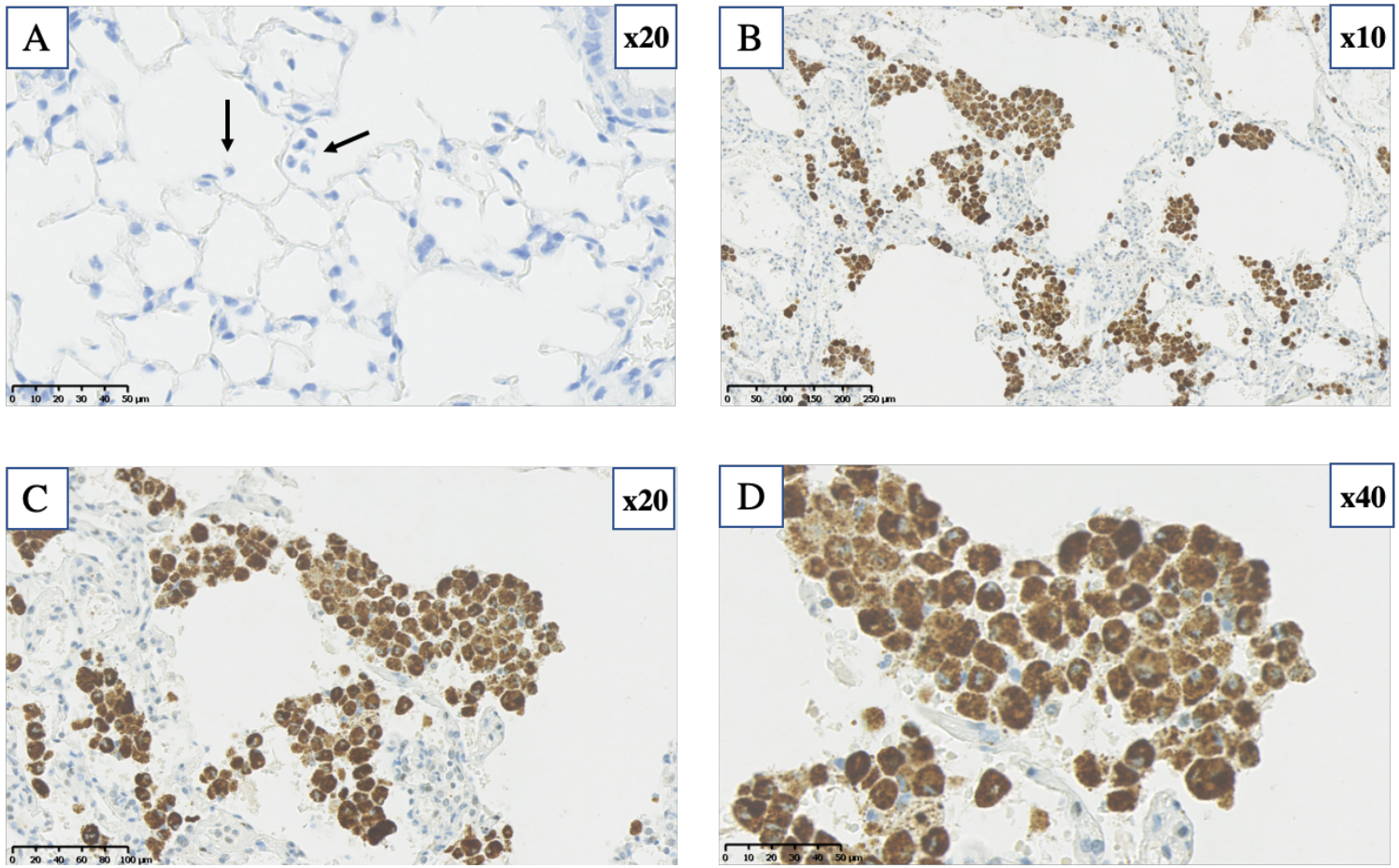

Figure 3.2.2-1 Sema3F expression is seen in the myeloid population in the alveoli of patients with COPD.
Lung sections taken at time of tumour resection from non-tumour regions of patients with moderate severity COPD were stained for Sema3F (B-D). An isotype matched control is shown in (A). Positively stained cells are indicated by the black arrows. These images were obtained using a x40 optical lens.

3.2.3 Murine neutrophil Sema3F mRNA levels rise acutely following lung injury

To further explore the expression profile of neutrophil Sema3F, qPCR was performed for Sema3F transcript in murine neutrophils recruited to the lung following LPS induced lung injury. Following nebulized LPS, mice were culled at 6, 24 and 48 hours and bronchioalveolar lavage (BAL) performed; neutrophils were isolated from the cellular infiltrate found in the BAL. Neutrophils were further purified using negative selection. From the cell pellets mRNA was extracted and cDNA made, using a Taqman assay quantification of the mRNA was detected. Beta-actin was selected as the endogenous control as it is highly expressed in neutrophils and is not influenced by inflammation. [8,217] To assess transcript expression 2^{Δ}dCT was determined for the experimental conditions relative to unstimulated wild-type bone marrow derived neutrophils. The fold change of Sema3F mRNA compared to peripheral blood neutrophils (time 0) was calculated and is shown in figure 3.2.3-1. The amount of Sema3F mRNA rises acutely at 6 hours (mean 0.31±0.007 n=4, ***P<0.001) following recruitment of the inflammatory neutrophil to the injured airway and is sustained at 24 & 48 hours at slightly lower levels (24 hours:0.31± 0.007 n=6 & 48 hours: mean 0.28± 0.007 n=4, ***P<0.001).

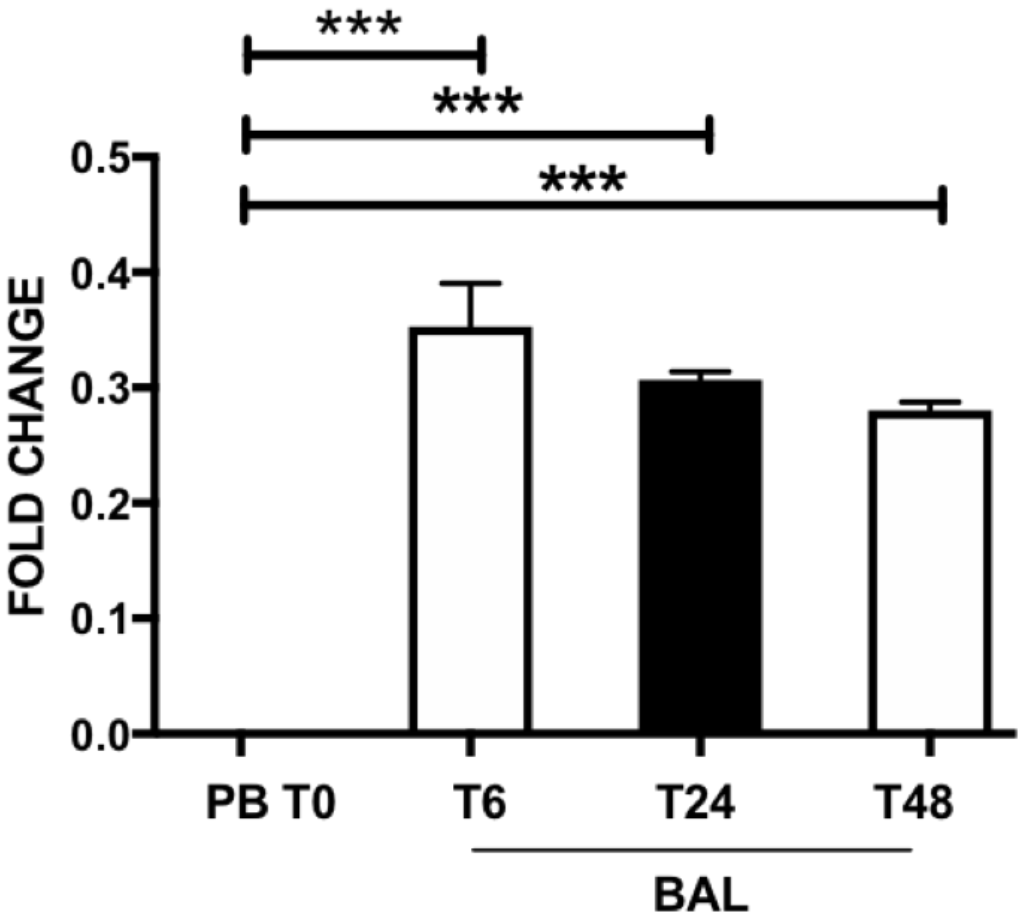

Figure 3.2.3-1 Murine Sema3F mRNA levels rise acutely following LPS induced lung injury

Fold change in Sema3F mRNA expression following acute lung injury with LPS. Mice were sacrificed at 6, 24 and 48 hrs post installation, bronchoalveolar lavage performed (BAL) neutrophils collected, and cDNA extracted. TaqMan analysis of cDNA was performed with data normalized to beta-actin (ACTB) expression and 2^{Δ}dCt calculated (control: wild-type unstimulated bone marrow derived neutrophils). Data show mean± SEM of fold change compared to peripheral blood neutrophils (PB T0), n=4-6 analysed by one-way ANOVA, ***P<0.001.

3.2.4 Murine neutrophils express Sema3F

Wild type mice were nebulised with 1mg/ml of LPS and sacrificed at 24 hours. Serial sections stained for a Sema3F isotype control, Ly6G (neutrophils) and Sema3F respectively are shown in figure 3.2.4-1 in images A, B & C; image D is of murine brain tissue used as a positive tissue control. For details of the primary antibodies used for immunohistochemistry see appendix VI. In image A there is an infiltration of neutrophils to the injured lung at 24 hours post LPS induced lung injury. At this time >90% of the infiltrating population would be neutrophils.[218] In image A no non-specific staining was seen in the isotype control supporting the specificity of the staining seen in images B, C and D in the figure. The murine brain tissue in D has positive staining located most likely on purkinje cells and on a subset of cells in the Inner Granular Layer as expected for Sema3F and provides a positive tissue control.[219] In image A, there is only nuclear staining, this highlights the unique morphology of the neutrophil multi-lobar nucleus and draws a sharp contrast to the surrounding cells, clearly identifying the neutrophils (identified by the black arrow) shown in the representative paired image to the right of A. Ly6G (Lymphocyte antigen 6 complex locus G6D) is a 21-25kD glycosylphosphatidylinositol (GPI)-linked differentiation antigen that is expressed by myeloid-derived cells in a tightly developmentally-regulated manner. Monocytes express Ly6G transiently during maturation within the bone marrow. In terms of recruited myeloid cells Ly6G is exclusively expressed by neutrophils.[220,221] In figure 3.2.4-1 image B there is an abundance of neutrophils in the injured lung, these cells are positive for Ly6G staining confirming they are neutrophils shown in the representative image to the right of C. In the sequential serial slice C the neutrophils positive for Ly6G are also positive for Sema3F.

The progression of Sema3F protein production during acute lung injury in the lung tissue is shown in figure 3.2.4-2. Sema3F expression is seen at 6 hours following LPS induced lung injury in wild-type mouse lung tissue image A. The black arrows indicate epithelial cells (*E) and neutrophils (*N) that are

positively stained for Sema3F at 6 hours post injury. At 24 hours post injury Sema3F is also seen in the macrophages (*M). Later at 48 hours, the level of Sema3F staining is subjectively reduced when compared to both 6 and 24 hours and there is no staining seen in the epithelial cells (image C).

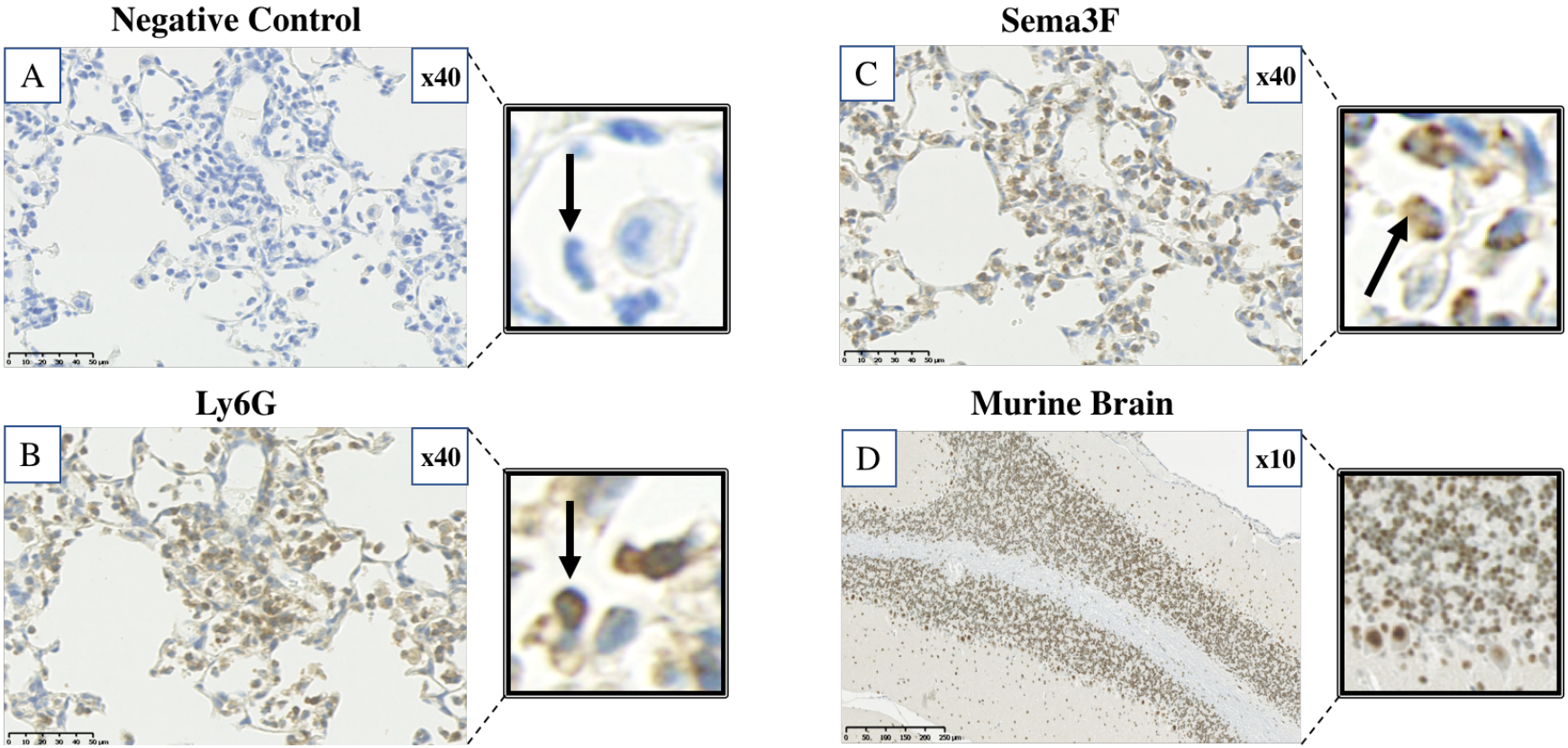

Figure 3.2.4-1 Following LPS induced lung injury recruited murine neutrophils express Sema3F
An acute lung injury was induced by LPS nebulisation, mice were sacrificed at 24 hours and serial lung sections stained for expression of the neutrophil marker Ly6G (B) and Sema3F (C). The negative isotype control is shown (A) and positive tissue control, murine brain tissue (D). To the right of each lung section image (A, B & C) there is an example of a neutrophil from the parent image. For image D a blown-up image highlights the positive staining in both purkinje cells and a subset of cells in the Inner Granular Layer. Example neutrophils and blown-up tissue areas were achieved using digital magnification with black arrows indicating an individual neutrophil. Original magnification x40.

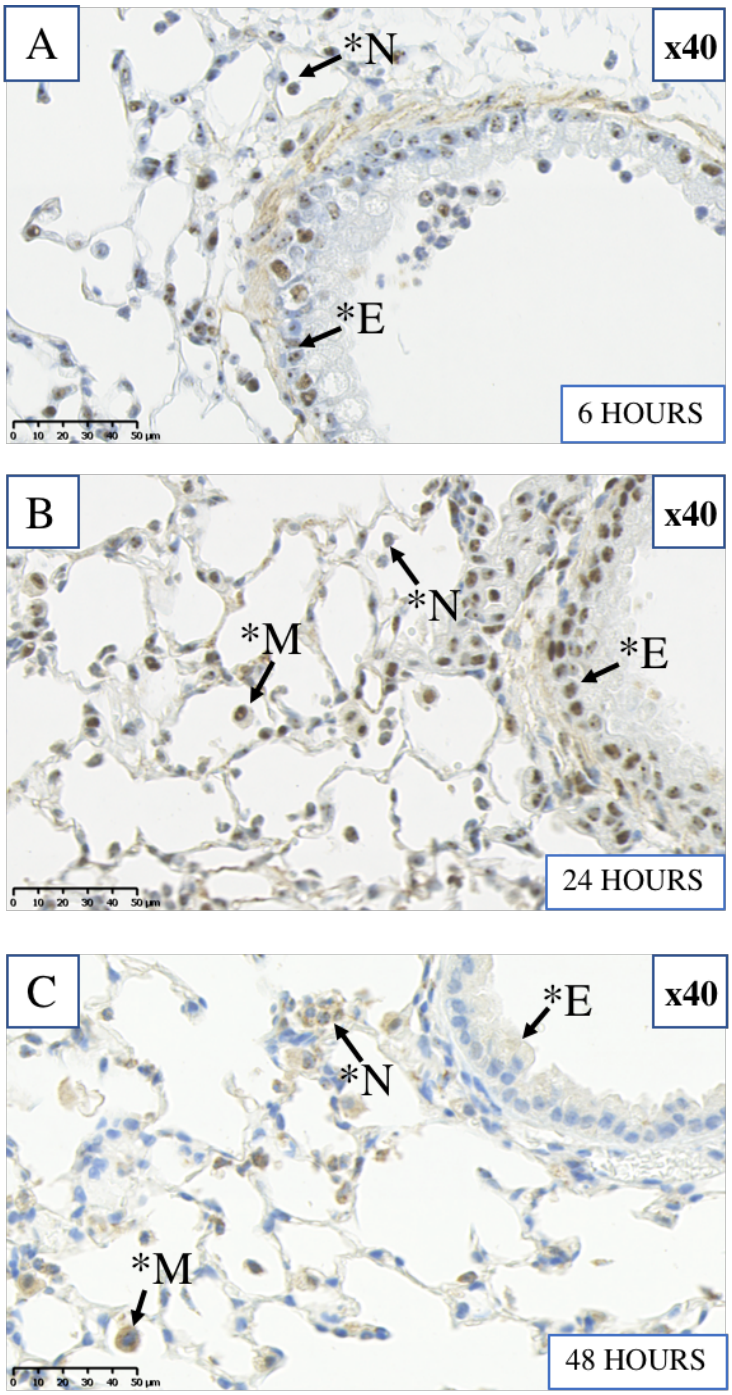

Figure 3.2.4-2 Following lung injury Sema3F protein expression is seen acutely in both the myeloid cell population and the epithelial layer
Images shown are of stained lung sections from wild type mice following acute lung injury. At 6 hours (A) there is evidence of Sema3F within both the recruited neutrophils (black arrow *N) and the airway epithelial cells (black arrow *E). At 24 hours staining is also seen in the macrophage population (black arrow *M). At 48 hours there is no Sema3F staining found within the epithelial cell layer (black arrow *E), however there are some macrophages (black arrow *M) and neutrophils (black arrow *N) that show positive staining. Original magnification is x40.

3.3 Co-receptor NRP2 expression

3.3.1 NRP2 is expressed by recruited lung neutrophils in COPD

To ascertain whether it is possible for neutrophil Sema3F autocrine signaling to occur in *vivo* and ensure that this is relevant to human lung disease, patient samples were obtained from the NHS Research Scotland (NRS) biorepositories and NRP2 expression identified using immunohistochemistry. Neuropilin NRP2 expression is seen in transmigrated human neutrophils. Non-tumour containing lung sections were taken from patients at the time of lung resection with concomitant COPD. The sections were stained for NRP2 (dark brown staining) and similar to Sema3F staining this is associated with the myeloid population found in the airspaces of the lung (figure 3.3.1-1, Images B and C). For details of the primary antibodies used in immunohistochemistry see appendix VI.

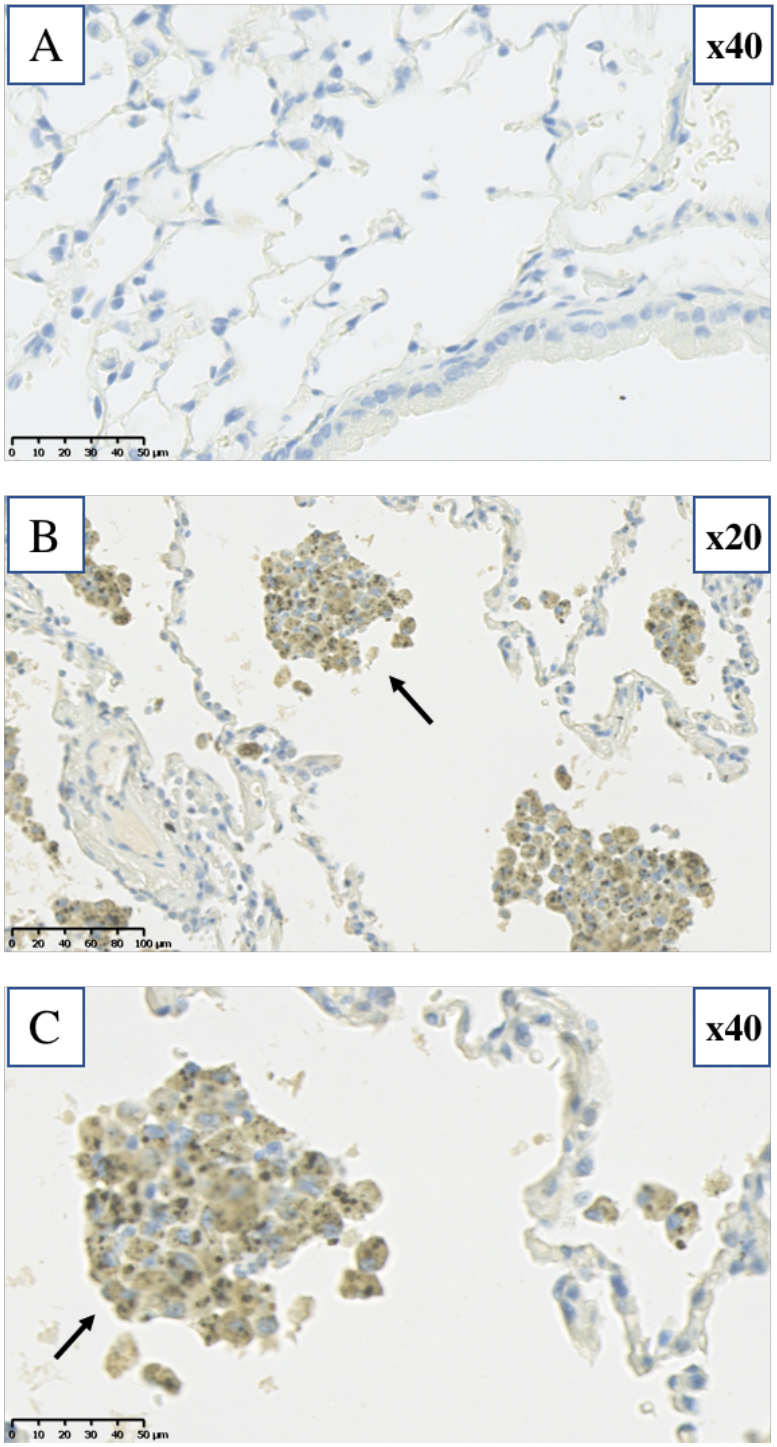

Figure 3.3.1-1 COPD lung neutrophils express NRP2
Lung sections taken at time of tumour resection from non-tumour regions of patients with COPD were stained for NRP2 (B&C). An isotype matched control is shown in (A). Positively stained cells are indicated by the black arrows. These images were obtained using a x40 optical lens.

3.3.2 Human neutrophil NRP1 and NRP2 co-receptor expression can be detected by flow cytometry

To explore the surface expression of NRP1 and 2 in human neutrophils I optimised a flow cytometry panel of antibodies. Whole blood was taken from healthy volunteers and was subjected to a red cell lysis optimised for the preservation of the neutrophil and monocytes populations. Then, using a previously validated panel to identify neutrophils from whole blood, the neutrophil expression profile of NRP2 and NRP1 was evaluated.[222,223] Figure 3.3.2-1 demonstrates the gating strategy for the neutrophil populations (Panel A) and subsequently the NRP2 (B & C) and NRP1 (D & E) positive neutrophils. Monocytes provided a biological positive for NRP1 staining which is shown in a later figure 3.3.4-1.[224]

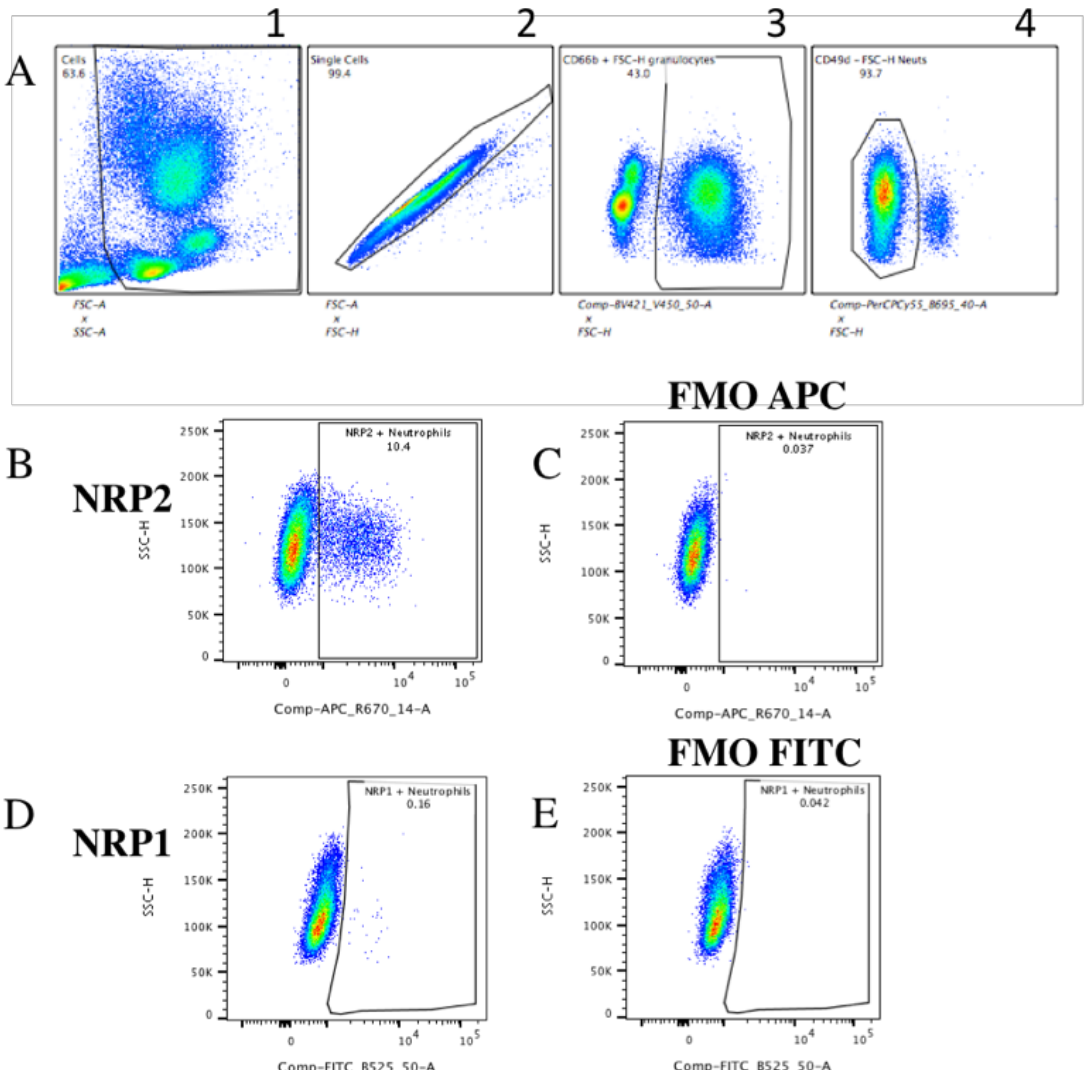

Figure 3.3.2-1 Surface expression of NRP1 and NRP2 co-receptors on human neutrophils analysed by flow cytometry

Following red cell lysis human whole blood was analysed using flow cytometry to determine NRP1 and NRP2 surface expression. In panel A, plot 1 shows identification of cells over debris using FSC-A/SSC-A, single cells are selected rejecting doublets (A plot 2), plot 3 shows gating for CD66b positive granulocytes (43% of single cells) and plot 4 shows CD49d negative granulocytes which are the neutrophil population (93.7% of granulocytes). Plot B shows the gate for the NRP2 positive neutrophil population (10.4% of neutrophils) which is based on the C, the corresponding fluorochrome minus-one (FMO) for the APC conjugated NRP2 receptor antibody signal. D & E show similar for the NRP1 receptor antibody which was conjugated to FITC (0.16% NRP1 positive neutrophils).

3.3.3 Cell viability and fluorescence-activated cell sorting (FACS) of human neutrophils expressing NRP2

In addition to the previously described panel to identify human neutrophils from lysed whole blood as shown in the figure 3.3.3-1 (panel A), a fixable live/dead stain was added. Using this it was evident that < 5% of identified neutrophils were dead at the time of fixation (plot, B). The panel was designed for FACS of NRP2 positive human neutrophils (with thanks to QRMI flow cytometry Unit and Dr Shonna Johnston). Cytospins were made of the resulting cell pellet, the neutrophils were identified by morphology. They were exclusively neutrophils and there was < 1% apoptosis seen; a representative image is shown in figure 3.3.3-1, image C. Of the cells that appeared dead, using the viability dye in the flow cytometry panel, very few were identified as NRP2 positive neutrophils shown in plot D.

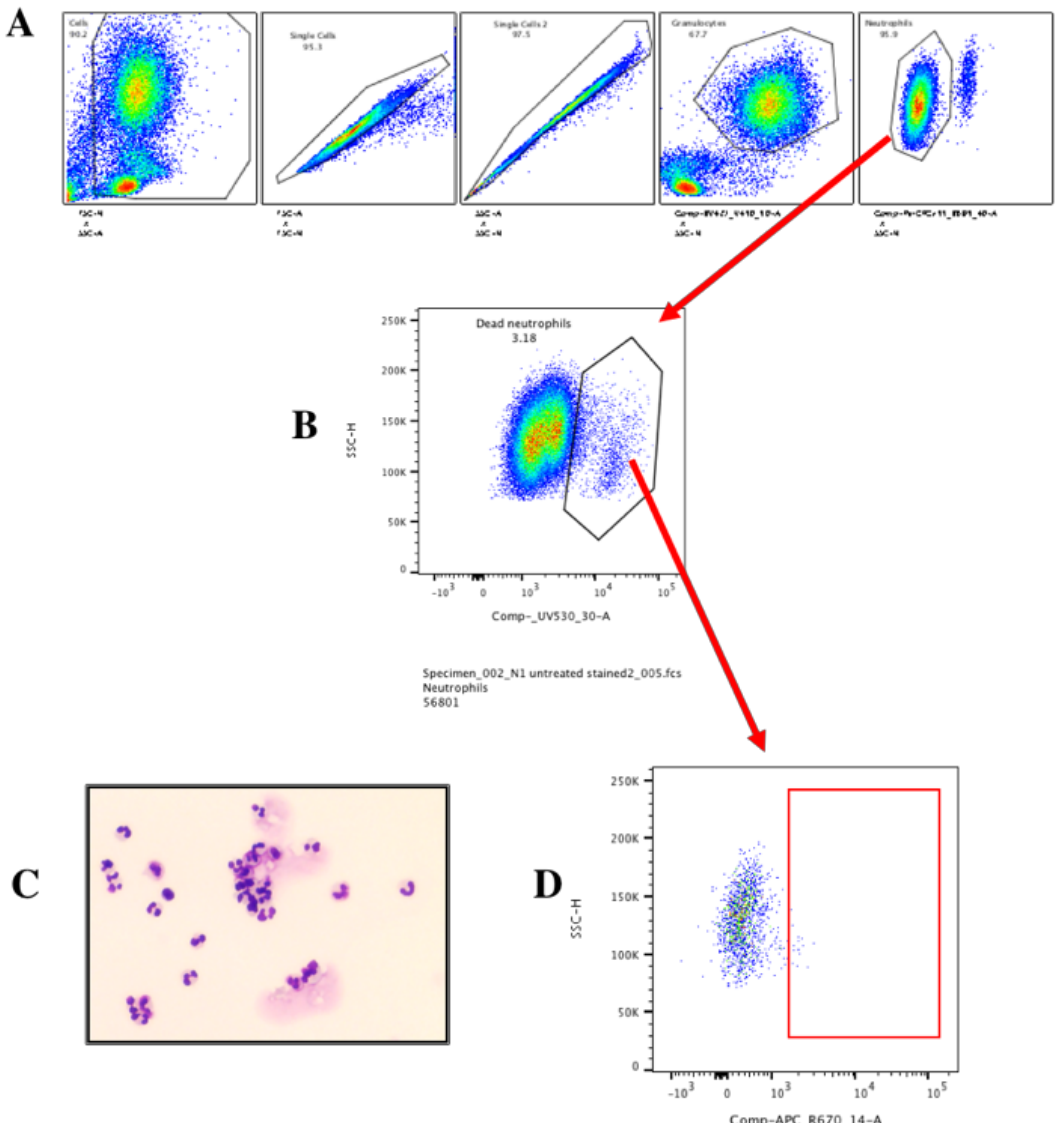

Figure 3.3.3-1 NRP2 positive neutrophils are viable and FACS sorted NRP2 positive neutrophils morphologically confirm an accurate identification of a neutrophil subpopulation

Following red lysis and fixation a fixable live/dead stain was used to identify dead cells. Neutrophils were identified as shown in panel A. The amount of neutrophil death using this protocol was consistently < 5% as shown in the representative plot in B (dead neutrophils 3.18% of the neutrophil population). Using this panel cells underwent flow assisted cell sorting (FACS) and a representative cytospin of the resulting cell population is shown in C, by morphology this is a pure neutrophil sub-population. NRP2 positive neutrophils are not identified as dying or dead and are viable, shown in plot D.

3.3.4 NRP2 and not NRP1 is predominately expressed in human neutrophils

In order to confirm that NRP1 staining was accurate other cell types were identified in the flowcytometry panel to use as biological controls. This included monocytes as show in figure 3.3.4-1, panel A and eosinophils in panel B. Following the gating shown in plots 1 and 2 of both panel A & B, monocytes were identified as being CD66b negative, then CD49d and CD14 double positive (14.8% of CD66b negative single cells). Eosinophils in contrast were CD66b positive, CD49d positive (6.14% of CD66b granulocytes). In the literature it has been previously shown that monocytes are NRP1 positive cells and have lower NRP2 expression.[146] This was replicated using my flow cytometry panel as shown in graph C, where the relative percentage of NRP1 and NRP2 positive monocytes and neutrophils are shown. In contrast neutrophils appear to be the reverse of this, having significantly more NRP2 receptor expression than NRP1, (NRP2 expression, mean 9.61% vs NRP1 expression, mean 2.93%). Monocytes in keeping with the literature have lower levels of Neuropilin expression, with more NRP1 (mean 3.85%) than NRP2 (mean 1.73%). There are significantly more NRP2 positive neutrophils, than NRP1 positive neutrophils (***P=0.0009, n=3).

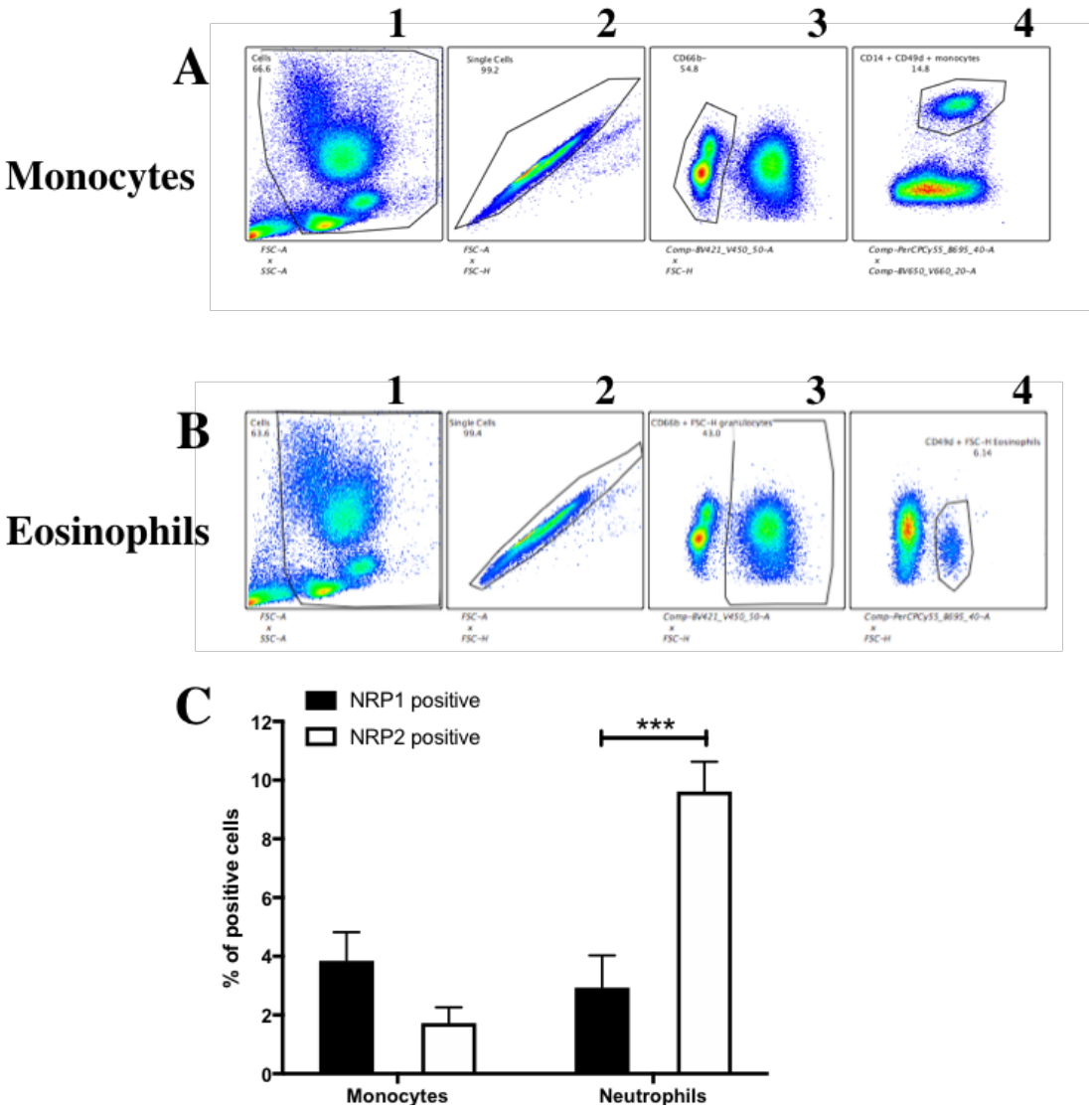

Figure 3.3.4-1 Human Neutrophils predominately express NRP2 and monocytes NRP1

Whole blood from healthy volunteers was subjected to red cell lysis and stained for flow cytometry analysis. In panel A and B, flow plots 1 and 2 show identification of single cells. In A panel B, flow plot 3 the CD66b population is shown, of the CD66b negative sub-population the monocytes are defined as the CD14 and CD49d positive cells, 14.8% of the parent population. From the CD66b positive sub-population, eosinophils are identified as CD49d+ positive cells. (6.14% of the parent population). Graph C shows the relative expression of NRP1 and NRP2 on neutrophils and monocytes at baseline. There are significantly higher NRP2 positive neutrophils than NRP1 positive neutrophils. NRP2 is expressed at a low level on monocytes. Data shown are mean ± SEM, n= 3 performed as 3 independent experiments. P values were calculated using two-way ANOVA and Sidak multiple comparison test performed, ***P<0.001.

3.3.5 Neutrophil NRP2 expression increases in response to inflammatory stimuli

Whether neutrophil NRP2 receptor expression is altered by the inflammatory environment remained a key question. To address this, I assessed the surface expression of NRP1 and NRP2 co-receptors on isolated human neutrophils following culture with inflammatory stimuli. Despite using a discontinuous Percoll gradient to purify the cells for culture, I applied an identical flow cytometry panel as used in the human whole blood experiments, in part, to ensure purity and also to allow comparison between this experiment and previous. Graph A in figure 3.3.5-1 shows NRP1 and NRP2 expression following 4 hours of culture. As seen in figure 3.3.4-1 neutrophils express significantly more NRP2 receptor than NRP1 following stimulation by the inflammatory mediators LPS, TNF-α and IL-1β for 4 hours. IL-1β treatment more than doubles the percentage of neutrophils expressing NRP2 from 8.18% to 18.47%, with a mean difference of -12.85% (Graph B). In contrast neutrophil expression of NRP1 remains unchanged regardless of the culture condition (graph C).

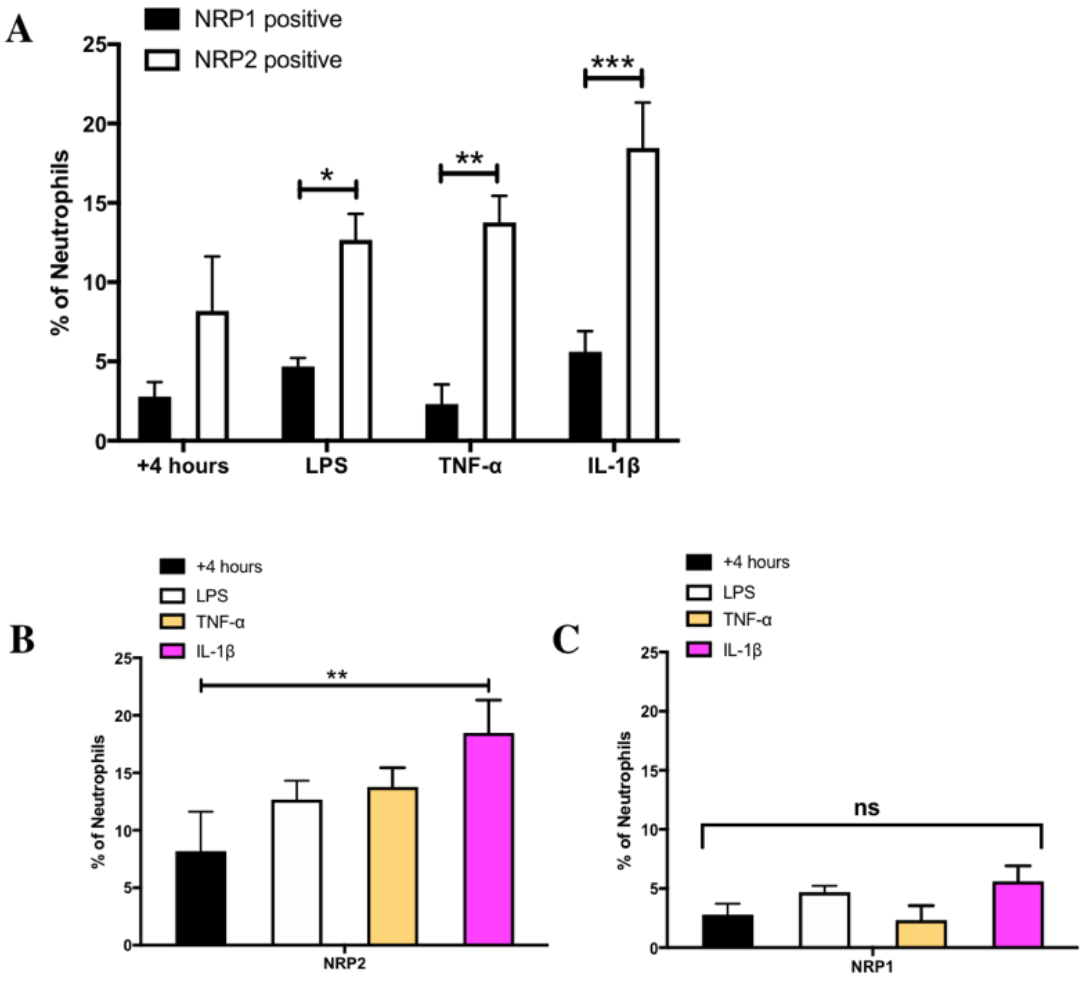

Figure 3.3.5-1 Neutrophil NRP2 surface express is enhanced by the addition of inflammatory stimuli

Isolated human neutrophils were cultured with LPS [10ng/ml], TNF-α and IL-1β [both 100nM] for four hours, then fixed and stained using the previously optimised Neuropilin flow cytometry panel. There was significantly more surface NRP2 than NRP1 expression seen following the addition of inflammatory stimuli; the highest significance is seen following IL-1β with a mean of 18.47% expression, Graph A. Data shown are mean ± SEM, n= 3 performed as 3 independent experiments, P values were calculated using two-way ANOVA and a Sidak multiple comparison post-test, *P<0.05, **P<0.01 & ***P<0.001. Graph B shows the data for NRP2 receptor expression only, there was a significant increase in NRP2 receptor surface expression following stimulation with IL-1β. Graph C shows there was no significant difference in neutrophil expression of NRP1 following treatment with the same inflammatory mediators. Data shown are mean ± SEM, n= 3 performed as 3 independent experiments, P values were calculated using unpaired *t*-tests, **P=0.0034.

3.3.6 NRP2 is detected in murine neutrophils the injured lung

Next, I evaluated the expression of NRP1 and NRP2 in murine neutrophils. NRP2 is an obligatory co-receptor for Sema3F and forms the receptor complex with a plexin (A1-A4), through which class 3 Semaphorins signal. Sema3F has higher affinity for NRP2 over NRP1. To evaluate the expression of NRP2, sections from murine lung taken at 6 hours following LPS induced lung injury were stained for NRP2 and NRP1. In figure 3.3.6-1 image A shows the isotype control which demonstrates no positive non-specific staining and in (B) positive staining for NRP2 is seen. Box C shows a blown-up area of positive staining from image B to highlight the positive staining for NRP2 of the neutrophil. There appears to be no staining for NRP1 in the murine lung section; the NRP1 stained image E is similar to the negative isotype control in image D.

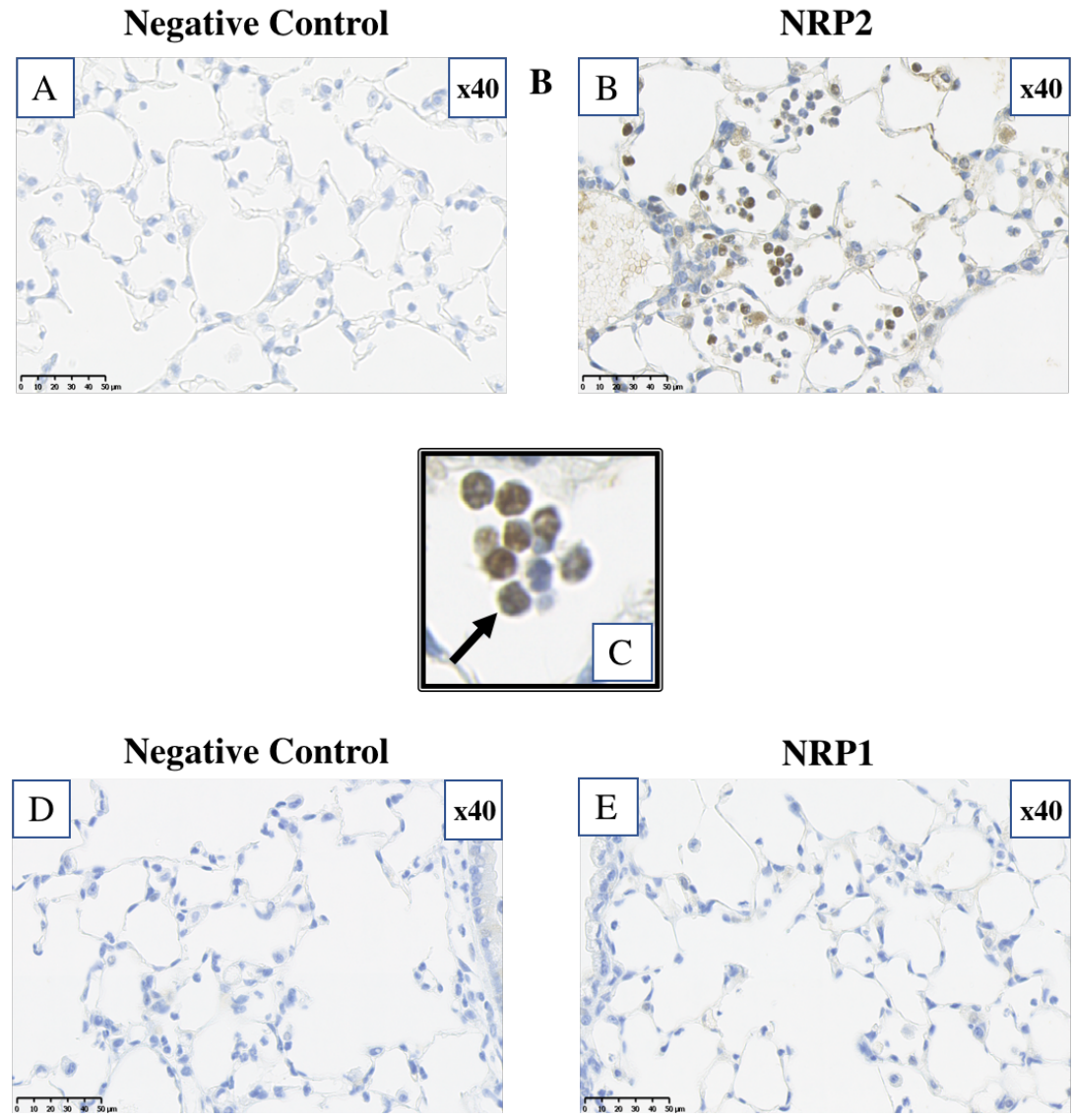

Figure 3.3.6-1 NRP2 is preferentially expressed over NRP1 in recruited neutrophils following acute lung injury in mice
Images A to E show murine lung sections from mice culled 6 hours following LPS induced lung injury and stained for NRP2 and NRP1 respectively, where A is the isotype control for B, and D represents the isotype control for E. Image C is an exploded area using digital magnification to demonstrate positively stained neutrophils. Original magnification x40.

3.3.7 Neutrophil NRP2 mRNA increases following acute lung injury in mice

To gain insight into the expression profile of NRP2 I looked for the neutrophil NRP2 mRNA transcript at 6, 24 and 48 hours following LPS induced lung injury, using cDNA collected as described in section 3.2.3. Here, beta-actin was again selected as the endogenous control, 2^{Δ}dCT was calculated relative to unstimulated wild-type bone marrow neutrophils. The graph in figure 3.3.7-1 shows the 2^{Δ}dCT values and not a fold change of peripheral blood as, unlike Sema3F mRNA expression there is NRP2 mRNA expression seen at time 0. There is a significant increase in NRP2 mRNA acutely following lung injury at 6 hours (*P<0.05) and a non-significant increase at 24 and 48 following the LPS insult.

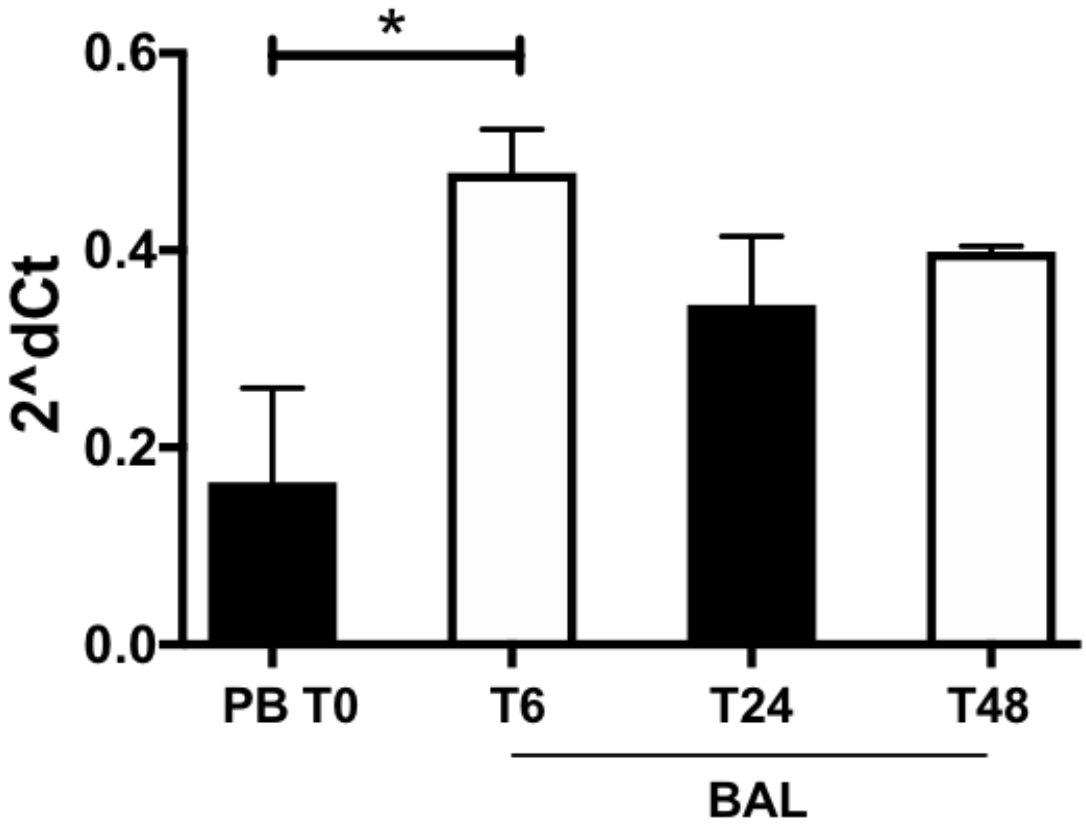

Figure 3.3.7-1 Murine neutrophil NRP2 mRNA levels increase acutely following lung injury

Mice were sacrificed at 6, 24 and 48 hrs post LPS installation, BAL neutrophils collected, and cDNA extracted. TaqMan analysis of cDNA was performed with data normalized to beta-actin (ACTB) expression. To calculate 2^{Δ}dCT unstimulated bone marrow derived neutrophils were used. Data shown are mean ± SEM of fold change compared to peripheral blood neutrophils (PB T0), n=4-6 analysed by two-way ANOVA, *P<0.05.

3.3.8 Following lung injury in mice NRP2 expression is initially seen in the recruited neutrophil and later in the lung epithelium

To ascertain whether surface expression of the NRP2 receptor correlated with mRNA levels immunohistochemistry was performed. LPS lung injury was induced in wild type mice. In images A, in figure 3.3.8-1 there is positive staining in the neutrophils, indicated by the black arrows (*N). At 24 and 48 hours post ALI, shown in images C and D the patchy NRP2 staining is found only in the epithelial layer. This indicates that inflammatory neutrophils acutely express the Sema3F co-receptor NRP2 following lung injury.

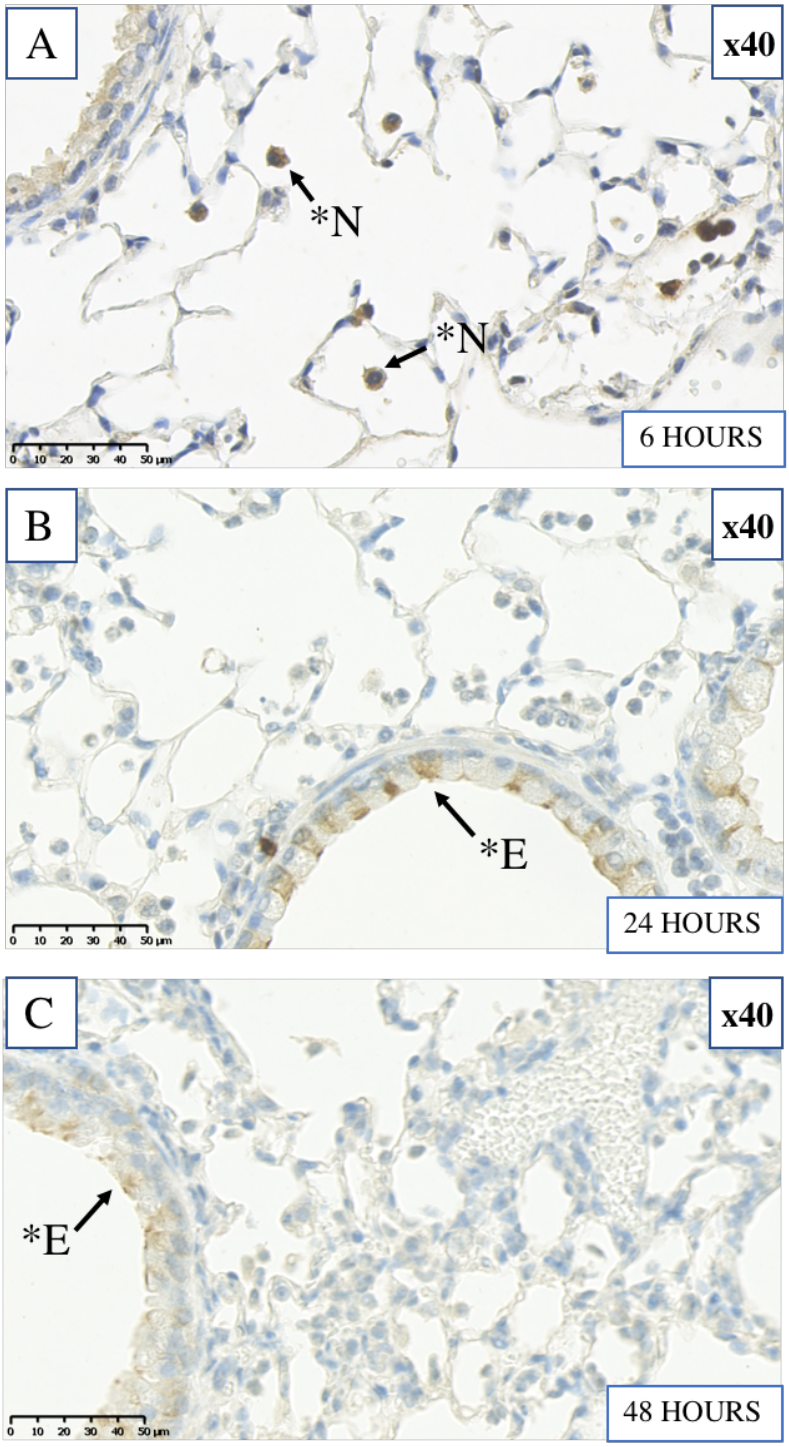

Figure 3.3.8-1 NRP2 expression within the murine lung tissue changes with time following LPS induced lung injury

Lung tissue was obtained following LPS induced lung injury from wild type mice. Mice were culled at times 6, 24 and 48 hours post LPS and lung tissue stained for NRP2. In images A neutrophils expressing NRP2 (black arrows *N). At the later time points patchy staining for NRP2 is seen only in the epithelium indicated by the black arrows *E. Original magnification was x40.

3.4 Exogenous Sema3F treatment in vivo increases neutrophil retention in a murine model of LPS induced acute lung injury

3.4.1 Intra-tracheal instillation (IT) of Sema3F at 24 hours increases retention of neutrophils in a mouse model of LPS induced lung injury

To investigate the effects of exogenous Sema3F on neutrophil function in *vivo* C57BL/6 mice were treated with nebulised LPS, then after 24 hours intratracheal instillation (IT) of 1 μM of recombinant Sema3F was compared to phosphate buffered saline (PBS). The use of a higher dose of recombinant Sema3F (1 μM) was to ensure the delivery of the protein to the alveoli, a large percentage of drug will be lost in the airways proximal to this. [225] A summary diagram of the experimental protocol is shown in figure 3.4.1-1. Graph A shows the total cell counts at 48 hours. There are more cells in the BAL in the Sema3F treated mice (mean value $4.33x10^6$ cells ± 0.45, n=8) compared to the PBS treated group (mean 2.94 $x10^6$ cells ± 0.34, n=8), this was found to be significant, *P=0.02. There is retention of neutrophils in the airway at 24 hours after IT Sema3F (mean 3.18 $x10^6$ neutrophils ± 0.26 n=8) compared to IT PBS (mean $2.32x10^6$ neutrophils ± 0.3, n=8) *p=<0.05. At the later time-point of 72 hours there was no difference seen in total or neutrophil counts between PBS control or Sema3F treatment. At both time points there was no difference observed in the neutrophil apoptosis counts performed by assessment of morphology.

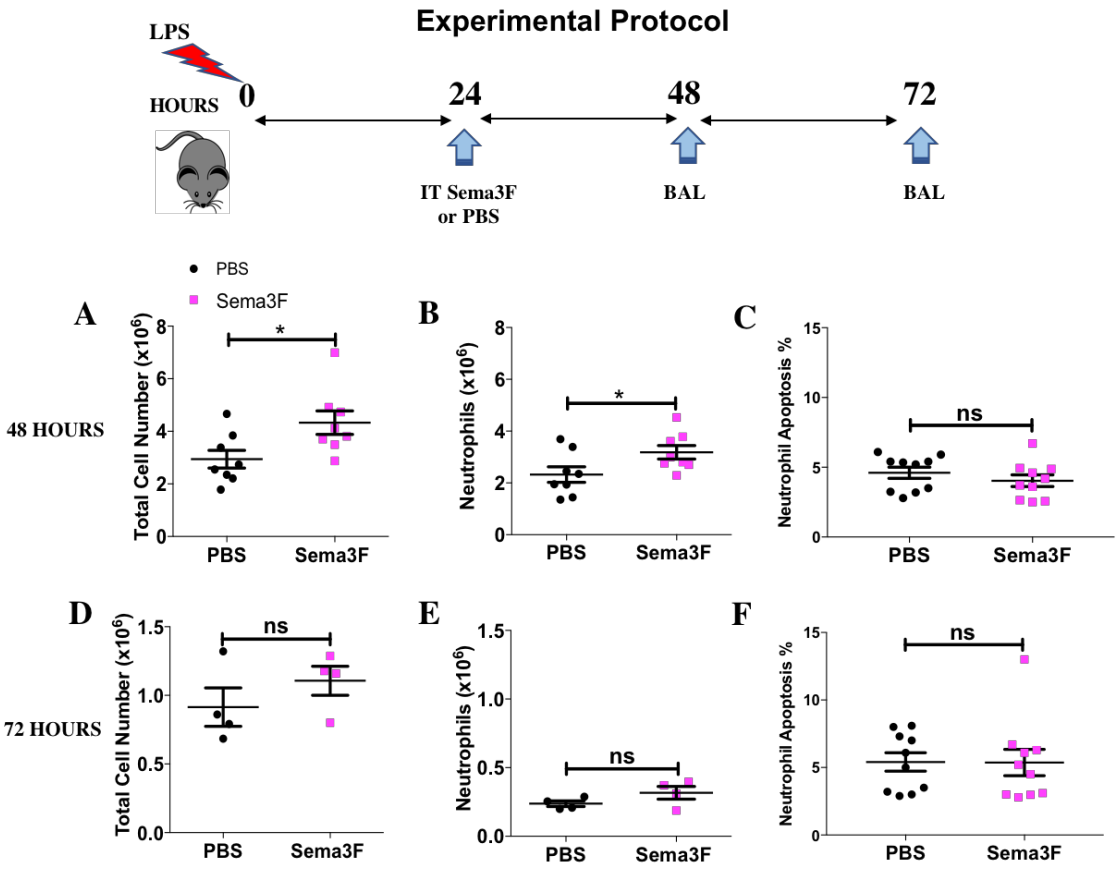

Figure 3.4.1-1 Intra-tracheal instillation of Sema3F in a murine model of acute lung injury retains recruited neutrophils at the injury site

Intra-tracheal recombinant Sema3F (1μM) was administered to C57BL/6 mice 24 hours post nebulised LPS challenge or phosphate buffered saline (PBS). Mice were then sacrificed after a further 48 hours and 72 hours and bronchoalveolar lavage performed; the protocol is shown in above the graphs. Some lungs were harvested without bronchoalveolar lavage and retained for lung slice imaging. Using the BAL obtained total, differential and apoptosis cell/neutrophil counts are shown for 48 hours in graphs A-C and 72 hours in D-E. Data shown are mean ± SEM n=4-8 analysed using an unpaired *t*-test, *P< 0.05.

3.4.2 Intra-tracheal instillation of Sema3F at 24 hours increases cellular infiltration seen in murine

H&E stained murine lung sections were obtained from mice that underwent the same experimental procedure detailed in the diagram in figure 3.4.1-1. In figure 3.4.2-1 images A and C are taken at x4 magnification. Further images at x20 magnification are of a representative area of A and C respectively. Following LPS then Sema3F or PBS treatment changes associated with lung injury including thrombi are seen in the post-capillary venules (images A & C, black arrows) alongside infiltration of neutrophils into the interstitial space and septal thickening (images B & D, black arrows). To provide further comment on these isolated samples the observed differences between PBS and Sema3F treated tissue were scored using the Matute-Bello lung injury scoring system. Image B (PBS treated lung) scored 7 compared to Sema3F treated lung which scored a 12 (where a higher score denotes more lung injury). [226] For scoring system see appendix XV.

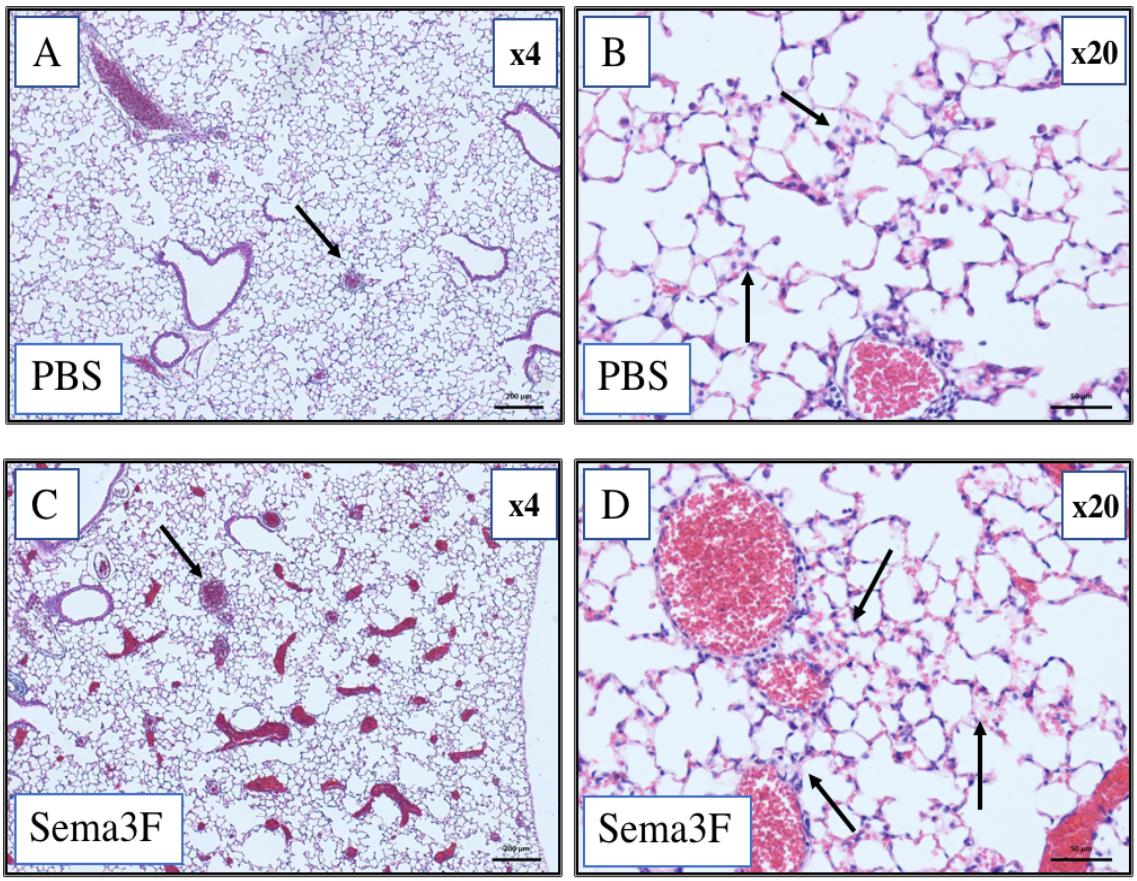

Figure 3.4.2-1 Intra-tracheal instillation of Sema3F at 24 hours increases post-capillary thrombi, neutrophil infiltration and alveolar-septal thickening seen in murine lung sections

Mice were sacrificed at 48 hours post LPS-induced lung injury after receiving intra-tracheal injection (IT) Sema3F 1 μM or PBS. Representative lung sections taken from the time of cull were fixed with 10% formalin at 20 cmH_2O, paraffin embedded and stained with H&E. Images A and B show sections at x4 and x20 magnification respectively from a mouse receiving IT PBS. Images C and D show sections at x4 and x20 magnification respectively from a mouse receiving IT Sema3F. Original magnification was x20. The black arrows in A and B show post-capillary venules with associated thrombi. The black arrows in B and D show areas of neutrophil infiltration and alveolar septal thickening.

3.5 Murine model of neutrophil specific knockdown of Semaphorin3F

3.5.1 Proof of knockdown at DNA, mRNA and protein levels

We wanted to explore how the loss of neutrophil Sema3F would alter neutrophil behaviour following LPS-induced lung injury in mice. Prior to using this murine model of neutrophil specific loss of Sema3F it was imperative to prove knockdown of the Sema3F gene, mRNA and protein in the neutrophils of this transgenic animal. The Sema3F^{floxflox}MRP8CRE$^{-/-}$ (WT) and Sema3F^{floxflox}MRP8CRE$^{-/+}$ (KO) were previously crossed with a reporter strain, where green fluorescent protein is only expressed in tissues with Cre activity (Materials and Methods 2.9.2 and Appendix VIII). Following LPS induced lung injury, at 24 hours mice were culled, BAL cells extracted and stained for flow cytometry analysis. Granulocytes were identified based on FSC-A/SSC-A position and CD45 positivity, from this population both neutrophils (Ly6G positive) and monocytes (Ly6G negative) populations determined. In the KO animal the neutrophils were GFP positive. Seen in figure 3.5.1-1 flow plot A, there is a lack of GFP signal in the WT neutrophils and, in contrast there is a right shift in Geomean fluorescence intensity seen the KO neutrophils (plot C). The monocyte population has minimal GFP signal (plots C & D). Graph E shows the percentage of neutrophils and monocytes that express the GFP protein determined from flow cytometry analysis. In the KO animal 95% of neutrophils ± 1.1 (n=4) express the GFP reporter protein, this is compared to 4.15% ± 0.830 of the WT neutrophils. The WT and KO monocytes express low levels of the reporter protein being 6.1% ± 0.8 and 3.18% ± 0.48 respectively. This demonstrates that there is Cre recombinase activity in the neutrophil population.

To further validate the model, I looked at the expression of Sema3F mRNA and protein levels. Using BAL cells obtained at 24 hours post LPS induced lung injury, I compared the Sema3F transcript level in WT and KO neutrophils. In order to do this, primers were generated to lie within the deleted region of the Sema3F gene found in my transgenic animal. Bone marrow derived

neutrophils were used as the control as they are known to express low levels of Sema3F.[227] In figure 3.5.1-2, the graph G shows a marked reduction in neutrophil Sema3F mRNA in the KO mouse compared with WT. Figure 3.5.1-3 shows images A-F representing stained lung slice obtained from mice following lung injury at 48 hours. A-C and D-F represent sequential serial sections. The first image is the negative control for each set of serial sections, next is stained for Ly6G (neutrophils) and the final image stained for Sema3F. It is evident that in the WT lung sections the cells that are positive for Ly6G are also positive for Sema3F. In comparison in the KO animal there is loss of positive staining for Sema3F in the neutrophils. This supports that the model has achieved successful knockdown of neutrophil Sema3F at the protein level.

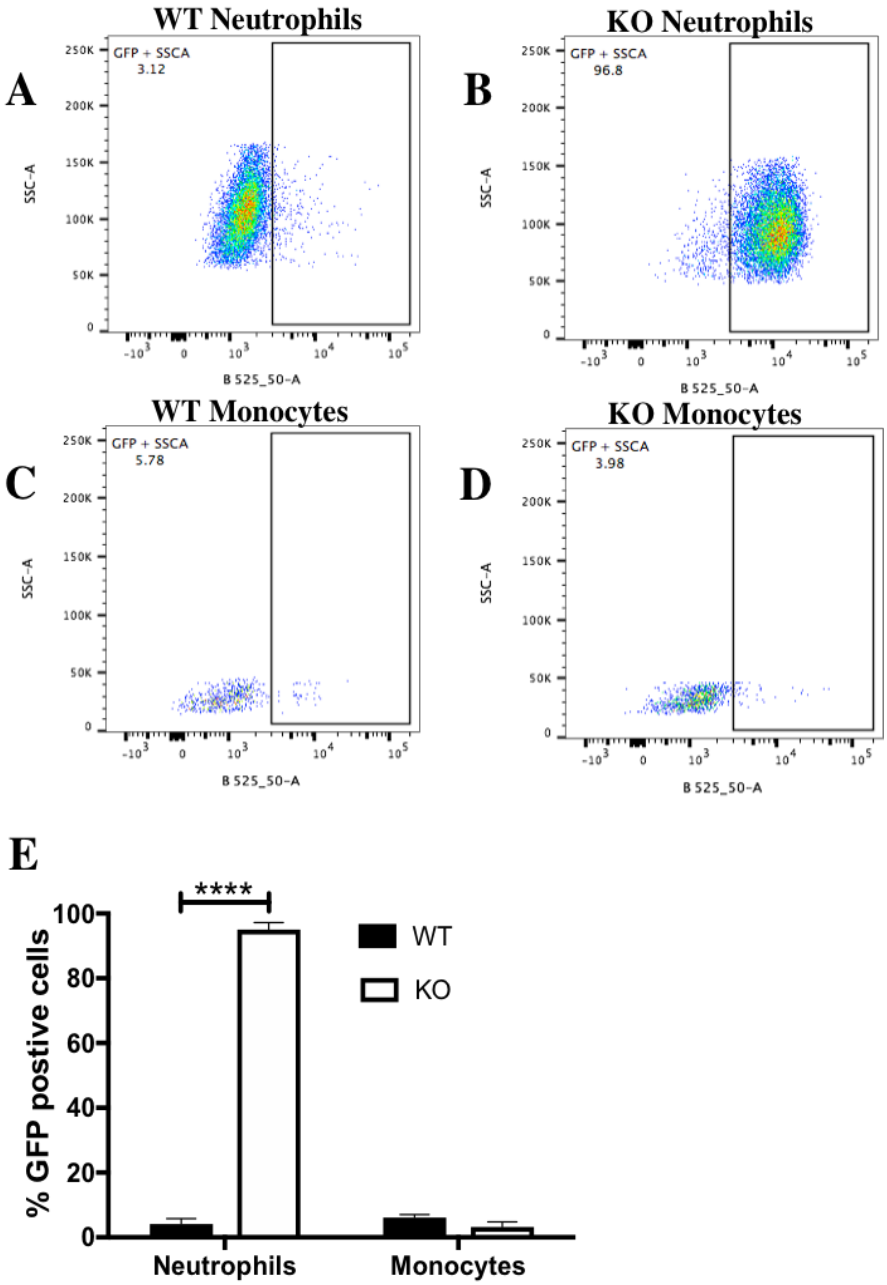

Figure 3.5.1-1 Neutrophil knockdown of Sema3F demonstrated by detection of a GFP reporter by flow cytometry

Sema3F^{floxflox}MRP8CRE$^{-/-}$ (WT) and Sema3F^{floxflox}MRP8CRE$^{-/+}$ (KO) underwent LPS induced lung injury and were sacrificed at 24 hours and bronchioalveolar lavage performed. Following identification of the neutrophils and monocyte cell populations in the BAL the geometric fluorescent intensity of the GFP signal was determined by flow cytometry (plots A-D). In the flowcytometry plots side scatter intensity is plotted against fluorescent intensity in the GFP channel (B525_50-A). The percentage of GFP positive neutrophils and monocytes is shown in graph E, the GFP reporter protein is only significantly expressed in Sema3F KO neutrophils. Data shown are mean ± SEM n=4 analysed using a two-way ANOVA, ****<0.0001.

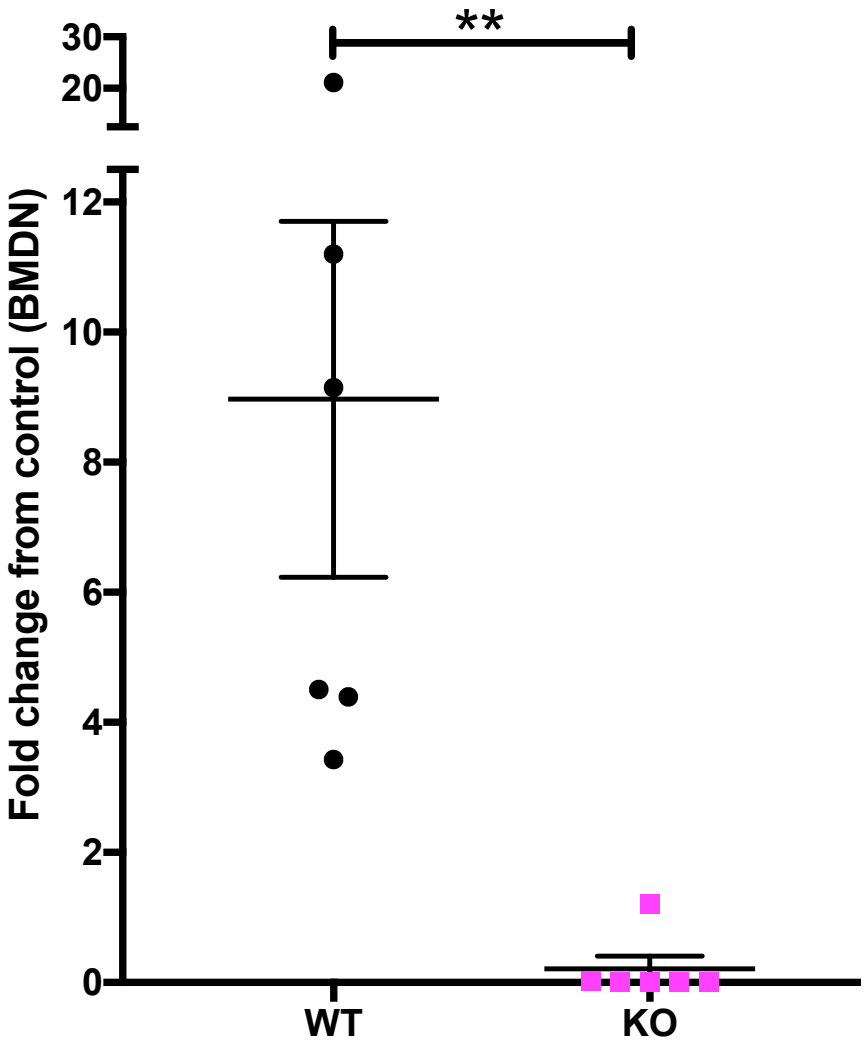

Figure 3.5.1-2 Sema3F is successfully knocked down in the neutrophil population at the mRNA level
Sema3F^{floxflox}MRP8CRE$^{-/-}$ (WT) and Sema3F^{floxflox}MRP8CRE$^{-/+}$ (KO) underwent LPS induced lung injury and were sacrificed at 24 hours, BAL neutrophils collected, and cDNA extracted. TaqMan analysis of cDNA was performed with data normalized to beta-actin (ACTB) expression. The graph shows fold change in Sema3F gene expression following acute lung injury with LPS in both the WT vs KO neutrophil. Data show mean ± SEM of fold change compared to bone marrow derived neutrophils, n=6 analysed by an unpaired *t*-test, **P=0.0096.

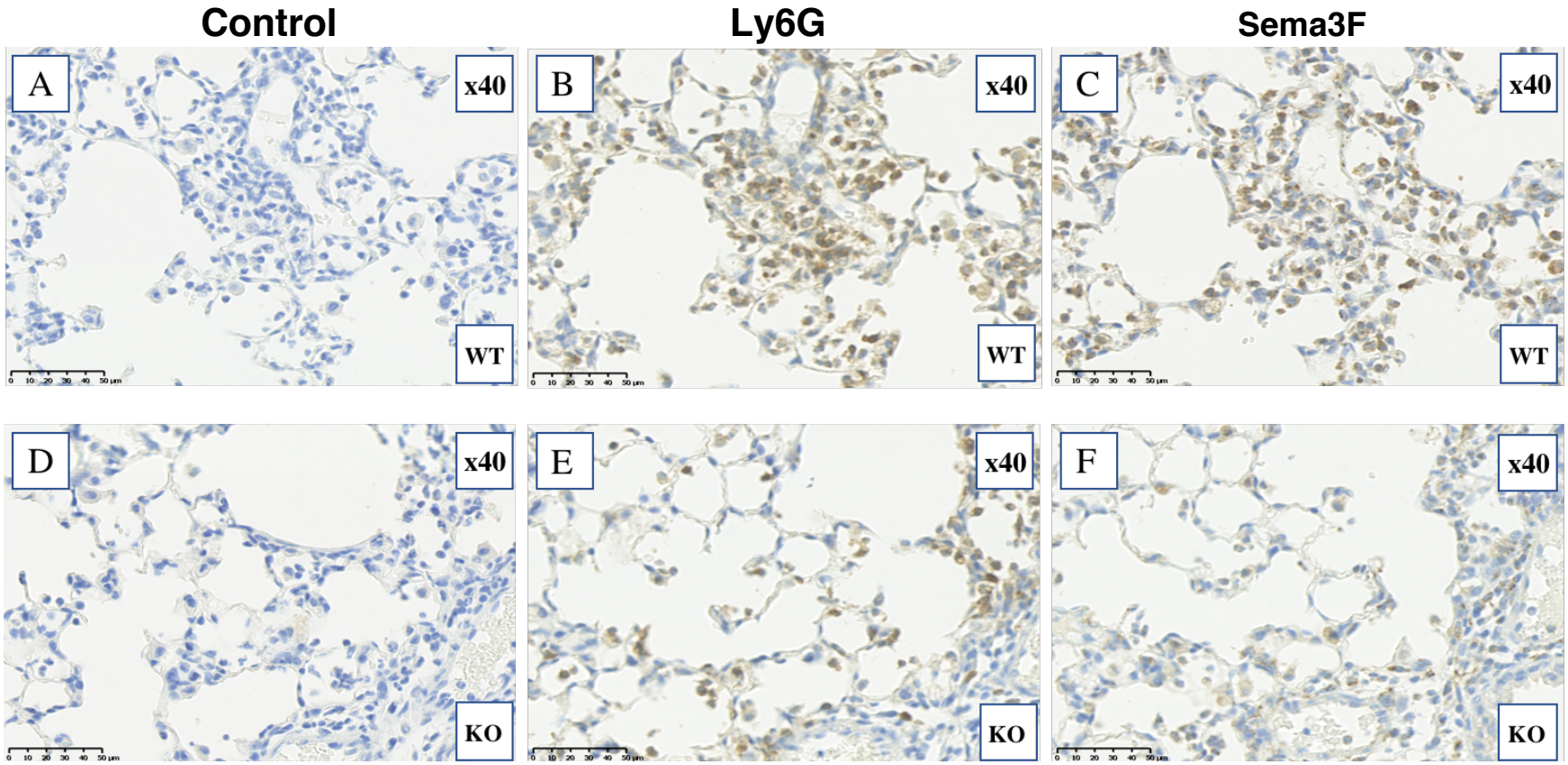

Figure 3.5.1-3 Sema3F is successfully knocked down in the neutrophil population at the protein level

Sema3F^{floxflox}MRP8CRE$^{-/-}$ (WT) and Sema3F^{floxflox}MRP8CRE$^{-/+}$ (KO) underwent LPS induced lung injury and were sacrificed at 48 hours and lung tissue taken, serial sections made and stained for Ly6G and Sem3F. Images and A and D represent the isotype controls. Images A-C and D-F are two sets of three serial sections from the WT and KO animals showing the staining for neutrophils (Ly6G) and Sema3F respectively. There is a reduction in the amount of staining for Sema3F seen in the neutrophils in the KO compared to WT animal.

3.6 Neutrophil specific knockdown of Semaphorin3F increases both recruitment and clearance of neutrophils without altering apoptotic responses

3.6.1 Neutrophil Sema3F knockdown enhances recruitment and resolution

To investigate the effect of neutrophil specific loss of the autocrine Sema3F signal an in *vivo* lung injury model was used. KO mice Sema3F$^{flox/flox}$MRP8Cre$^{+/-}$ and WT mice Sema3F$^{flox/flox}$MRP8Cre$^{-/-}$ were nebulised with LPS and culled at 6, 24 and 48 hours. Following BAL both total and differential cell counts were performed. In figure 3.6.1-1, In Graph A in the KO animal the peak recruitment is seen at 6 hours with a significant increase in the recruited neutrophil count KO compared to WT mice. Mean values for the knockout mice were $8.97x10^6 \pm 0.8$ and wild type were $5.51x10^6 \pm 0.7$. At 24 and 48 hours counts were comparable between groups.

The resolution of neutrophilic inflammation occurs between 24 and 48 hours. The rate of decline in neutrophils numbers is higher in the KO than WT animal during the period. In graph B hypothesised lines have been drawn between timepoints to graphically show the rate of change for the WT and KO mice. The T_{50} for each genotype was calculated by identifying the maximal neutrophil recruitment number and the time taken to achieve a 50% reduction in neutrophil count from this peak. The resolution of neutrophilic inflammation occurs 9.1 hours earlier in the KO than the WT animal. Therefore, neutrophil specific loss of Sema3F enhanced the resolution of neutrophilic inflammation in this model.

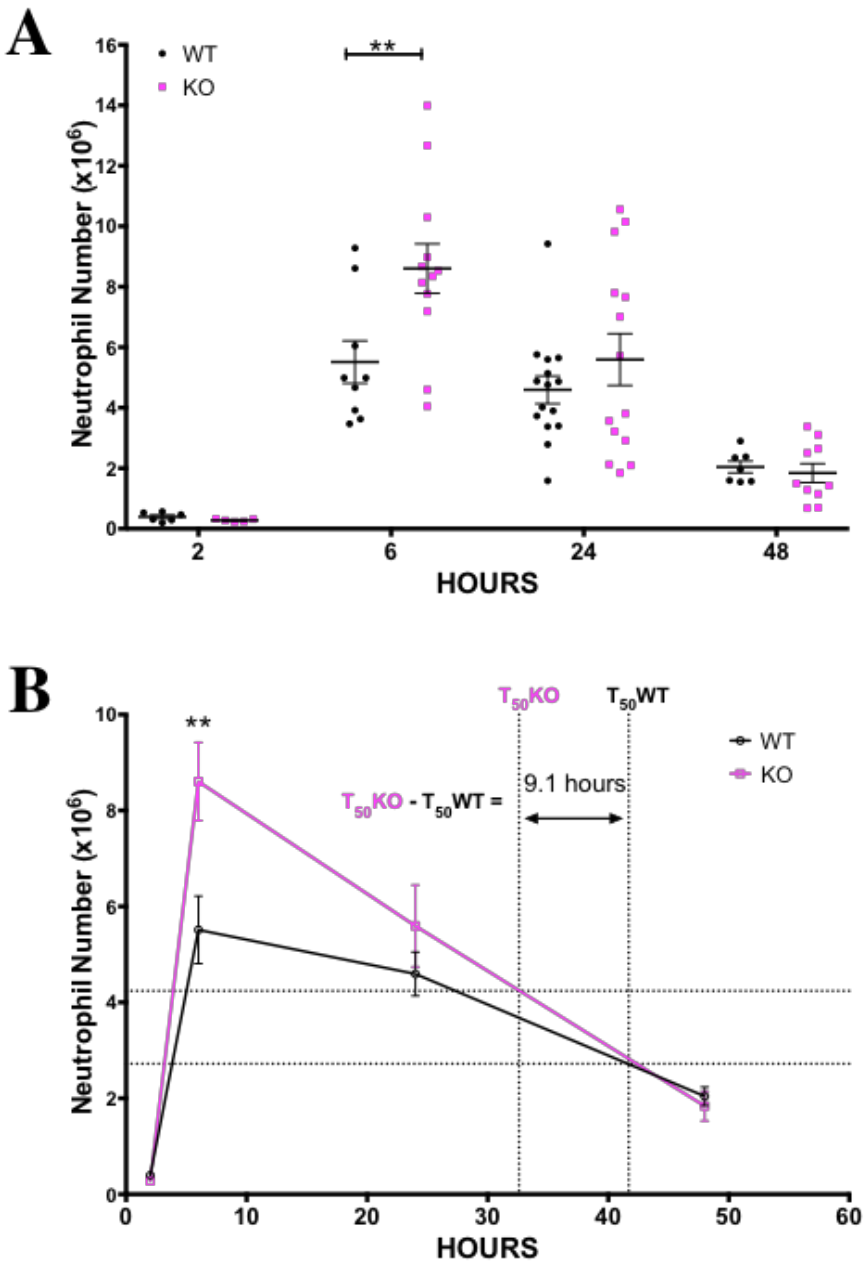

Figure 3.6.1-1 Neutrophil specific knockdown of Sema3F enhances both recruitment and resolution post LPS induced lung injury
Sema3F^{floxflox}MRP8cre$^{-/-}$ WT and Sema3Ff^{loxflox}MRP8cre$^{+/-}$ KO were challenged with LPS, sacrificed at 2, 6, 24 and 48 hours and bronchoalveolar lavage fluid obtained. Cell counts were performed by haemocytometer and the differential cell count established using cytospins. Graph A shows the individual mice during the time course. Data are shown mean ± SEM, n=6-12 over 3 individual experiments analysed using two-way ANOVA, **P=0.014. Graph B shows the time taken for a 50% reduction in the number neutrophils at peak recruitment calculated individually for each genotype (T_{50}) occurring 9.1 hours earlier in the KO compared to WT.

3.6.2 Neutrophil Sema3F deficiency does not increase neutrophil apoptosis or macrophage numbers following LPS induced lung injury

Apoptosis is a route of neutrophil clearance following LPS induced lung injury. To determine if apoptosis was increased to account for the increased rate of resolution seen in the KO mice apoptosis counts were performed. Cytospins of BAL samples from the same mice were analysed and percentage apoptosis assessed by morphological changes. Examples of the features used to define an apoptotic neutrophil is shown in image B figure 3.6.2-1. Graph A shows that, at all three times points, there is no difference in the percentage of apoptosis between genotypes.

Macrophages and neutrophils often have complementary and overlapping roles within the innate immune response. The behaviour and longevity of neutrophils are controlled, in part, by macrophage signals and the phagocytosis of dying neutrophils by macrophages. The neutrophil specific Cre driver used in the construct $Sema3F^{flox/flox}MRP8Cre^{+/-}$ is described in the literature as having minimal expression in macrophages/monocyte population and I have confirmed this in the context of my transgenic model (figure 3.5.1-1).[187] To ascertain whether the neutrophil specific KO of Sema3F has a neutrophil specific phenotype in the context of the LPS induced lung injury model, I determined macrophage numbers from the BAL differential counts of the mice. The macrophage counts are shown in Graph C and are similar at all time points. This supports the conclusion that the phenotype seen when there is a deficiency in neutrophil Sema3F is neutrophil specific, as is not due to a change in either macrophage counts during recruitment or resolution. Differences between genotypes are only observed in the neutrophils counts during ALI.

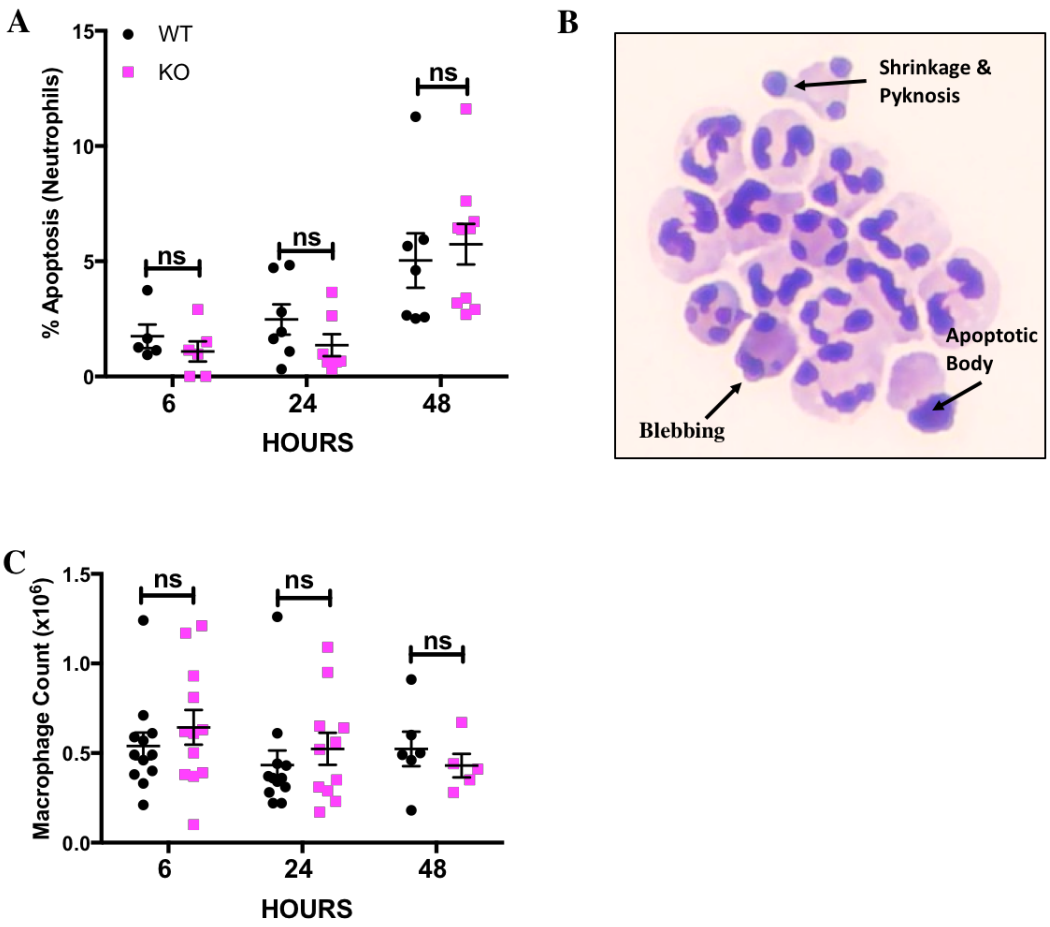

Figure 3.6.2-1 Loss of neutrophil Sema3F does not increase neutrophil apoptosis or macrophage number during the course of acute lung injury
Graph A shows apoptosis counts of BAL neutrophils performed by assessment of typical apoptotic morphology of cytospins at times 6, 24 and 48 following LPS induced acute lung injury. Image B shows a representative image demonstrating some of the characteristic features used to identify apoptotic neutrophils. These include blebbing of the cytoplasm, shrinkage and pyknosis of the multi-lobed nuclei and the formation of the apoptotic body (with thanks to Dr Rob Grecian). Graph C shows the macrophage differential cell counts at these times points. (A) n=6-12 (B) n=5-12, Data are shown mean ± SEM analysed using two-way ANOVA.

3.7 Discussion

I have demonstrated that human neutrophils express Sema3F at the protein level (figure 3.2.1-1) and its expression is under the control of the inflammatory mediators LPS but not TNF-α or IL-1β. While LPS and IL-1β are both pro-inflammatory signals that activate neutrophils there some differences. It has been postulated that LPS signalling through the Toll-like receptor 4 (TLR4) activates neutrophils but does not elicit a pro-survival response.[209] LPS may enhance neutrophil survival in the presence of peripheral blood mononuclear cells producing IL-1β.[209] In contrast IL-1β stimulation has been shown to both activate and extend the neutrophil life-span and is related to a later stage of sterile inflammation.[228] In the murine acute lung injury model, following loss of neutrophil Sema3F, we did not see any differences in apoptosis (figure 3.6.2-1). Sema3F mRNA and protein levels rise acutely following lung injury (mRNA: figure 3.2.3-1, protein: figure 3.2.4-1).

It was important to relate Sema3F expression to inflammatory lung disease and to establish whether Sema3F may have role in the pathogenesis of such diseases therefore an evaluation of COPD patient samples was undertaken. As the aetiology of COPD and lung cancer share smoking exposure as a common and important risk factor, there is often a co-existence of these pathologies. Lung tissue was taken from non-tumour regions during resection for lung cancer (figure 3.2.2-1) and stained for Sema3F. The recruited inflammatory cells found in the airspace, consisting predominately of neutrophils and a smaller proportion of macrophages, stained positively for Sema3F. This indicates that Sema3F may have role to play in the regulation of these cell types in COPD.

Following this it became clear that Sema3F, in the context of the regulation of lung inflammation, warranted further investigation. To this end, an in *vivo* model of lung acute injury was used to ascertain the role of Sema3F in the innate immune response. I looked at murine neutrophils to ascertain whether

they also expressed Sema3F following LPS induced lung injury. Sema3F mRNA rises acutely with the initiation of lung injury and is maintained at a slightly reduced level at 24 and 48 hours (figure 3.2.3-1). There is no expression of Sema3F mRNA found in unstimulated peripheral blood neutrophils. This supports the hypothesis that Sema3F is involved in the regulation of neutrophil inflammation and as consequence is not found in the quiescent blood neutrophil.

Sema3F is detected in murine neutrophils at the protein level, (figure 3.2.4-1). The Ly6G positive neutrophils in the adjacent serial section stain positively for Sema3F within the cell cytoplasm. This is keeping with what is known about class 3 Semaphorins, that they are released as exogenous proteins. In figure 3.2.4-2, images of lung sections from mice are shown for time points 6, 24 and 48 following LPS induced lung injury, depicting the temporal-spatial staining pattern for Sema3F protein during lung injury. Throughout the time-course there is expression seen in both the neutrophils and macrophages. At 6 and 24 hours following acute lung injury staining is also seen in the epithelial layer; this is not apparent at 48 hours. The highest level of staining level is observed at 24 hours. The Sema3F mRNA does not directly correspond to the protein expression, in that the acute uplift in mRNA are seen at 6 hours, whereas subjectively the highest levels of staining for Sema3F is seen at 24 hours post lung injury. There may be a lag phase between mRNA and protein translation to account for this. Similarly, the lowest Sema3F staining levels are seen at 48 hours despite the maintenance of the mRNA levels. There may be other factors controlling mRNA and protein levels, these include the regulation of protein translation and mRNA/protein degradation, trafficking within the cell and release mechanisms. There is a clear dynamic co-ordination of Sema3F expression which correlates with the stage of lung injury. It appears that resolution is associated with overall lower levels of Sema3F mRNA and protein expression. The amount of intracellular Sema3F could have an inverse

relationship with the amount of the exogenous active Sema3F protein present in the inflammatory milieu, which is not accounted for by this data.

In conjunction with the investigation into neutrophil Sema3F expression, I also examined the expression of the Sema3F co-receptors, Neuropilins 1 and 2 (NRP1 and 2). It was important to establish that neutrophil Sema3F-Neuropilin signalling is relevant to the human system and that Sema3F autocrine regulation of neutrophils remained a credible hypothesis. COPD patient lung samples, as described previously, were stained for NRP2. As is the case for the Sema3F staining in these samples, the positive signal was seen in the myeloid population resident in the inflamed airways (figure 3.3.1-1). I went on to characterise the human neutrophil surface expression of NRP 1 and 2 in health. The receptors were identified through a validated flow cytometry panel (figure 3.3.2-1). The panel successfully identified neutrophils that express NRP2. These neutrophils are seen to be viable, following fluorescent assisted cell sorting using this panel and a detailed study of the morphology of the selected neutrophils (figure 3.3.3-1). Human neutrophils express significantly more NRP2 than monocytes, and as such, monocytes provide both a biological negative control for NRP2 expression and a positive control for NRP1 expression (figure 3.3.4-1). Following stimulation with the inflammatory mediators LPS, TNF-α and IL-1β there are higher levels of NRP2 expression where NRP1 expression remains unchanged (figure 3.3.5-1). Interestingly, in contrast to human Sema3F protein expression seen in figure 3.2.1-1, it is IL-1β treatment that induces a doubling of the percentage of neutrophils that express NRP2 and LPS has the least effect on surface expression. The opposite effect of these proinflammatory mediators on Sema3F protein expression and NRP2 surface expression suggests differential regulation of the Sema3F ligand and co-receptor NRP2 by the inflammatory environment. This may also relate to an overall temporal co-ordination of the innate immune response to lung injury involving Sema3F and its co-receptor NRP2. LPS and IL-1β induce individual neutrophil responses and are prominent during different

phases of lung injury. Thus, variation in the expression of the ligand Sema3F and NRP2 throughout lung injury, could be co-ordinated by inflammatory mediators such as LPS and IL-1β and in turn alter the neutrophil behaviour. Equally, temporal co-ordination of the ligand and receptor could be required for successful signal transduction. Following Sema3F protein translation, release of exogenous Sema3F has to occur and the ligand and receptor must be in proximity to allow binding for signal transduction. The timing of each of these steps could provide a level of regulation. Another consideration is the evidence that soluble NRP2 can be secreted by alveolar macrophages adding another layer of complexity.[149] While the exact relationship between neutrophil Sema3F and its receptors has yet to be established, it is clear that Sema3F autocrine signalling has a role throughout acute lung injury from recruitment to resolution.

Using a murine in *vivo* model system was crucial to understanding the role of Sema3F signalling in greater detail. Likewise, it was imperative to establish the presence of the Sema3F co-receptors in murine neutrophils. At 6 hours following LPS induced lung injury murine neutrophils express the NRP2 receptor but no NRP1 was identified (3.3.6-1). Unlike Sema3F mRNA, neutrophils express NRP2 mRNA at baseline (unstimulated peripheral blood neutrophils). Following injury there is a significant induction of NRP2 mRNA, at 24 and 48 hours levels are reduced but maintained above baseline (figure 3.3.7-1). In the WT mice, at 6 hours, NRP2 protein expression is present in the neutrophil population, following this it appears to be exclusively located in the epithelial layer and cells adjacent to the blood vessels (figure 3.3.8-1).

To investigate the effects of Sems3F in the context of an in *vivo* system, C6/BL57 wild-type mice were used, 24 hours following acute lung injury intra-tracheal Sema3F [1μM] or PBS (experimental protocol, figure 3.4.1-1). Following Sema3F given at peak recruitment neutrophils were retained at the site of injury (graphs A & B, figure 3.4.1-1). Neutrophil retention was not sustained at 48 hours following Sema3F treatment (graphs C & D). Alongside

this, lung sections were taken from mice treated using this protocol and culled at 24 hours post treatment. As a general observation there is an increase in the features of ALI following Sema3F treatment although this is not quantified (figure 3.4.2-1). This may suggest that a more severe lung injury is sustained following Sema3F treatment due to the increase in retained neutrophil numbers. The thrombi seen in the post capillary venules in acute lung injury are not generally thought to be a hallmark of underlying thromboembolic disorders but related to acute and localised alterations in the coagulation pathway.[229] Whether this Sema3F-retention of neutrophils is due to an effect on neutrophil migration or an alteration in the pattern of neutrophil recruitment over the time course remains unclear. Sema3F treatment could reduce the reverse migration of neutrophils from the pulmonary vasculature to the wider circulation so greater numbers are in close proximity ready to be recruited or impede loss to body through the mucociliary escalator. This experiment discounted the possibility that Sema3F acts as a potent pro-survival stimulus. No difference was observed in neutrophil apoptosis counts between PBS or Sema3F treated mice at either 48 or 73 hours post ALI.

In view of the response to excess exogenous Sema3F I wondered if the converse would hold true. To begin to answer this I used a transgenic neutrophil specific KO of Sema3F ($Sema3F^{floxflox}MRP8cre^{+/-}$) to further explore the role of Sema3F in neutrophil migration and lung inflammation. Semaphorin signalling has been shown to be autocrine in both tumour and endothelial cells.[160,195,197] As such the neutrophil specific knockout of Sema3F provided a precise construct with which I could begin to interrogate the role of neutrophil Sema3F as an autocrine signal in the context of lung injury. MRP8 acts a driver for Cre in this transgenic construct and is highly specific for neutrophils. MRP8 (S100A8/Calgranulin A) Cre mice show specific deletion in neutrophils, with minimal expression in macrophages, monocytes, natural killer (NK) cells, mast cells, basophils, or eosinophils.[187] As the MRP8-Cre transgene contains an IRES-GFP cassette, I can also follow Cre expression by flow cytometry (figure

3.5.1-1). I have also demonstrated knockdown of neutrophil Sema3F at the mRNA and protein level (figures 3.5.1-2 & 3.5.1-3). Following lung, the loss of neutrophil Sema3F leads to peak recruitment being seen at 6 hours and a significant increase in the number of neutrophils within the airspace (figure 3.6.1-1, graph A). After 6 hours, between 24 and 48 hours there is no significant difference between the KO and WT mice. At 48 hours the neutrophil numbers are virtually identical between genotypes. The rate at which the numbers of neutrophils fall, between 24 and 48 hours, is greater in the KO animal. Whether this represents a resolution phenotype is not fully answered by my data in this project. However, the rate of change in neutrophil number is greater in the KO mouse (figure 3.6.1-1 graph B) and it is evident that both phases of recruitment and resolution are occurring at this faster rate. Calculating the T_{50} confirms this, whereby the time taken for a 50% reduction from the maximal number of neutrophils recruited into the lung is 9.1 hours earlier in the KO than the WT animal. Rather than being related to an absence of neutrophil Sema3F expression, the increased rate of resolution could represent an upregulation in tissue homeostasis mechanisms responding to the greater influx of neutrophils in the KO mouse. These findings point towards an overall increase in the speed of neutrophil transit during acute lung injury.

Apoptosis is a route for the disposal of neutrophils during resolution and yet the numbers of apoptotic neutrophils are unchanged between genotypes (figure 3.6.2-1, graph A). It must be acknowledged that even small differences in percentage of apoptosis, at a single time point, can alter the rate of apoptosis and have a major effect on levels of neutrophil clearance.[115,230] This finding suggests that neutrophil specific KO of Sema3F can increase neutrophil recruitment and resolution without altering apoptotic responses. Semaphorins are known to control cell motility and it may be that the Sema3F deficient neutrophils have an increased propensity to migrate, to and away from, the injury site which would yield differences in both neutrophil recruitment and resolution. Macrophages also play a crucial role in the regulation of neutrophil

numbers and neutrophilic inflammation by phagocytosis of apoptotic neutrophils. Macrophages can control the behaviour of neutrophils by the production of inflammatory mediators, which can modulate both neutrophil recruitment and apoptosis. In this transgenic model I did not see alterations in macrophage numbers (figure 3.6.2-1, graph B).

Both in *vivo* and in *vitro* LPS switches on neutrophil Sema3F production which appears to act as a “brake” to neutrophil transmigration. Recruited neutrophils are retained following exogenous Sema3F treatment and neutrophils deficient in Sema3F show a pattern of enhanced recruitment and resolution following lung injury. The main co-receptor for Sema3F is expressed on both murine and human neutrophils under the control of inflammatory stimuli. Taken together this supports the hypothesis that Sema3F is an important signal in lung injury and may act in autocrine manner to differentially influence the magnitude of the inflammatory response. In this way neutrophil Sema3F production and the Sema3F co-receptor NRP2 are highly relevant to the development of new therapeutic agents for inflammatory lung diseases.

4 Results chapter: Sema3F retains neutrophils in the injured lung by inducing neutrophil F-actin disassembly

Introduction.

4.1.1 Neutrophil migration in lung injury

The response to tissue injury requires a complex communication network and signals such as Sema3F may direct the traffic of neutrophils, retaining or permitting emigration from the injury site. This could occur through reverse migration, or loss to body and clearance by the mucociliary-escalator of the lungs. Certainly, dysfunctional migratory neutrophil behaviour is seen in patients with COPD, where recruited and inflammatory neutrophils are retained in the injured lung and contribute to the ongoing tissue distruction.[231,232] Another class 3 Semaphorin, Sema3A, has been shown to modulate the migration of cells including macrophages and endothelial cells and has also been shown to control growth through alterations in the cytoskeleton by promoting F-actin disassembly.[233,234] Changes in the F-actin cytoskeleton structure will not only affect cell migration, but will have clear implications for the exocytosis of neutrophil granules (degranulation) and the subsequent release of their potent histotoxic contents, which includes enzymes such as myeloperoxidase and elastase.[235] Likewise a retention signal could increase the number of neutrophils releasing granules which would have a direct effect on the amount of histotoxic agents in the inflammatory milieu potentiating tissue damage.

Enhanced or reduced neutrophil recruitment to the injury site is defined both by the ability of the cell to migrate, therefore the speed and directionality of neutrophil locomotion, but also the physical barriers breached during transmigration. In this regard, the human lung has key differences from other organs. It has been proposed, that even in health, 51% of circulating neutrophils are found in the marginated pool within the lung vasculature, approximately 33.15×10^7 cells/kg.[60] These marginated neutrophils are poised in close proximity ready to respond rapidly to lung injury. The lungs participate

in the first line of host defence and have an enormous alveolar surface area of ~143m^2 which is in contact with the external environment.[236] The human pulmonary capillary bed is proportionally large, with between 51-72 million 1st order pulmonary arteries and a capillary blood volume of 95m^3, the capillary vessels themselves are narrow with an average diameter of 6.3μm.[237] In order to enter the pulmonary vasculature neutrophils are required to undergo shape change and appear elongated; in turn their transit time in the capillary network is extended compared to red blood cells.[238] This results in generating a pool of marginated neutrophils within the pulmonary capillary network of a healthy lung which are ready for rapid recruitment.[239] In lung injury the process of sequestration of neutrophils follows the recognition of damage within the lung. Unlike in other organs the narrow diameter of the pulmonary capillary does not allow rolling. Neutrophil migration into the lung parenchyma is selectin and, in certain contexts, β2-integrin independent.[240]

Yipp et al. (2013) used intra-vital imaging of transgenic murine lungs to identify that neutrophils survey the pulmonary vasculature for bloodstream pathogens and from this position, capture bacteria from the blood stream.[22] Human subjects responded to intra-venous LPS with a rapid 50% reduction in circulating neutrophil counts, as these neutrophils were sequestered to the lung, adding to the already existing marginated pool of neutrophils. In the mice the canonical recruitment pathway did not occur and only upregulation of CD11b through TLR4 and Myd88 activation was required for neutrophil crawling leading to successful bacterial capture. [241] Downstream of TLR4 and Myd88 Abl-kinase inhibition reduced neutrophil crawling; interestingly Abl-kinase is responsible for inside out signaling and modulation of both the cytoskeleton and integrins. Similarly, Sema7A promotes neurite outgrowth through inside out integrin signaling and cytoskeletal re-arrangements.[242]

L-selectin deficient mice have a normal marginated pool of neutrophils and P- and E selectin are not expressed on the capillary endothelium.[243-245] The CD11/CD18 adhesion pathway accounts for 60-80% of neutrophil migration

from the pulmonary capillary bed to the distal airspaces in response to LPS; of note 20-40% of neutrophil migration is therefore independent.[62,63,246] Doerschuck et al. (1987) demonstrated that following an injection of complement fragments, neutropenia is observed in rabbits within 1 minute of the infusion, and there is a corresponding increase in neutrophils within the pulmonary capillaries. These sequestered neutrophils require the CD11/CD18 adhesion to maintain accumulation in the lung after 7 minutes. Blocking of neutrophil recruitment using a CD18 specific monoclonal antibody mAb 60.3 is successful only after 7 minutes and not prior to this.[239,247] It is therefore likely that the marginated pool of neutrophils is initially controlled by the transit time of the neutrophil, which in turn is regulated by the neutrophil deformability.[60] Yoshia et al. (2012) directly link a decrease in neutrophil deformability and increased sequestration to the lung in a rat model of bacterial pneumonia.[248] Neutrophils with low-deformability were identified by the formation of an F-actin rim, this appeared to control sequestration independently of adhesion either through selectins or CD11/CD18. The deformability of the neutrophil is determined by changes in the neutrophil cytoskeleton. Neutrophil rigidity is altered by cytocalasin B and not directly by colchicine, which suggests that actin and not microtubules, is primarily responsible for changes in deformability and therefore lung sequestration.[249] Dynamic actin re-structuring and distribution appears to affect not only deformability but also neutrophil shape. F-actin amount and distribution relates to neutrophil function and activation status. Circulating unstimulated neutrophils are mostly round with lower levels of F-actin distributed both centrally and at the periphery. In contrast to the circulating neutrophil, quiescent bone marrow (BM) neutrophils have more F-actin and are almost exclusively round and spherical, with some F-actin centrally, but most is located at the submembrane region.[250] In response to fMLF, circulating neutrophils undergo a dramatic shape change and F-actin levels increase and are distributed to the submembrane region.[250,251] In BM neutrophils there is a less extreme response to fMLF and only small irregularities appear in the plasma membrane. Yet in both circulating and BM

neutrophils there is loss of central F-actin in response to fMLF. The BM neutrophils are stiffer due to the predominance of submembrane F-actin distribution and as a result sequester better than circulating neutrophils to the lung.[24,26] The key regulators of the actin cytoskeleton include the Rho family of GTPases. Neutrophils deficient in the Rac2 had 20-25% less F-actin content at baseline and a reduction in F-actin increase in response to fMLF. Associated with this they have impaired directionality and chemotaxis.[252] Dooley et al. (2009) found that following immune-complex mediated lung injury in Rac2 -/- mice there was increased neutrophil recruitment when compared to WT mice at 6 hours.[253] The reduction in baseline F-actin, may promote neutrophil sequestration which translates into enhanced acute neutrophil recruitment post lung injury. The Rac2-/- neutrophils had normal expression of adhesion molecules CD11a, CD11b, CD11c, CD18, and CD61.

Neutrophil deformability and cytoskeletal arrangements appear to define sequestration to the pulmonary vasculature which can occur independently of CD11/CD18 adhesion, however retention of sequestered neutrophils requires adhesion through the CD11/CD18 and L-selectin pathways. The next stage of transmigration requires transendothelial migration (TEM) or diapedesis and occurs in the absence of rolling, due to the small diameter of the pulmonary capillaries. Neutrophils migrate through the endothelial layer via the transcellular or paracellular route. The biomechanical changes required involve both actin and microtubules and are far more complex than the earlier stage of sequestration. Changes in the endothelial cell cytoskeleton are also required.[91,254] Once across the endothelial cell layer, the neutrophil triggering receptor expressed on myeloid cells 1 (TREM-1) is essential for neutrophil transepithelial migration into the distal airspace.[64] Prior to this neutrophils must migrate through the lung interstitium; less is known about the regulation of migration through this compartment of the lung.

Lung transmigration may not represent a one-way system. Reverse neutrophil transendothelial migration (rTEM) has been shown to occur in other organs

where subsequent neutrophil accumulation in the lung is a secondary event.[75] There is not yet evidence that neutrophils undergo reverse migration originating in the lung itself.[96] The neutrophil is key in instigating reverse transendothelial migration elsewhere and the LTB4 - elastase axis is critical to the process.[96] While there remains uncertainty regarding the possibility of true rTEM in the lung, neutrophils do return from the pulmonary vasculature to the remaining circulation. It has been posited that the lungs act as a neutrophil de-priming station. The activated neutrophils are recruited to the pulmonary vasculature but do not undergo TEM. Once de-primed they are allowed to enter the circulation again; if prior to the de-priming further activation occurs or de-priming fails, these primed neutrophils are recruited to the interstitial space and may cause lung injury.[20] During sterile injury neutrophils leave the tissue, return to the blood stream then enter the lungs where CXCR4 is upregulated promoting the return of the neutrophils to the bone marrow.[23,255] Adrenaline and exercise have been shown to mobilise neutrophils from the marginated pool in the bone marrow.[256]

In a zebrafish model of reverse migration, neutrophils which have been shown to reverse migrate were significantly less spherical and this may suggest they have are activated and remained primed.[85] If the lung is indeed a center for de-priming neutrophils after which they return to the bone marrow, this may explain why reverse migration of activated neutrophils is not observed. This observation highlights a link between neutrophil migration, activation status, neutrophil effector functions and neutrophil roundness and sphericity.

4.1.2 Neutrophil functions and their relationship to the actin cytoskeleton

Neutrophils are professional phagocytes. Phagocytosis has three distinct stages: 1) the particle binding 2) pseudopod extension 3) phagosome closure. As such it is evident that phagocytosis requires dramatic changes in the neutrophil actin cytoskeleton. The Rho family of GTPases differentially regulates phagocytosis. For example Cdc42 regulates the formation of the

pseudopod, while Rac1 controls the closure of the phagosome.[257] Rac1 and Rac2 have been shown to have distinct roles in actin organisation within hematopoietic stem cells.[258] Inhibitors of actin polymerisation such as Latrunculin or, Cytocalasin B which prevents actin turnover, inhibit neutrophil phagocytosis.[259,260] The pox virus and Semaphorin family member A39R both evade host defence by inhibiting neutrophil phagocytosis.[168]

Neutrophils produce ROS as part of an oxygen-dependent antimicrobial system. Stimulated neutrophils consume oxygen to generate superoxide; neutrophils can also be primed and following this initial signal the generation of ROS is enhanced. The bacterial peptide fMLF can both prime and trigger low levels of ROS. Neutrophil NADPH oxidase (NOX2) generates superoxide which dismutates and is used by the heme enzyme myeloperoxidase to generate both ROS and hydrogen peroxide. Neutrophil ROS is found intra-cellularly in phagosomes, ready to kill engulfed bacteria but can be found at other sites or released to the environment.[261] The generation of NADPH oxidase dependent ROS has been shown to be reliant on cytoskeletal rearrangements and the small GTPase Rac2. [262] The depolymerisation of actin is enhanced by ROS.[263] Levels of intracellular ROS have been shown to control neutrophil migration.[264,265]

Myeloperoxidase is a hemoprotein contained within neutrophil primary (azurophilic granules) and can be released through exocytosis which is a process dependent on actin cytoskeletal dynamics.[235] This enzyme forms hypochlorous acid (HOCL), hydrogen peroxide (H_2O_2) and chloride anions from radical oxygen species. This toxic cocktail is released as part of the neutrophils' role in host defence against invading pathogens.[266] Primary granules undergo exocytosis, by relocation to the internal neutrophil membrane granules then they tether, dock and fuse to the phagolysosomes or expel their contents into the extra-cellular matrix. Translocation of primary granules to the internal neutrophil membrane is largely through Rac2 signaling and the actin cytoskeleton.[267]

4.1.3 Semaphorins regulate the cytoskeleton

Semaphorins have been shown to regulate cell migration and the actin cytoskeleton. Sema3E has recently been shown to act as a neutrophil chemorepellent in a murine model of allergic asthma.[193] In results chapter 3 I described that neutrophil Sema3F deficiency resulted in enhanced recruitment and resolution in a murine model of acute lung injury. Furthermore, that following intra-tracheal instillation of Sema3F recruited inflammatory neutrophils were retained in the injured airway. This suggests that Sema3F has a role as a retention signal rather than chemorepellent, in the control of neutrophilic inflammation. This is possibly through the modulation of neutrophil migration from the blood to airspace by alterations in the neutrophil cytoskeleton. Semaphorins have been shown to regulate cell migration and axonal growth in an integrin dependent fashion.[160,169,242] Class 3 Semaphorins have been shown to regulate integrin activation status and affect vascular morphogenesis.[160] The interplay between Sema3F modulation of actin cytoskeletal dynamics and shape and potentially also adhesion pathways may begin to explain the mechanism of neutrophil retention and enhanced recruitment seen in response to Sema3F treatment or loss. This regulation of neutrophil function and behaviour could be harnessed to create new therapies to ameliorate the consequences of pathological neutrophilic inflammation.

Neutrophil Sema3F autocrine signaling determines neutrophil transit to the lung during ALI. There are many aspects to neutrophil transit including neutrophil kinetics, intrinsic properties of the neutrophil (deformability, adhesion pathways, cytoskeletal arrangements) and clearance, through expectoration, cell death, phagocytosis and migration away from the lung to distant sites such as the bone marrow. Clearly there exists a complex interplay between all these factors. A single signal which might cut through this all this ‘noise’, such as the retention signal Sema3F, could participate in the regulation of neutrophil recruitment and resolution by inducing a well-timed pause thus allowing the neutrophil to do its important work.

4.1.4 Neutrophil elastase in health and disease

Elastase is a chymotrypsin serine protease and is responsible for the degradation of a variety of substances including: elastin, extracellular matrix proteins, collagen types I–IV, proteoglycan, fibronectin, platelet IIb/IIIa receptor, complement receptor, thrombomodulin, lung surfactant, and cadherins.[268-270] Neutrophils contain large amounts of elastase approximately 5 mM and up to 3 pg and as such are a major source of elastase in the injured lung .[271] Elevated elastase levels promote inflammation and delays wound healing.[272] Similarly, in the lung excessive elastase activity leads to destruction of the epithelial capillary barrier, pulmonary oedema and acute lung injury. [273] It is a dysregulation of the balance between proteases (elastase) and-anti proteases that can lead to this type of lung damage.[274] While elastase has been shown to be increased in the BAL of patients with ARDS, this has not been seen in all studies conducted using similar patient groups.[275-277] Elastase has a very short half-life of 0.6ms which may account for a lack of correlation between elastase levels and the clinical picture.[278] Likewise, elastase can remain bound to the neutrophil membrane and at this site is more resistant to inactivation by endogenous protease inhibitors. Detection of membrane bound elastase is prohibited when studying BAL fluid or supernatant samples.[279-281] In view of this, as levels of protease inhibitors correlate well with ARDS risk, they are potentially better biomarkers of lung injury.[282]

4.2 Neutrophil specific knockout of Sema3F does not alter neutrophil transit through the lung tissue

4.2.1 Ex-vivo lung imaging shows exogenous Sema3F in vivo retains neutrophils external to the vasculature

As shown in chapter 3 neutrophil transit time to the alveolus and neutrophilic resolution is manipulated by Sema3F signalling. To assess neutrophil transit during ALI the location of the neutrophil population needed to be determined. In order to delineate the location of the WT, KO or Sema3F treated neutrophils I collaborated with Dr Leo Carlin at the Beatson institute. Following ALI, mice were culled, and lungs instilled with agarose gel, fixed and sectioned. They were stained to identify the neutrophils (S100A9 red) and blood vessels (CD31 green) and slices were imaged using confocal microscopy (figure 4.2.1-1, image A). Images were processed, and rendered in 3D by Imaris software, shown in the small blown up section of image A (B). Using the definitions shown in diagram C, neutrophils were identified and counted. Then locations were assigned to the neutrophils as shown in Figure 4.2.1-1: alveolar space D, peri-vascular E and vascular F. Following the protocol shown in figure 4.2.1-2 A, it was observed that intra-tracheal Sema3F treatment at peak recruitment, 24 hours post ALI, retained neutrophils in alveolar space. This supports the previous observation of elevated BAL counts following IT Sema3F treatment. There were more neutrophils in the Sema3F treated lung compared to PBS per μm^3 (****P<0.0001, n=13) (figure 4.2.1-2, graph B). This was accounted for by a significant increase in neutrophils in alveolar space rather than those associated with vasculature (****P<0.0001, n=13).

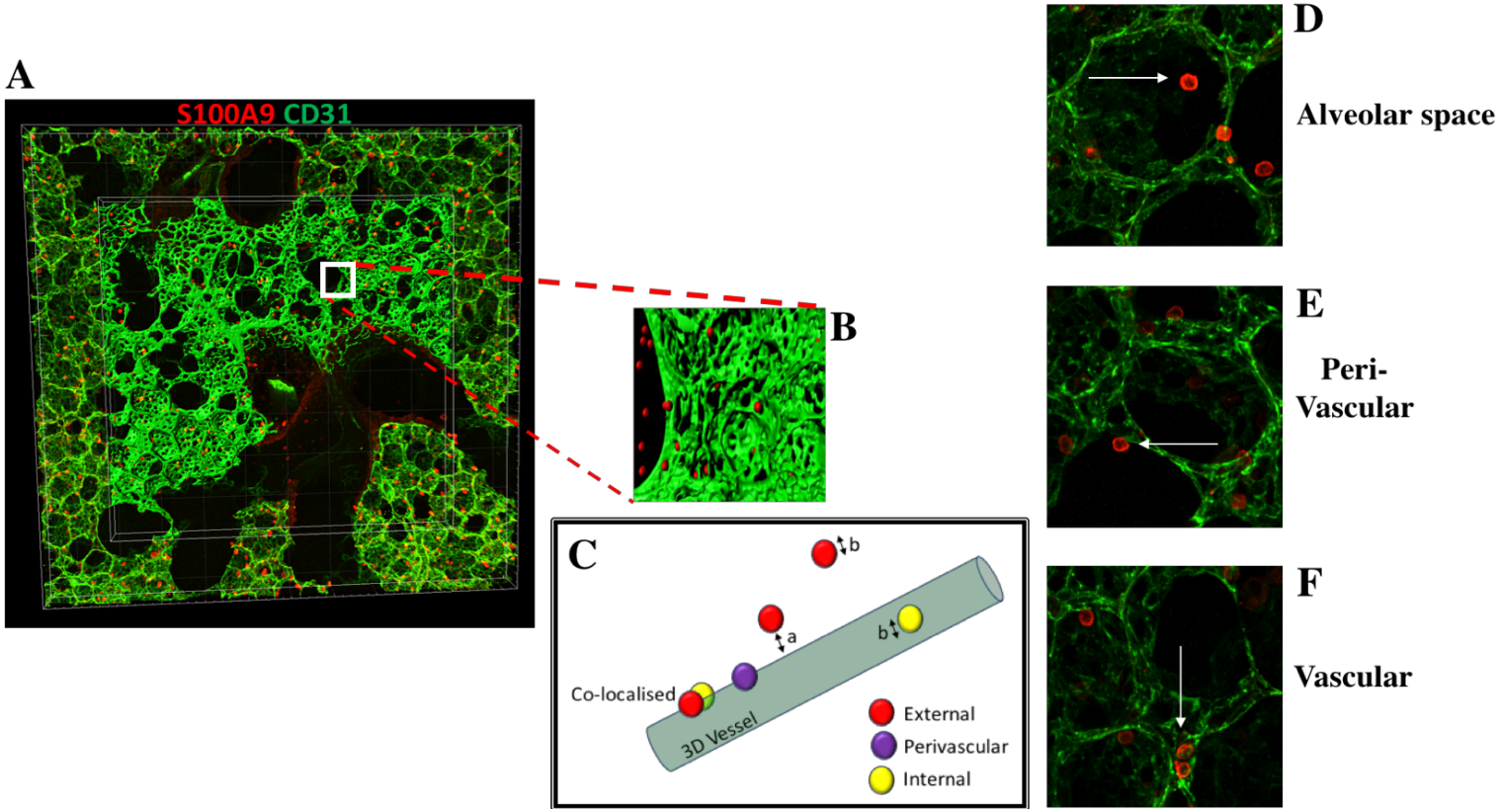

Figure 4.2.1-1 Identification of the location of neutrophils with respect to the pulmonary vasculature in fixed murine lung slices
Murine lungs were instilled with agarose gel and fixed, then stained for CD31 (green) to denote the endothelial cells and S100A9 (red) identifying the neutrophil population. Lungs were imaged using a confocal microscopy (Zeiss LSM 880 with Airyscan) (A). For each animal 2 x 1mm areas of lung were imaged and analysed using Imaris software (Imaris V 8.3). Each slice underwent 3D reconstruction of the vessels shown in the inner square in image B. Further to this, neutrophils were identified as being external to the vessel (>10μm from the vessel surface distance "a" and larger than internal neutrophils size "b") or internal (smaller than external neutrophils size "b") (diagram C). Where alveolar space (D) and vascular (F) neutrophils co-localised these were classified as peri-vascular neutrophils (E).

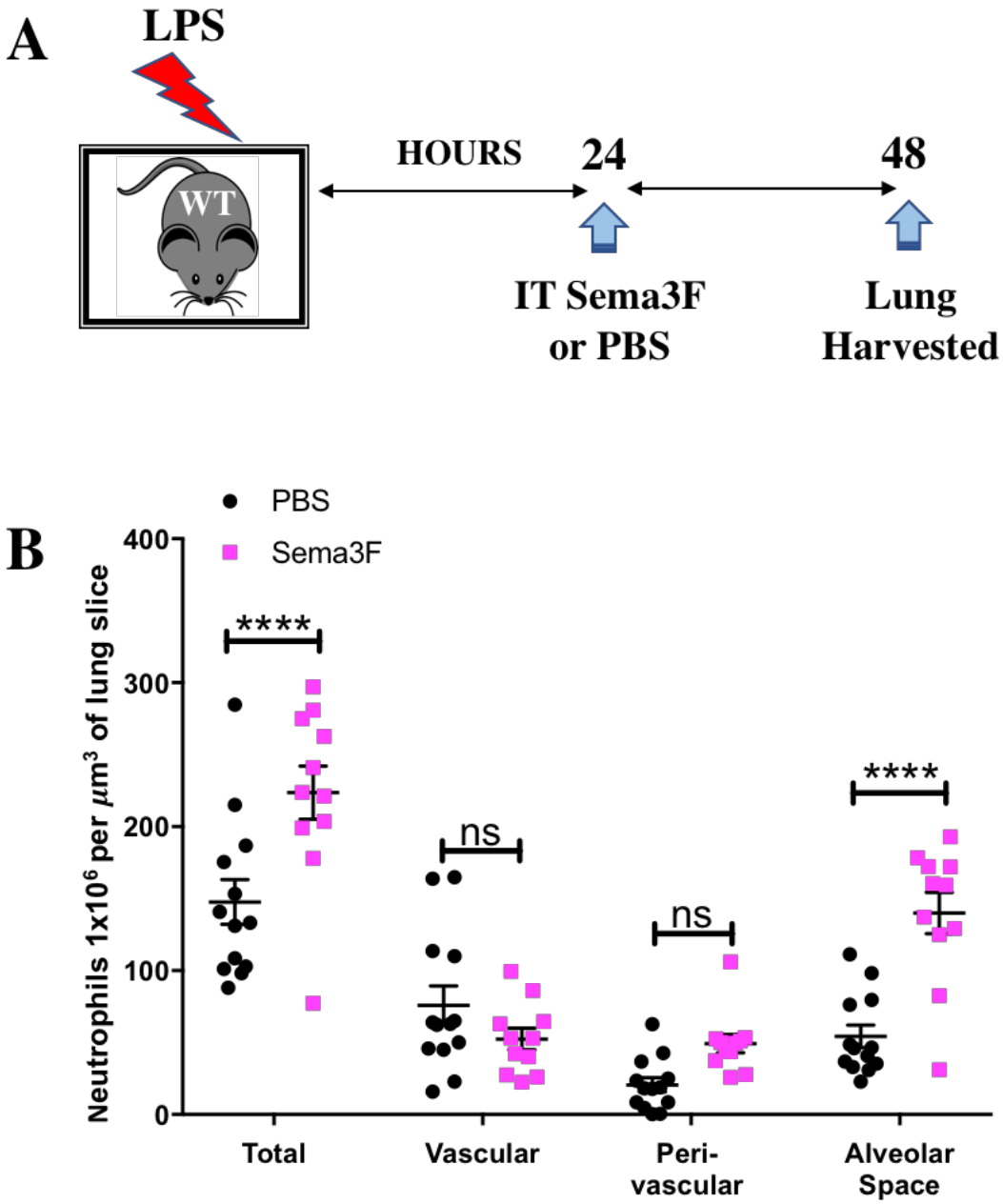

Figure 4.2.1-2 Exogenous Sema3F retains recruited neutrophils in a murine model of lung injury at 24 hours

Intra-tracheal (IT) recombinant Sema3F (1μM) or phosphate buffered saline (PBS) was administered to wildtype C57BL/6 mice 24 hours post nebulised LPS challenge and were sacrificed at 48 and 72 hours (Experimental protocol A). Murine lungs were instilled with agarose gel, fixed and stained to identify the location of the neutrophil population. Lungs were imaged using a confocal microscopy and neutrophil location assigned using Imaris software (Imaris V 9.1) and neutrophil number per μm^3 of lung tissue is shown. There are significantly more neutrophils in the lung tissue following IT Sema3F treatment compared to PBS and this is accounted for by a rise in neutrophils found in the alveolar space. Data are shown mean ± SEM, n=13 over 2 experiments. Analysed using two-way ANOVA, with a post-test correction for multiple comparisons (Sidak), ****P<0.0001.

4.2.2 Sema3F deficient neutrophils transit from blood to alveolar space faster than wild-type neutrophils in early acute lung injury

Following on from the finding that neutrophils deficient in Sema3F are recruited more avidly into the injured murine lung 6 hours post ALI (Figure 4.2.2-1, graph A) I began to investigate the mechanism of this enhanced transit. Neutrophils transmigrate from the blood, through the adjacent endothelial layer and lung tissue to emerge, following transmigration of the epithelial layer, into the alveolar space (4.2.2-1, diagram B - red arrow). It has been demonstrated that in health the majority of circulating neutrophils form a marginated intravascular pool and further neutrophil sequestration occurs following an insult to the lungs.[9,15] Neutrophil transit time through the cell layers is dependent on many processes. These include neutrophil shape, chemotaxis and adhesion. Also changes in the cell layer to be transmigrated play a part, for example alterations in junctional molecules of endothelial cells allow neutrophil passage.[53] In order to narrow the list of potential candidate mechanisms for Sema3F regulation of neutrophil transmigration I investigated the relative proportion of neutrophils in each compartment: blood, lung tissue and alveolar space (4.2.2-2, diagram A-C).

In parallel to differential BAL neutrophils counts at 2, 6, 24 and 48 hours shown in figure 4.2.2-2, graph A. I looked at both the blood and lung tissue compartments (figure 4.2.2-2, graphs B & C). Following lung injury WT and KO mice were culled at 0 and 6 hours and full blood counts conducted using the Coulter counter method. The differential neutrophil count is shown in graph C. There was no significant difference between WT or KO mice peripheral blood neutrophil counts (P=0.2337). Blood monocyte counts were also unremarkable (data not shown). I quantified the numbers of neutrophils within the murine lung tissue at 2 and 6 hours. Whole lung tissue was isolated from Sema3F KO and WT mice. Using this tissue, I performed a pre-optimised lung digest protocol and then stained cells with a validated antibody panel to identify the neutrophil population by flow cytometry. Total cell counts were also performed.

The data is shown in figure 4.2.2-2 graph C: there was no difference in neutrophil numbers between the WT and KO animal at any of the timepoints investigated. Unpaired *t*-tests were performed: 2 hours (P= 0.472) and 6 hours (P= 0.352) n=6. Despite a clear neutrophil recruitment phenotype seen in the Sema3F KO animal it was surprising there was no difference seen in the lung tissue neutrophil population between genotypes. The full blood versus lung tissue neutrophil counts has limited resolution. The full blood counts would not include the marginated or sequestered neutrophil population.[91] Neutrophils that are marginated/sequestered to the pulmonary capillaries or adhered to the endothelium could be variably accounted for in the lung digest experiment thus the proportion of neutrophils spread across the compartments during transmigration cannot be fully understood from these experiments.

I have previously demonstrated that neutrophil specific loss of Sema3F enhances recruitment to the airways at 6 hours following the initiation of the lung injury (4.2.2-1, graph A). Using the same method employed in 4.2.1, I focused on this 6-hour timepoint and neutrophil location data was collected for the WT and KO animals. The mean total neutrophil count for the WT lung was 180.1 neutrophils per μm^3 and 136.6 neutrophils per μm^3 for the KO lung. From these raw counts there appeared to less neutrophils in the KO lung however there was no statistical difference between groups (*t*-test, P=0.5049 n=5). When looking at the relative percentage of neutrophils in each location by genotype there is a significant increase in the percentage of neutrophils found in the alveolar space in the KO animal (*P=0.0401, n=5). As a reflection of the increased neutrophil percentage in the alveolar space, there is a trend towards lower neutrophils percentages in both the peri-vascular and vascular compartments of the KO animal (P=0.727 and P=0.0844, respectively).

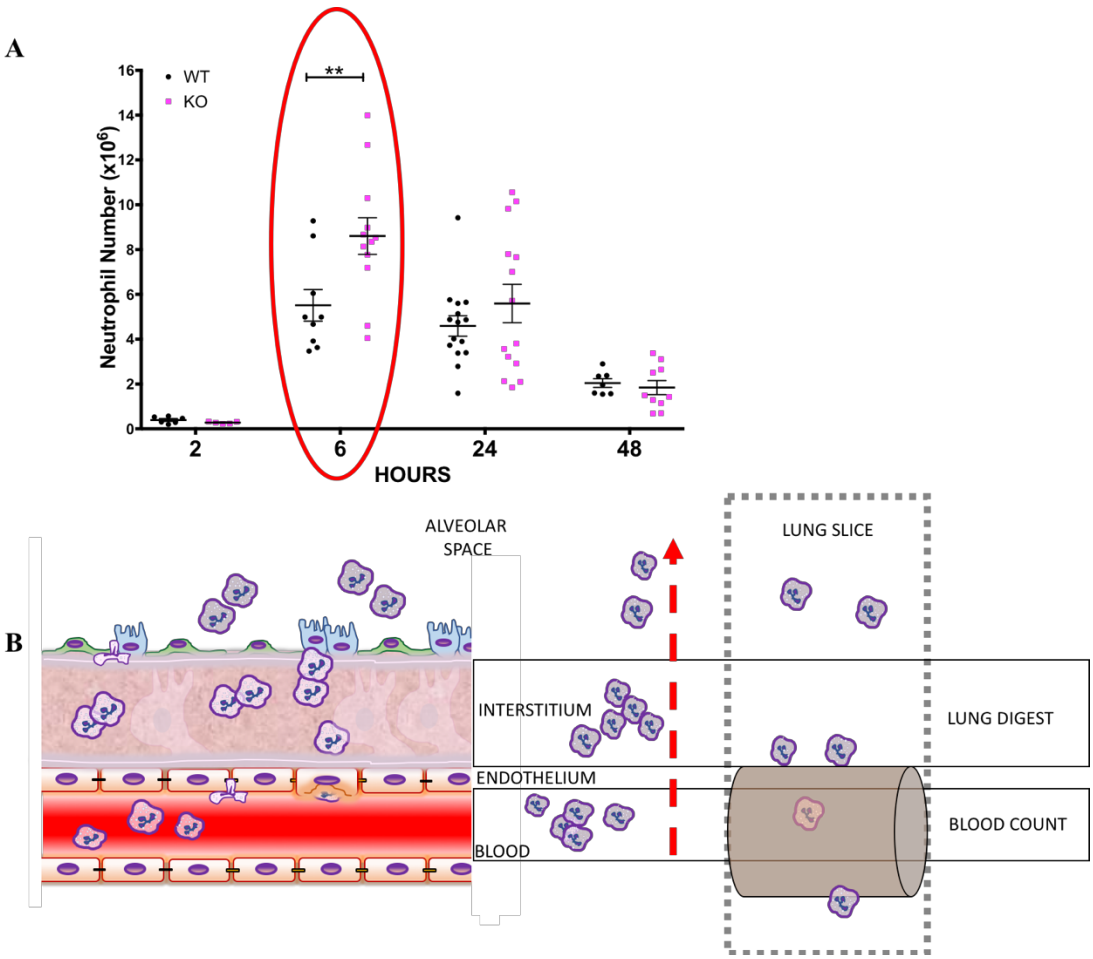

Figure 4.2.2-1 Investigating the transit of Sema3F deficient neutrophils 6 hours post-acute lung injury

Graph A (also shown in figure 3.6.1-1) highlights that following ALI more Sema3F deficient neutrophils are found in the injured lung at 6 hours. Diagram B shows neutrophil transit (red arrow) from the pulmonary capillary where neutrophils crawl and undergo transmigration through both the endothelium (via either transcellular or paracellular route) and the lung interstitium to finally emigrate through the epithelial layer into the alveolus. Also identified are the experimental approaches to quantifying neutrophil transit at this time point. The blood count which identifies the circulating neutrophil count, the lung digest which demonstrates the neutrophil population in the lung tissue and the lung slice which pinpoints the location of the neutrophil with respect to the endothelium.

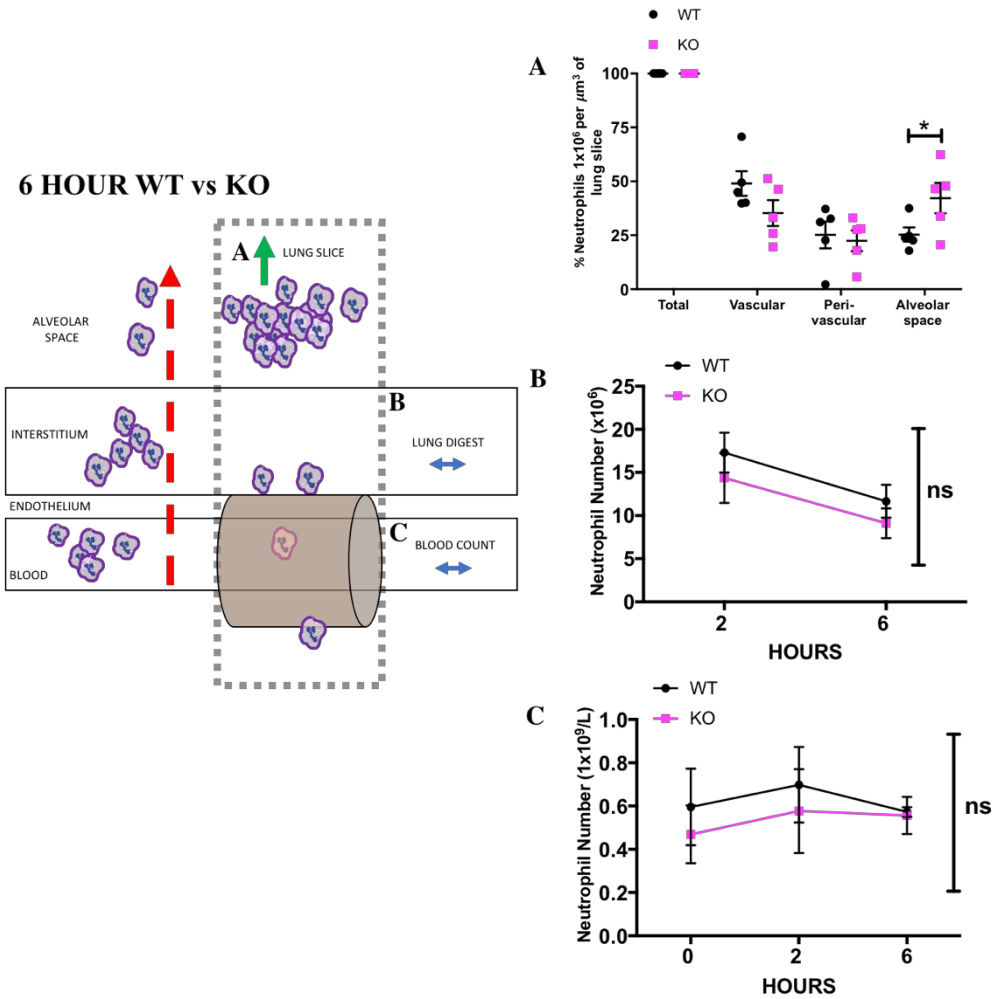

Figure 4.2.2-2 Loss of neutrophil Sema3F increases neutrophil transit from the blood to the alveolus

The diagram relates each data set to the lung compartment examined: A. Lung slice [neutrophil relationship to endothelium] B. lung tissue and peripheral blood C. (A) WT (Sema3F^{floxflox}MRP8cre$^{-/-}$) and KO (Sema3F^{floxflox}MRP8cre$^{+/-}$) were challenged with LPS and sacrificed at 6 hours and lung tissue obtained. Murine lungs were instilled with agarose gel, fixed and stained to identify the location of the neutrophil population. Lungs were imaged using a confocal microscopy and neutrophil location assigned using Imaris software (Imaris V 9.1). The percentage of the neutrophil number per μm^3 of lung tissue is shown (A). There is a significant increase in the proportion in the airway (alveolar space) in the KO animal compared to WT. Data are shown mean ± SEM, n=5 over 2 experiments. Analysed using two-way ANOVA, *P<0.05. (A) At 0, 2 and 6 hours following nebulised LPS, WT and KO mice were sacrificed. Venepuncture was performed and full blood counts analysed, neutrophils numbers are shown in graph B, data are shown ± SEM n=3 analysed by two-way ANOVA. (C) WT mice and KO murine lungs from 2 and 6 hours were harvested and enzymatically digested. Cellular populations were identified using flow cytometry. Data are shown ± SEM n=4-6, analysed by unpaired *t*-tests. (

.

4.3 Sema3F modulates neutrophil function in vitro

4.3.1 Sema3F treated neutrophils display blunted chemotactic responses

In order to gain access to sites of inflammation neutrophils migrate through challenging microenvironments towards chemoattractants.[283] I had established that acutely, neutrophils deficient in Sema3F migrate faster into the air space post lung injury. Previous data shown in this chapter did not highlight a significant corresponding decrease in Sema3F KO neutrophils in either the wider circulation or associated with the pulmonary vasculature which would be expected if adhesion pathways were altered, facilitating rapid transit. As such, it suggests that this recruitment phenomenon was probably due an intrinsic property of the cell rather than an interaction between the neutrophil and the barriers to transmigration. As such, I wished to determine the effect of Sema3F upon neutrophil migration. I isolated peripheral human neutrophils and observed chemotaxis in a simple Boyden chamber assay, where human neutrophils are co-incubated with Sema3F (top of chamber) and migration towards known chemoattractants (well of chamber) measured (figure 4.3.1-1, diagram of chamber A). Neutrophils were cultured in exogenous recombinant Sema3F [100nM] and chemotaxis was measured towards known neutrophil chemoattractants either IL8 [100nM] or fMLF [100nM] (figure 4.3.1-1). A positive control (incubation without Sema3F), negative control (no fMLF or IL8) and chemokinesis control (incubation with fMLF or IL8) were included. Whilst Sema3F is not a chemoattractant itself, incubation with sema3F inhibits ex-vivo human neutrophils migrating towards both chemoattractants. Sema3F 100nM reduced neutrophil migration toward both high dose fMLF [100nM] and dose IL8 [100nM] (**$P<0.01$ and ****$P<0.0001$ respectively n=4-6). Sema3F treatment modulated fMLF- and IL8-induced neutrophil chemotaxis in a dose-dependent manner.

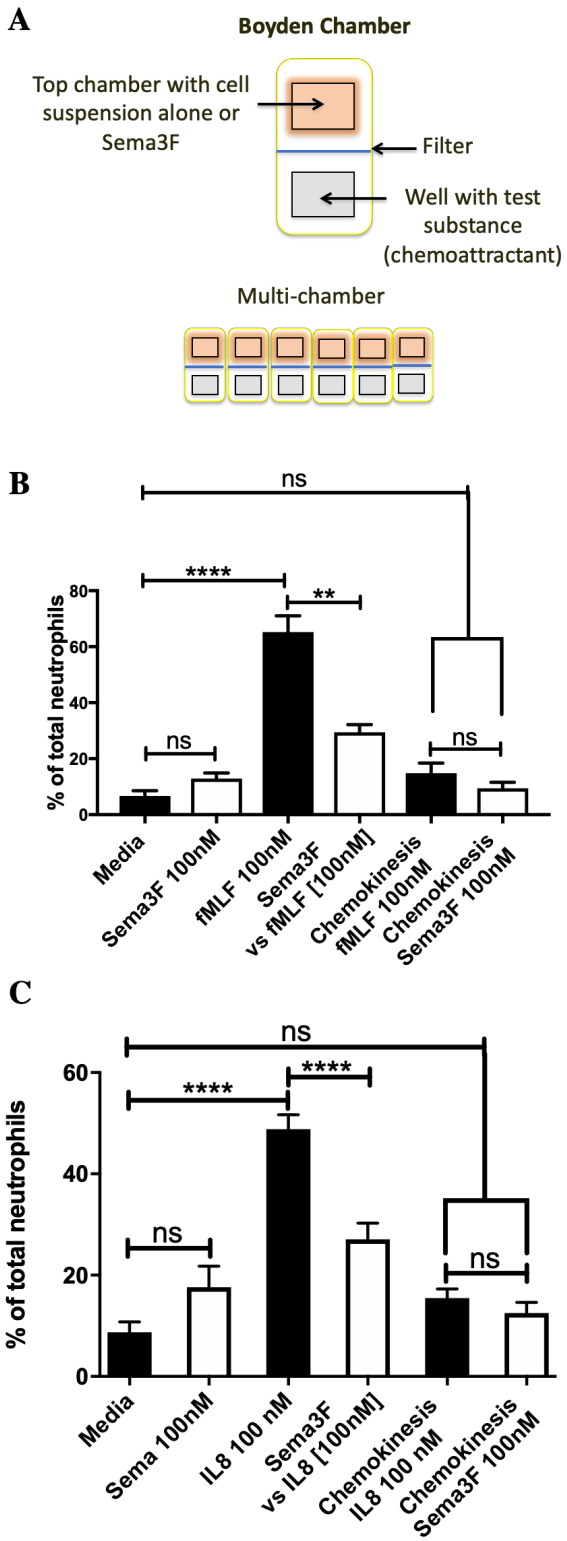

Figure 4.3.1-1 Sema3F treated neutrophils display blunted chemotactic responses. Diagram A shows Boyden-type transwell assay, neutrophils are incubated with Sema3F above the filter and chemoattractant is placed into the well. (B&C) Isolated peripheral blood neutrophils from healthy volunteers were incubated with recombinant Sema3F [100nM], and the chemotactic behaviour of neutrophils to both fMLF & IL8 [100nM] determined by Boyden chamber. ,Data shown are mean ± SEM, n=4-6 analysed using two-way ANOVA; **P<0.01, ***P<0.001 & ****P<0.0001.

4.3.2 Sema3F acts as a neutrophil retention signal in *vitro*

Transwell assays have significant limitations to assess neutrophil migration yet are relatively easy and therefore widely used. It gives an endpoint readout only and provides no further information on the pattern of cell migration. To investigate further the effect of Sema3F on neutrophil migration I collaborated with Dr Felix Ellett a Clinical Fellow at Harvard medical school. The chemoattractant LTB4 is loaded into the chamber and washed through the channels creating a stable gradient for up to eight hours.[89] The narrow 8μm diameter channels replicate the pulmonary capillaries. A drop of whole human blood is placed on the opposing pole and only the neutrophil population are able to migrate to the start of the channels through the first section of the chip assay (figure 4.3.2-1, diagram A). Real-time light microscopy is used to monitor the neutrophil journey to the chamber and retrotaxis (against the preserved gradient, away from the chamber). Every ~5min the percentage of maximal recruitment to the chamber was calculated. The inflection point represents maximal recruitment; after this point declining percentages represent retrotaxis and not apoptosis as these cells can be viewed actively leaving the chamber against the maintained gradient.

Graph B (figure 4.3.2-1) shows accumulative percentage of maximal recruitment to the chamber over time. With Sema3F pre-incubation, there is a significant dose-dependent reduction in recruitment. Untreated neutrophils moved to the chamber significantly faster than those pre-treated with Sema3F 10nM (P**=0.0019). Increasing the dose of Sema3F to 100nM slowed neutrophil locomotion further (P****=0.0001). Maximal dose of Sema3F 1000nM resulted in the largest reduction in neutrophil migration to the chamber over time (P***=0.0006). Moreover, after reaching the inflection point (where maximal recruitment is achieved) the highest dose of Sema3F, 1000nM (black line) retains the neutrophils in the chamber for 90 minutes. In contrast, the lower doses of Sema3F and untreated neutrophils appear to move away from the chamber and against the LTB4 gradient performing retrotaxis in a dose

dependent manner. The untreated group has the largest percentage of neutrophils that undergo retrotaxis.

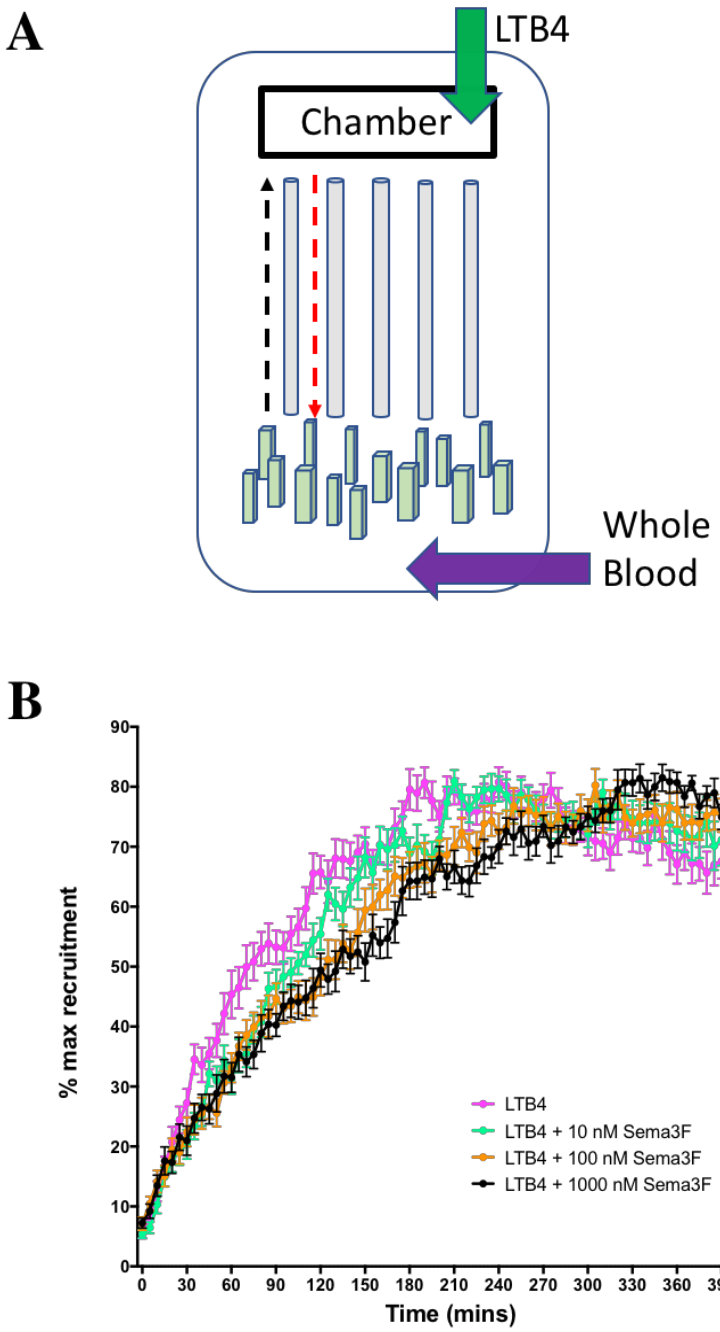

Figure 4.3.2-1 Pre-treatment with Sema3F retains neutrophils with reduced chemotaxis and retrotaxis

A chip assay was used to assay the migration of human neutrophils in response to LTB4 [100nM] diagram A, where only neutrophils can exit the blood and progress to the migration channels. In graph B a significant dose dependent reduction in neutrophil migration seen following Sema3F pre-treatment [0-1000nM]. Data shown are mean ± SEM, n=3 analysed by two-way ANOVA with Dunnett's post-test correction for multiple comparisons. LTB4 vs LTB4 & Sema3F 10nM P**=0.0019 LTB4 vs LTB4 & Sema3F 100nM P****=0.0001 LTB4 vs LTB4 & Sema3f 1000nM P***=0.0006.

4.3.3 Sema3F does not alter neutrophil expression of Cd11b or L-selectin in response to LPS

Loss of neutrophil Sema3F enhances neutrophil transit into the alveolus post LPS lung injury. Semaphorins have been shown to regulate integrin adhesion and expression in tumour cells, axons, dendritic cells and during angiogenesis.[169,233,242,284] Following culture with LPS, CD11b expression increases in a dose dependent manner (figure 4.3.3-1, graph A) and L-selectin is shed (graph B). This is consistent with the literature and the well characterised neutrophil response to LPS, where CD11b surface expression is rapidly up regulated with concurrent loss of L-selectin.[285] Sema3F treatment does not alter this pattern of expression, and Sema3F alone causes no change in neutrophil expression of either CD11b or L-selectin.

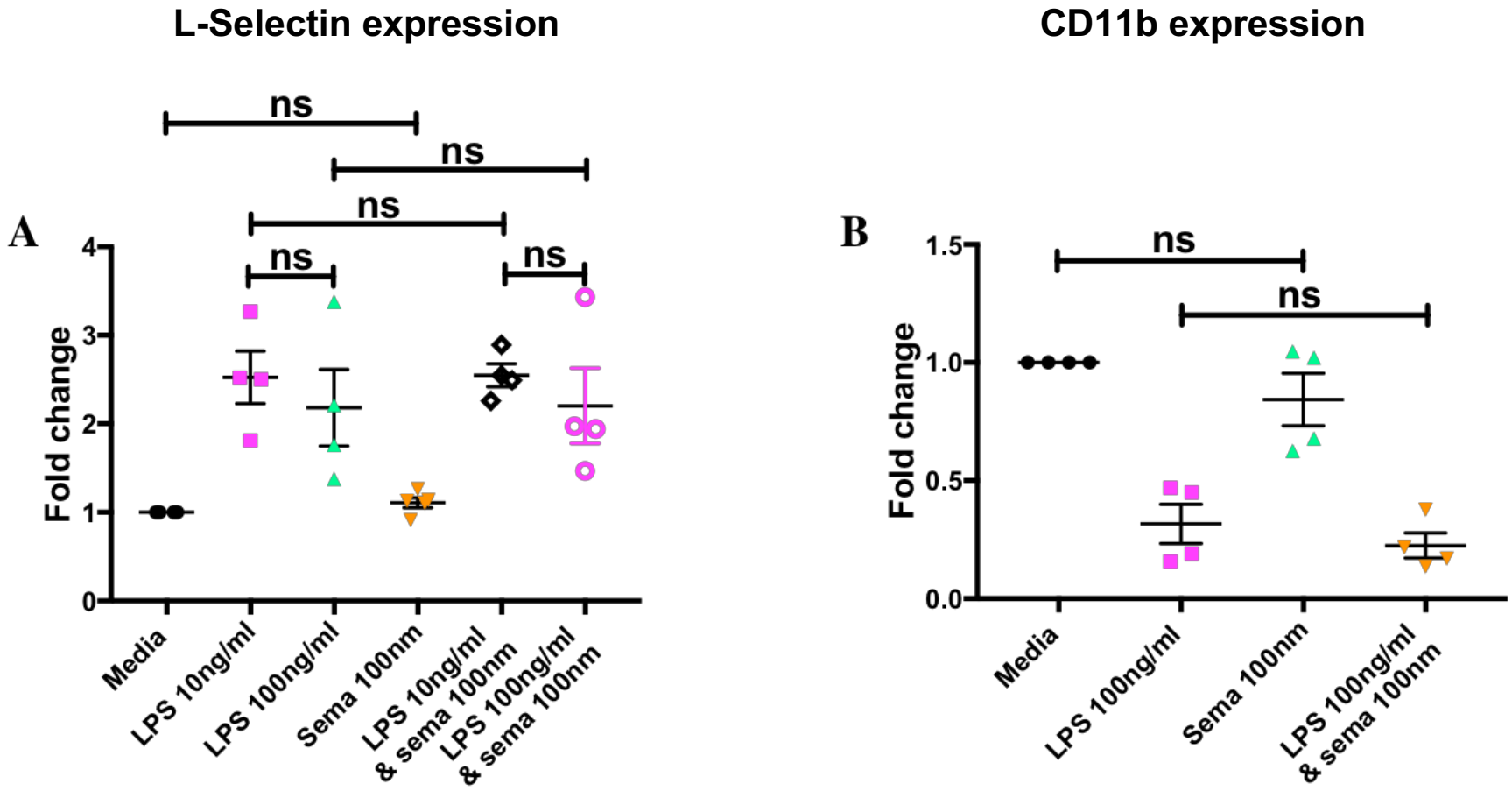

Figure 4.3.3-1 Sema3F does not alter the expression of CD11b or L-selectin following treatment with LPS
Human neutrophils were cultured in the presence/absence of LPS (0, 10 or 100ng/ml) and Sema3F (0 or 100nm), then stained with PE-anti-CD11b (A) or PE-anti-L-selectin (B) and geometric mean fluorescence determined by flow cytometry and fold change from control (media and vehicle control) data are shown ± SEM, n=4 analysed by two-way ANOVA.

4.3.4 Sema3F treated neutrophils undergo cell rounding

Neutrophil sequestration in the lung is closely linked to the property of deformability which is regulated by the F-actin cytoskeletal arrangements and is associated with submembrane F-actin deposition and neutrophil roundness.[56,57] Similarly, the formation of pseudopodia and lamellipodia are integral for cell motility. Generalized loss of these protrusions leads to cell rounding.[163] During the migration assays I observed that Sema3F treatment caused marked rounding of neutrophils. Images in figure 4.3.4-1 are examples of this observation, images A-C show untreated quiescent neutrophils, D-F show fMLF shaped changed neutrophils and G-I show hyper-round Sema3F treated neutrophils. While assessing Sema3F-treated neutrophils during multiple experiments this phenotype appeared clear to me as the observer, but exact quantification was required to establish objectively whether Sema3F causes cell rounding.

To answer this question, I isolated neutrophils from healthy volunteers and cultured them in media with autologous serum and Sema3F [10nM, 100nM]. Following 40mins of incubation with Sema3F, cultured neutrophils were treated with 100nM of fMLF and fixed after 15 minutes. These neutrophils were then stained to differentiate the nucleus, cytoplasm and actin. Images were taken using the Operetta high content imaging system. Example images are shown in figure 4.3.4-1 these were taken at x40 magnification to show the morphology of the hyper-round Sema3F treated cells compared to control or fMLF treated neutrophils. Associated software was used to quantify cell roundness and the results are shown in the graph in figure 4.3.4-2. Images for the roundness analysis were taken at x20 magnification as this increased the number of cells analysed. Each well represents a treatment group and had a minimum of 4 replicates; within each well 23 fields were imaged and on average 1000 cells per field analysed. Roundness was determined by the sequential use of cell masks in an optimized algorithm and roundness values displayed between 0 and 1, where 0 represents a line and 1 a perfect circle.

Neutrophils were rounder when co-incubated with Sema3F [10nM, 100nM] in a dose dependent manner (figure 4.3.4-2). The rounding effect was overcome by treatment with fMLF [100nM]. Untreated neutrophils in culture medium had a mean roundness value of 0.935 ± 0.005 compared to Sema3F treated neutrophils which had a significantly higher roundness value of 0.966 ± 0.005 (****P=0.0003).

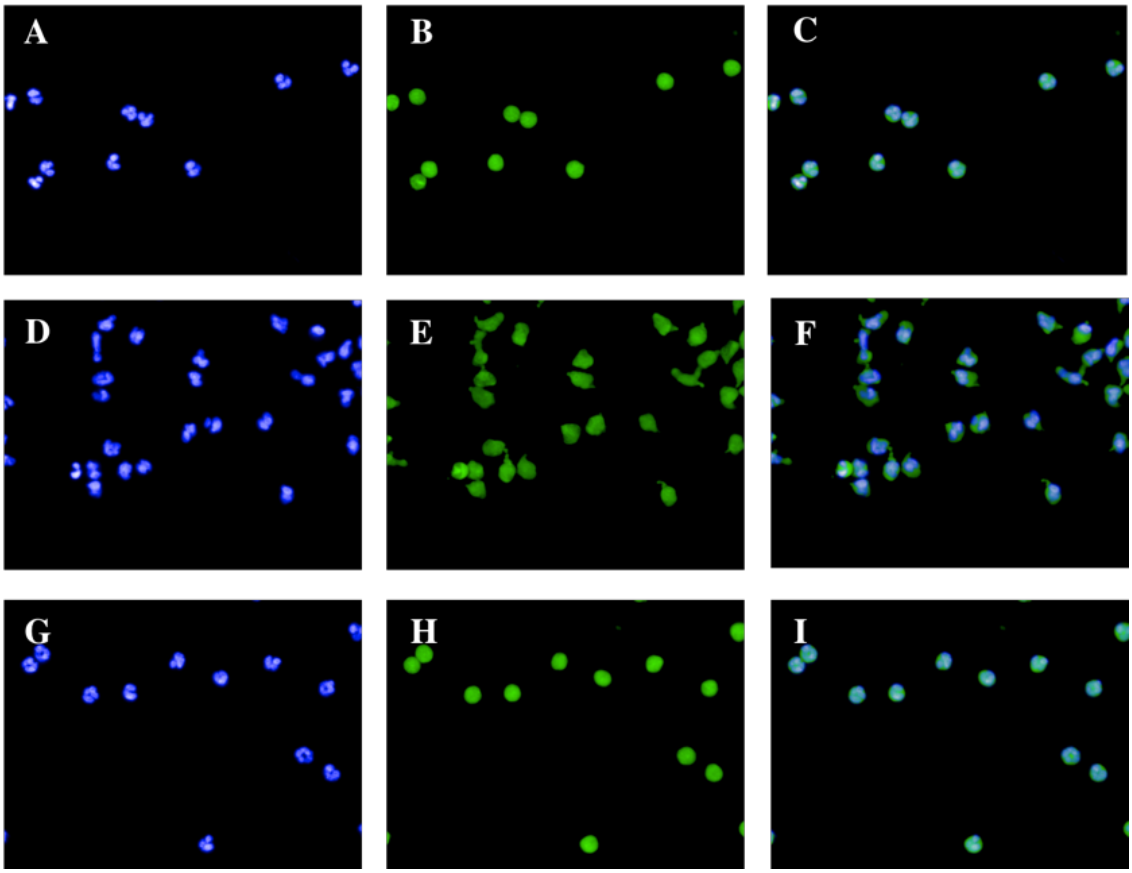

Figure 4.3.4-1 Sema3F treated neutrophils undergo cell rounding
Isolated peripheral blood neutrophils from healthy volunteers were incubated with recombinant Sema3F [0-100nM] and fMLF 100nM. Neutrophils were cultured in media for 40 mins then treated with fMLF and fixed after 15 minutes. Cells were then stained with DAPI (4',6-Diamidino-2-Phenylindole, Dihydrochloride), HCS CellMask™ Green stain and Alexa Fluor® 594 conjugated Phalloidin. Images were obtained using an Operetta High-Content Imaging System. Representative images taken at x40 magnification are shown in the figure; DAPI (A, D & G), HCS CellMask™ Green (B, E & H) and dual staining (C, F & I). Images A-C show untreated neutrophils, images D-F show neutrophils treated with fMLF and images G-I show neutrophils treated with Sema3F 100nM.

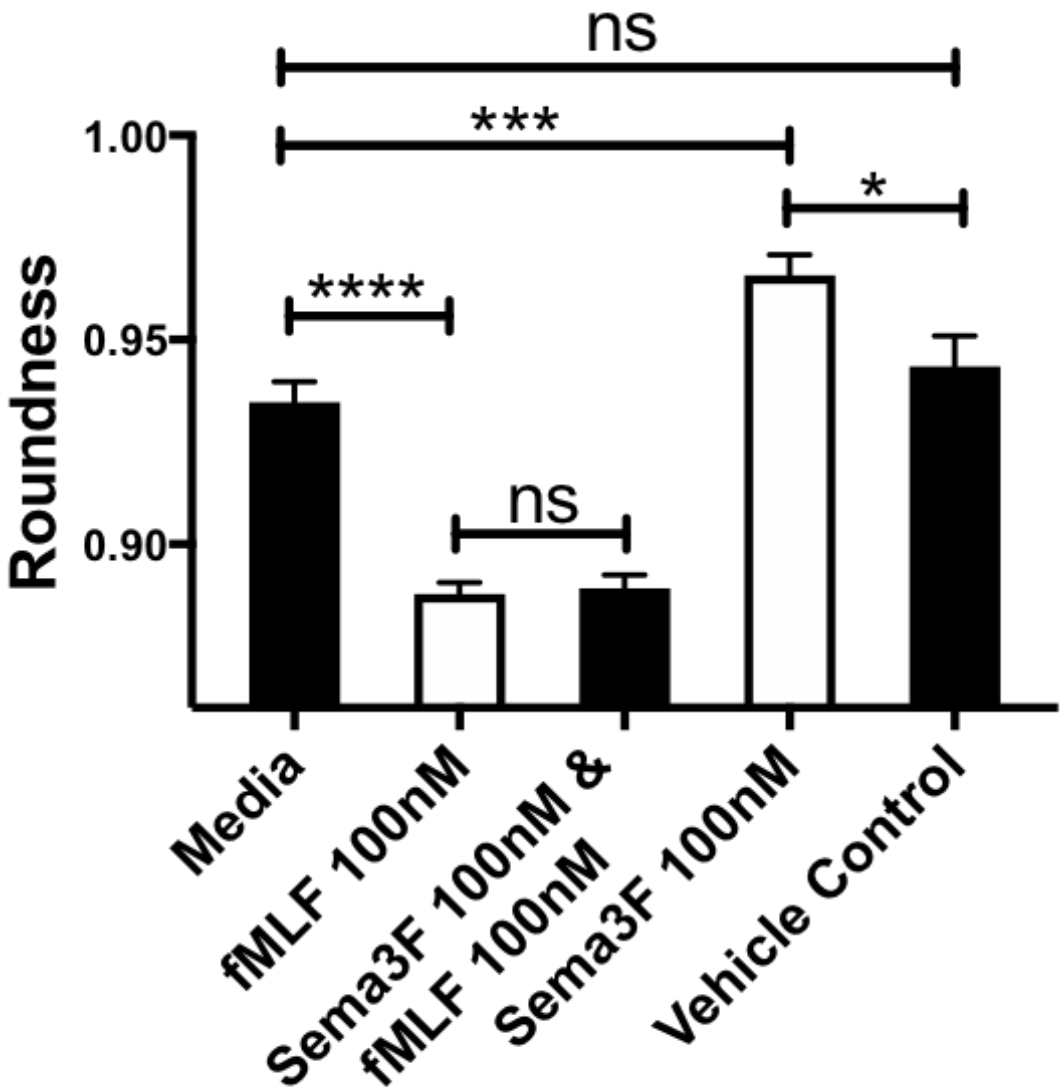

Figure 4.3.4-2 Sema3F treated neutrophils are rounder
Isolated peripheral blood neutrophils from healthy volunteers were incubated with recombinant Sema3F [0-100nM] and fMLF 100nM. Neutrophils were cultured in media for 40 mins then treated with fMLF and fixed after 15 minutes. Cells were then stained with DAPI (4',6-Diamidino-2-Phenylindole, Dihydrochloride), HCS CellMask™ Green stain and Alexa Fluor® 594 conjugated Phalloidin. Images were obtained using an Operetta High-Content Imaging System and analysis of roundness performed by Harmony® analysis Software. Data shown are mean ± SEM, n=4 analysed using paired *t*-tests, *P<0.05, **P<0.01 & ****P<0.001.

4.3.5 Human neutrophils treated with Sema3F have preserved phagocytosis

Sema3F signalling alters neutrophil migratory behaviour. Phagocytosis is an important cytotoxic neutrophil function which is regulated by cell shape and actin dynamics. To determine whether Sema3F could also inhibit phagocytosis I examined the phagocytosis of both Zymosan granules and fluorescent labelled *E. coli* results are shown in figure 4.3.5-1, graph A. Neutrophils were co-incubated with opsonised Zymosan A particles and phagocytic index (PI) calculated, negative controls were included where Zymosan granules were absent [not shown]. There was no inhibition of phagocytosis in the neutrophils treated with Sema3F as shown in graph A. The mean PI for untreated was 0.53±0.071 compared to Sema3F treated which was 0.585±0.071, P=0.58. Neutrophils were incubated with fluorescently labelled *E. coli* and internalization assessed by flow cytometry. Sema3F did not significantly reduce internalisation of the labelled *E. coli*, P=0.27, n=3 (figure 4.3.5-1, graph B).

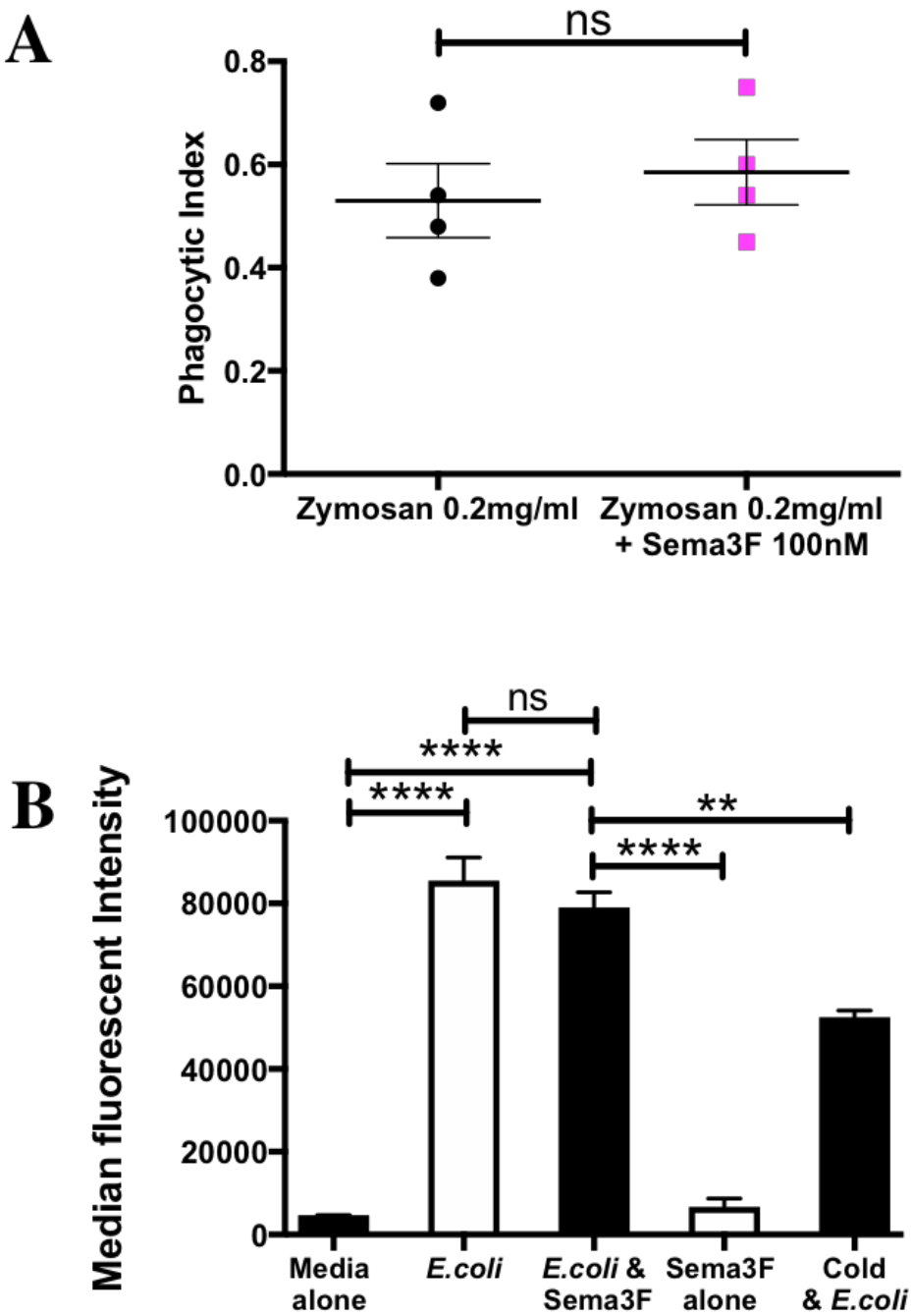

Figure 4.3.5-1 Human neutrophils treated with Sema3F have normal phagocytosis

(A) The phagocytotic index was calculated from cytospins of healthy human neutrophils treated with Sema3F and cultured with opsonised Zymosan particles for 30 minutes. (B) Flow cytometry analysis of intracellular Alex® 488 *E. coli* was undertaken following 30 minutes culture of human neutrophils. A cold control was performed, neutrophils were also incubated with Alex® 488 *E. coli* at 4°C to identify the energy dependent internalisation from external binding of the labelled *E. coli* to the neutrophils. Data shown are mean ± SEM, n=4 (A) and n=3 (B) analysed using unpaired *t*-tests, *P<0.05, **P<0.01 & ****P<0.001.

4.3.6 Sema3F reduces neutrophil myeloperoxidase activity

While Sema3F treatment does not alter phagocytosis, I wondered if other neutrophil effector functions would be modulated by Sema3F. Given that the accumulating evidence suggested that Sema3F regulates the neutrophil cytoskeletal and, that the re-arrangement of the actin cytoskeleton is necessary for neutrophil degranulation I looked at the one of the functional consequences of neutrophil degranulation - myeloperoxidase (MPO) activity.[235] The activity assay measures the peroxidase capacity of the myeloperoxidase enzyme released during neutrophil degranulation in culture supernatant. Neutrophils were cultured with and without Sema3F for 1 hour, then stimulated with GM-CSF for 30 minutes and fMLF for 10 mins ensuring maximal degranulation.[286] The supernatant was immediately removed and promptly analysed. The myeloperoxidase-catalysed oxidation of 3,5,3‘,5‘-Tetramethylbenzidine (TMB), which uses H_2O_2 as a substrate, results in a colour change and is analysed using spectrometry. In figure 4.3.6-1 A, the graph shows that following Sema3F 100nM treatment there is a significant reduction in MPO activity.

In a similar manner, to elucidate whether Sema3F treatment can regulate neutrophil degranulation and enzyme activity I assessed the elastase activity (graph B). This was performed following the same conditions used for the myeloperoxidase assay. Elastase is another component of primary granules; unlike MPO it is a peptidase and breaks down proteins. In this way elastase driven enzymatic digestion of a quenched fluorochrome removes the quenching and produces a signal. This assay did not show any differences in elastase activity following Sema3F treatment (P=0.5146).

These two enzymes were chosen for their important role in host defence and tissue damage. They may also have a role as biomarkers of ongoing lung inflammation and have been used as markers of lung injury throughout the literature. [11,268] Both are contained within the same neutrophil granule (primary/azurophilic granules) when released from activated neutrophils.

There exists debate over the relevance of granule specify to the pathogenesis of tissue injury. It is postulated that different neutrophil granules release a spectrum of enzymatic and toxic contents and as such may not form a useful experimental or biological distinction. These assays do not directly evaluate neutrophil granule exocytosis itself and would be an interesting future area of research beyond the scope of this current project. [2]

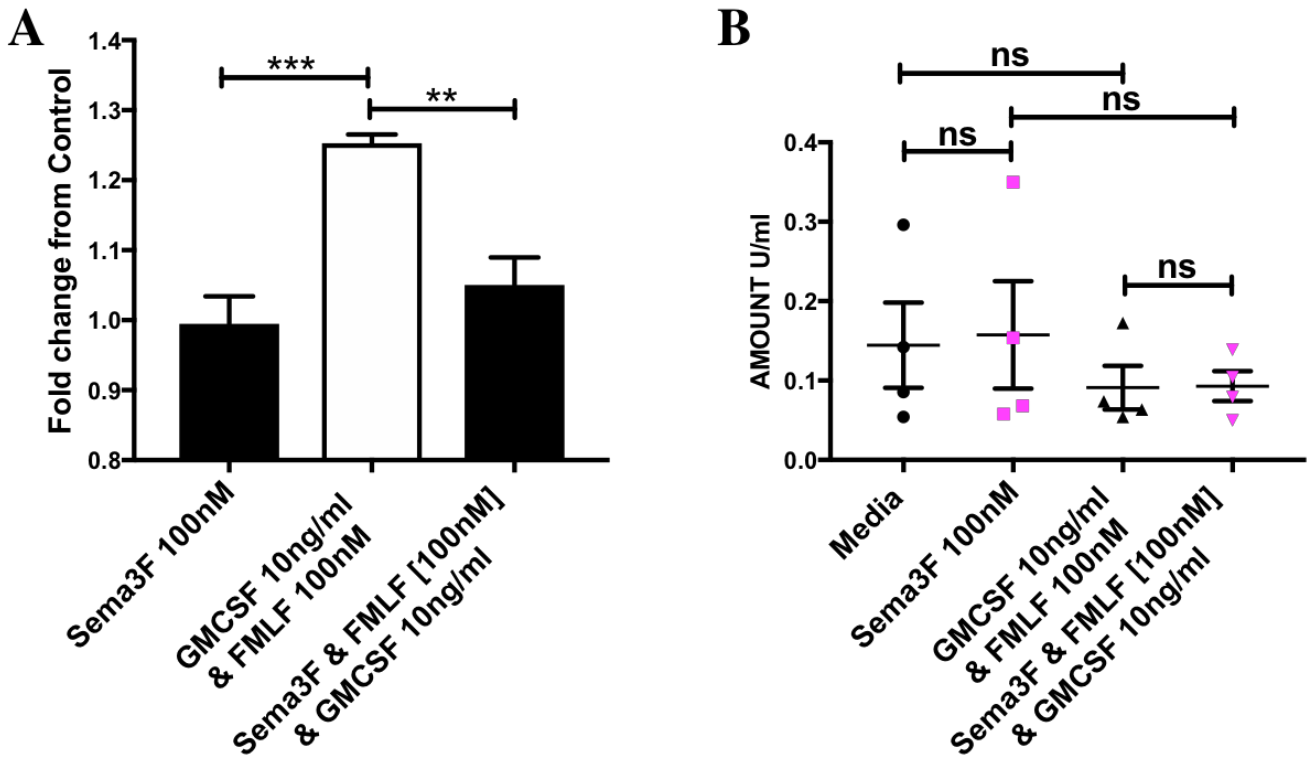

Figure 4.3.6-1 Pre-treatment with Sema3F does not alter neutrophil elastase activity in cell culture supernatant but neutrophil Myeloperoxidase activity is reduced

Following culture with Sema3F for 1 hour, Granulocyte-macrophage colony-stimulating factor (GMCSF) was given for 30min and FMLF for the final 10 min, then supernatant harvested. Either the peroxidase utilisation of 3,3′,5,5′-Tetramethylbenzidine (TMB, Sigma) by MPO was measured and fold change from control (media alone) shown in graph A or elastase activity in a fluorometric assay graph B. Data shown are mean ± SEM, (A n=3, B n=4) analysed using one-way ANOVA, **p<0.001 & ***p<0.001.

4.3.7 Following stimulation with Sema3F neutrophils treated with N-formylmethionyl-leucyl-phenylalanine have increased radical oxygen species production

Neutrophils generate radical oxygen species (ROS) through the enzyme NADPH oxidase as part of an antimicrobial defence strategy.[4] Following on from the observed reduction in neutrophil MPO activity in response to Sema3F treatment, I hypothesised that other histotoxic agents would be similarly reduced or inhibited and ROS could be reduced by Sema3F treatment. ROS has a unique and direct relationship with the actin cytoskeleton and has been shown to dynamically alter the actin through reversible glutathionylation promoting depolymerisation.[44,61-63] In addition ROS has also been implicated in the internalisation of receptors that detect chemoattractant cues and can arrest neutrophil migration.[264] Given this, I investigated the effect of Sema3F on neutrophil ROS production. In figure 4.3.7-1 the graph shows DCF fluorescence (the ROS detector) following neutrophil culture with various conditions. For each n number, which formed an individual experiment, the values were normalised to the unstained sample to remove any variability in both signal and detection between each experiment. In the media alone group, DCFH-DA was added to delineate a baseline value. As expected fMLF induced a positive in increase in DCF signal and therefore intracellular neutrophil ROS production (media alone vs fMLF *P=0.0131), surprisingly with the addition of pre-incubation with Sema3F 100nM the response to fMLF was increased by 157% (% mean increase, *P=0.0135). There was no difference between fMLF alone and Sema3F 10nM/fMLF (P=0.9573). Sema3F alone at either 10nM or 100nM did not induce ROS production (P=0.6234 & P=0.6429 respectively).

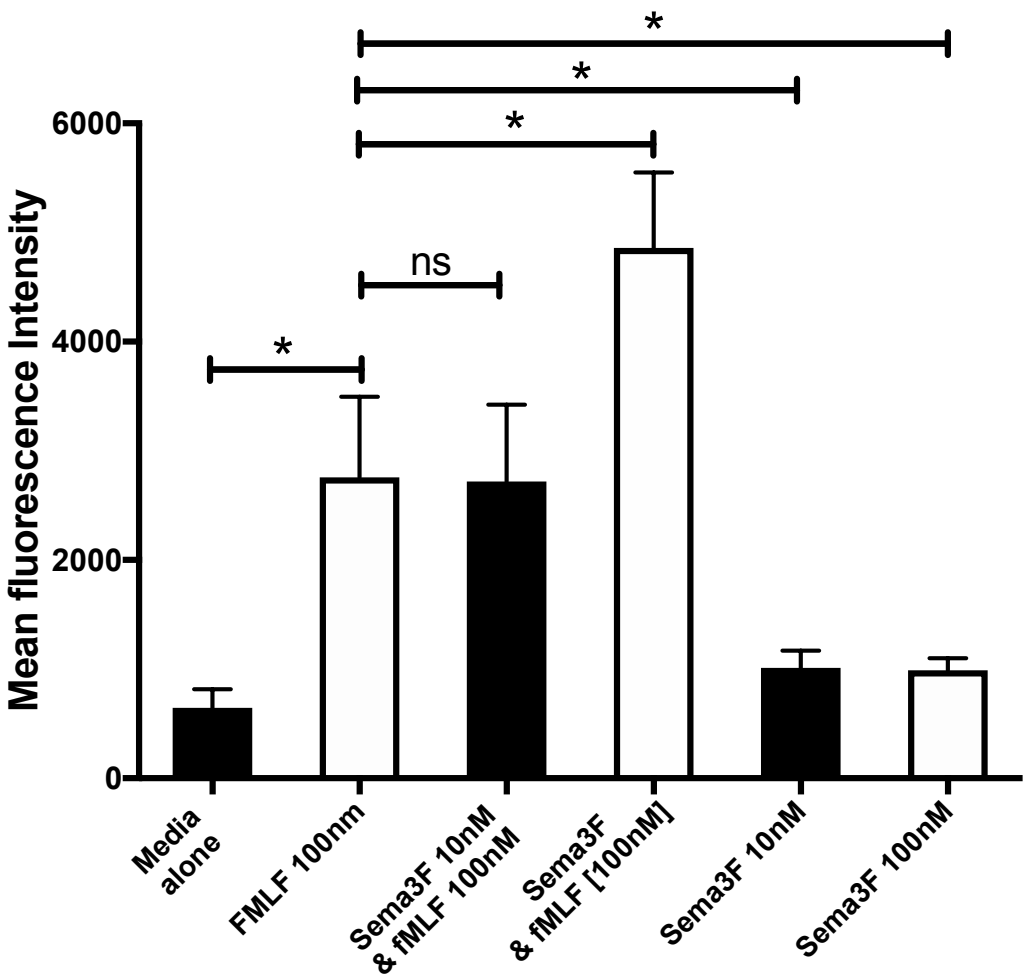

Figure 4.3.7-1 Pre-treatment with Sema3F enhances fMLF induced intra-cellular radical oxygen species in neutrophils
Intra-neutrophil radical oxygen species (ROS) generation was determined following a 1-hour pre-incubation with Sema3F and treatment with fMLF for 30 minutes. The ROS detector substance DCF was measured by flowcytometry. Data shown are mean ± SEM n=3 analysed using one-way ANOVA, *P<0.05.

4.4 In vivo Sema3F reduces neutrophil locomotion through reduction of F-actin content

4.4.1 In vivo Sema3F treated neutrophils are slower but maintain directionality

When investigating the effect Sema3F had on chemotaxis in human neutrophils it became apparent that real-time analysis of neutrophil movement was superior. During neutrophil chemotaxis directionality and speed are linked, however to some degree, they can be regulated independently.[287,288] In order to begin to measure this, a live lung culture experiment was optimised in collaboration with Dr Leo Carlin, Beatson Institute, using Catchup$^{IVM\text{-}RED;LifeAct\text{-}GFP}$ mice. In this transgenic model the murine neutrophils express both the reporter tdTomato and the peptide LifeAct-GFP; the latter facilitates the visualisation of neutrophil F-actin. This allowed accurate locating of the neutrophils in *vivo* and may be amenable to future F-actin quantification. In figure 4.4.1-1 the schematic shows the details of the experimental protocol. The unstimulated transgenic mice were culled, lungs instilled with agarose and sliced. The slice was then placed in RPMI (1% FCS) at 37°C in 5% CO_2. The duration of real-time confocal image acquisition is shown in timeline A. Lung 1 and lung 2 were treated simultaneously, with Sema3F treatment omitted and PBS treatment given to lung 1. Following this 10μM of fMLF was given; this higher dose promotes ROS production and neutrophil chemotaxis declines.[63,64] Initially lung slice movement during imaging created substantial movement artefact which was reduced by: 1) allowing the slice to equilibrate fully to temperature for 1 hour before imaging within the chamber; 2) The tissue harp and steel washer was used to hold the tissue in situ when the stage moved allowing imaging of the other slice, however they did not interfere with either treatments or imaging (B). Image C and D represent the two lung slices, imaged sequentially at positions 1,2,3,4. Only one position can be imaged at a time, to compare conditions in real-time alternating positions were used. All 4 positions were imaged within 60 seconds. Treatments were given in the assigned locations, as shown in diagrams C and D. Using this protocol imaging data was acquired over 110 minutes. Each section of the timeline was

analysed independently using Imaris software and the data is shown in graphs A - C in figure 4.4.1-2. Automated analysis of speed and directionality [track straightness] was used to avoid observer error and bias. The analysis was then manually checked for accuracy. In graph A, average track speed is shown [track length / time between first and last position] and there is no difference between lung 1 & 2 prior to treatments (P=0.21). Following application of Sema3F 100nM neutrophils are significantly slower compared with both the control lung 1 at baseline (***P=0.0003) and the PBS treated lung (lung 1 60 mins vs lung 2 60 mins, *P=0.021). The average speed of the neutrophils in slice 1 at baseline compared to PBS treated slice is unchanged (P=0.112). There is a significant reduction in neutrophil mean track speed following fMLF in both the treated and untreated slices (lung 1 60 mins vs lung 1 30 mins; lung 2 60 min vs lung 2 30 mins). There is no difference between lung 1 and 2 following fMLF (lung 1 30 mins vs lung 2 30 mins). In parallel, track straightness was recorded (straightness=displacement [distance between first and last position]/length [of tracks]) where the value of 1 represents a straight line and < 1 an indirect path. The starting and endpoint needed to be visible throughout the recording, this did generate some variability in the numbers of neutrophils amenable to analysis per slice. As shown in graph B directionality [track straightness] is preserved following Sema3F treatment. Track straightness decreased in the PBS treated groups over time. As the track straightness decreases the number of track branches increase and the neutrophil must perform increasing numbers of “turns”. Each turn will require additional time and slow locomotion. Therefore, to confirm the effect of Sema3F on neutrophil speed I also analysed the maximal speed of each neutrophil, graph C. Following Sema3F treatment there is a significant reduction in maximal neutrophil speed compared to PBS treatment (**P=0.0084) but not compared to baseline [initial 20mins without either fMLF or vehicle control PBS] (P=0.1579). There was no significant difference observed at baseline during the initial 20 minutes of recording (P=0.1827). Following fMLF there is no difference between treatment groups. The maximal

speed is less significantly reduced following Sema3F & fMLF sequential treatment compared to PBS & fMLF treatment (lung 1 60 mins with PBS vs lung 1 fMLF ***P=0.0001 - lung 2 60 mins with Sema3F vs lung 1 fMLF *P=0.0120). The maximal neutrophil speed does not appear to decline with time, changes from baseline are only seen following treatments.

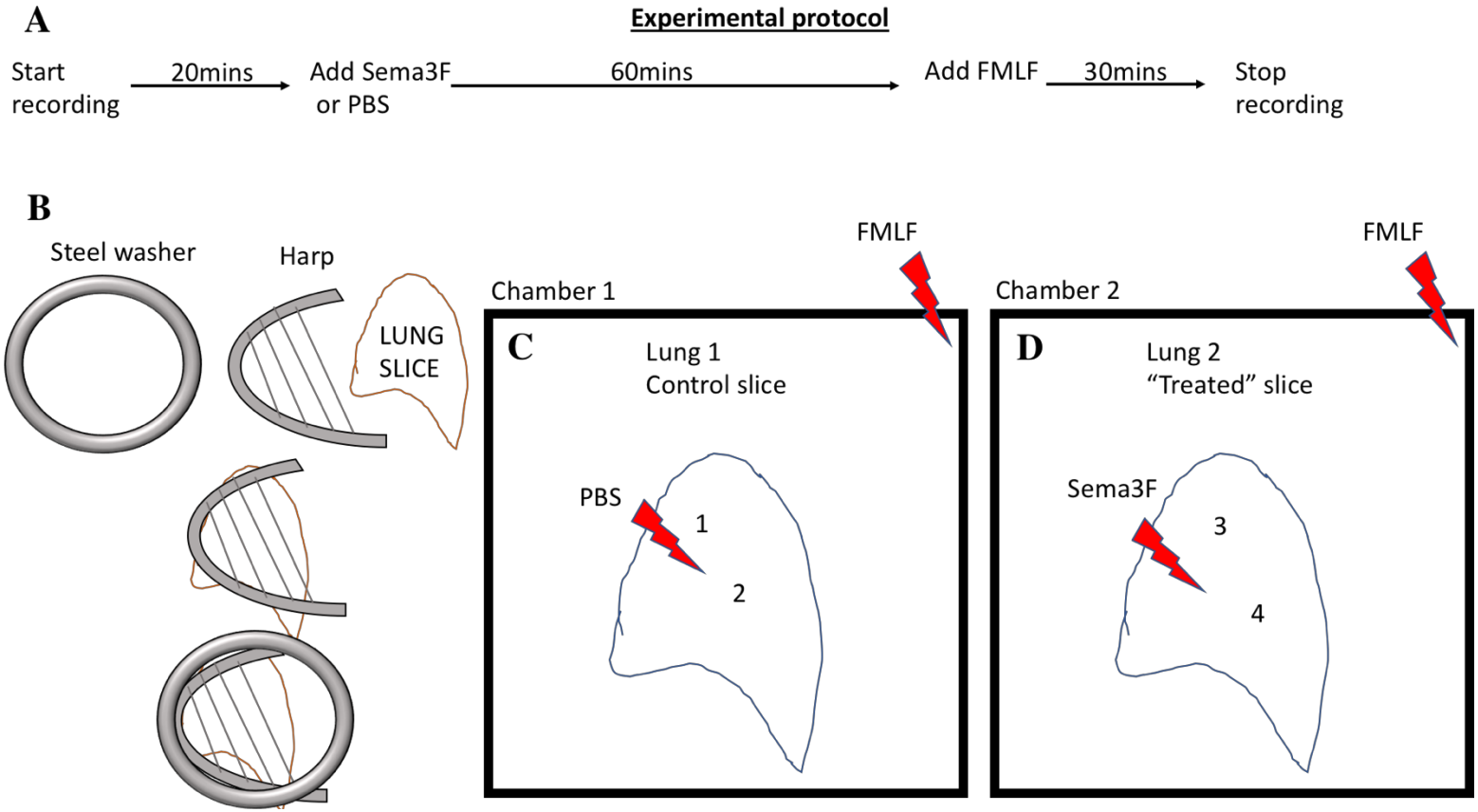

Figure 4.4.1-1 Experimental protocol for live lung imaging

Timeline A shows the recording of the live lung imaging with the serial conditions indicated, in the first 20 minutes the tissue equilibrates to 37°C, following this either Sema3F or PBS is added for 60 minutes and finally fMLF is added and recording continues for another 30 minutes. Image B shows the system employed to hold the slice in situ during movement of the stage allowing for continuous and alternating imaging of lung slide 1 and 2. C and D are schematics of the parallel chambers, a 30-frame recording is made at site 1, 3, 2 and 4 throughout the duration of the recording. PBS or Sema3F is added to the central area of the slice and FMLF to the top right-hand corner.

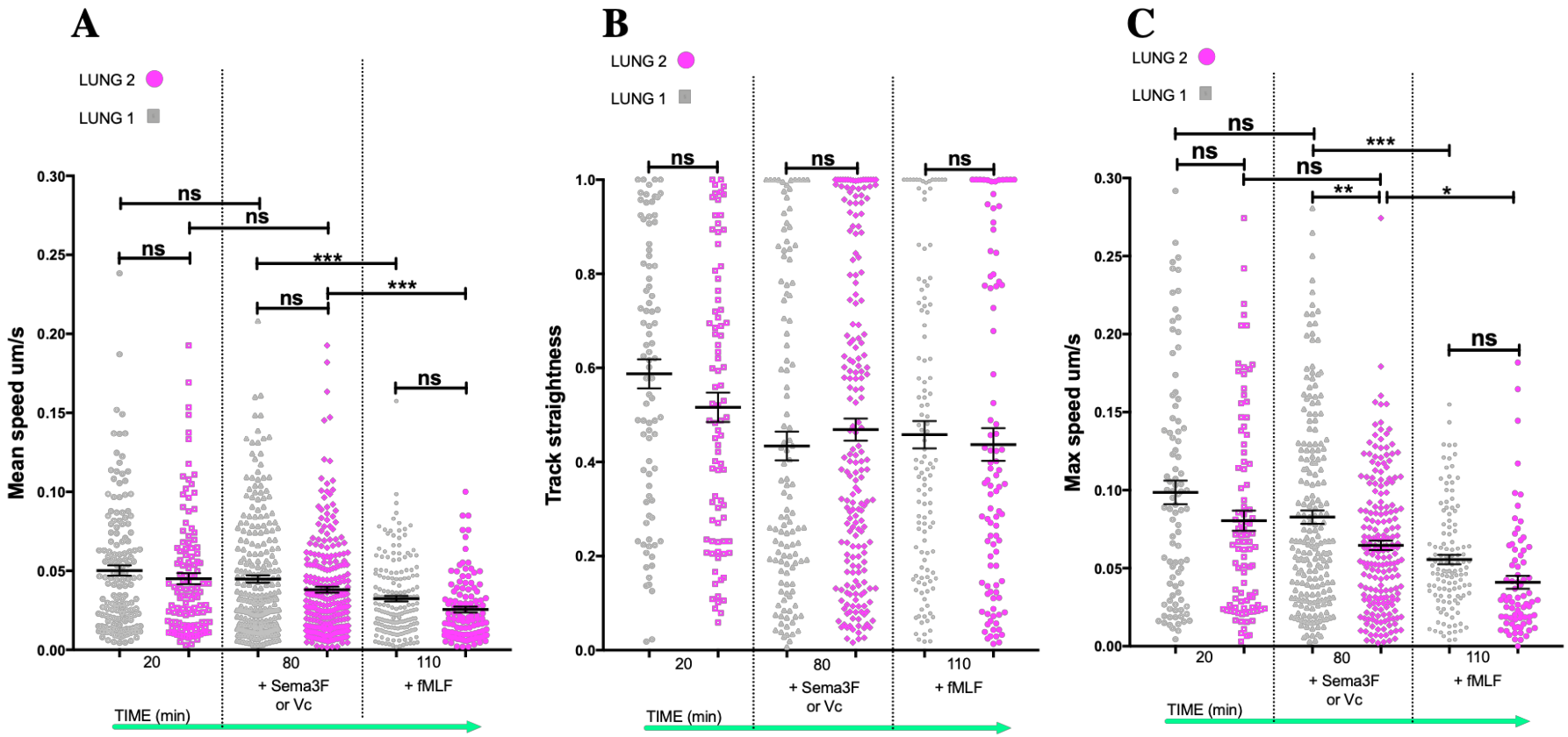

Figure 4.4.1-2 Sema3F signalling slows ex *vivo* neutrophils but directionality is unchanged
Catchup$^{IVM\text{-}RED;Lifeact\text{-}GFP}$ were sacrificed and lungs were instilled with agarose gel. Lungs were sliced and imaged using a confocal microscopy for 110 minutes. Neutrophil speed (A) and track straightness (directionality) (B) and maximum track speed (C) were measured and analysed using Imaris software (Imaris V 9.1). Data shown are mean ± SEM, biological replicate of 3, analysed using one-way ANOVA *P<0.05, **P<0.001, ***P<0.001 & ****P<0.0001

4.4.2 Sema3F increases neutrophil sphericity in the injured murine lung

Many of the neutrophil behaviours and functions altered by Sema3F signaling are associated with modifications of cytoskeleton dynamics. I have shown that Sema3F affects neutrophil cell rounding in *vitro* and that, at 24 hours post ALI neutrophils treated with Sema3F, are retained in the injured airway. Therefore, I hypothesised that the Sema3F retained neutrophils would be rounder, or indeed more spherical, than those treated with PBS in *vivo.* Mice were culled at 48 hours post ALI and after receiving IT Sema3F, lungs were instilled with agarose gel, fixed, sliced, stained and neutrophils identified. Using Imaris software, the neutrophils number were counted, and sphericity assessed, where 1 is considered a perfect sphere and 0 would be an extremely polarised neutrophil. It may be expected that in this context recruited neutrophils would be very shaped-changed in response to the multitude of inflammatory signals.[289] In figure 4.4.2-1, graph A is a representative histogram showing data from one pair of lung slices. In this graph frequency is the percentage of neutrophils of the total number of neutrophils (per standardised area imaged). Sema3F increases the frequency (percentage) of neutrophils that are highly round, evident in the right shift of the Sema3F treated population compared to the PBS. In graph B the mean sphericity value for the neutrophil population, in each pair of treated lungs, is shown. This mean is derived from counting > 270 cells (the number of neutrophils contained per slice in the imaged area), two areas were imaged per lung and the data compared. To analyse this data, *t*-tests were conducted using the n number and SEM for the data set. Graph B demonstrates that when neutrophils when are treated with Sema3F in *vivo* are significantly more spherical than those treated with vehicle control, PBS. Mean sphericity increases from 0.74±0.04 to 0.8253±0.04 following Sema3F treatment (****P<0.0001).

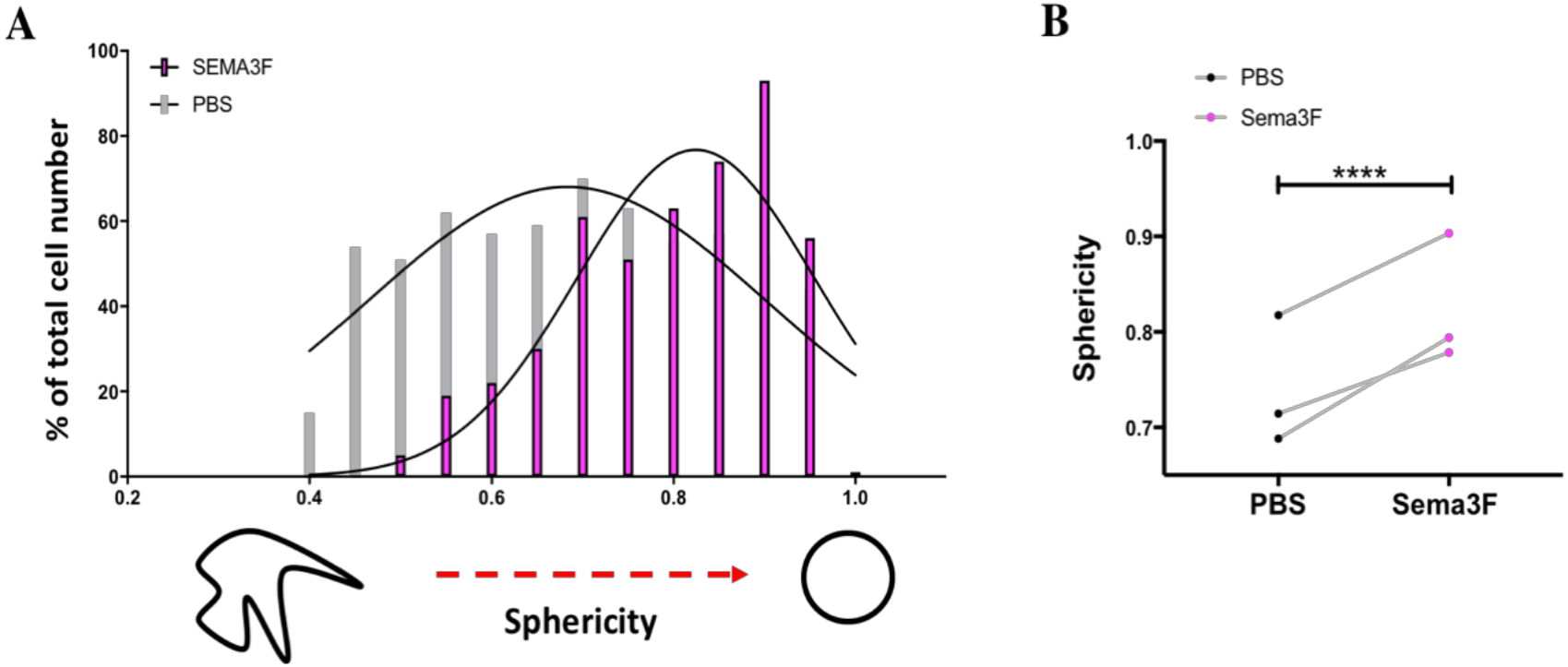

Figure 4.4.2-1 Sema3F treatment of recruited inflammatory neutrophils increases neutrophil sphericity

Intra-tracheal (IT) recombinant Sema3F (1μM) or phosphate buffered saline (PBS) was administered to wildtype C57BL/6 mice 24 hours post nebulised LPS challenge and were sacrificed at 48 hours. Murine lungs were instilled with agarose gel, fixed and stained to identify the location of the neutrophil population. Lungs were imaged using a confocal microscopy and neutrophil location assigned using Imaris software (Imaris V 9.1) and neutrophil sphericity analysed. Example A shows n=1, where all data points are represented in the histogram. Sema3F treatment affects a right shift in the histogram towards increased sphericity with a maximal value of 1. Graph B shows a summary, data are shown mean, n=3 over 3 experiments. Data: donor 1 - PBS, mean=0.71 ± 008 (297 cells) vs Sema3F, 0.77 ± 009 (307 cells); donor 2 - PBS, mean=0.69 ± 0061 (639 cells) vs Sema3F, 0.79 ± 0.0053 (475 cells); donor 3 - PBS, mean=0.818 ± 0.080 (270 cells) vs Sema3F, 0.903 ± 0.048 (301 cells); analysed using unpaired *t*-test, ****P<0.0001.

4.4.3 Sema3F differentially regulates myeloperoxidase and elastase activity in bronchioalveolar lavage fluid during acute lung injury

Neutrophil degranulation occurs through dynamic cytoskeletal arrangements which can be regulated by Sema3F. I have shown in culture that exogenous Sema3F treatment of human neutrophils results in a reduced in MPO activity in the cell-culture supernatant. Following IT Sema3F at peak recruitment (24 hours), at 48 hours there is significantly less MPO activity in the BAL fluid (figure 4.4.3-1, graph B *P=0.0113). I wondered if the converse would hold true and hypothesised following recruitment of Sema3F deficient neutrophils to the injured lung there would be an increase in MPO activity. The graph A shows that at 24 hours following lung injury there is a significant increase in MPO activity in the supernatant (*P=0.0301). Loss of neutrophil Sema3F results in enhanced recruitment and significantly more neutrophils in the alveolus at 6 hours and not 24. Therefore, while this increase in MPO activity does directly correspond to the timepoint where increased neutrophil numbers are seen this could relate to an increase in accumulated MPO from this prior timepoint.

Neutrophil elastase was significantly reduced at 48 hours in the Sema3F KO animal compared to WT (*P=0.0249). This is the timepoint that follows the enhanced resolution period seen in the KO animal. The reduction in elastase could reflect this ‘enhanced’ resolution. There is no effect of IT Sema3F when compared to IT PBS on BAL levels of neutrophil elastase.

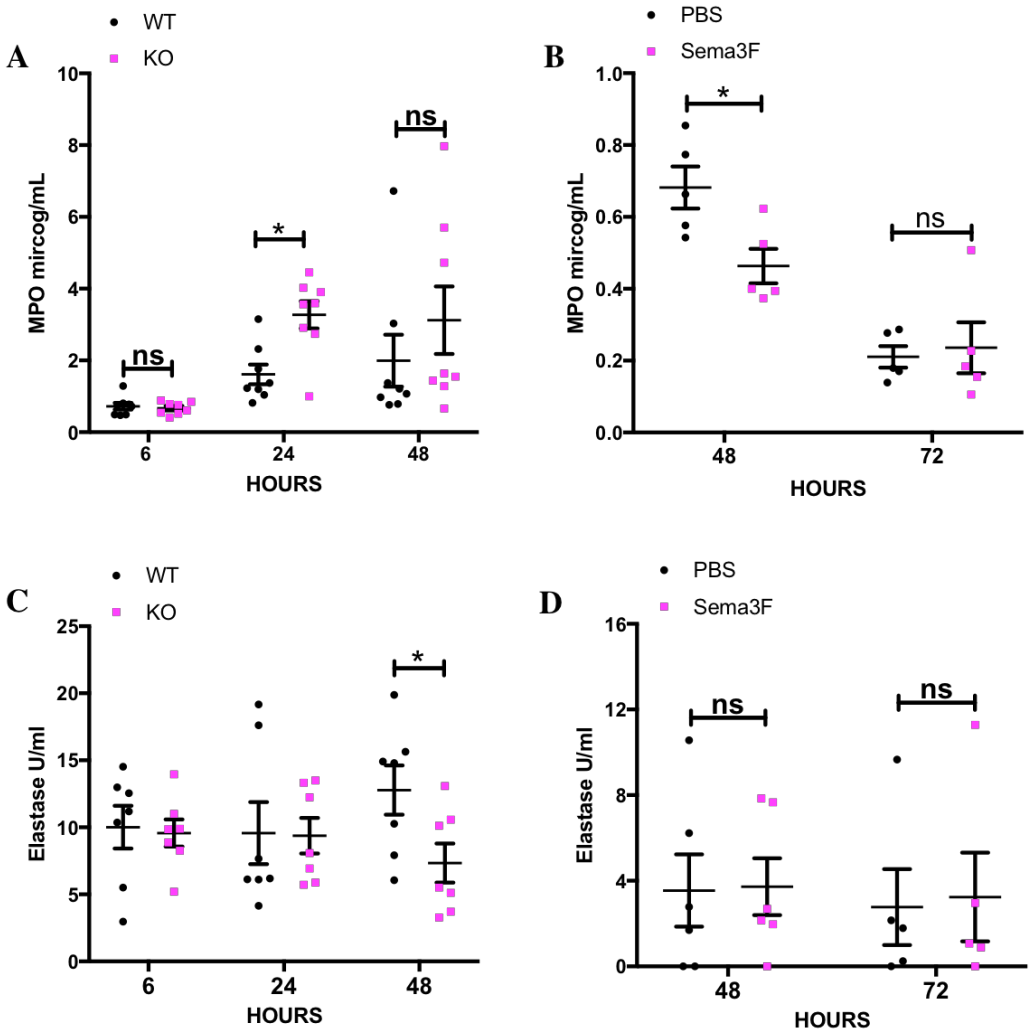

Figure 4.4.3-1 Sema3F differentially regulates both elastase and myeloperoxidase activity

Sema3F^{floxflox}MRP8cre$^{-/-}$ (WT) and Sema3Ff^{loxflox}MRP8cre$^{+/-}$ (KO) or C57BL/6 mice were challenged with LPS. WT and KO mice were sacrificed at 6, 24 and 48 hours then bronchoalveolar lavage fluid obtained (A & C). C57BL/6 mice were given IT PBS or Sema3F at 24 hours and culled at 48 and 72 hours following this BAL fluid was extracted (B & D). BAL fluid was tested and the peroxidase utilisation of 3,3′,5,5′-Tetramethylbenzidine (TMB, Sigma) by MPO measured or elastase activity in a fluorometric assay graph. Quantities of MPO and elastase were derived using standard curve method. Data are shown mean ± SEM analysed using two-way ANOVA. Graph A, *P=0.0301 n=8 over 2 individual experiments. Graph B, *P=0.0113 n=5 over 1 experiment, graph C *P=0.0249 n=8 over 2 individual experiments and Graph D n=5-6 over 1 experiment.

4.4.4 Sema3F treatment reduces neutrophil steady state F-actin content but does not alter polarity

Sema3F reduces the speed of neutrophil chemotaxis and transit in *vivo* and *vitro*. This could be through the induction of neutrophil F-actin disassembly. Following fMLF stimulation neutrophils undergo a well characterized response. Initially between 0 to 75 seconds there is an actin polymerisation phase, neutrophils appear round and this is not dependent upon fMLF dose. Following this there is depolymerisation to an intermediate level which leads into the stable state between 5 and 10 minutes. The depolymerisation phase is inversely dependent upon fMLF dose. It is only the maximal polymerisation point and the steady state that is dose dependent. [290]

I looked at the neutrophil F-actin content at key timepoints starting at 0, 75, 90 seconds then 3,10,15 & 30 minutes as shown in figure 4.4.4-1, graph A. After pre-incubation with Sema3F, the neutrophil F-actin levels are significantly reduced only once the steady state is reached at 10 minutes shown in graph A (*P=0.0150). This is not surprising as the rapid polymerisation rate is not proportional to the fMLF dose and may be a fixed response. It is possible that Sema3F promotes an extended second phase of depolymerisation resulting in a reduced F-actin content. The F-actin distribution, shown in graph B by the co-variance of the pixel intensity, becomes increasingly disparate overtime to the same degree in both treatment groups. This infers that neutrophil polarisation is preserved and despite a reduction in total F-actin the distribution of F-actin is unchanged by Sema3F treatment. At 10 minutes the neutrophils have maximally polarised shown by the higher heterogenicity of their F-actin signal. This would support the ex *vivo* findings, that Sema3F does not alter track straightness and that neutrophil polarisation (F-actin heterogeneity) and directionality are maintained. Sema3F does reduce neutrophil speed in *vivo* with a corresponding reduction in F-actin neutrophil content in *vitro*.

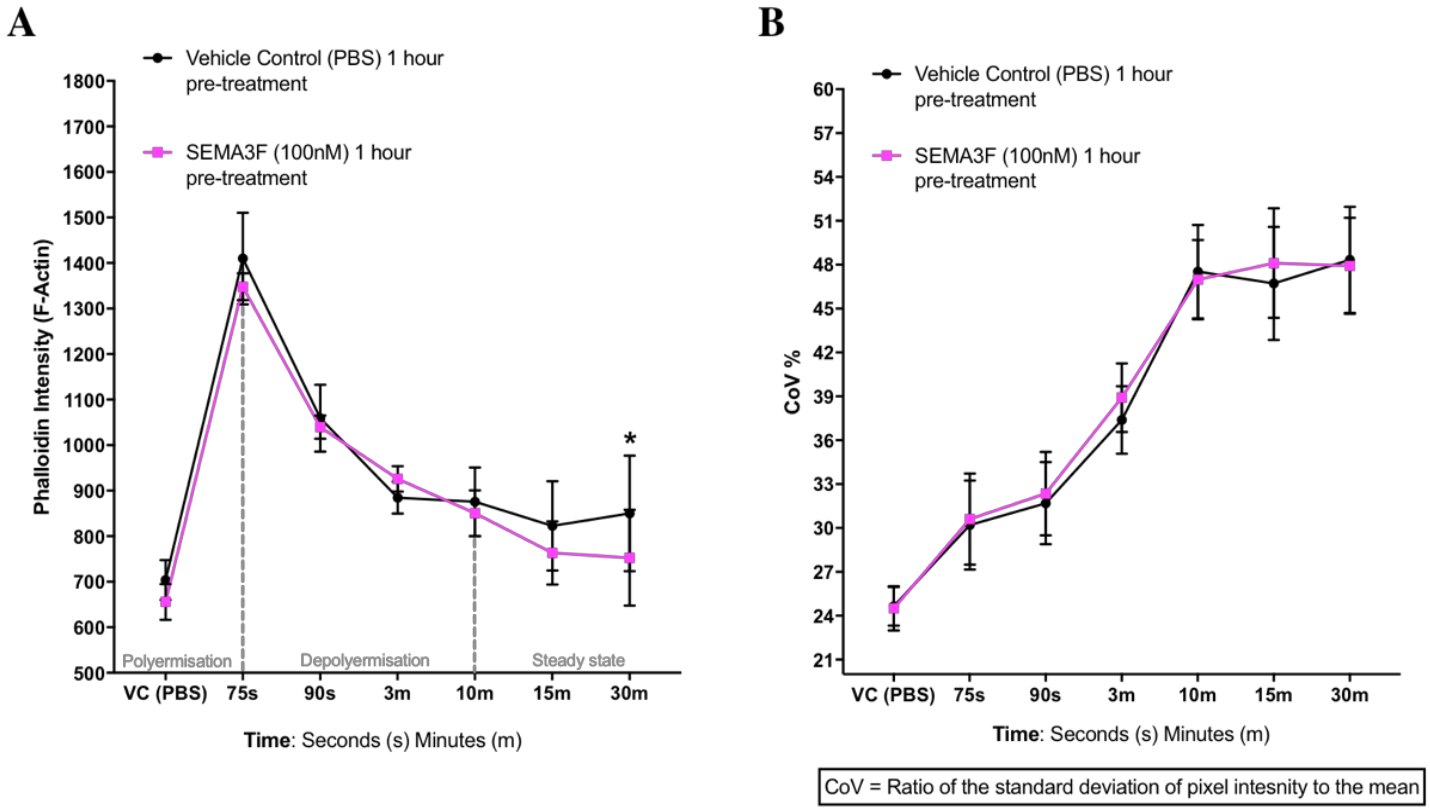

Figure 4.4.4-1 Sema3F reduces steady state F-actin content in neutrophils while distribution is unchanged

Isolated peripheral blood neutrophils from healthy volunteers were incubated with recombinant Sema3F [100nM] and then treated with fMLF 100nM. Neutrophils were cultured in media for 60 mins with and without Sema3F then treated with fMLF and fixed at the timepoints shown in graph A and B for 15 minutes. Following permeabilisation cells were then stained with DAPI (4',6-Diamidino-2-Phenylindole, Dihydrochloride), and Alexa Fluor® 488 conjugated Phalloidin. The characteristic of F-actin kinetics is marked in grey on graph A. Images were obtained using an Operetta High-Content Imaging System and analysis of F-actin was performed by Harmony® analysis Software. Data shown are mean ± SEM, n=3 analysed using two-way ANOVA, *P=0.015.

.

4.4.5 Intra-tracheal Sema3F retains neutrophils in the injured airway through F-actin disassembly

I wanted to elucidate the mechanism by which Sema3F treatment retained recruited neutrophils in the injured lung. I hypothesised that neutrophils retained in *vivo* by Sema3F treatment would have less F-actin content. To do this I assessed the F:G actin ratio within each neutrophil. As filamentous F-actin depolymerises into G actin the ratio declines figure 4.4.5-1, diagram B. Wild type mice were given nebulised LPS and I obtained neutrophils 48 hours following IT Sema3F or PBS treatment at 24 hours. The mice were culled, and lungs instilled with a gentle fixative to preserve the F-actin cytoskeleton in *vitro* (experimental protocol is shown in diagram A). The method of permeabilisation employed maintained the characteristic neutrophil FSC-A and SCC-A profile to assist analysis. Following staining with Phalloidin-conjugated and DNAse I conjugated probes, the ratiometrics were determined on a flow cytometer shown in graph C, in figure 4.4.5-1. A subset of the PBS and Sema3F treated neutrophils were neutrophils not immediately fixed and were first treated with Latrunculin A (Lat A) for 30 minutes. This is a potent effector of F-actin collapse and provided a positive control shown in graph B, where following treatment with Lat A the F:G ratio is extremely low. There was no difference observed between groups post Lat A treatment. The neutrophils treated with Sem3F have a significantly lower F:G actin ratio (**P=0.089) and less F-actin content.

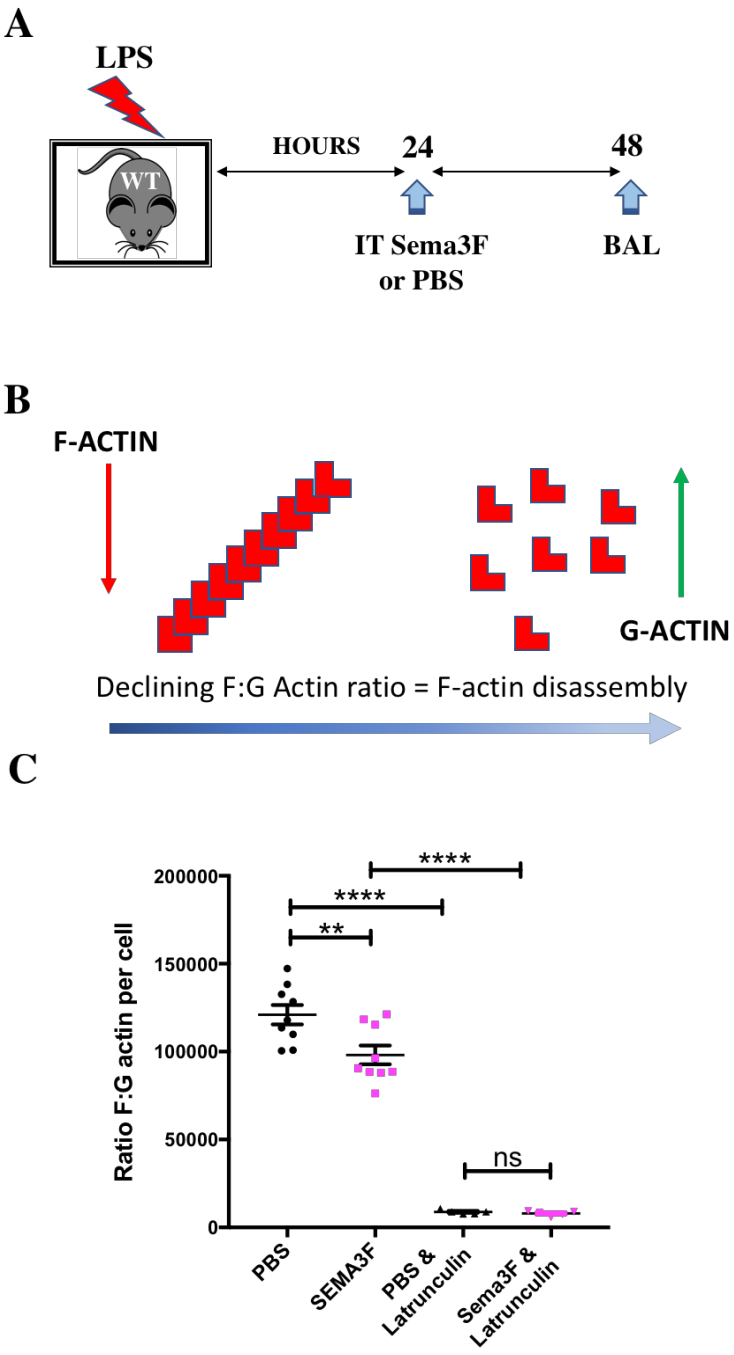

Figure 4.4.5-1 Inflammatory neutrophils are retained in the injured airway by Sema3F induced F-actin disassembly

Using the experimental protocol shown in diagram A, BALs were performed with fixative and neutrophils permeabilised. The F:G actin ratio is defined in diagram B; after intracellular staining for F and G actin, this ratio was determined for each neutrophil using flowcytometry. A subset of neutrophils was treated prior to staining with Latrunculin A [10μM] to collapse the F-actin cytoskeleton as a positive control. Data shown are mean ± SEM n=9 over two individual experiments, analysed using unpaired *t*-tests. **P<0.01 & ****P<0.0001

4.5 Discussion

Neutrophil transit into the injured lung tissue is altered by both exogenous Sema3F and neutrophil loss of Sema3F. Analysis of the neutrophil location demonstrated that in the lung treated with exogenous Sema3F there were significantly more neutrophils per μm^3 of lung tissue (as defined by the area of the capillary vessel network) (figure 4.2.1-2). This was largely accounted for by a significant increase in neutrophils found in the alveolar space. The retention of neutrophils to the alveolus may simply occur as this is the location where the neutrophil would sense the exogenous Sema3F signal. Alternatively, reduction in clearance of neutrophils from the distal airway would account for this. In this setting neutrophil clearance occurs partially through apoptosis and subsequent phagocytosis by macrophages.[114] The neutrophil counts made in the lung slices may include neutrophils in early apoptosis. This is less likely as during this phase in the LPS induced lung injury model, neutrophil survival is enhanced and it is doubtful that this route of clearance is a significant contributor.[9] While neutrophil reverse migration has been confirmed in other organs, this has not been observed from the alveolar space into the pulmonary vessels and remains unlikely due to the complexity of the barriers to migration.[75] It has however been shown that neutrophils may return from a marginated state, where they are in close proximity to the blood vessel wall to the wider circulation.[20] This would not account for the differences seen in alveolar space neutrophil populations. Once the neutrophil arrives in the distal airway it is permanently captured in the lipid rich mucus. The mucociliary escalator is a mechanism for the clearance of particles in the lung; this also extends to cells, including both macrophages and neutrophils.[25,291] If the amount cleared is in excess and cannot be swallowed this results in cough and the generation of sputum. In health and following induction of sputum neutrophils represent 37% of the cell types found and this dramatically increases in inflammation to 80%.[25] Another explanation is that PBS treated neutrophils are removed from the distal airway more efficiently than those treated with Sema3F. For example, neutrophils that are more amenable to

migrate, be captured and then propelled from the alveolus mucus, to the start of the “escalator” adjacent to the ciliated distal airway would be cleared faster. As mice swallow all sputum and do not have a cough reflex this is difficult to evaluate in a murine model.

Following the discovery that neutrophils deficient in Sema3F are recruited into the injured airway in significantly greater numbers at 6 hours post ALI, it remained unclear whether this neutrophil specific phenotype due overall to an increase in circulating neutrophils in the KO animal or due to faster neutrophil transit to the distal airspaces. Neutrophil release from, and recapture in, the bone marrow partly regulates the numbers of neutrophils in circulation. In health the circulating pool of neutrophils is a small percentage (1-2%) of the total number of mature neutrophils present in the bone marrow (BM).[60] During an inflammatory insult, stimulation by G-MCSF and inhibition of retention signals through the receptor CXCR4 ensures neutrophils are released from the bone marrow. Sema3A autocrine loops regulate BM endothelial cell behaviour.[197] Likewise following sterile injury neutrophils move to the lungs and through CXCR4 relocate back to the BM.[23] While no role has been described for Semaphorins in the regulation of neutrophil release from the BM, it was possible that the Sema3F deficient neutrophils could be released, retained or recaptured by the bone marrow differently from their WT counterparts. At baseline (0 and 6 hours), the circulating differential neutrophil count was similar between genotypes (figure 4.2.2-2, C). Baseline neutrophil blood counts were at the lower end of what is expected for the C57BL/6J background strain; mean counts between 0-6 hours range from 0.469-0.6983 $1x10^9$/L.[292] This suggests that loss of Sema3F did not alter the pool of circulating neutrophils in health. “Time 0” could occur up to 20 minutes following induction of ALI. Intravenous injections of bacterial peptide fMLF, complement factor C5, IL8, LTB4 have all been shown in animal models to induce neutropenia rapidly between 30 and 90 seconds.[293] In humans intravenous LPS results in neutropenia within 30 minutes.[22] Rapid neutropenia

occurs due to the sequestration of neutrophils following systemic circulation. While LPS in this case was delivered via nebulisation and not given IV, this delay could allow for the rapid sequestration of neutrophils to the pulmonary vasculature and the low normal counts between 0 and 6 hours. If this were true there is no identifiable difference in rapid sequestration between WT and KO neutrophils.

To capture the neutrophil flux through the interstitium during ALI, lung digests were performed following LPS induced lung injury at 2 & 6 hours. Cell suspensions were counted and stained with an established antibody panel to allow identification of granulocyte populations, then flow cytometry performed. In figure 4.2.2-2 graph B shows the neutrophil count per ml of digest. There was no significant difference observed between genotypes. Overall, there is a decline in neutrophil numbers in the lung tissue, a trough is seen at 6 hours concurrent with the timing of enhanced neutrophil recruitment seen in the KO mice. Taken together the data regarding the relative neutrophil populations in the blood and lung tissue suggest that Sema3F regulation of neutrophil transit is independent of interactions with these compartments and points to regulation of an intrinsic neutrophil property.

Sema3F may regulate neutrophil cytoskeleton, shape and deformability which are important determinants of neutrophil transit in ALI. Of circulating neutrophils 20% are found in the healthy lung and of these, 90% are found in the pulmonary capillaries. The airspace neutrophil population is dramatically increased following an inflammatory insult. The narrow diameter of pulmonary capillaries requires neutrophils to deform in order to enter and neutrophil migration into the lung capillary bed is largely independent of P or L selectin adhesion, or integrin mediated rolling.[62,245,294] In a rat model of *E. coli* pneumonia model, requiring CD11/CD18 mediated neutrophil adhesion, there was no reduction in neutrophil sequestration. Levels of selectin adhesion or neutrophil platelet binding also had no effect and it was the presence of neutrophil F-actin rims that largely accounted for neutrophil

sequestration.[12,20,22,47] Cytocalasin D, an inhibitor of actin polymerisation inhibits sequestration into the lung; similarly increased deformability of neutrophils resulted in shorter transit times into the lung.[248,293,295] Cytocalasin D reduces the overall turnover of the actin cytoskeleton and dynamic cytoskeletal arranges that probably increase cell deformability. The enhanced recruitment of KO neutrophils to the injured lung at 6 hours point to an early event in the transmigration of recruited neutrophils being adjusted, such as sequestration. There is strong evidence that it is the biomechanical properties of the neutrophil and the slow blood flow of the pulmonary capillaries that determine the rate of neutrophil sequestration into the lung over selectin or integrin interactions.[296,297] The lack of disparity in neutrophil blood and lung tissue numbers between genotypes attests the hypothesis that the autocrine Sema3F signal regulates an intrinsic property of the neutrophil and not an interaction between the neutrophil and other cell types.

In results chapter 3 I demonstrated that neutrophil specific loss of Sema3F results in enhanced recruitment to the injured airway at 6 hours. The circulating differential neutrophil count does not include the marginated/sequestered neutrophil population. Lung tissue digests will include neutrophils adherent to the endothelial layer, but as the pulmonary vasculature is washed out with PBS prior to resection, it will also not include the marginated population. Therefore, patterns of neutrophil transit may be obscured by a lack of resolution. To address this limitation, I looked at lung tissue taken from WT and KO mice at 6 hours, to assess whether the recruitment phenotype was reflected by an altered location of the neutrophils (figure 4.2.2-2, graph A). There was no significant difference in the absolute number of neutrophils per μm^3 between genotypes. I then calculated the percentage of neutrophils at each location from the total number of neutrophils in the slice. Using this method there were significantly more Sema3F deficient neutrophils found in the alveolus at 6 hours post injury. Following bronchoalveolar lavage the KO animal had a statistically significant enhancement of neutrophil recruitment (figure 4.2.2-1

graph A). This discrepancy between lung slice and BAL counts could relate to the BAL fluid representing a more comprehensive airway neutrophil quantification. Neutrophils that are in the distal airways and larger airways, will not be captured by the lung slice which includes small airways and alveoli, whereas the entire bronchial tree would be reflected in a BAL count. If the mucociliary escalator is reached earlier by the faster KO neutrophils I would hypothesise that the larger airways would contain more neutrophils than the distal or alveolus. In conjunction with increased percentage of Sema3F deficient neutrophils in the alveolus there is a non-significant reduction in both vascular and peri-vascular neutrophils. These compartments probably represent the marginated (vascular) and those undergoing transendothelial and/or transepithelial migration (peri-vascular). This points to an increase in the neutrophil rate of transit, over a decrease in adhesive forces alone, as both marginated neutrophils and those undergoing diapedesis are affected. In addition, the total numbers of neutrophils per lung slice remain similar between genotypes; it is the portion of cells that have migrated to the finish line - the alveolar space, which is increased. In summary, in diagrams A & B, figure 4.5-1, I have summarized the trends in neutrophil transmigration observed across multiple experiments in response to both exogenous Sem3F and neutrophil specific loss of Sema3F. What is clear from this diagram is that Sema3F signal is able to alter the pattern of neutrophil transit thus both recruitment and resolution. This appears to begin acutely and there is a suggestion that it is independent of adhesion pathways. The differences in recruitment at 6 hours in the transgenic animal and at 24 hours in the exogenous Sema3F experiment are not reflected in significant decreases in other compartments. It is possible that these neutrophils are recruited differently from a marginated pool of neutrophils which would not affect baseline circulating blood counts. Alternatively, the relative speed of neutrophil transit time may be enhanced following loss of Sema3F.

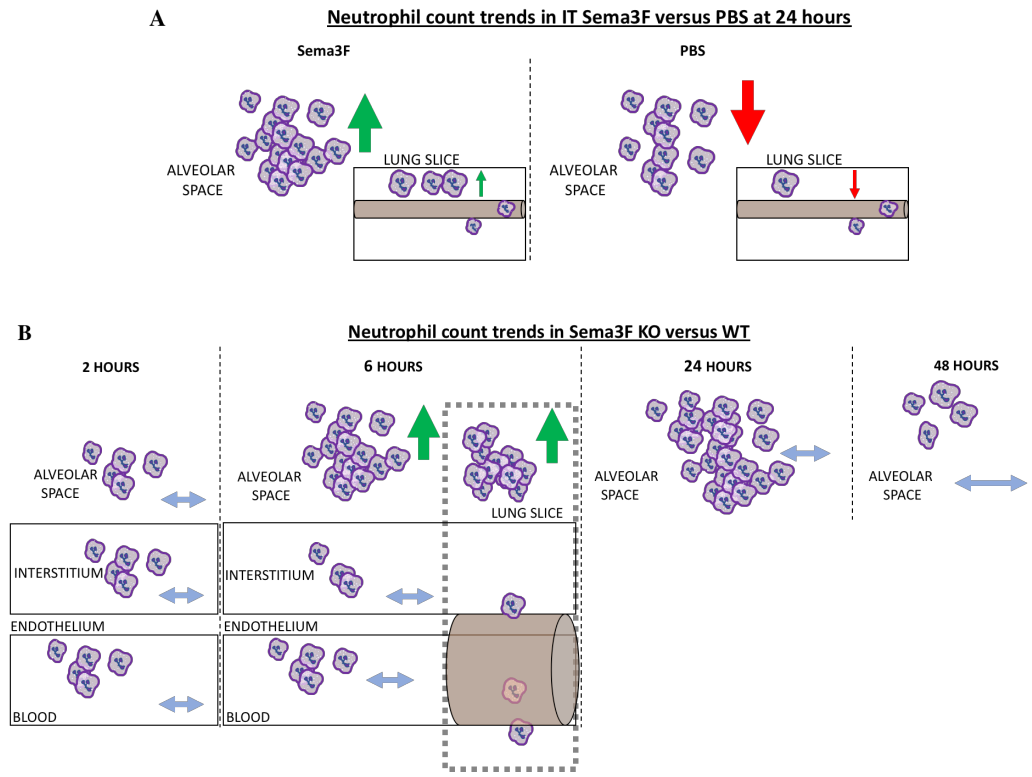

Figure 4.5-1 A comparison of trends in neutrophil distribution during LPS lung injury in the murine lung
A summary of data from separate experiments to show neutrophil transit during ALI. Diagram A shows the increased neutrophils found in the alveolar space by lung slice imaging and by differential white cell counts performed on BAL fluid. Diagram B shows the changes in the KO mouse compared to WT in circulation (Blood) in the interstitium (lung digest) relative to the pulmonary capillary blood vessels (lung slice) and in the BAL (differential cell counts). Blue sideways arrows indicate where there is no significant difference. Green arrows indicate an increased count in the KO versus WT animal, red arrows indicate a relative decrease and blue arrows no difference. In the KO (compared to WT) animal an increase in neutrophil numbers is seen in both BAL and alveolar space at 6 hours. Not all experiments were conducted for each time point.

Semaphorins have been shown to control cell migration; rapid recruitment to the site of injury is a pre-requisite of neutrophils as the first responder of innate immunity.[148,169,193,298-301] As such, I began to examine the effect of Sema3F behaviour on neutrophil migration. Human neutrophils were co-incubated with Sema3F for the duration of the transwell assay shown in the diagram A in figure 4.3.1-1. The chemoattractants fMLF and IL8 were placed in the well and the percentage of neutrophils that had successfully traversed the filter and chemotaxed to the well recorded. Sema3F significantly inhibited neutrophil chemotaxis towards both fMLF (figure 4.3.1-1, graph B) and IL8 (not shown). Chemokinesis for Sema3F was similar to that of media alone. Sema3F alone was not a chemoattractant as it reduced (rather than enhanced) chemotaxis towards the chemoattractant when co-incubated with neutrophils in the top of the transwell system. Sema3E, another class 3 Semaphorin, has been demonstrated in chronic allergy[188] to act as a chemorepellent, Sema3F itself was initially described as chemorepellent[293] in the nervous system and to human thymocyte migration[148,193,302] Sema3F does not act as neutrophil chemorepellent in this assay. These initial results confirmed that Sema3F treatment slows the neutrophils ability to move from the top chamber into the well. This could be a result of changes in speed and/or ability to deform to migrate through the 5μm pore. Sema3F can signal through Neuropilin (NRP) 1 or 2 and Plexins A1-A4, as shown in chapter 1 neutrophils express higher levels of NRP2 than 1 which is enhanced by inflammatory stimuli (figure 3.3.4-1). The surface expression of Neuropilins and Plexins varies between cell types, for example human thymocytes express predominately NRP2 and this similar to neutrophils as shown in chapter 3. [193] This could, in part, determine specific role of Semaphorin signalling in this cell type. However, Neuropilin expression may not always be relevant. For example Sema3E is the only class 3 Semaphorin that can signal directly through Plexins without requiring a co-receptor.[148,193] In this manner varied receptor expression may explain how Sema3F has diverse effects on cell behaviour.

As mentioned, the transwell assay has limitations and to overcome these a microfluidic chemotaxis assay was performed (figure 4.3.2-1). This demonstrated that Sema3F reduces neutrophil chemotaxis in a dose dependent manner to LTB4 and retains neutrophils in the chamber by a reduction in the speed/rate of retrotaxis. Following the maximal dose of Sema3F 1000nM the neutrophils remain in the chamber for 90 minutes, while the LTB4 gradient reduces by 70% after 2 hours. Yet there is still > 1% LTB4 gradient maintained over 8 hours, the minimum for neutrophil chemotaxis or retrotaxis. It has been suggested that neutrophils can consume chemoattractant signals, thus creating self-generated gradients on a local scale.[106] These neutrophil derived gradients would not occur in isolation and the environmental gradient may be more relevant in chemotaxis over longer distances. After maximal recruitment neutrophils could consume a large amount of the chemoattractant in the chamber, such that the chemoattract levels are then higher in the adjacent channel, promoting chemotaxis and not retrotaxis away from the chamber. In either case it remains evident that Sema3F, in a dose dependent manner, slows neutrophil chemotaxis.

I have demonstrated that in *vivo* and *vitro* Sema3F slows neutrophil chemotaxis and acts as a retention signal. This begins to explain the increased neutrophil transit into the injured lung when the Sema3F signal is lost. In addition to regulating neutrophil locomotion I questioned whether Sema3F could regulate the expression of CD11b and loss of L-selectin in response to LPS. I found there was no effect of Sema3F treatment on integrin CD11b or L-selectin surface expression and the characteristic response to LPS stimulation was preserved (figure 4.3.3-1).[285] This supports the view that Sema3F increases neutrophil transit into the lung not through altering the surface expression of adhesion molecules. It must be noted that this simple experiment does not assess integrin activation state which is known to be altered by other Semaphorins. [242]

During the migration assays I had observed the neutrophils treated with Sema3F were very round. A F-actin sub-cortical rims and neutrophil roundness have been identified as features that selectively promote the sequestration to the lung capillaries.[296] Semaphorins themselves have been shown to affect F-actin disassembly, growth cone collapse and reduce lamellipodia, all of which could give rise to neutrophil rounding.[155,163,174] Neutrophils receiving Sema3F rounded up in culture (figure 4.3.4-2). Sema3F rounding was overcome by fMLF 100nM. This be may an effect of the dose of fMLF chosen, which may not reflect physiological conditions within the specific inflammatory milieu. Rounder neutrophils would have the potential to travel faster within fluids such as blood but may have reduced deformability which may limit sequestration and transmigration. Sema3F-induced changes in the neutrophil cytoskeleton could be manifold: a reduction in actin turnover, actin stabilisation, destabilisation of the existing F-actin structure or increased branching. A varying combination of these could yield the neutrophil phenotype observed. In human Glioma cells Sema3F-NRP2/Plexin A1 signalling has been shown to reduce F-actin stability and the formation of stress fibres, essential for the contractile forces behind locomotion.[303] Inhibition of neutrophil production of LTB4 has been shown to reduce chemotaxis to fMLF.[304] In a similar manner neutrophil chemotaxis could be regulated by neutrophil production of an autocrine retention signal, such as Sema3F, in the context of inflammation.

Phagocytosis is another key neutrophil function that is dependent upon dynamic cytoskeletal changes. It represents a complex process with a large degree of redundancy.[305] Therefore, it may be unsurprising that following treatment with Sema3F phagocytosis is preserved to both opzonised Zymosan granules and labelled *E. coli* (figure 4.3.5-1). The divergent effects of Sema3F on phagocytosis, chemotaxis and cell shape relate to the alternative pathways involved in each. These pathways are often discussed and portrayed as being separate whereas they are interconnected. There is significant overlap between the downstream regulators of the actin cytoskeleton in chemotaxis

and phagocytosis. They may appear to be mutually exclusive events, where a neutrophil is required to promote one function above all else. As such they are often studied in isolation, as is the case here. The migrating neutrophil is thought to pause to complete phagocytosis as this action requires changes in the cell cytoskeleton that are possibly inhibitory to cell chemotaxis. This is probably a limited view and there is data involving immunophysical single cell modelling which suggests that cells may phagocytosis on the move, as a specialised continuum of chemotaxis.[306]

Polarisation is an initiating event that is common to both processes.[180,305] In a zebrafish model of inflammation, following tailfin injury, Sema3F over-expression had no effect on either neutrophil polarisation or PI-3K kinase activity as judged by PH-GFP disposition (unpublished data, Prof Sarah Walmsley). In other cell types (glioblastoma cells, melanocyte cells, Jurkat T lymphocytes and endothelial cells) Nakayama et al. (2015) demonstrated that Sema3F, through NRP2-Plexin A1 signaling, inhibited PI3-K activity within 20 minutes.[307] It is known that Plexins are linked to the Rho family of small GTPases. The Sema3F-Plexin signal transduction might involve redox enzymes such as Mical1 as a direct link to the actin cytoskeleton, or regulatory proteins such as GAPs or GEFs, which control GTPase activity.[173] [109] There are distinct roles for the Rho family members Cdc42, Rac1 and Rac2 in phagocytosis; their roles are related to the 'stage' of the process.[26] The distinct spatial and temporal patterns of Rho GTPases and the interplay of divergent Plexin signalling pathways would allow for a single signal, Sema3F, to have disparate effects on multiple and concurrent cytoskeleton dependent neutrophil functions.

Other neutrophil functions include generating the armament of histotoxic contents and their dispersal as part of a host-defense response. Neutrophil Myeloperoxidase is contained in primary (azurophil) granules and release is dependent upon actin remodeling. Myeloperoxidase is a peroxidase which produces the bactericide hypochlorous acid (HOCl) (or the equivalent from a

non-chlorine halide) from hydrogen peroxide (H_2O_2) and chloride anion (Cl^-).[308] It is an enzyme which is crucial for the bactericidal role of neutrophils but causes extensive tissue damage when inappropriately released.[309] Mitchell et al. (2008) demonstrated that during exocytosis of granules cortical actin is redistributed to the primary sites of granule translocation involving Rac-dependent cortical actin depolymerisation.[235] While low doses of Latrunculin B (Lat B) and Cytocalasin B (CB) induce exocytosis, the actin stabiliser Jaspokinalide inhibits exocytosis as too did high doses of CB and Lat B.[235] I observed that pre-incubation with Sema3F significantly reduced neutrophil myeloperoxidase activity in culture (figure 4.3.6-1, graph A). GM-CSF and fMLF sequential neutrophil stimulation was used to stimulate maximal granule release.[310] While MPO activity assays cannot directly correlate to the exocytosis or degranulation rates, with suitable controls this assay can begin to describe the effect Sema3F has upon myeloperoxidase function. The amount of exocytosis/degranulation will still be a crucial rate limiting step. Yet it is improbable that Sema3F or downstream effectors have the potential to regulate the activity of myeloperoxidase, rather than the rate of release. This highly potent redox enzyme has proven difficult to inhibit therapeutically as it often oxidises many inhibitors.[308] Inhibitors either disrupt the catalytic cycling of the enzyme or act as suicide inhibitor and by virtue of this are free radical containing acids or substances that covalently bind to the heme group. Therefore, there is little scope for Sema3F to directly affect MPO activity in culture. Furthermore, I have reported the fold change from baseline so known effects on MPO activity by gender, age and polymorphism are controlled for.[311] If we assume Sema3F does not directly affect myeloperoxidase activity then the likely the determinant of fold change in MPO activity in cell culture supernatant is exocytosis magnitude. This is supported by the finding that Sema3F only alters upstream of GM-CSF and fMLF exocytosis simulation. This suggests that Sema3F may regulate the neutrophil cytoskeleton such that exocytosis of primary granules is reduced. Rounder Sema3F neutrophils may represent an increase in sub-cortical F-actin, this may prevent normal levels of

exocytosis being achieved by disrupting the balance between cortical actin depolymerisation and redistribution to sites of granule translocation heralding exocytosis.[235]

In contrast to Sema3F's ability to alter neutrophil MPO activity, the amount of elastase in cell culture was unchanged following pre-treatment with Sema3F (figure 4.3.7, graph B). Low level readings were obtained in this assay which may suggest a submaximal degranulation response. This could also reflect the short half-life of elastase in the extracted supernatant. Alternatively a proportion of the total enzyme may remain bound to the neutrophil membrane and therefore not available in the supernatant. [278,279][280,281]

In a similar fashion following IT instillation of either Sema3F or PBS at peak neutrophil recruitment, there was no effect observed on the levels of elastase found in the BAL fluid (figure 4.4.3-1, graph D). Again, this could also represent a submaximal neutrophil degranulation or an artificially low elastase level due to inhibited detection. In this experiment the timepoints are much later in the LPS lung injury time course and represent the resolution phase. During resolution elastase levels would be expected to be lower. In terms of protease inhibitors, their presence in the BAL fluid could inhibit the elastase more effectively in *vivo* post-harvest than in *vitro*. In the BAL and supernatant fluid there is no membrane bound elastase. This elastase is more resistant to the effects of protease inhibitors. In this setting there are also no neutrophils to replace the rapidly degraded elastase leading to an underestimate of the physiological level. Indeed, there are many other proteases that would be able to degrade the quenching structure in the fluorochromatic assay. These include: protease 3, cathepsin (G, L & S), macrophage elastase and gelatinase.[272] In addition other cells such as monocytes and mast cells can produce elastase.[312]

Despite all these caveats, the assay may still generate valid results. The variables affecting elastase measurement described would be present and

equal in all the in *vivo* elastase assays. So, it remains important that loss of neutrophil specific Sema3F reduces elastase activity at 48 hours post ALI. This may be a sequela of the enhanced resolution seen in the KO animal between 24 and 48 hours. Neutrophil elastase itself is not just a protease but can also generate further chemoattractive signals such as GMCSF, IL-6 and IL-8.[313] As such it has a pivotal role in ongoing lung injury and reduction of elastase could be very beneficial in the context of pathological inflammation and tissue damage.

The neutrophil's ability to produce ROS, the respiratory burst, is crucial to its function as a front-line responder to invading pathogens.[3,4] As other histotoxic functions such as myeloperoxidase activity were reduced it may have been expected that neutrophil ROS production was also inhibited. I have demonstrated that neutrophils have a significant increase in ROS production in response to fMLF following pre-incubation with Sema3F (figure 4.3.7-1). The ROS detector Dichlorodihydrofluorescein diacetate (DCFH-DA) is a cell membrane permeable probe, that is widely used to detect ROS. Two-electron oxidation converts DCFH-DA into a fluorescent and therefore detectable signal. There are limitations to this method, the oxidation of DCFH-DA is not limited to one type of ROS and not directly with H_20_2. It may also take part in itself in redox-cycling and therefore enhance ROS. With stable culture conditions, controls and repeated measurements some of these concerns can be mitigated.[314] The actin cytoskeleton and ROS have an intimate relationship. Leukocyte Rho GTPases and cytoskeletal dynamics have been shown to be involved in the production of ROS, and in turn are influenced by ROS. Leukocytes contain the inducible electron transport chain NADPH, reducing equivalents are transferred from NADPH to oxygen producing superoxide anions. NADPH exits in a dormant resting state in unstimulated neutrophil and upon stimulation is relocated to the cell membrane associating with cytochrome B. This relocation to facilitate NADPH assembly has been shown to be dependent on actin polymerisation.[315-317] It has been suggested that Rho

family GTPases might be even more intimately involved with the NAPDH complex. Rac is required for the transfer of electrons from NADPH to cytochrome b-associated FAD, then to cytochrome b heme and finally to molecular oxygen.[318] Leukocyte adhesion stimulated inhibition of ROS production is suggested to be specifically through Rac2, whereby integrins act to suppress both Rac2 activation and assembly into the functional membrane NADPH oxidase complex.[319] NADPH oxidase-dependent generated ROS negatively regulates actin polymerisation through reversible actin glutathionylation.[320] Glutathionylation of a critical cysteine, Cys374, in actin, has been shown to reduce the ability of G-actin to polymerise into F-actin polymers.[263] Sema3F alone appears to have no effect on neutrophil ROS generation. Sema3F could have dual roles as a retention and neutrophil priming signal, similar to LPS and other inflammatory stimuli.[320] It may be that the hyper-round Sema3F treated neutrophil with a lower predisposition for integrin mediated adhesion leads to a reduction in the inhibition of ROS production via Rac2 signaling, and this is only unmasked on further treatment with fMLF. Sema3F increases in intracellular ROS may result in higher levels of glutathionylation and thus reduce actin polymerisation, which could result in reduced neutrophil chemotaxis.[263] Sema3F may not only act as neutrophil retention signal but it would appear it could also potentiate specific cytotoxic features such as increased intracellular ROS alongside a preserved phagocytosis ability.

To explore whether Sema3F altered neutrophil locomotion in *vivo* I collaborated with Dr Leo Carlin. We constructed an experimental system where the movement of Ly6G labelled neutrophils & LifeAct-GFP labelled actin could be tracked in a live-culture lung slice (figure 4.4.1-1). Confocal images were taken as described throughout 110 minutes, at the allotted timepoints PBS verses Sema3F was given, this was followed by fMLF. As expected in the first 20 minutes there was no difference in neutrophil behaviour, after the first treatment there was a significant reduction in neutrophil speed in response to

Sema3F alone, with the addition of fMLF this was exacerbated (figure 4.4.1-2, graph A). Rather counterintuitively fMLF treatment also reduced the speed of neutrophils in the non-Sema3F treated lung slice perhaps related to the high dose of fMLF used generating ROS production. At this level the fMLF dose is inversely proportional to neutrophil locomotion speed.[321] The effect of culture of the ex-*vivo* lung slice tissue and associated neutrophils may alter the neutrophil behaviour overtime and this could correspond to changes in neutrophil chemotaxis. The comparison between parallel lung slices, (lung 1[control] and lung 2[Sema3F) helped to identify the specific effect of exogenous Sema3F. There is significant difference between lung 1 (PBS then fMLF) and lung 2 (Sema3F then fMLF), with slowing of the neutrophil movement following Sema3F treatment. The chemoattractant fMLF will disperse quickly through the media following its addition and there may not be a sustained differential chemokine gradient. Chemokines and cytokine gradients do not act in isolation and it has also been demonstrated that neutrophils can make their own gradients.[322] So a lack of “true” fMLF gradient may be irrelevant to neutrophil migration in this context.

In this experiment track straightness remained similar between PBS and Sema3F treated neutrophils (figure 4.4.1-2 graph B). Track straightness is the displacement of the neutrophils (distance between the first and last recorded position) divided by the length from the start to end position. A straight line would give a higher value, however as the length increases but the displacement does not this would reduce the value. Therefore, an increase in chemokinesis would reduce track straightness. There appears to be no effect in chemokinesis or track straightness between treatment groups, there does appear to be an effect with time and fMLF treatment. While fMLF has been shown to promote a convergent (direct) over divergent (exploratory) migratory pattern, without a sustained source of fMLF and a gradient, neutrophil chemokinesis would be increased and would further reduce track straightness.[263] The track average speed is calculated based on the track

length divided by the time between the first and last positions. With a decrease in track straightness, an increase in chemokinesis and/or direction the average track speed could be lower despite the actual speed of the neutrophil remaining stable or increasing. Therefore, I also looked at the max speed recorded, as this measurement would overcome variation due to migration pattern. There was a significant reduction in neutrophil maximum speed following treatment with Sema3F compared to PBS (figure 4.4.1-2 graph C). Overall there was a reduction in speed following fMLF in both treatment groups and Sema3F treatment did not exacerbate this. In this case there was not a reduction seen over time (PBS: 20mins vs 60mins) in max speed and this supports the suggestion that the differences in track straightness and average speed seen with increased culture time is a function of a change in migratory pattern.

As mentioned the slowing of neutrophil chemotaxis in response to fMLF has multiple explanations. In part it could be due to dysfunctional chemotaxis, as seen in the neutrophils of burns patient, whereby following fMLF stimulation there is a 75% reduction in neutrophil velocity.[106] The absence or dwindling production of other signals, for example GM-CSF may reduce fMLF neutrophil chemotaxis.[304] Neutrophils also display environmentally dependent hierarchical chemotaxis, for example LPS may induce expression of the human FPR1 receptor and enhance chemotactic responses to fMLF.[287,323] These lungs were deliberately unstimulated as part of a reductionist strategy to assess the underlying mechanisms. Furthermore, desensitisation to the fMLF may occur following internalization of the FPR1 receptor. A higher dose of fMLF given was (10μM), required for the full response of murine neutrophil which will elicit ROS production. The effect of increased ROS could result in actin depolymerisation through increased glutathionylation and reduced maximal speed. Howard et al. (1984) demonstrated that up to 10nM concentrations of fMLF F-actin and mean rate of locomotion (mROL) of

neutrophils increased simultaneously. At doses > 10nM while F-actin content did increase, there was a steady decline in mROL.[324]

Neutrophil roundness is increased in culture by Sema3F treatment, in *vivo* measurements in 3D describe neutrophil sphericity. Increased sphericity has been linked to enhanced neutrophil sequestration, thus slowing neutrophil transit to the lung tissues.[325] This shape change occurs as a rapid and transient first response to inflammatory mediators such as complement fractions.[321] Zebrafish with neutrophil specific mutant Rac2 had a rounder morphology compared to WT and were retained in haemopoietic tissues.[296] The underlying change in the actin cytoskeleton requires redistribution of central actin to the sub-cortical regions and thus reduces neutrophil deformability.[296] In the literature sphericity has been linked to neutrophil function and location, highly spherical neutrophils are less motile and are found on the luminal surface.[326] A hallmark of neutrophils that have undergone reverse migration is their lack of sphericity.[296] In lung slices from mice treated at peak recruitment with intra-tracheal Sema3F neutrophils are retained in the airway. They are significantly more spherical compared with PBS treated neutrophils (figure 4.4.2-1). This is in keeping with previous in *vitro* data where I demonstrated that cultured neutrophils following Sema3F treatment are rounder, which was overcome by fMLF treatment. The in *vivo* response to Sema3F signal occurs following LPS induced inflammation and is not overcome by inflammatory stimuli. This could be accounted for by the dose of Sema3F used in the in *vivo* experiment being 1μM, compared to 100nM in culture. This is unlikely as it is expected that intra-tracheal instillation will result in a delivery of considerably lower actual doses to the alveolus due to distribution and loss in the preceding proximal respiratory tract. Alternatively, LPS may not antagonise the effect of Sema3F rounding in a similar manner to fMLF, it is also possible that measurement of cell roundness is less sensitive than that of sphericity or indeed less specific. With these caveats in mind it still suggests that Sema3F inhibition of chemotaxis and neutrophil retention both in *vivo* and in *vitro* relates to increased neutrophil

roundness and sphericity as either a consequence or cause. This is in keeping with observations in the literature regarding the phenotype of highly spherical or round neutrophils, suggesting neutrophils in this shape-conformation have specific properties that determine both location and function.

In both *vitro* and *vivo* I observed a significant reduction in neutrophil MPO activity following Sema3F treatment. IT Sema3F treatment at 24 hours following LPS resulted in less MPO activity in the BAL fluid at 48 hours (figure 4.4.3-1, graph B). At 48 hours it is expected that MPO levels will be declining as this timepoint is during the resolution phase of the LPS lung injury model. Following IT Sema3F these levels are further reduced compared with IT PBS. In contrast loss of neutrophil Sema3F enhanced MPO activity in the BAL fluid at 24 hours compared to WT (figure 4.4.3-1, graph A). Whereas the increased neutrophil number in the KO animal is seen at 6 hours and WT and KO recruited neutrophil numbers are similar at 24 hours. Therefore, the increase in MPO does not relate directly to more neutrophils releasing the substance at 24 hours. It could be an accumulation of MPO from the previous 6-hour timepoint. As the half-life of MPO is 10 hours, therefore 18 hours later there could still be active MPO produced during this previous timepoint.[327,328] At 48 hours there are similar lower levels of MPO in the BAL fluid in both WT and KO. Alveolar macrophages have been shown to scavenger MPO so that accumulation is limited.[329] This suggests that Sema3F may regulate neutrophil degranulation taken alongside other data: reduced neutrophil chemotaxis/speed, neutrophil retention and the altered effector functions observed strongly suggest that Sema3F may regulate the neutrophil cytoskeleton as an overarching mechanism.

Initially I looked at neutrophil F-actin content in *vitro* and identified that Sema3F reduced F-actin content during the steady state following fMLF stimulation (figure 4.4.4-1, graph A) while the polarisation or heterogeneity of the F-actin distribution was unchanged (figure 4.4.4-1, graph B). I then went on to test the hypothesis that F-actin disassembly is the underlying mechanism by which

Sema3F signaling results in these observations. If true there would be less F-actin in the Sema3F retained neutrophils in *vivo*. I again used the murine ALI model, where IT Sema3F or PBS was given at peak recruitment and investigated the F:G ratio at 48 hours (figure 4.4.5-1). In solution monomeric actin or G actin will spontaneously self-assemble into polarised bi-helical filamentous actin, even in steady state these are dynamic structures and this process is ATP dependent.[113,114] I assumed that neutrophil retention at 48 hours would be the result of a lower F-actin steady state in these cells. An F: G actin ratio was derived by using conjugated labels: Phalloidin (F-actin) and Deoxyribonuclease I (G-actin). Phalloidin is considered the gold-standard for labelling endogenous actin in fixed samples.[330] Phalloidin is a toxin which requires fixation and permeabilisation of the cell, it stabilises the F-actin structure by reducing the dissociation of G-subunits to zero. Methanol was avoided as this can create artifacts upon phalloidin staining within the cytoskeleton. Theoretically detection by phalloidin staining could underestimate F-actin, as binding can be inhibited by actin regulator proteins; this would be a consistent caveat in all treatment groups and experiments.[331] Likewise, DNase I has been shown to be specific for G actin when used with a detergent and paraformaldehyde fixation; it can also detect G-actin when bound to Latrunculin A.[117,118] Flowcytometry ratiometrics (the ratio of decreasing signal over increasing signal) has been established as a method to quantify calcium flux in cells.[332] I harnessed this system using Phalloidin Alexa 488 and DNAse I 594 to detect F: G actin ratio. These specific and sensitive probes attached to stable complementary fluorophores give a reliable signal. Determining the ratiometric value per neutrophil corrects for artifactual changes in fluorescence due to variations in dye loading, bleaching effects and changes in equipment.

The F: G actin ratio per neutrophil was found to be significantly lower in the Sema3F treated group 24 hours following IT administration (figure 4.4.5-1). This demonstrates that the Sema3F treated neutrophils have less F-actin and

therefore have undergone relatively more F-actin disassembly, in concert with this G-actin is increased. Both PBS and Sema3F treated neutrophils displayed an extremely significant reduction in F: G actin ratio following treated with Latrunculin A (Lat A). This confirms the validity of the ratio as a measure of F-actin disassembly. Lat A binds to the actin monomer (G-actin) and prevents incorporation to form a polymer or F-actin, it affects disassembly through preventing the continuing treadmilling of actin structures by promoting only disassembly.[333] The Sema3F treated neutrophils have a less significant amount of F-actin disassembly compared with both the Lat A treated groups, suggesting that Sema3F (by this route and dose) does not inflict complete F-actin disassembly. Therefore, it may only serve to modulate F-actin dependent functions rather than prevent them. This is in keeping with the in *vitro* phenotypes I have observed where neutrophil chemotaxis is inhibited yet other neutrophil functions, such as phagocytosis are preserved. A reduction in the F: G actin ratio indicates net F-actin depolymerisation this does not identify the specific mechanism. For example, this could be a result of alterations in actin turnover, F-actin stability, structure divergence (branching) or a combination of these.

The effects of Sema3F signaling can be explained by alterations in the neutrophil cytoskeleton, more specifically a reduction in neutrophil total F-actin. I have demonstrated that Sema3F treatment enhances ROS generation. The regulation of the neutrophil cytoskeleton by Sema3F will inform patterns of neutrophil migration but also the functional phenotype including ROS production. Equally, the increases in ROS seen in Sema3F treated neutrophils may go some way to explaining the mechanism by which Sema3F causes dynamic actin rearrangement. Terman et al. (2011) identify MICAL, a large multi domain flavo monooxygenase that directly links Sema3A-Plexin A1 signaling to the actin cytoskeleton.[334,335] Sema3A-Plexin mediated relief of autoinhibition of MICAL allows this enzyme to oxidise actin at the methionine 44 residue within the D-loop of the actin helix promoting decreasing

polymerisation.[174] Sema3A, has also been shown to affect neurite growth cone collapse through F-actin disassembly mediated by sequential inhibition and activation through cofilin phosphorylation by LIM-kinase resulting in an actin severing.[336] There appears to be a synergistic relationship between MICAL and cofilin, such that MICAL induced oxidation enhances cofilin binding and severing of F-actin ensuring instability and dismantling of the F-actin network.[337,338] MICAL establishes a role for neutrophil redox reactions in the regulation of the cytoskeleton. Increases in ROS directly promote F-actin disassembly and balance actin dynamics[320] Low levels of ROS also regulate actin. There is a deficiency in the generation of NADPH oxidase-dependent ROS in the phagocytes of patients with chronic granulomatous disease (CGD). Neutrophils from these patients have defective migration, with an increase in the frequency of pseudopodia and reduction in directionality and speed. This has been recapitulated with siRNA inhibitors of NADPH and in murine models of CGD.[265,339]

An extract of green tea, epigallocatechin gallate (EGCG) flavoprotein monooxygenase inhibitor, neutralised Sema3A axonal repulsion in culture.[340] EGCG is a non-specific inhibitor of flavoproteins. As MICAL cannot be selectively inhibited and genome editing through transfection is not effective in neutrophils it is difficult to ascertain whether MICAL is involved in Sema3F F-actin disassembly. I have demonstrated that Sema3F signaling results in F-actin disassembly in neutrophils, the upstream regulators of this process remain unclear. Certainly, we known that neutrophils express the MICAL 1 protein (unpublished data, Prof Sarah Walmsley) and thus it could link the Sema3F-Plexin-actin pathway. ROS and the regulators of neutrophil ROS production could also be candidates.

The lack of availability to me of a non-functioning blocking antibody for the Sema3F binding site on the NRP2 co-receptor means I cannot confirm the direct effect of Sema3F by this method. But considering the concordance between my varied model systems showing in *vivo* and *vitro* data. Alongside

what is already known about class 3 Semaphorins, there is little doubt that these results are due to Sema3F and its signaling pathway. Future work will focus on this pathway to delineate the key players and identify novel susceptibilities to therapeutic interventions.

5 Discussion

The regulation of neutrophil migration and retention has implications for the magnitude of the inflammatory response. In pathological neutrophilic inflammation there is an exaggerated response with the sequelae of tissue damage leading to disease. Signals that curtail excessive inflammation are directly relevant to the generation of novel anti-inflammatory therapies.

5.1 Summary of findings

Human neutrophils express Sema3F and its co-receptor NRP2 and are therefore amenable to autocrine regulation by Sema3F. Expression of both ligand and receptor are under the control of the inflammatory mediators. Sema3F mRNA and protein are up regulated in response to LPS and neutrophil surface expression of NRP2 is significantly increased by IL-1β (see table 5.1-1).

Neutrophil Expression of:		
Sema3F		
Stimuli/disease	mRNA expression	Protein expression
LPS	UP **P<0.001 (6 hours Murine fig 3.2.3-1)	IHC – present (murine fig. 3.2.5-1)
		WB- UP **P=0.0058 (human fig.3.2.1-1)
TNF-α	?	WB-present (human fig.3.2.1-1)
IL-1β	?	WB-present (human fig.3.2.1-1)
COPD	?	IHC – present (human fig. 3.2.2-1)
NRP2		
LPS	UP *P<0.05 (6 hours Murine fig 3.3.7-1)	IHC – present (murine fig. 3.2.5-1)
		FlowC-present (human fig 3.3.5-1)
TNF-α	?	FlowC-present (human fig 3.3.5-1)
IL-1β	?	FlowC-UP **P=0.0034 (human fig 3.3.5-1)
COPD	?	IHC – present (human fig. 3.3.1-1)

Table 5.1-1 The regulation of Sema3F and NRP2 expression
A summary of results detailing Sema3F and NRP2 expression as determined by immunohistochemistry (IHC) Western blot (WB) and Flow cytometry (FlowC)

Both Sema3F and the co-receptor NRP2 are expressed by recruited COPD neutrophils in the inflamed lung. Murine neutrophil Sema3F is induced acutely following ALI and persists throughout injury. Temporal differences between Sema3F and NRP2 murine neutrophil expression, at both the mRNA and protein level, were noted during the course of ALI. This suggests that a level of regulation of the signalling pathway occurs through Sema3F and NRP2 expression. In a murine model of LPS induced ALI exogenous Sema3F acts a in *vivo* retention signal to neutrophils following peak recruitment. Whereas loss of neutrophil Sema3F generates the converse phenotype, with increased neutrophil transit resulting in enhanced recruitment to the lung and resolution of neutrophilic inflammation. This occurs without alterations in neutrophil apoptosis, macrophage populations or disruption to the characteristic neutrophil surface expression of adhesion molecules CD11b and L-selectin in response to LPS.[341]

Following deletion of neutrophil Sema3F no differences were observed in the baseline circulating neutrophil counts. The phenotype was only uncovered following the induction of LPS induced lung injury. On induction of lung injury prior to, or at 6 hours both circulating and lung tissue neutrophil counts were similar for both genotypes. Loss of neutrophil Sema3F did lead to an increased BAL count and an earlier peak in neutrophil recruitment occurred at 6 hours in the KO animal. The observed increase in the neutrophil count was exclusive to the alveolar space. As such neutrophil Sema3F does not alter neutrophil adhesive interactions with constituents of the blood or lung tissue compartments namely: the lung endothelium, interstitium or epithelial layers allowing rapid neutrophil transit. It is more probable that Sema3F controls an intrinsic neutrophil property resulting in differential neutrophil transit times. This supports the view that following neutrophil sequestration, transmigration into the lung can be through an adhesion independent pathway.[82,240] Sema3F treatment inhibits convergent chemotaxis and acts as a neutrophil retention signal both in *vivo* and *vitro*. Neutrophils become rounder and more spherical

in response to Sema3F and this can be antagonised by fMLF. The effect of Sema3F on neutrophil histotoxic related functions is divergent. On one hand, ROS generation is promoted, and phagocytosis preserved, but in contrast MPO activity is reduced both in *vivo* and *vitro*. For MPO activity the converse holds true where loss of neutrophil Sema3F enhances MPO activity in the BAL fluid following ALI. There was no effect observed on neutrophil elastase activity following Sema3F treatment in *vitro*. In *vivo* the Sema3F KO animal had reduced elastase levels in the BAL fluid at 48 hours. This was associated with a period of enhanced resolution of the neutrophilic inflammation seen in the KO animal. This identifies a potential anti-inflammatory role for an antagonist of Sema3F signalling. This divergent behaviour of neutrophils in response to Sema3F in the context of inflammation could reflect a) the specific activation status of the Sema3F treated neutrophil or b) provide mechanistic insights. For example it is known that neutrophil ROS, which is up regulated by Sema3F treatment, is intimately related to the F-actin cytoskeleton.[263]

Sema3F pre-treatment reduces the level of neutrophil F-actin achieved during the steady state following the initial rapid polymerisation and depolymerisation phases characteristic of the neutrophil response to fMLF. Neutrophils that are retained by Sema3F in *vivo* have a decreased total F-actin. They are also more spherical and are slower with persevered directionality correlating with the in *vitro* chemotaxis data. These data taken together establish that Sema3F acts as a neutrophil retention signal by slowing down neutrophil migration through the induction of F-actin disassembly leading to more spherical neutrophils with altered effector functions. What remains to be elicited is the link between the Sema3F signal and downstream F-actin disassembly. Candidates include the observed increase in intracellular ROS resulting in a promotion of F-actin depolymerisation or redox enzymes such as MICAL which directly link Semaphorin-signalling to F-actin disassembly.

5.2 Limitations

I identified the presence of the receptors NRP1 and 2 using both flow cytometry and immunohistochemistry on neutrophils. The NRP2 receptor is the preferential co-receptor for Sema3F and a focus of this project as this presented a potential future therapeutic target.[342] I demonstrated that NRP2 expression is under the regulation of inflammation and is present on 10-18% of circulating human neutrophils. This is less than I expected given the size of the neutrophil response to both exogenous Sema3F and loss of neutrophil Sema3F. These methods would not identity NRP2 if it was either released as a soluble form in *vivo*, lost prior to fixation, or following fixation during sample processing. While this may result in an underestimate of the levels of NRP2 neutrophil surface expression, the relative ratios of the receptor expression between conditions would remain constant. Certainly, we know that murine neutrophil NRP2 mRNA is seen to rise acutely following LPS induced lung injury. Reassuringly, NRP2 is then observed at the protein level in recruited murine neutrophils in the injured lung. This supports the hypothesis that NRP2 is involved in Sema3F signalling and the generation of the phenotypes observed during this work. This project did not attempt to address which Plexin A1-A4 is expressed by neutrophils, as the NRP2 is an obligatory co-receptor. NRP2 is an ideal therapeutic target as it has no intracellular component and blocking agents are less likely to affect downstream pathways.

Having said this, NRP2 can bind other ligands, although at a separate binding site to Sema3F. This includes the vascular endothelial growth factor (VEGF) and antagonism between VEGF and Sema3F has been observed.[343,344] This interplay could be relevant to the Sema3F autocrine regulation of neutrophils. In the context of both a plethora of ligands, varied receptor combinations and expression profiles and the potential for receptor solubility, a reductionist strategy was employed in the first instance. This does not preclude the existence of further layers of complexity regarding Sema3F signal and its detection by neutrophils. In terms of the specificity of the Sema3F signal in these experiments it cannot be stated that they are a direct effect of Sema3F-

NRP2 binding. One constraint was the lack of a commercially available NRP2 non-functioning blocking antibody. In the context of the receptor complexity I have described this, single blockade would not have been sufficient to ensure that this was indeed due to a direct effect of Sema3F-NRP2 signalling. My hypothesis is further supported as the converse phenotype is seen in the neutrophil specific KO murine model. This result suggests that Sema3F does impact on neutrophil migration as predicted from extrapolations of both the in *vitro* and exogenous Sema3F murine experimental results. Therefore, it is highly likely that this is a result of direct Sema3F signalling.

It remains unknown whether the Sema3F signal in the injured lung is only from neutrophils. I observed that Sema3F was produced in epithelial cells in the injured airways of mice. The contribution to the overall Sema3F signal by cell type was not quantified. To address this the neutrophil specific knockout of Sema3F identified the impact of the neutrophil contribution to overall Sema3F signal by the resulting alteration in neutrophil behaviour. Semaphorins have been shown to affect integrin conformation and cell adhesion.[284,345] While I looked at neutrophil expression of CD11b and L-selectin I did not look at the activation status of these adhesive molecules or the ability of the neutrophil to adhere following Sema3F treatment. Neutrophil migration in the pulmonary vasculature can be adhesion pathway independent. The location and transit profile of the Sema3F deficient neutrophil suggests that the differences observed are likely due to adhesion pathway independent mechainsims.[240]

Finally, in the situation of neutrophil Sema3F loss the resolution of neutrophilic inflammation occurred at a faster rate. What this data cannot say is the route of enhanced neutrophil loss. I did not investigate either neutrophil reverse migration or loss to body through expectoration. There are significant challenges with measuring both of these potential routes of neutrophil loss and this fell beyond the scope of this current project. I did not observe alterations in apoptosis at individual timepoints which gave no indication that Sema3F alters neutrophil survival.

5.3 Future work

As identified in the limitations of this work there are many potential avenues to explore. The temporal regulation of neutrophil Sema3F expression is not known. How Sema3F production is switched on in the neutrophil and other cell types is crucial to understanding the signal during ALI and lung disease. In a similar manner I have not identified the Sema3F receptor profile over the injury course, or how the Sema3F autocrine loop functions; both would be essential in understanding this process in greater detail. It may be possible to use techniques such as mass spectrometry or Cytometry by Time of Flight (CyTOF) for detailed phenotypic analysis of the cells types implicated in the neutrophil Sema3F signalling pathway.[346] This method is able to use a far more extensive panel of antibodies than standard flowcytometry and is directed at both extra-and intracellular components. Using this it would be interesting to observe the production and release of Sema3F in neutrophils, macrophages and endothelial cells. This assessment would describe the contributions of various cell types to the total Sema3F signal and the individual cell-types response to Sema3F. This could be done by way of expression patterns of adhesion molecules and changes in cytoskeletal proteins. I could use this information to define how neutrophil transit is up and down regulated in response to Sema3F. It has been shown that myeloid specific ablation of NRP2 increased leukocyte infiltration into LPS injured lungs and delayed resolution[149] Similarly, loss of neutrophil Sema3F also enhanced leukocyte infiltration but resolution was not delayed. This may suggest Sema3F from a non-neutrophil source, or another antagonist of NRP2 is an important regulator of the myeloid population during resolution. To this end I have also begun work on a LysmCre driven Sema3F floxed mouse line to delineate the role of monocytes/macrophages in this signalling pathway. I also have preliminary immunohistochemistry data to describe the Plexin profile of the lung tissue during ALI. To further this I will generate a new flow panel to assess the neutrophil expression of the Sema3F Plexin receptors A1 to A4.

In the situation of loss of neutrophil Sema3F there is a causal relationship between increased neutrophil transit and enhanced resolution, but the mechanism remains unknown. Experiments to investigate neutrophil kinetics in this system might unmask the route of enhanced neutrophil clearance. My hypotheses are that enhanced clearance is due to: 1) greater loss to the body and the mucociliary escalator; 2) a reduction in the adjacent sequestered pool of neutrophils through reverse migration to the wider circulation resulting in a reduction in the availability of neutrophils to recruit to the airspaces; or 3) increased homeostatic clearance mechanisms engaged by the earlier peak in neutrophil recruitment seen in the Sema3F KO animal. When the mucociliary escalator fails the alveoli fill with mucus and gaseous exchange is reduced. This is seen in chronic lung diseases such as primary ciliary dyskinesia and cystic fibrosis. A role for the mucociliary escalator in acute lung injury cannot be completely discounted as there is no evidence to refute that clearance of neutrophils via this route would not influence the level of local inflammation in the alveoli following injury. Experimentally neutrophils could be followed through this journey and loss measured, for example monitoring labelled neutrophils in alveolus, small and large airways and sputum over a time course, this would begin to describe the fate of Sema3F deficient neutrophils following acute lung injury in mice. While ARDS It is known that reverse migrated neutrophils upregulate ICAM 1, CD54 and are $CXCR1^{Low}$.[61,323] Neutrophil surface expression of these markers could be assessed by flow cytometry to identify reverse transendothelial migrated neutrophils.

I would like to maintain the focus of research on potential therapeutic agents that could be used in the treatment of respiratory diseases. As such the Sema3F-NRP2 signalling pathway is pivotal. Two arms to this future work would include focusing on the receptor NRP2 and investigating the downstream effects of Sema3F signalling on the F-actin cytoskeleton. This would include investigating the consequence of NRP2 neutrophil specific knockout in an animal model, to recapitulate the Sema3F phenotype and

investigate the autocrine signalling loop. In addition, using NRP2 blockade by a non-functioning antibody to demonstrate that Sema3F-NRP2 binding is an initiating step in the pathway activation. The antibody could also be used in an animal model as an in *vivo* therapy, where nebulised NRP2 would be hypothesised to enhance neutrophil resolution and lessen lung tissue damage. Lung damage would be assessed through measurements of markers associated with progressive disease elastase, such as myeloperoxidase and albumin alongside immunohistochemistry of lung tissue.

It would be vital to establish the role of neutrophil Sema3F in host-pathogen responses in order to assess whether this pathway could yield a viable treatment for inflammatory lung conditions. In part, this is because sterile lung inflammation often occurs concurrently with infection either super-imposed on the inflammation or as a preceding injury to the lung leading to inflammation. As such, investigating the response of the Sema3F KO mouse to pneumonia or hypoxia would further deepen our understanding of the role of Sema3F as a retention signal and the potential for exploiting this to modify disease. In this situation the timing of the exogenous Sema3F or NRP2 blockade could dictate whether this treatment is harmful or helpful to the host. For example, delivery of the NRP2 blockade early in a pneumonia model may reduce the helpful neutrophil responses, as recruitment and resolution are both enhanced, resulting in a detrimental persistence of the infective agent. Equally, the enhanced peak recruitment could be sufficient to clear the pathogens and recovery from pneumonia expedited. Likewise, exogenous Sema3F given at peak recruitment or before could enhance the neutrophil response and bacterial clearance. It is unclear whether this would result in damage to the host as neutrophilic resolution is subsequently delayed.

In concert with interrogating the physiological effects of Sema3F in the context of lung disease, elucidating the underlying mechanism is required. To investigate the F-actin cytoskeletal changes in relation to Sema3F I would use the ex-*vivo* lung slice set-up with real-time imaging. By using Ly6G-LifeAct-

GFP neutrophils I can heat-map the F-actin distribution in real-time in response to treatment and stimuli. Other ways to address this could include high-resolution con-focal microscopy of neutrophils with staining for F and G actin or fluorescent speckle microscopy.[347] This may highlight which downstream actin associated regulators are involved and these could be targeted to control neutrophil migration downstream of Sema3F.

As discussed, the redox protein MICAL and intracellular ROS are candidates which could link Sema3F-Plexin signalling to the cytoskeletal.[173,263,338,348,349] F-actin disassembly can be the result of multiple cytoskeletal re-arrangements and modifications involving proteins such as: cofilin and ARP2 complex promoting actin severing and branching respectively, or other such as fascin an actin bundling protein and formin an actin nucleation factor. Directionality is preserved in the Sema3F deficient murine neutrophils and supported by unpublished zebrafish data from my lab group. We know the Sema3F signal alters the actin cytoskeleton downstream of the formation of the leading edge which excludes actin associated proteins upstream of this. This suggests the family of Rho GTPases, in particular Rac1 and 2, could be involved in the generation of the divergent effects on neutrophil effector functions seen in response to Sema3F. An understanding of the downstream mechanisms in the Sema3F signalling pathway may guide the generation and application of future therapeutic interventions based on this science.

5.4 Therapeutic targeting of Sema3F signalling pathway in neutrophils

I have eluded to the use of NRP2 blockade as a way to regulate neutrophilic inflammation. This poses the danger of altering an essential innate immune response and could potentially render the patient susceptible to infection. If the NRP2 blocker was given too early this could enhance neutrophil recruitment and exacerbate the problem. As yet, we do not fully understand how the Sema3F signal causes enhanced recruitment and later resolution, or the interplay with other key signals. Manipulating the actin cytoskeletal responses

downstream of the Sema3F signal appears attractive. This could negate effects on VEGF binding and off target effects of NRP2 receptors on other cells. This is a risky proposal as these are ubiquitous targets and modulators of actin cytoskeleton are often cytotoxic, such as phalloidin and the chemotherapy agent Paclitaxel.

It may be that NRP2 blockade could be used in conjunction with other therapies. The beneficial anti-angiogenic effect of the VEGF-A monoclonal antibody (bevacizumab) on patients with glioblastoma is short lived. This is associated with NRP1 down regulation due to internalisation following binding transforming growth factor βs (TGFβs).[350] In this case dual therapy with NRP1 blockade could give a better response to anti-cancer therapy. SEMA3F is a known tumor suppressor in lung cancer; this is downregulated by TGFβ1 but NRP2 is upregulated during TGFβ1-driven epithelial-mesenchymal transitioning.[351] This suggests NRP2, in this context, is transducing a pro-cancer signal which is antagonised by Sema3F. In this manner, rather than non-functioning blockade of NRP2, Sema3F treatment itself may have a role in cancer therapy. Overall there are many promising therapeutic applications for Sema3F and its co-receptor NRP2 in respiratory disease. It is with greater knowledge of the ligand and receptor we can produce both targeted and personalised therapies for our patients with enhanced efficacy and improved side effect profiles.

6 References

1. Savill, J. S., Henson, P. M. & Haslett, C. Phagocytosis of aged human neutrophils by macrophages is mediated by a novel 'charge-sensitive' recognition mechanism. *J. Clin. Invest.* **84,** 1518–1527 (1989).
2. Borregaard, N. & Cowland, J. B. Granules of the Human Neutrophilic Polymorphonuclear Leukocyte. *Blood* **89,** 3503–3521 (1997).
3. Segal, AW., Geisow, M., Garcia, R., Harper, A. & Miller, R. The respiratory burst of phagocytic cells is associated with a rise in vacuolar pH. *Nature* **290,** 406–409 (1981).
4. Segal, A. W. How Neutrophils Kill Microbes. *Annual review of immunology* **23,** 197–223 (2005).
5. Hampton, M. B., Kettle, A. J. & Winterbourn, C. C. Inside the Neutrophil Phagosome: Oxidants, Myeloperoxidase, and Bacterial Killing. *Blood* **92,** 3007–3017 (1998).
6. Whyte, M. K., Meagher, L. C., MacDermot, J. & Haslett, C. Impairment of function in aging neutrophils is associated with apoptosis. (1993).
7. Sabroe, I., Prince, L. R., Jones, E. C., Horsburgh, M. J., Foster, S. J., Vogel, S. N., Dower, S. K. & Whyte, M. K. B. Selective roles for Toll-like receptor (TLR)2 and TLR4 in the regulation of neutrophil activation and life span. *The Journal of Immunology* **170,** 5268–5275 (2003).
8. Walmsley, S. R. *et al.* Hypoxia-induced neutrophil survival is mediated by HIF-1alpha-dependent NF-kappaB activity. *J Exp Med* **201,** 105–115 (2005).
9. Lee, A., Whyte, M. K. & Haslett, C. Inhibition of apoptosis and prolongation of neutrophil functional longevity by inflammatory mediators. *J Leukoc Biol* **54,** 283–288 (1993).
10. Bernard, G. R. *et al.* Report of the American-European consensus conference on ARDS: Definitions, mechanisms, relevant outcomes and clinical trial coordination. *Intensive Care Med* **20,** 225–232 (1994).
11. Pittet, J. F., Mackersie, R. C., Martin, T. R. & Matthay, M. A. Biological markers of acute lung injury: prognostic and pathogenetic significance. *Am. J. Respir. Crit. Care Med.* **155,** 1187–1205 (1997).
12. Anderson, W. R. & Thielen, K. Correlative Study of Adult Respiratory Distress Syndrome by Light, Scanning, and Transmission Electron Microscopy. *Ultrastructural Pathology* **16,** 615–628 (2009).
13. Laufe, M. D., Simon, R. H., Flint, A. & Keller, J. B. Adult respiratory distress syndrome in neutropenic patients. *The American Journal of Medicine* **80,** 1022–1026 (1986).

14. Williams, A. E. *et al.* Evidence for chemokine synergy during neutrophil migration in ARDS. *Thorax* **72,** 66–73 (2017).
15. Steinberg, K. P. *et al.* Evolution of bronchoalveolar cell populations in the adult respiratory distress syndrome. *Am. J. Respir. Crit. Care Med.* **150,** 113–122 (1994).
16. Grommes, J. & Soehnlein, O. Contribution of neutrophils to acute lung injury. *Mol. Med.* **17,** 293–307 (2011).
17. Brun-Buisson, C. *et al.* Epidemiology and outcome of acute lung injury in European intensive care units. *Intensive Care Med* **30,** 51–61
18. Bellingan, G. J. The pulmonary physician in critical care • 6: The pathogenesis of ALI/ARDS. *Thorax* **57,** 540–546 (2002).
19. Matthay, M. A. & Zimmerman, G. A. Acute Lung Injury and the Acute Respiratory Distress Syndrome. *American Journal of Respiratory Cell and Molecular Biology* (2005).
20. Singh, N. R. P. *et al.* Acute lung injury results from failure of neutrophil de-priming: a new hypothesis. *European Journal of Clinical Investigation* **42,** 1342–1349 (2012).
21. Summers, C. *et al.* Pulmonary retention of primed neutrophils: a novel protective host response, which is impaired in the acute respiratory distress syndrome. *Thorax* **69,** 623–629 (2014).
22. Yipp, B. G. *et al.* The Lung is a Host Defense Niche for Immediate Neutrophil-Mediated Vascular Protection. *Science immunology* **2,** eaam8929 (2017).
23. Wang, J. *et al.* Visualizing the function and fate of neutrophils in sterile injury and repair. *Science* **358,** 111–116 (2017).
24. Kubes, P. The enigmatic neutrophil: what we do not know. *Cell Tissue Res.* **371,** 399–406 (2018).
25. Quint, J. K. & Wedzicha, J. A. The neutrophil in chronic obstructive pulmonary disease. *Journal of Allergy and Clinical Immunology* **119,** 1065–1071 (2007).
26. Huang, G. *et al.* Neutrophilic Inflammation in the Immune Responses of Chronic Obstructive Pulmonary Disease: Lessons from Animal Models. *J Immunol Res* **2017,** 7915975–9 (2017).
27. Kamath, A. V., Pavord, I. D., Ruparelia, P. R. & Chilvers, E. R. Is the neutrophil the key effector cell in severe asthma? *Thorax* **60,** 529–530 (2005).
28. Gharaee-Kermani, M., Gyetko, M. R., Hu, B. & Phan, S. H. New insights into the pathogenesis and treatment of idiopathic pulmonary fibrosis: a potential role for stem cells in the lung parenchyma and implications for therapy. *Pharm. Res.* **24,** 819–841 (2007).
29. Gifford, A. M. & Chalmers, J. D. The role of neutrophils in cystic fibrosis. *Current Opinion in Hematology* **21,** 16–22 (2014).
30. Pittman, K. & Kubes, P. Damage-associated molecular patterns control neutrophil recruitment. *J Innate Immun* **5,** 315–323 (2013).

31. Ng, L. G. *et al.* Visualizing the neutrophil response to sterile tissue injury in mouse dermis reveals a three-phase cascade of events. *J. Invest. Dermatol.* **131,** 2058–2068 (2011).
32. Niethammer, P., Grabher, C., Look, A. T. & Mitchison, T. J. A tissue-scale gradient of hydrogen peroxide mediates rapid wound detection in zebrafish. *Nature* **459,** 996–U123 (2009).
33. Yoo, S. K., Starnes, T. W., Deng, Q. & Huttenlocher, A. Lyn is a redox sensor that mediates leukocyte wound attraction in vivo. *Nature* **480,** 109–112 (2011).
34. Klyubin, I. V., Kirpichnikova, K. M. & Gamaley, I. A. Hydrogen peroxide-induced chemotaxis of mouse peritoneal neutrophils. *Eur J Cell Biol* **70,** 347–351 (1996).
35. McDonald, B. *Intravascular danger signals guide neutrophils to sites of sterile inflammation (October, pg 362, 2010)*. (Science, 2011).
36. Lämmermann, T. In the eye of the neutrophil swarm—navigation signals that bring neutrophils together in inflamed and infected tissues. *J Leukoc Biol* **100,** jlb.1MR0915–403–63 (2015).
37. Sai, J., Raman, D., Liu, Y., Wikswo, J. & Richmond, A. Parallel phosphatidylinositol 3-kinase (PI3K)-dependent and Src-dependent pathways lead to CXCL8-mediated Rac2 activation and chemotaxis. *J. Biol. Chem.* **283,** 26538–26547 (2008).
38. Afonso, P. V. *et al.* LTB4 is a signal-relay molecule during neutrophil chemotaxis. *Developmental Cell* **22,** 1079–1091 (2012).
39. Lindley, I. *et al.* Synthesis and expression in Escherichia coli of the gene encoding monocyte-derived neutrophil-activating factor: biological equivalence between natural and recombinant neutrophil-activating factor. *PNAS* **85,** 9199–9203 (1988).
40. de Oliveira, S. *et al.* Cxcl8 (IL-8) mediates neutrophil recruitment and behavior in the zebrafish inflammatory response. *J. Immunol.* **190,** 4349–4359 (2013).
41. Devalaraja, R. M. *et al.* Delayed wound healing in CXCR2 knockout mice. *J. Invest. Dermatol.* **115,** 234–244 (2000).
42. Li, L. *et al.* New development in studies of formyl-peptide receptors: critical roles in host defense. *J Leukoc Biol* **99,** 425–435 (2016).
43. Kansas, G. S. Selectins and their ligands: current concepts and controversies. *Blood* **88,** 3259–3287 (1996).
44. Yago, T. *et al.* E-selectin engages PSGL-1 and CD44 through a common signaling pathway to induce integrin αLβ2-mediated slow leukocyte rolling. *Blood* **116,** 485–494 (2010).
45. Hidalgo, A., Peired, A. J., Wild, M. K., Vestweber, D. & Frenette, P. S. Complete Identification of E-Selectin Ligands on Neutrophils Reveals Distinct Functions of PSGL-1, ESL-1, and CD44. *Immunity* **26,** 477–489 (2007).

46. Chesnutt, B. C. *et al.* Induction of LFA-1-Dependent Neutrophil Rolling on ICAM-1 by Engagement of E-Selectin. *Microcirculation* **13,** 99–109 (2009).
47. Kadono, T., Venturi, G. M., Steeber, D. A. & Tedder, T. F. Leukocyte rolling velocities and migration are optimized by cooperative L-selectin and intercellular adhesion molecule-1 functions. *The Journal of Immunology* **169,** 4542–4550 (2002).
48. Shamri, R. *et al.* Lymphocyte arrest requires instantaneous induction of an extended LFA-1 conformation mediated by endothelium-bound chemokines. *Nature Immunology* **6,** 497–506 (2005).
49. Kim, M., Carman, C. V. & Springer, T. A. Bidirectional transmembrane signaling by cytoplasmic domain separation in integrins. *Science* **301,** 1720–1725 (2003).
50. Kinashi, T. Intracellular signalling controlling integrin activation in lymphocytes. *Nature Reviews Immunology* **5,** 546–559 (2005).
51. Phillipson, M. *et al.* Intraluminal crawling of neutrophils to emigration sites: a molecularly distinct process from adhesion in the recruitment cascade. *J Exp Med* **203,** 2569–2575 (2006).
52. Shaw, S. K., Bamba, P. S., Perkins, B. N. & Luscinskas, F. W. Real-time imaging of vascular endothelial-cadherin during leukocyte transmigration across endothelium. *The Journal of Immunology* **167,** 2323–2330 (2001).
53. Nourshargh, S., Krombach, F. & Dejana, E. The role of JAM-A and PECAM-1 in modulating leukocyte infiltration in inflamed and ischemic tissues. *J Leukoc Biol* **80,** 714–718 (2006).
54. Cinamon, G., Shinder, V., Shamri, R. & Alon, R. Chemoattractant signals and beta 2 integrin occupancy at apical endothelial contacts combine with shear stress signals to promote transendothelial neutrophil migration. *The Journal of Immunology* **173,** 7282–7291 (2004).
55. Millán, J. *et al.* Lymphocyte transcellular migration occurs through recruitment of endothelial ICAM-1 to caveola- and F-actin-rich domains. *Nature Cell Biology* **8,** 113–123 (2006).
56. Nieminen, M. *et al.* Vimentin function in lymphocyte adhesion and transcellular migration. *Nature Cell Biology* **8,** 156–162 (2006).
57. Hallmann, R. *et al.* Expression and Function of Laminins in the Embryonic and Mature Vasculature. *Physiological Reviews* **85,** 979–1000 (2005).
58. Wang, S. *et al.* Venular basement membranes contain specific matrix protein low expression regions that act as exit points for emigrating neutrophils. *J Exp Med* **203,** 1519–1532 (2006).
59. Wang, S., Dangerfield, J. P., Young, R. E. & Nourshargh, S. PECAM-1, α6 integrins and neutrophil elastase cooperate in mediating neutrophil transmigration. *Journal of Cell Science* **118,** 2067–2076 (2005).

60. Summers, C. *et al.* Neutrophil kinetics in health and disease. *Trends in Immunology* **31,** 318–324 (2010).
61. Hanger, C. C., Wagner, W. W., Janke, S. J., Lloyd, T. C. & Capen, R. L. Computer simulation of neutrophil transit through the pulmonary capillary bed. *J. Appl. Physiol.* **74,** 1647–1652 (1993).
62. Doerschuk, C. M., Tasaka, S. & Wang, Q. CD11/CD18-dependent and -independent neutrophil emigration in the lungs: how do neutrophils know which route to take? *American Journal of Respiratory Cell and Molecular Biology* **23,** 133–136 (2000).
63. Kubo, H. *et al.* L- and P-Selectin and CD11/CD18 in Intracapillary Neutrophil Sequestration in Rabbit Lungs. *Am. J. Respir. Crit. Care Med.* **159,** 267–274 (2012).
64. Klesney-Tait, J. *et al.* Transepithelial migration of neutrophils into the lung requires TREM-1. *J. Clin. Invest.* **123,** 138–149 (2013).
65. Cicchetti, G., Allen, P. G. & Glogauer, M. Chemotactic signaling pathways in neutrophils: from receptor to actin assembly. *CROBM* **13,** 220–228 (2002).
66. Hirsch, E. *et al.* Central role for G protein-coupled phosphoinositide 3-kinase gamma in inflammation. *Science* **287,** 1049–1053 (2000).
67. Stephens, L., Ellson, C. & Hawkins, P. Roles of PI3Ks in leukocyte chemotaxis and phagocytosis. *Current Opinion in Cell Biology* **14,** 203–213 (2002).
68. Orlando, K. & Guo, W. Membrane Organization and Dynamics in Cell Polarity. *Cold Spring Harb Perspect Biol* **1,** a001321–a001321 (2009).
69. Srinivasan, S. *et al.* Rac and Cdc42 play distinct roles in regulating PI(3,4,5)P3 and polarity during neutrophil chemotaxis. *J Cell Biol* **160,** 375–385 (2003).
70. Lam, P.-Y., Yoo, S. K., Green, J. M. & Huttenlocher, A. The SH2-domain-containing inositol 5-phosphatase (SHIP) limits the motility of neutrophils and their recruitment to wounds in zebrafish. *J Cell Sci* **125,** 4973–4978 (2012).
71. Mondal, S., Subramanian, K. K., Sakai, J., Bajrami, B. & Luo, H. R. Phosphoinositide lipid phosphatase SHIP1 and PTEN coordinate to regulate cell migration and adhesion. *Mol. Biol. Cell* **23,** 1219–1230 (2012).
72. Buckley, C. D., Gilroy, D. W., Serhan, C. N., Stockinger, B. & Tak, P. P. The resolution of inflammation. *Nature Reviews Immunology* **13,** 59–66 (2013).
73. Elks, P. M. *et al.* Activation of hypoxia-inducible factor-1α (Hif-1α) delays inflammation resolution by reducing neutrophil apoptosis and reverse migration in a zebrafish inflammation model. *Blood* **118,** 712–722 (2011).
74. Buckley, C. D. *et al.* Identification of a phenotypically and functionally distinct population of long-lived neutrophils in a model

of reverse endothelial migration. *J Leukoc Biol* **79,** 303–311 (2006).
75. Nourshargh, S., Renshaw, S. A. & Imhof, B. A. Reverse Migration of Neutrophils: Where, When, How, and Why? *Trends in Immunology* **37,** 273–286 (2016).
76. Nourshargh, S. & Alon, R. Leukocyte migration into inflamed tissues. *Immunity* **41,** 694–707 (2014).
77. Mathias, J. R. *et al.* Resolution of inflammation by retrograde chemotaxis of neutrophils in transgenic zebrafish. *J Leukoc Biol* **80,** 1281–1288 (2006).
78. Renshaw, S. A. *et al.* A transgenic zebrafish model of neutrophilic inflammation. *Blood* **108,** 3976–3978 (2006).
79. Robertson, A. L. *et al.* A Zebrafish Compound Screen Reveals Modulation of Neutrophil Reverse Migration as an Anti-Inflammatory Mechanism. *Science Translational Medicine* **6,** 225ra29–225ra29 (2014).
80. Auffray, C. *et al.* Monitoring of blood vessels and tissues by a population of monocytes with patrolling behavior. *Science* **317,** 666–670 (2007).
81. Kelly, M., Hwang, J. M. & Kubes, P. Modulating leukocyte recruitment in inflammation. *Journal of Allergy and Clinical Immunology* **120,** 3–10 (2007).
82. Nourshargh, S., Hordijk, P. L. & Sixt, M. Breaching multiple barriers: leukocyte motility through venular walls and the interstitium. *Nature Reviews Molecular Cell Biology* **11,** 366–378 (2010).
83. Hughes, J. *et al.* Neutrophil fate in experimental glomerular capillary injury in the rat. Emigration exceeds in situ clearance by apoptosis. *Am. J. Pathol.* **150,** 223–234 (1997).
84. Elks, P. M. *et al.* Activation of hypoxia-inducible factor-1α (Hif-1α) delays inflammation resolution by reducing neutrophil apoptosis and reverse migration in a zebrafish inflammation model. *Blood* **118,** 712–722 (2011).
85. Ellett, F., Elks, P. M., Robertson, A. L., Ogryzko, N. V. & Renshaw, S. A. Defining the phenotype of neutrophils following reverse migration in zebrafish. *J Leukoc Biol* **98,** 975–981 (2015).
86. Tauzin, S., Starnes, T. W., Becker, F. B., Lam, P.-Y. & Huttenlocher, A. Redox and Src family kinase signaling control leukocyte wound attraction and neutrophil reverse migration. *J Cell Biol* **207,** 589–598 (2014).
87. Woodfin, A. *et al.* The junctional adhesion molecule JAM-C regulates polarized transendothelial migration of neutrophils in vivo. *Nature Immunology* **12,** 761–769 (2011).
88. Duffy, D. *et al.* Neutrophils transport antigen from the dermis to the bone marrow, initiating a source of memory CD8+ T cells. *Immunity* **37,** 917–929 (2012).

89. Hamza, B. & Irimia, D. Whole blood human neutrophil trafficking in a microfluidic model of infection and inflammation. *Lab Chip* **15,** 2625–2633 (2015).
90. Huttenlocher, A. & Poznansky, M. C. Reverse leukocyte migration can be attractive or repulsive. *Trends Cell Biol.* **18,** 298–306 (2008).
91. Doerschuk, C. M. Mechanisms of leukocyte sequestration in inflamed lungs. *Microcirculation* **8,** 71–88 (2001).
92. Phillipson, M., Heit, B., Colarusso, P., of, L. L. J.2006. Intraluminal crawling of neutrophils to emigration sites: a molecularly distinct process from adhesion in the recruitment cascade. *jem.rupress.org*
93. Geissmann, F. *et al.* Intravascular Immune Surveillance by CXCR6+ NKT Cells Patrolling Liver Sinusoids. *PLoS Biol.* **3,** e113 (2005).
94. Rodero, M. P. *et al.* Immune surveillance of the lung by migrating tissue monocytes. *cdn.elifesciences.org*
95. Woodfin, A. *et al.* The junctional adhesion molecule JAM-C regulates polarized transendothelial migration of neutrophils in vivo. *Nature Immunology* **12,** 761–769 (2011).
96. Colom, B. *et al.* Leukotriene B4-Neutrophil Elastase Axis Drives Neutrophil Reverse Transendothelial Cell Migration In Vivo. *Immunity* **42,** 1075–1086 (2015).
97. de Oliveira, S., Rosowski, E. E. & Huttenlocher, A. Neutrophil migration in infection and wound repair: going forward in reverse. *Nature Reviews Immunology* **16,** 378–391 (2016).
98. Tharp, W. G. *et al.* Neutrophil chemorepulsion in defined interleukin-8 gradients in vitro and in vivo. *J Leukoc Biol* **79,** 539–554 (2006).
99. Enyedi, B., Kala, S., Nikolich-Zugich, T. & Niethammer, P. Tissue damage detection by osmotic surveillance. *Nature Cell Biology* **15,** 1123–1130 (2013).
100. Hamza, B. *et al.* Retrotaxis of human neutrophils during mechanical confinement inside microfluidic channels. *Integr. Biol.* **6,** 175–183 (2014).
101. Hamza, B. *et al.* Retrotaxis of human neutrophils during mechanical confinement inside microfluidic channels. *Integr. Biol.* **6,** 175–183 (2014).
102. Colom, B. *et al.* Leukotriene B4-Neutrophil Elastase Axis Drives Neutrophil Reverse Transendothelial Cell Migration In Vivo. *Immunity* **42,** 1075–1086 (2015).
103. Holmes, G. R. *et al.* Repelled from the wound, or randomly dispersed? Reverse migration behaviour of neutrophils characterized by dynamic modelling. *J R Soc Interface* **9,** 3229–3239 (2012).

104. Opfermann, P. *et al.* A pilot study on reparixin, a CXCR1/2 antagonist, to assess safety and efficacy in attenuating ischaemia–reperfusion injury and inflammation after on-pump coronary artery bypass graft surgery. *Clin. Exp. Immunol.* **180,** 131–142 (2015).
105. Leaker, B. R., Barnes, P. J. & O'Connor, B. Inhibition of LPS-induced airway neutrophilic inflammation in healthy volunteers with an oral CXCR2 antagonist. *Respiratory Research 2008 9:1* **14,** 137 (2013).
106. Tweedy, L., Susanto, O. & Insall, R. H. Self-generated chemotactic gradients — cells steering themselves. *Current Opinion in Cell Biology* **42,** 46–51 (2016).
107. Gambardella, L. & Vermeren, S. Molecular players in neutrophil chemotaxis--focus on PI3K and small GTPases. *Journal of leukocyte biology* **94,** 603–612 (2013).
108. Welch, M. D., Iwamatsu, A. & Mitchison, T. J. Actin polymerization is induced by Arp 2/3 protein complex at the surface of Listeria monocytogenes. *, Published online: 16 January 1997; | doi:10.1038/385265a0* **385,** 265–269 (1997).
109. Insall, R. H. & Machesky, L. M. Actin dynamics at the leading edge: from simple machinery to complex networks. *Developmental Cell* **17,** 310–322 (2009).
110. Pollard, T. D. & Borisy, G. G. Cellular Motility Driven by Assembly and Disassembly of Actin Filaments. *Cell* **112,** 453–465 (2003).
111. Chhabra, E. S. & Higgs, H. N. The many faces of actin: matching assembly factors with cellular structures. *Nature Cell Biology* **9,** 1110–1121 (2007).
112. Pantaloni, D., Le Clainche, C. & Carlier, M.-F. Mechanism of Actin-Based Motility. *Science* **292,** 1502–1506 (2001).
113. Levy, B. D., Clish, C. B., Schmidt, B., Gronert, K. & Serhan, C. N. Lipid mediator class switching during acute inflammation: signals in resolution. *Nature Immunology* **2,** 612–619 (2001).
114. Savill, J. Apoptosis in resolution of inflammation. *J Leukoc Biol* **61,** 375–380 (1997).
115. Rossi, A. G. *et al.* Cyclin-dependent kinase inhibitors enhance the resolution of inflammation by promoting inflammatory cell apoptosis. *Nat Med* **12,** 1056–1064 (2006).
116. Green, D. R. & Kroemer, G. The Pathophysiology of Mitochondrial Cell Death. *Science* **305,** 626–629 (2004).
117. McGrath, E. E. *et al.* TNF-related apoptosis-inducing ligand (TRAIL) regulates inflammatory neutrophil apoptosis and enhances resolution of inflammation. *J Leukoc Biol* **90,** 855–865 (2011).
118. Colotta, F., Re, F., Polentarutti, N., Sozzani, S. & Mantovani, A. Modulation of granulocyte survival and programmed cell death by cytokines and bacterial products. *Blood* **80,** 2012–2020 (1992).

119. Walmsley, S. R. *et al.* Prolyl hydroxylase 3 (PHD3) is essential for hypoxic regulation of neutrophilic inflammation in humans and mice. *J. Clin. Invest.* **121,** 1053–1063 (2011).
120. Serhan, C. N. *et al.* Resolvins A Family of Bioactive Products of Omega-3 Fatty Acid Transformation Circuits Initiated by Aspirin Treatment that Counter Proinflammation Signals. *J Exp Med* **196,** 1025–1037 (2002).
121. Ariel, A. & Serhan, C. N. Resolvins and protectins in the termination program of acute inflammation. *Trends in Immunology* **28,** 176–183 (2007).
122. Fujisawa, H. & Kitsukawa, T. Receptors for collapsin/semaphorins. *Current Opinion in Neurobiology* **8,** 587–592 (1998).
123. Kruger, R. P., Aurandt, J. & Guan, K.-L. Semaphorins command cells to move. *Nature reviews. Molecular cell biology* **6,** 789–800 (2005).
124. Jongbloets, B. C. & Pasterkamp, R. J. Semaphorin signalling during development. *Development* **141,** 3292–3297 (2014).
125. Luo, Y., Raible, D. & Raper, J. A. Collapsin: a protein in brain that induces the collapse and paralysis of neuronal growth cones. *Cell* **75,** 217–227 (1993).
126. Kolodkin, A. L., Matthes, D. J. & Goodman, C. S. The semaphorin genes encode a family of transmembrane and secreted growth cone guidance molecules. *Cell* **75,** 1389–1399 (1993).
127. Pasterkamp, R. J. & Kolodkin, A. L. Semaphorin junction: making tracks toward neural connectivity. *Current Opinion in Neurobiology* **13,** 79–89 (2003).
128. Love, C. A. *et al.* The ligand-binding face of the semaphorins revealed by the high-resolution crystal structure of SEMA4D. *Nature Structural & Molecular Biology* **10,** 843–848 (2003).
129. Ohta, K. *et al.* Plexin: A novel neuronal cell surface molecule that mediates cell adhesion via a homophilic binding mechanism in the presence of calcium ions. *Neuron* **14,** 1189–1199 (1995).
130. Tong, Y. & Buck, M. 1H, 15N and 13C Resonance assignments and secondary structure determination reveal that the minimal Rac1 GTPase binding domain of plexin-B1 has a ubiquitin fold. *J. Biomol. NMR* **31,** 369–370 (2005).
131. Janssen, B. J. C. *et al.* Structural basis of semaphorin-plexin signalling. *Nature* **467,** 1118–1122 (2010).
132. He, Z. & Tessier-Lavigne, M. Neuropilin is a receptor for the axonal chemorepellent Semaphorin III. *Cell* **90,** 739–751 (1997).
133. Janssen, B. J. C. *et al.* Neuropilins lock secreted semaphorins onto plexins in a ternary signaling complex. *Nature Structural & Molecular Biology* **19,** 1293–1299 (2012).
134. Soker, S., Takashima, S., Miao, H. Q., Neufeld, G. & Klagsbrun, M. Neuropilin-1 is expressed by endothelial and tumor cells as an

isoform-specific receptor for vascular endothelial growth factor. *Cell* **92,** 735–745 (1998).
135. Takahashi, T. & Strittmatter, S. M. Plexina1 autoinhibition by the plexin sema domain. *Neuron* **29,** 429–439 (2001).
136. Kong, Y. *et al.* Structural Basis for Plexin Activation and Regulation. *Neuron* **91,** 548–560 (2016).
137. Guo, H.-F. & Vander Kooi, C. W. Neuropilin Functions as an Essential Cell Surface Receptor. *J. Biol. Chem.* **290,** 29120–29126 (2015).
138. Püschel, A. W. The function of neuropilin/plexin complexes. *Adv. Exp. Med. Biol.* **515,** 71–80 (2002).
139. Negishi, M., Oinuma, I. & Katoh, H. Plexins: axon guidance and signal transduction. *Cellular and Molecular Life Sciences* **62,** 1363–1371 (2005).
140. Swendeman, S. *et al.* VEGF-A Stimulates ADAM17-Dependent Shedding of VEGFR2 and Crosstalk Between VEGFR2 and ERK Signaling. *Circulation Research* **103,** 916–918 (2008).
141. Werneburg, S. *et al.* Polysialylation and lipopolysaccharide-induced shedding of E-selectin ligand-1 and neuropilin-2 by microglia and THP-1 macrophages. *Glia* **64,** 1314–1330 (2016).
142. Kumanogoh, A. & Kikutani, H. Immunological functions of the neuropilins and plexins as receptors for semaphorins. *Nature Reviews Immunology* **13,** 802–814 (2013).
143. Tamagnone, L. *et al.* Class 3 semaphorins control vascular morphogenesis by inhibiting integrin function. **424,** 391–397 (2003).
144. Casazza, A. *et al.* Impeding macrophage entry into hypoxic tumor areas by Sema3A/Nrp1 signaling blockade inhibits angiogenesis and restores antitumor immunity. *Cancer Cell* **24,** 695–709 (2013).
145. Piper, M., Salih, S., Weinl, C., Holt, C. E. & Harris, W. A. Endocytosis-dependent desensitization and protein synthesisl[ndash]ldependent resensitization in retinal growth cone adaptation. *Nature Neuroscience* **8,** 179–186 (2005).
146. Ji, J. D., Park-Min, K.-H. & Ivashkiv, L. B. Expression and function of semaphorin 3A and its receptors in human monocyte-derived macrophages. *Human Immunology* **70,** 211–217 (2009).
147. Curreli, S., Arany, Z., Gerardy-Schahn, R., Biological, D. M. J. O.2007. Polysialylated neuropilin-2 is expressed on the surface of human dendritic cells and modulates dendritic cell-T lymphocyte interactions. *ASBMB*
148. Mendes-da-Cruz, D. A. *et al.* Semaphorin 3F and Neuropilin-2 Control the Migration of Human T-Cell Precursors. *PLOS ONE* **9,** e103405 (2014).
149. Immormino, R. M. *et al.* Neuropilin-2 regulates airway inflammatory responses to inhaled lipopolysaccharide. *American*

Journal of Physiology - Lung Cellular and Molecular Physiology **266,** L278 (2018).
150. Nasarre, P. *et al.* Semaphorin SEMA3F and VEGF Have Opposing Effects on Cell Attachment and Spreading. *Neoplasia* **5,** 83–92 (2003).
151. Maden, C. H. *et al.* NRP1 and NRP2 cooperate to regulate gangliogenesis, axon guidance and target innervation in the sympathetic nervous system. *Dev. Biol.* **369,** 277–285 (2012).
152. Mitsui, N. *et al.* Involvement of Fes/Fps tyrosine kinase in semaphorin3A signaling. *The EMBO Journal* **21,** 3274–3285 (2002).
153. Gu, Y. & Ihara, Y. Evidence that collapsin response mediator protein-2 is involved in the dynamics of microtubules. *J. Biol. Chem.* **275,** 17917–17920 (2000).
154. Turner, L. J., Nicholls, S. & Hall, A. The activity of the plexin-A1 receptor is regulated by Rac. *J. Biol. Chem.* **279,** 33199–33205 (2004).
155. Jin, Z. & Strittmatter, S. M. Rac1 mediates collapsin-1-induced growth cone collapse. *J. Neurosci.* **17,** 6256–6263 (1997).
156. Andrea B Huber, Alex L Kolodkin, David D Ginty & Cloutier, J.-F. SIGNALING AT THE GROWTH CONE: Ligand-Receptor Complexes and the Control of Axon Growth and Guidance. *http://dx.doi.org/10.1146/annurev.neuro.26.010302.081139* **26,** 509–563 (2003).
157. Bagri, A., Cheng, H.-J., Yaron, A., Pleasure, S. J. & Tessier-Lavigne, M. Stereotyped Pruning of Long Hippocampal Axon Branches Triggered by Retraction Inducers of the Semaphorin Family. *Cell* **113,** 285–299 (2003).
158. Dent, E. W., Barnes, A. M., Tang, F. & Kalil, K. Netrin-1 and semaphorin 3A promote or inhibit cortical axon branching, respectively, by reorganization of the cytoskeleton. *J. Neurosci.* **24,** 3002–3012 (2004).
159. Shelly, M. *et al.* Semaphorin3A regulates neuronal polarization by suppressing axon formation and promoting dendrite growth. *Neuron* **71,** 433–446 (2011).
160. Serini, G. *et al.* Class 3 semaphorins control vascular morphogenesis by inhibiting integrin function. *Nature* **424,** 391–397 (2003).
161. Behar, O., Golden, J. A., Mashimo, H., Schoen, F. J. & Fishman, M. C. Semaphorin III is needed for normal patterning and growth of nerves, bones and heart. *, Published online: 10 October 1996; | doi:10.1038/383525a0* **383,** 525–528 (1996).
162. Oinuma, I., Ishikawa, Y., Katoh, H. & Negishi, M. The Semaphorin 4D Receptor Plexin-B1 Is a GTPase Activating Protein for R-Ras. *Science* **305,** 862–865 (2004).

163. Barberis, D. *et al.* Plexin signaling hampers integrin-based adhesion, leading to Rho-kinase independent cell rounding, and inhibiting lamellipodia extension and cell motility. *FASEB J.* **18,** 592–594 (2004).
164. Kumanogoh, A. *et al.* Requirement for the lymphocyte semaphorin, CD100, in the induction of antigen-specific T cells and the maturation of dendritic cells. *The Journal of Immunology* **169,** 1175–1181 (2002).
165. Oh, W.-J. & Gu, C. The role and mechanism-of-action of Sema3E and Plexin-D1 in vascular and neural development. *Seminars in Cell & Developmental Biology* **24,** 156–162 (2013).
166. Comeau, M. R. *et al.* A Poxvirus-Encoded Semaphorin Induces Cytokine Production from Monocytes and Binds to a Novel Cellular Semaphorin Receptor, VESPR. *Immunity* **8,** 473–482 (1998).
167. Walzer, T., Galibert, L. & De Smedt, T. Poxvirus semaphorin A39R inhibits phagocytosis by dendritic cells and neutrophils. *European Journal of Immunology* **35,** 391–398 (2005).
168. Walzer, T., Galibert, L. & Smedt, T. D. Poxvirus semaphorin A39R inhibits phagocytosis by dendritic cells and neutrophils. *European Journal of Immunology* **35,** 391–398 (2005).
169. Walzer, T., Galibert, L., Comeau, M. R. & De Smedt, T. Plexin C1 engagement on mouse dendritic cells by viral semaphorin A39R induces actin cytoskeleton rearrangement and inhibits integrin-mediated adhesion and chemokine-induced migration. *The Journal of Immunology* **174,** 51–59 (2005).
170. Sekido, Y. *et al.* Human semaphorins A(V) and IV reside in the 3p21.3 small cell lung cancer deletion region and demonstrate distinct expression patterns. *PNAS* **93,** 4120–4125 (1996).
171. Brambilla, E., Constantin, B., Drabkin, H. & Roche, J. Semaphorin SEMA3F localization in malignant human lung and cell lines: A suggested role in cell adhesion and cell migration. *The American Journal of Pathology* **156,** 939–950 (2000).
172. Bielenberg, D. R. *et al.* Semaphorin 3F, a chemorepulsant for endothelial cells, induces a poorly vascularized, encapsulated, nonmetastatic tumor phenotype. *J. Clin. Invest.* **114,** 1260–1271 (2004).
173. Hung, R.-J. *et al.* Mical links semaphorins to F-actin disassembly. *Nature* **463,** 823–827 (2010).
174. Hung, R.-J., Pak, C. W. & Terman, J. R. Direct redox regulation of F-actin assembly and disassembly by Mical. *Science* **334,** 1710–1713 (2011).
175. Pascoe, H. G., Wang, Y. & Zhang, X. Structural mechanisms of plexin signaling. *Prog. Biophys. Mol. Biol.* **118,** 161–168 (2015).
176. Toyofuku, T. *et al.* FARP2 triggers signals for Sema3A-mediated axonal repulsion. *Nature Neuroscience* **8,** 1712–1719 (2005).

177. Parent, C. A. & Devreotes, P. N. A cell's sense of direction. *Science* **284,** 765–770 (1999).
178. Parent, C. A., Blacklock, B. J., Froehlich, W. M., Murphy, D. B. & Devreotes, P. N. G Protein Signaling Events Are Activated at the Leading Edge of Chemotactic Cells. *Cell* **95,** 81–91 (1998).
179. Brown, J. A. & Bridgman, P. C. Disruption of the cytoskeleton during Semaphorin 3A induced growth cone collapse correlates with differences in actin organization and associated binding proteins. *Developmental Neurobiology* **69,** 633–646 (2009).
180. Wong, K., Pertz, O., Hahn, K. & Bourne, H. Neutrophil polarization: spatiotemporal dynamics of RhoA activity support a self-organizing mechanism. *PNAS* **103,** 3639–3644 (2006).
181. Nobes, C. D. & Hall, A. Rho GTPases control polarity, protrusion, and adhesion during cell movement. *J Cell Biol* **144,** 1235–1244 (1999).
182. Protocols, Y. H. L. M. A.2012. Isolation of human and mouse neutrophils ex vivo and in vitro. *Springer*
183. Garvey, C. M., Spiller, E., Lindsay, D., reports, C. C. S.2016. A high-content image-based method for quantitatively studying context-dependent cell population dynamics. *nature.com*
184. Matsuda, I., Shoji, H., Yamasaki, N., Miyakawa, T. & Aiba, A. Comprehensive behavioral phenotyping of a new Semaphorin 3 F mutant mouse. *Mol Brain* **9,** 15 (2016).
185. Regano, D. *et al.* Sema3F (Semaphorin 3F) Selectively Drives an Extraembryonic Proangiogenic Program. *Arteriosclerosis, Thrombosis, and Vascular Biology* **37,** ATVBAHA.117.308226–1721 (2017).
186. Rammes, A. *et al.* Myeloid-related protein (MRP) 8 and MRP14, calcium-binding proteins of the S100 family, are secreted by activated monocytes via a novel, tubulin-dependent pathway. *J. Biol. Chem.* **272,** 9496–9502 (1997).
187. Abram, C. L., Roberge, G. L., Hu, Y. & Lowell, C. A. Comparative analysis of the efficiency and specificity of myeloid-Cre deleting strains using ROSA-EYFP reporter mice. *Journal of Immunological Methods* **408,** 89–100 (2014).
188. Hasenberg, A. *et al.* Catchup: a mouse model for imaging-based tracking and modulation of neutrophil granulocytes. *Nature Methods 2015 12:5* **12,** 445–452 (2015).
189. de Souza Xavier Costa, N. *et al.* Early and late pulmonary effects of nebulized LPS in mice: An acute lung injury model. *PLOS ONE* **12,** e0185474 (2017).
190. Thompson, A. A. R. *et al.* Hypoxia-inducible factor 2α regulates key neutrophil functions in humans, mice, and zebrafish. *Blood* **123,** 366–376 (2014).
191. Karadjian, G. *et al.* Migratory phase of Litomosoides sigmodontis filarial infective larvae is associated with pathology and transient

increase of S100A9 expressing neutrophils in the lung. *PLOS Negl Trop Dis* **11,** e0005596 (2017).
192. Walmsley, S. R. *et al.* Prolyl hydroxylase 3 (PHD3) is essential for hypoxic regulation of neutrophilic inflammation in humans and mice. *J. Clin. Invest.* **121,** 1053–1063 (2011).
193. Movassagh, H. *et al.* Chemorepellent Semaphorin 3E Negatively Regulates Neutrophil Migration In Vitro and In Vivo. *J. Immunol.* 1601093 (2016). doi:10.4049/jimmunol.1601093
194. Kusy, S. *et al.* Selective Suppression of In Vivo Tumorigenicity by Semaphorin SEMA3F in Lung Cancer Cells. *Neoplasia* **7,** 457–465 (2005).
195. Potiron, V. A. *et al.* Semaphorin SEMA3F Affects Multiple Signaling Pathways in Lung Cancer Cells. *Cancer Res* **67,** 8708–8715 (2007).
196. Caunt, M. *et al.* Blocking Neuropilin-2 Function Inhibits Tumor Cell Metastasis. *Cancer Cell* **13,** 331–342 (2008).
197. Vacca, A. *et al.* Loss of inhibitory semaphorin 3A (SEMA3A) autocrine loops in bone marrow endothelial cells of patients with multiple myeloma. *Blood* **108,** 1661–1667 (2006).
198. Taylor, P. C. & Feldmann, M. Anti-TNF biologic agents: still the therapy of choice for rheumatoid arthritis. *Nature Reviews Rheumatology 2009 5:10* **5,** 578–582 (2009).
199. Barnes, P. J. Cytokine-directed therapies for asthma. *J. Allergy Clin. Immunol.* **108,** S72–S76 (2001).
200. Feldmann, M. Development of anti-TNF therapy for rheumatoid arthritis. *Nature Reviews Immunology* **2,** 364–371 (2002).
201. Ben-Horin, S., Kopylov, U. & Chowers, Y. Optimizing anti-TNF treatments in inflammatory bowel disease. *Autoimmunity Reviews* **13,** 24–30 (2014).
202. Reumaux, D., Hordijk, P. L., Duthilleul, P. & Roos, D. Priming by tumor necrosis factor-alpha of human neutrophil NADPH-oxidase activity induced by anti-proteinase-3 or anti-myeloperoxidase antibodies. *J Leukoc Biol* **80,** 1424–1433 (2006).
203. Murray, J. *et al.* Regulation of neutrophil apoptosis by tumor necrosis factor-alpha: requirement for TNFR55 and TNFR75 for induction of apoptosis in vitro. *Blood* **90,** 2772–2783 (1997).
204. Lokuta, M. A., Biol, A. H. J. L.2005. TNF-promotes a stop signal that inhibits neutrophil polarization and migration via a p38 MAPK pathway. *Citeseer*
205. Proudfoot, A. *et al.* Novel anti-tumour necrosis factor receptor-1 (TNFR1) domain antibody prevents pulmonary inflammation in experimental acute lung injury. *Thorax* thoraxjnl–2017–210305 (2018). doi:10.1136/thoraxjnl-2017-210305
206. Patton, L. M., Saggart, B. S., Ahmed, N. K., Leff, J. A. & Repine, J. E. Interleukin-1<Emphasis Type='Italic'>β</Emphasis>-induced

neutrophil recruitment and acute lung injury in hamsters. *Inflammation* **19,** 23–29 (1995).
207. Alten, R. *et al.* Efficacy and safety of the human anti-IL-1beta monoclonal antibody canakinumab in rheumatoid arthritis: results of a 12-week, phase II, dose-finding study. *BMC Musculoskeletal Disorders 2011 12:1* **12,** 153 (2011).
208. Biondo, C. *et al.* The Interleukin-1β/CXCL1/2/Neutrophil Axis Mediates Host Protection against Group B Streptococcal Infection. *Infect. Immun.* **82,** 4508–4517 (2014).
209. Prince, L. R. *et al.* The role of interleukin-1beta in direct and toll-like receptor 4-mediated neutrophil activation and survival. *Am. J. Pathol.* **165,** 1819–1826 (2004).
210. Renshaw, S. A. *et al.* Inflammatory neutrophils retain susceptibility to apoptosis mediated via the Fas death receptor. *J Leukoc Biol* **67,** 662–668 (2000).
211. Edwards, S. W., Derouet, M., Howse, M. & Moots, R. J. Regulation of neutrophil apoptosis by Mcl-1. *Biochemical Society Transactions* **32,** 489–492 (2004).
212. Wardle, D. J. *et al.* Effective Caspase Inhibition Blocks Neutrophil Apoptosis and Reveals Mcl-1 as Both a Regulator and a Target of Neutrophil Caspase Activation. *PLOS ONE* **6,** e15768 (2011).
213. Youle, R. J. & Strasser, A. The BCL-2 protein family: opposing activities that mediate cell death. *Nature Reviews Molecular Cell Biology* **9,** 47–59 (2008).
214. Czabotar, P. E., Lessene, G., Strasser, A. & Adams, J. M. Control of apoptosis by the BCL-2 protein family: implications for physiology and therapy. *Nature Reviews Molecular Cell Biology* **15,** 49–63 (2014).
215. Serhan, C. N. & Savill, J. Resolution of inflammation: the beginning programs the end. *Nature Immunology* **6,** 1191–1197 (2005).
216. Parker, M. W., Hellman, L. M., Xu, P., Fried, M. G. & Vander Kooi, C. W. Furin Processing of Semaphorin 3F Determines Its Anti-Angiogenic Activity by Regulating Direct Binding and Competition for Neuropilin. *Biochemistry* **49,** 4068–4075 (2010).
217. Zhang, X., Ding, L. & Sandford, A. J. Selection of reference genes for gene expression studies in human neutrophils by real-time PCR. *BMC Mol. Biol.* **6,** 4 (2005).
218. Nick, J. A. *et al.* Selective Suppression of Neutrophil Accumulation in Ongoing Pulmonary Inflammation by Systemic Inhibition of p38 Mitogen-Activated Protein Kinase. *The Journal of Immunology* **169,** 5260–5269 (2002).
219. Matsuda, I. *et al.* Development of the somatosensory cortex, the cerebellum, and the main olfactory system in Semaphorin 3F knockout mice. *Neuroscience Research* **66,** 321–329 (2010).

220. Rose, S., Misharin, A. & Perlman, H. A novel Ly6C/Ly6G-based strategy to analyze the mouse splenic myeloid compartment. *Cytometry Part A* **81A,** 343–350 (2012).
221. Daley, J. M., Thomay, A. A., Connolly, M. D., Reichner, J. S. & Albina, J. E. Use of Ly6G-specific monoclonal antibody to deplete neutrophils in mice. *J Leukoc Biol* **83,** 64–70 (2008).
222. Lakschevitz, F. S. *et al.* Identification of neutrophil surface marker changes in health and inflammation using high-throughput screening flow cytometry. *Exp. Cell Res.* **342,** 200–209 (2016).
223. Picot, T. *et al.* Evaluation by Flow Cytometry of Mature Monocyte Subpopulations for the Diagnosis and Follow-Up of Chronic Myelomonocytic Leukemia. *Front Oncol* **8,** 109 (2018).
224. Carrer, A. *et al.* Neuropilin-1 identifies a subset of bone marrow Gr1- monocytes that can induce tumor vessel normalization and inhibit tumor growth. *Cancer Res* **72,** 6371–6381 (2012).
225. Borghardt, J. M., Kloft, C. & Sharma, A. Inhaled Therapy in Respiratory Disease: The Complex Interplay of Pulmonary Kinetic Processes. *Canadian Respiratory Journal* **2018,** 1–11 (2018).
226. Matute-Bello, G., Downey, G., of, B. M. A. J.2011. An official American Thoracic Society workshop report: features and measurements of experimental acute lung injury in animals. *atsjournals.org*
227. Shay, T. & Kang, J. Immunological Genome Project and systems immunology. *Trends in Immunology* **34,** 602–609 (2013).
228. Rider, P. *et al.* IL-1α and IL-1β recruit different myeloid cells and promote different stages of sterile inflammation. *J. Immunol.* **187,** 4835–4843 (2011).
229. medicine, M. B. A. O. P. L.2010. The pathologist's approach to acute lung injury. *archivesofpathology.org.* doi:10.1043/1543-2165-134.5.719
230. Renshaw, S. A. *et al.* Acceleration of human neutrophil apoptosis by TRAIL. *The Journal of Immunology* **170,** 1027–1033 (2003).
231. Sapey, E. *et al.* Behavioral and structural differences in migrating peripheral neutrophils from patients with chronic obstructive pulmonary disease. *Am. J. Respir. Crit. Care Med.* **183,** 1176–1186 (2011).
232. Sapey, E. *et al.* Phosphoinositide 3-kinase inhibition restores neutrophil accuracy in the elderly: toward targeted treatments for immunosenescence. *Blood* **123,** 239–248 (2014).
233. Serini, G. *et al.* Class 3 semaphorins control vascular morphogenesis by inhibiting integrin function. *Nature* **424,** 391–397 (2003).
234. Casazza, A. *et al.* Impeding macrophage entry into hypoxic tumor areas by Sema3A/Nrp1 signaling blockade inhibits angiogenesis and restores antitumor immunity. *Cancer Cell* **24,** 695–709 (2013).

235. Mitchell, T., Lo, A., Logan, M. R., Lacy, P. & Eitzen, G. Primary granule exocytosis in human neutrophils is regulated by Rac-dependent actin remodeling. *American Journal of Physiology-Cell Physiology* **295,** C1354–C1365 (2008).
236. Gehr, P., Bachofen, M. & Weibel, E. R. The normal human lung: ultrastructure and morphometric estimation of diffusion capacity. *Respiration Physiology* **32,** 121–140 (1978).
237. Townsley, M. I. *Structure and Composition of Pulmonary Arteries, Capillaries, and Veins*. **2,** 675–709 (American Cancer Society, 2011).
238. Doerschuk, C. M., Beyers, N., Applied, H. C. J. O.1993. Comparison of neutrophil and capillary diameters and their relation to neutrophil sequestration in the lung. *Am Physiological Soc*
239. Doerschuk, C. M. *et al.* Marginated pool of neutrophils in rabbit lungs. *J. Appl. Physiol.* **63,** 1806–1815 (1987).
240. Nourshargh, S. & Alon, R. Leukocyte Migration into Inflamed Tissues. *Immunity* **41,** 694–707 (2014).
241. Yipp, B. G. & Kubes, P. Antibodies against neutrophil LY6G do not inhibit leukocyte recruitment in mice in vivo. *Blood* **121,** 241–242 (2013).
242. Pasterkamp, R. J., Peschon, J. J., Spriggs, M. K. & Kolodkin, A. L. Semaphorin 7A promotes axon outgrowth through integrins and MAPKs. *Nature* **424,** 398–405 (2003).
243. Doyle, N. A. *et al.* Neutrophil margination, sequestration, and emigration in the lungs of L-selectin-deficient mice. *J. Clin. Invest.* **99,** 526–533 (1997).
244. Doerschuk, C. M. *et al.* The role of P-selectin and ICAM-1 in acute lung injury as determined using blocking antibodies and mutant mice. *The Journal of Immunology* **157,** 4609–4614 (1996).
245. Mulligan, M. S. *et al.* Neutrophil-dependent acute lung injury. Requirement for P-selectin (GMP-140). *J. Clin. Invest.* **90,** 1600–1607 (1992).
246. Qin, L. *et al.* The roles of CD11/CD18 and ICAM-1 in acute Pseudomonas aeruginosa-induced pneumonia in mice. *The Journal of Immunology* **157,** 5016–5021 (1996).
247. molecular, C. D. A. J. O. R. C. A.1992. The role of CD18-mediated adhesion in neutrophil sequestration induced by infusion of activated plasma in rabbits. *Am Thoracic Soc*
248. Yoshida, K., Kondo, R., Wang, Q. & Doerschuk, C. M. Neutrophil Cytoskeletal Rearrangements during Capillary Sequestration in Bacterial Pneumonia in Rats. *Am. J. Respir. Crit. Care Med.* **174,** 689–698 (2012).
249. Tsai, M. A., Waugh, R. E. & Keng, P. C. Passive mechanical behavior of human neutrophils: effects of colchicine and paclitaxel. *Biophys. J.* **74,** 3282–3291 (1998).

250. Saito, H., Lai, J., Rogers, R. & Doerschuk, C. M. Mechanical properties of rat bone marrow and circulating neutrophils and their responses to inflammatory mediators. *Blood* **99,** 2207–2213 (2002).
251. Segura, E. F., García, J. M., Santos, J. L. & Campos, A. Shape, F-actin, and surface morphology changes during chemotactic peptide-induced polarity in human neutrophils. *The Anatomical Record* **241,** 519–528 (2005).
252. Roberts, A. W. *et al.* Deficiency of the Hematopoietic Cell-Specific Rho Family GTPase Rac2 Is Characterized by Abnormalities in Neutrophil Function and Host Defense. *Immunity* **10,** 183–196 (1999).
253. Dooley, J. L. *et al.* Regulation of inflammation by Rac2 in immune complex-mediated acute lung injury. *American Journal of Physiology - Lung Cellular and Molecular Physiology* **297,** L1091–102 (2009).
254. Bochsler, P. N., Neilsen, N. R., Dean, D. F. & Slauson, D. O. Stimulus-dependent actin polymerization in bovine neutrophils. *Inflammation* **16,** 383–392 (1992).
255. Devi, S. *et al.* Neutrophil mobilization via plerixafor-mediated CXCR4 inhibition arises from lung demargination and blockade of neutrophil homing to the bone marrow. *J Exp Med* **210,** jem.20130056–2336 (2013).
256. Davis, J. M. *et al.* Increased neutrophil mobilization and decreased chemotaxis during cortisol and epinephrine infusions. *J Trauma* **31,** 725–31– discussion 731–2 (1991).
257. Castellano, F., Chavrier, P. & Caron, E. Actin dynamics during phagocytosis. *Seminars in Immunology* **13,** 347–355 (2001).
258. Gu, Y. Hematopoietic Cell Regulation by Rac1 and Rac2 Guanosine Triphosphatases. *Science* **302,** 445–449 (2003).
259. de Oliveira, C. A. & Mantovani, B. Latrunculin A is a potent inhibitor of phagocytosis by macrophages. *Life Sci.* **43,** 1825–1830 (1988).
260. Esmann, L. *et al.* Phagocytosis of Apoptotic Cells by Neutrophil Granulocytes: Diminished Proinflammatory Neutrophil Functions in the Presence of Apoptotic Cells. *The Journal of Immunology* **184,** 391–400 (2010).
261. Winterbourn, C. C., Kettle, A. J. & Hampton, M. B. Reactive Oxygen Species and Neutrophil Function. *Annu. Rev. Biochem.* **85,** 765–792 (2016).
262. Diebold, B. A. & Bokoch, G. M. Molecular basis for Rac2 regulation of phagocyte NADPH oxidase. *Nature Immunology* **2,** 211–215 (2001).
263. Wang, J. *et al.* Reversible glutathionylation regulates actin polymerization in A431 cells. *J. Biol. Chem.* **276,** 47763–47766 (2001).

264. Wong, W. Arresting migrating neutrophils with ROS. *Sci. Signal.* **9,** ec226–ec226 (2016).
265. Hattori, H. *et al.* Small-molecule screen identifies reactive oxygen species as key regulators of neutrophil chemotaxis. *PNAS* **107,** 3546–3551 (2010).
266. Nicholls, S. J. & Hazen, S. L. Myeloperoxidase and cardiovascular disease. *Arteriosclerosis, Thrombosis, and Vascular Biology* **25,** 1102–1111 (2005).
267. Lacy, P. Mechanisms of Degranulation in Neutrophils. *Allergy, Asthma & Clinical Immunology 2006 2:3* **2,** 98 (2006).
268. Carden, D. *et al.* Neutrophil elastase promotes lung microvascular injury and proteolysis of endothelial cadherins. *Am. J. Physiol. Heart Circ. Physiol.* **275,** H385–H392 (1998).
269. Ginzberg, H. H. *et al.* Neutrophil-mediated epithelial injury during transmigration: role of elastase. *American Journal of Physiology-Gastrointestinal and Liver Physiology* **281,** G705–G717 (2001).
270. Liau, D. F., Yin, N. X., Huang, J. & Ryan, S. F. Effects of human polymorphonuclear leukocyte elastase upon surfactant proteins in vitro. *Biochimica et Biophysica Acta (BBA) - Lipids and Lipid Metabolism* **1302,** 117–128 (1996).
271. Liou, T. G., Biochemistry, E. C.1995. Nonisotropic enzyme-inhibitor interactions: a novel nonoxidative mechanism for quantum proteolysis by human neutrophils. *ACS Publications*
272. Lee, W. L. & Downey, G. P. Leukocyte Elastase. *Am. J. Respir. Crit. Care Med.* **164,** 896–904 (2012).
273. Med, M. B. C. C.1982. *Structural alterations of lung parenchyma in the adult respiratory distress syndrome*. *ci.nii.ac.jp*
274. Petty, T. L. Protease Mechanisms in the Pathogenesis of Acute Lung Injury. *Annals of the New York Academy of Sciences* **624,** 267–277 (1991).
275. Lee, C. T. *et al.* Elastolytic Activity in Pulmonary Lavage Fluid from Patients with Adult Respiratory-Distress Syndrome. *http://dx.doi.org.ezproxy.is.ed.ac.uk/10.1056/NEJM198101223040402* **304,** 192–196 (2010).
276. Idell, S. *et al.* Neutrophil Elastase-Releasing Factors in Bronchoalveolar Lavage from Patients with Adult Respiratory Distress Syndrome1–3. *American Review of Respiratory Disease* (2015). doi:10.1164/arrd.1985.132.5.1098
277. Weiland, J. E. *et al.* Lung Neutrophils in the Adult Respiratory Distress Syndrome. *American Review of Respiratory Disease* (2015). doi:10.1164/arrd.1986.133.2.218
278. Travis, J., biochemistry, G. S. A. R. O.1983. Human plasma proteinase inhibitors. *annualreviews.org*

279. Campbell, E. J. & Campbell, M. A. Pericellular proteolysis by neutrophils in the presence of proteinase inhibitors: effects of substrate opsonization. *J Cell Biol* **106,** 667–676 (1988).
280. Weitz, J. I., Landman, S. L., Crowley, K. A., Birken, S. & Morgan, F. J. Development of an assay for in vivo human neutrophil elastase activity. Increased elastase activity in patients with alpha 1-proteinase inhibitor deficiency. *J. Clin. Invest.* **78,** 155–162 (1986).
281. Campbell, E. J. *et al.* Proteolysis by Neutrophils: Relative Importance Of Cell-Substrate Contact And Oxidative Inactivation Of Proteinase Inhibitors In Vitro. *J. Clin. Invest.* **70,** 845–852 (1982).
282. Kerrin, A. *et al.* Proteolytic cleavage of elafin by 20S proteasome may contribute to inflammation in acute lung injury. *Thorax* **68,** 315–321 (2013).
283. Ridley, A. J. *et al.* Cell migration: integrating signals from front to back. *Science* **302,** 1704–1709 (2003).
284. Zheng, C. *et al.* Semaphorin3F down-regulates the expression of integrin alpha(v)beta3 and sensitizes multicellular tumor spheroids to chemotherapy via the neuropilin-2 receptor in vitro. *Chemotherapy* **55,** 344–352 (2009).
285. Simon, S. I. *et al.* Beta 2-integrin and L-selectin are obligatory receptors in neutrophil aggregation. *Blood* **82,** 1097–1106 (1993).
286. McGovern, N. N. *et al.* Hypoxia selectively inhibits respiratory burst activity and killing of Staphylococcus aureus in human neutrophils. *J. Immunol.* **186,** 453–463 (2011).
287. Hoang, A. N. *et al.* Measuring neutrophil speed and directionality during chemotaxis, directly from a droplet of whole blood. *Technology (Singap World Sci)* **1,** 49–57 (2013).
288. Weiner, O. D. Regulation of cell polarity during eukaryotic chemotaxis: the chemotactic compass. *Current Opinion in Cell Biology* **14,** 196–202 (2002).
289. Howard, T. H. & Meyer, W. H. Chemotactic peptide modulation of actin assembly and locomotion in neutrophils. *Journal of Cell Biology* **98,** 1265–1271 (1984).
290. Howard, T. H. & Oresajo, C. O. The kinetics of chemotactic peptide-induced change in F-actin content, F-actin distribution, and the shape of neutrophils. *J Cell Biol* **101,** 1078–1085 (1985).
291. Hoenderdos, K. & Condliffe, A. The Neutrophil in Chronic Obstructive Pulmonary Disease. Too Little, Too Late or Too Much, Too Soon? *American Journal of Respiratory Cell and Molecular Biology* **48,** 531–539 (2013).
292. Vietinghoff, von, S. & Ley, K. Homeostatic Regulation of Blood Neutrophil Counts. *The Journal of Immunology* **181,** 5183–5188 (2008).

293. Worthen, G. S., Schwab, B., Elson, E. L. & Downey, G. P. Mechanics of stimulated neutrophils: cell stiffening induces retention in capillaries. *Science* **245,** 183–186 (1989).
294. Doyle, N. A. *et al.* Neutrophil margination, sequestration, and emigration in the lungs of L-selectin-deficient mice. *J. Clin. Invest.* **99,** 526–533 (1997).
295. Markos, J., Doerschuk, C. M., English, D., Wiggs, B. R. & Hogg, J. C. Effect of positive end-expiratory pressure on leukocyte transit in rabbit lungs. *Journal of Applied Physiology* **74,** 2627–2633 (1993).
296. Motosugi, H. *et al.* Changes in neutrophil actin and shape during sequestration induced by complement fragments in rabbits. *Am. J. Pathol.* **149,** 963–973 (1996).
297. Rossaint, J. & Zarbock, A. Tissue-specific neutrophil recruitment into the lung, liver, and kidney. *J Innate Immun* **5,** 348–357 (2013).
298. van Rijn, A. *et al.* Semaphorin 7A Promotes Chemokine-Driven Dendritic Cell Migration. *The Journal of Immunology* **196,** 459–468 (2016).
299. Kruger, R. P., Aurandt, J. & Guan, K.-L. Semaphorins command cells to move. *Nature Reviews Molecular Cell Biology* **6,** 789–800 (2005).
300. Morote-Garcia, J. C., Napiwotzky, D., Köhler, D. & Rosenberger, P. Endothelial Semaphorin 7A promotes neutrophil migration during hypoxia. *PNAS* **109,** 14146–14151 (2012).
301. Tamagnone, L. & Comoglio, P. M. To move or not to move? Semaphorin signalling in cell migration. *EMBO Rep.* **5,** 356–361 (2004).
302. Giger, R. J., Urquhart, E. R., Gillespie, S., Neuron, D. L.1998. Neuropilin-2 is a receptor for semaphorin IV insight into the structural basis of receptor function and specificity. *Elsevier*
303. Shimizu, A. *et al.* ABL2/ARG tyrosine kinase mediates SEMA3F-induced RhoA inactivation and cytoskeleton collapse in human glioma cells. *J. Biol. Chem.* **283,** 27230–27238 (2008).
304. Boneschansker, L., Jorgensen, J., Ellett, F., Briscoe, D. M. & Irimia, D. Convergent and Divergent Migratory Patterns of Human Neutrophils inside Microfluidic Mazes. *Scientific Reports 2015 5* **8,** 1887 (2018).
305. May, R. C. & Machesky, L. M. Phagocytosis and the actin cytoskeleton. *J Cell Sci* **114,** 1061–1077 (2001).
306. Heinrich, V. & Lee, C.-Y. Blurred line between chemotactic chase and phagocytic consumption: an immunophysical single-cell perspective. *Journal of Cell Science* **124,** 3041–3051 (2011).
307. Nakayama, H. *et al.* Regulation of mTOR Signaling by Semaphorin 3F-Neuropilin 2 Interactions In Vitro and In Vivo. *Scientific Reports 2015 5* **5,** 11789 (2015).

308. Strzepa, A., Pritchard, K. A. & Dittel, B. N. Myeloperoxidase: A new player in autoimmunity. *Cell. Immunol.* **317,** 1–8 (2017).
309. Barnes, P. J., Shapiro, S. D. & Pauwels, R. A. Chronic obstructive pulmonary disease: molecular and cellularmechanisms. *European Respiratory Journal* **22,** 672–688 (2003).
310. Condliffe, A. M., Kitchen, E. & Chilvers, E. R. Neutrophil Priming: Pathophysiological Consequences and Underlying Mechanisms. *Clinical Science* **94,** 461–471 (1998).
311. Pulli, B., Wojtkiewicz, G., Am, M. A. R. S. N.2012. *Molecular Magnetic Resonance Imaging of the Inflammatory Enzyme Myeloperoxidase Can Distinguish Steatosis from Non-Alcoholic Steatohepatitis in a …*.
312. Lavie, G., Zucker-Franklin, D. & Franklin, E. C. Elastase-type proteases on the surface of human blood monocytes: possible role in amyloid formation. *The Journal of Immunology* **125,** 175–180 (1980).
313. Nakamura, H., Yoshimura, K., McElvaney, N. G. & Crystal, R. G. Neutrophil elastase in respiratory epithelial lining fluid of individuals with cystic fibrosis induces interleukin-8 gene expression in a human bronchial epithelial cell line. *J. Clin. Invest.* **89,** 1478–1484 (1992).
314. Kalyanaraman, B. *et al.* Measuring reactive oxygen and nitrogen species with fluorescent probes: challenges and limitations. *Free Radic. Biol. Med.* **52,** 1–6 (2012).
315. Suzuki, M., Kato, M., Hanaka, H., Izumi, T. & Morikawa, A. Actin assembly is a crucial factor for superoxide anion generation from adherent human eosinophils. *J. Allergy Clin. Immunol.* **112,** 126–133 (2003).
316. Lacy, P. The role of Rho GTPases and SNAREs in mediator release from granulocytes. *Pharmacology & Therapeutics* **107,** 358–376 (2005).
317. Shao, D., Segal, A. W. & Dekker, L. V. Subcellular localisation of the p40phox component of NADPH oxidase involves direct interactions between the Phox homology domain and F-actin. *Int. J. Biochem. Cell Biol.* **42,** 1736–1743 (2010).
318. Diebold, B. A., Fowler, B., Lu, J., Dinauer, M. C. & Bokoch, G. M. Antagonistic cross-talk between Rac and Cdc42 GTPases regulates generation of reactive oxygen species. *J. Biol. Chem.* **279,** 28136–28142 (2004).
319. Zhao, T., Benard, V., Bohl, B. P. & Bokoch, G. M. The molecular basis for adhesion-mediated suppression of reactive oxygen species generation by human neutrophils. *J. Clin. Invest.* **112,** 1732–1740 (2003).
320. Sakai, J. *et al.* Reactive Oxygen Species-Induced Actin Glutathionylation Controls Actin Dynamics in Neutrophils. *Immunity* **37,** 1037–1049 (2012).

321. Howard, T. H. & Meyer, W. H. Chemotactic peptide modulation of actin assembly and locomotion in neutrophils. *J Cell Biol* **98,** 1265–1271 (1984).
322. Hughes, J. E., Stewart, J., Barclay, G. R. & Govan, J. R. Priming of neutrophil respiratory burst activity by lipopolysaccharide from Burkholderia cepacia. *Infect. Immun.* **65,** 4281–4287 (1997).
323. Hamza, B. & Irimia, D. Whole blood human neutrophil trafficking in a microfluidic model of infection and inflammation. *Lab Chip* **15,** 2625–2633 (2015).
324. Shen, L. *et al.* Differential regulation of neutrophil chemotaxis to IL-8 and fMLP by GM-CSF: lack of direct effect of oestradiol. *Immunology* **117,** 205–212 (2006).
325. Wang, X., Qin, W., Zhang, Y., Zhang, H. & Sun, B. Endotoxin promotes neutrophil hierarchical chemotaxis via the p38-membrane receptor pathway. *Oncotarget* **7,** 74247–74258 (2016).
326. Deng, Q., Yoo, S. K., Cavnar, P. J., Green, J. M. & Huttenlocher, A. Dual roles for Rac2 in neutrophil motility and active retention in zebrafish hematopoietic tissue. *Developmental Cell* **21,** 735–745 (2011).
327. Yang, C.-T. *et al.* Neutrophils Exert Protection in the Early Tuberculous Granuloma by Oxidative Killing of Mycobacteria Phagocytosed from Infected Macrophages. *Cell Host Microbe* **12,** 301–312 (2012).
328. Proebstl, D. *et al.* Pericytes support neutrophil subendothelial cell crawling and breaching of venular walls in vivo. *J Exp Med* **209,** jem.20111622–1234 (2012).
329. Ellett, F., Elks, P. M., Robertson, A. L., Ogryzko, N. V. & Renshaw, S. A. Defining the phenotype of neutrophils following reverse migration in zebrafish. *J Leukoc Biol* **98,** 975–981 (2015).
330. Yogalingam, G. *et al.* Cellular Uptake and Delivery of Myeloperoxidase to Lysosomes Promote Lipofuscin Degradation and Lysosomal Stress in Retinal Cells. *J. Biol. Chem.* **292,** 4255–4265 (2017).
331. Schmekel, B., Hörnblad, Y., Linden, M., Sundström, C. & Venge, P. Myeloperoxidase in human lung lavage. II. Internalization of myeloperoxidase by alveolar macrophages. *Inflammation* **14,** 455–461 (1990).
332. Wulf, E., Deboben, A., Bautz, F. A., Faulstich, H. & Wieland, T. Fluorescent phallotoxin, a tool for the visualization of cellular actin. *PNAS* **76,** 4498–4502 (1979).
333. Kristó, I., Bajusz, I., Bajusz, C., Borkúti, P. & Vilmos, P. Actin, actin-binding proteins, and actin-related proteins in the nucleus. *Histochem Cell Biol* **145,** 373–388 (2016).
334. Dustin, L. B. Ratiometric analysis of calcium mobilization. *Clinical and Applied Immunology Reviews* **1,** 5–15 (2000).

335. Wendt, E. R., Ferry, H., Greaves, D. R. & Keshav, S. Ratiometric Analysis of Fura Red by Flow Cytometry: A Technique for Monitoring Intracellular Calcium Flux in Primary Cell Subsets. *Plos One* **10,** e0119532 (2015).
336. Aizawa, H. *et al.* Phosphorylation of cofilin by LIM-kinase is necessary for semaphorin 3A-induced growth cone collapse. *Nature Neuroscience* **4,** 367–373 (2001).
337. Grintsevich, E. E. *et al.* F-actin dismantling through a redox-driven synergy between Mical and cofilin. *Nature Cell Biology* **18,** 876–885 (2016).
338. Grintsevich, E. E. *et al.* Catastrophic disassembly of actin filaments via Mical-mediated oxidation. *Nat Commun* **8,** 2183 (2017).
339. Hattori, H., Subramanian, K. K. & Luo, H. R. Small-Molecule Screen Identifies ROS as Key Regulators of Actin Dynamics in Neutrophils. *Blood* **112,** 4641–4641 (2008).
340. Terman, J. R., Mao, T., Pasterkamp, R. J., Yu, H.-H. & Kolodkin, A. L. MICALs, a Family of Conserved Flavoprotein Oxidoreductases, Function in Plexin-Mediated Axonal Repulsion. *Cell* **109,** 887–900 (2002).
341. Sabroe, I., Jones, E. C., Usher, L. R., Whyte, M. K. B. & Dower, S. K. Toll-like receptor (TLR)2 and TLR4 in human peripheral blood granulocytes: a critical role for monocytes in leukocyte lipopolysaccharide responses. *The Journal of Immunology* **168,** 4701–4710 (2002).
342. Chen, H., Chédotal, A., He, Z., Goodman, C. S. & Tessier-Lavigne, M. Neuropilin-2, a novel member of the neuropilin family, is a high affinity receptor for the semaphorins Sema E and Sema IV but not Sema III. *Neuron* **19,** 547–559 (1997).
343. Soker, S., Takashima, S., Miao, H. Q., Neufeld, G. & Klagsbrun, M. Neuropilin-1 Is Expressed by Endothelial and Tumor Cells as an Isoform-Specific Receptor for Vascular Endothelial Growth Factor. *Cell* **92,** 735–745 (1998).
344. Nasarre, P. *et al.* Semaphorin SEMA3F Has a Repulsing Activity on Breast Cancer Cells and Inhibits E-Cadherin-Mediated Cell Adhesion. *Neoplasia* **7,** 180–189 (2005).
345. Nasarre, P. *et al.* Semaphorin SEMA3F and VEGF have opposing effects on cell attachment and spreading. *Neoplasia* **5,** 83–92 (2003).
346. Lamble, A. J., Dietz, M., Laderas, T., McWeeney, S. & Lind, E. F. Integrated functional and mass spectrometry-based flow cytometric phenotyping to describe the immune microenvironment in acute myeloid leukemia. *Journal of Immunological Methods* **453,** 44–52 (2018).

347. Cameron, L. A., Houghtaling, B. R. & Yang, G. Fluorescent speckle microscopy. *Cold Spring Harb Protoc* **2011,** pdb.top106–pdb.top106 (2011).
348. Giridharan, S. S. P. & Caplan, S. MICAL-family proteins: Complex regulators of the actin cytoskeleton. *Antioxid. Redox Signal.* **20,** 2059–2073 (2014).
349. Stojkov, D. *et al.* ROS and glutathionylation balance cytoskeletal dynamics in neutrophil extracellular trap formation. *J Cell Biol* **216,** 4073–4090 (2017).
350. Kwiatkowski, S. C. *et al.* Neuropilin-1 modulates TGFβ signaling to drive glioblastoma growth and recurrence after anti-angiogenic therapy. *PLOS ONE* **12,** e0185065 (2017).
351. Nasarre, P. *et al.* Neuropilin-2 Is Upregulated in Lung Cancer Cells during TGF-β1–Induced Epithelial–Mesenchymal Transition. *Cancer Res* **73,** 7111–7121 (2013).

7 Appendices

I. Human Sonification buffer

Sonication lysis buffer	Stock conc.	F/w	Molarity req.	Conc. Req.	Volume to add	Mass to add	Final volume
	M/L	g/M	M	g/L	ml	mg	ml
Tris pH 7.8 1M	1	-	0.1	-	10	-	100
EDTA		372.24	0.0015	0.5584		55.84	100
KCl		74.56	0.01	0.7456		74.56	100
DTT		154.25	0.0005	0.0771		7.71	100
Na orthovanadate		183.91	0.001	0.1839		18.39	100
Tetramisole		240.76	0.002	0.4815		48.15	100
dH2O					90		100

Add 50ul of protease-inhibitor containing water per 1ml of sonication buffer

II. Human 2XSDS Lysis buffer (hypotonic lysis buffer)

SDS lysis buffer	Stock Conc.	FW	Molarity	Conc.	% Required	Volume to add	Mass to add	Final volume
	M/L	g/M	M	g/L		ml	Mg	ml
DTT	1	154.25	0.2	30.8500			308.50	10
SDS	20%				4%	2		10
Glycerol 100%	100%				20.00%	2		10
Tris-HCl pH 6.8	0.5		0.1			2		10
Bromophenol Blue	2%				0.04%	0.1		10
Protease inhibitor cocktail						0.2		10
H2O						3.7		10

Protease-inhibitor containing water: To 1ml ddH20 add 1 tablet of cOmplete™, EDTA-free Protease Inhibitor Cocktail (Sigma-Aldrich). Store at -20ºC. PMSF (phenylmethylsulfonyl fluoride): 100mM stock made up in isopropanol Fw = 174.20 i.e. 87.1 mg in 5 ml isopropanol = 100 mM. Store in foil at 4ºC.

III. Running buffer for Western blots

10 X Running Buffer

Glycine	190g
Tris Base	30.3g
20% SDS	50ml
dH_2O	to 1 litre

IV. Transfer Buffer for Western blots

10 X Transfer Buffer

Glycine	145g
Tris Base	29g
dH_2O	to 800ml

1 X Transfer Buffer: Made immediately before use

10 X Transfer Buffer	10ml
Methanol	20ml
Water	70ml

V. Primary Antibodies used in Western Blotting

Antibody	**Dilution**	**Supplier**	**Code**
Anti-Sema3F Rabbit Polyclonal	1/100	Life Science Biosciences	LS-C135015-50
Anti-Mical Rabbit Polyclonal	1/100	Cambridge Bioscience	LS-C135015-50
Anti-NRP2	1/100	Atlas Antibodies	HPA054974
Anti-P38	1/2000	Abcam	ab197348

VI. Primary Antibodies used for immunohistochemistry

Antibody	**Dilution**	**Supplier**	**Code**
Anti-Sema3F (N-terminal) Rabbit Polyclonal	1/75	Sigma-Aldrich	SAB2700501
Anti-Neuropilin 1 Rabbit Polyclonal	1/100	R & D Systems	AF3870
Anti-Neuropilin 2 Rabbit Polyclonal	1/100	Santa Cruz	H300
Anti-Ly6G Rat monclonal	1/250	Abcam	ab25377

VII. Pipeline used to measure neutrophil roundness

Analysis Sequence "Tracie Cell morph try Cyto ABC"

Input Image	**Stack Processing :** Individual Planes **Flatfield Correction :** None		
Find Nuclei	**Channel :** DAPI **ROI :** None	**Method :** M Diameter : 13 µm Splitting Coefficient : 0.4 Common Threshold : 0.4	Output Population : Nuclei
Calculate Intensity Properties	**Channel :** DAPI **Population :** Nuclei **Region :** Nucleus	**Method :** Standard Mean	Output Properties : Intensity Nucleus DAPI
Calculate Morphology Properties	**Population :** Nuclei **Region :** Nucleus	**Method :** Standard Area	Output Properties : Nucleus
Select Population	**Population :** Nuclei	**Method :** Filter by Property Nucleus Area [µm²] : < 70 Intensity Nucleus DAPI Mean : < 5000 Boolean Operations : F1 and F2	Output Population : Nuclei Selected
Find Cytoplasm	**Channel :** Alexa 488 **Nuclei :** Nuclei Selected	**Method :** C Common Threshold : 0.45 Individual Threshold : 0.15	
Calculate Intensity Properties (2)	**Channel :** Alexa 594 **Population :** Nuclei Selected **Region :** Cytoplasm	**Method :** Standard Mean	Output Properties : Intensity Cytoplasm Phalloidin
Calculate Morphology Properties (2)	**Population :** Nuclei Selected **Region :** Cell	**Method :** Standard Area Roundness Width Length Ratio Width to Length	Output Properties : Cell

VIII. Genotyping for murine colonies

2% gels were used.

Mastermix

DNA	2ul
5xbuffer	2.4μl
MgCl2	0.96μl
dNTP (2.5mM)	0.96μl
Primer 1084	0.6μl
Primer 1085	0.6μl
Primer 7338	0.6μl
Primer 7339	0.6μl
Taq polymerase	0.03μl
dH20	3.25μl

2μl DNA + 10ul Mastermix into PCR thermocycler

PCR cycling conditions

Step	Temp. ºC	Time	Repeat
1	94	3 min.	
2	94	30 sec.	
3	51.7	1 min.	
4	72	1 min	Steps 2-4 for 35 cycles
5	72	1 min.	
6	10	Hold	

IX. Mowiol mounting medium; hard set

(adapted from CSHL protocols http://cshprotocols.cshlp.org/content/2006/1/pdb.rec10255.full?text_only=true)

Ingredients:

- Mowiol 4-88 (Sigma 81381)
- Glycerol (Sigma G5516)
- Tris-Cl (0.2 M, pH 8.5; see below)
- DABCO (1,4-diazabicyclo-[2,2,2]-octane; Sigma D27802)

Method:

1. In a 50 ml Falcon, add 2.4 g of Mowiol 4-88 to 6 g of glycerol. Stir to mix.
2. Add 6 mL of dH_2O and leave for several hours at room temperature.
3. Add 12 mL of 0.2 M Tris-Cl (pH 8.5) and heat to 50°C in rotating hybridization oven for up to 5 hrs. After the Mowiol dissolves, clarify by centrifugation at 5000*g* for 15 min.

4. Aliquot in airtight containers and store at −20°C.
5. To use for fluorescence detection, thaw, then add DABCO (antifade) to 2.5% (w/v) and dissolve on roller (approx. 45 mins), then stand upright at 4°C for approx. 30 mins before use to let bubbles rise.
6. Store excess at 4°C for a few weeks then discard if not used.

X. Percoll gradients used for Ultra-purification of Neutrophils

Concentrations	For 10ml (3 gradients)		For 20ml (6 gradients)		For 30ml (9 gradients)	
	90% Percoll	1xPBS	90% Percoll	1xPBS	90% Percoll	1xPBS
78%	8.7ml	1.3ml	17.3ml	2.7ml	26ml	4ml
69%	7.7ml	2.3ml	15.3ml	4.7ml	23ml	7ml
52%	5.8ml	4.2ml	11.6ml	8.4ml	17.3ml	2.7ml

XI. Critical region used as reference for Primer design customised prime-probe set

TCTGTAGCATCTTCCACCCCAACACCACTCCCATCTGCTCGTTAACCCTT
TCGGCCCCACCCTGAGTGGAAGCCTCTGCCCCCACCTGAGCAGGCTCT
TTGATGCCATCGCACACCCTGGGTTACACCCACGGCCCTTTCATTGGGA
TTAGCTTGGGCTGCCTGTGAATCAGGGTGTAGCTTTGGGTGTGGCCCC
TTCTCTGGCTTGTCTACATGTCCCACTTTCTCCTCCATGGACTGGCAGC
AACTGTAGAGGGAGCTAAGAGGGCCCTGGGGAAGGAATGGGAAGTTTA
GGACAGCCGCGGCCTCAGTGTCTCTCTTTCAGGGGGAATGTGTCCCTC
TCATTGGTGCCCTGCTTCTCATCCACAGAACTTAAGGCCACCGGTACCG
CCCACTTCTTCAACTTTCTGCTCAACACTACAGACTACAGAATCCTGCTC
AAGGATGAGGACCATGACCGCATGTATGTGGGCAGCAAGGACTACGTG
CTGTCCCTGGACCTGCATGACATCAACCGAGAGCCCCTTATTGTAAGGG
CTGGCCCGGAAATGGGACGAGGCAGGGTGAAGGGCGTGGAGCCCAGG
GTCAGGGTCCTGGCCAGCAGGCTGCATCCTCTAACCTTCATCTTTGGCA
GATCCATTGGGCAGCCTCCCCGCAGCGCATTGAGGAGTGCATACTGTC
AGGCAAGGATGGCAATGTGAGTGCAGTGGGGTCCACCGAGGGTGAGG
CCGTGATCTCAGAGATGGACAGACATGGGCAGTTGTCTGGGCATCCAC
ACAGCTTTCTGTCTGGCCACAGGGAGAGTGTGGTAACTTCGTCCGGCT
CATCCAGCCTTGGAACCGAACACACCTGTATGTGTGTGGGACCGGTGC
CTACAACCCCATGTGCACCTATGTGAACCGTGGCCGTCGCGCACAGGT
AAGCTCCTGCCAACCCTAGCTCTGTGCTGTCCCCCTCTGGTGGCTGTGT
TCCAAGGTCCTGATGGGAGGATGGGCTTAAGCCCCATCCTTAACCCTTC
CAGGCCCCATGGCCTTGGGTGAGTAAGTTGTTCAGCTCTCTGAGCCTC
GATTTTTCTCACCTGGAAATTGGGTTCACAGTTCCTTTCGAACAGGTCGA
TGTGAGGAAGAGGCAGTGAGTTAGTGCTCTCCAGCTAACGCTGTGCCT
GGCGCATTAGTAAGC.

Primer Design quality control data for custom made Sema3F primer-probe set

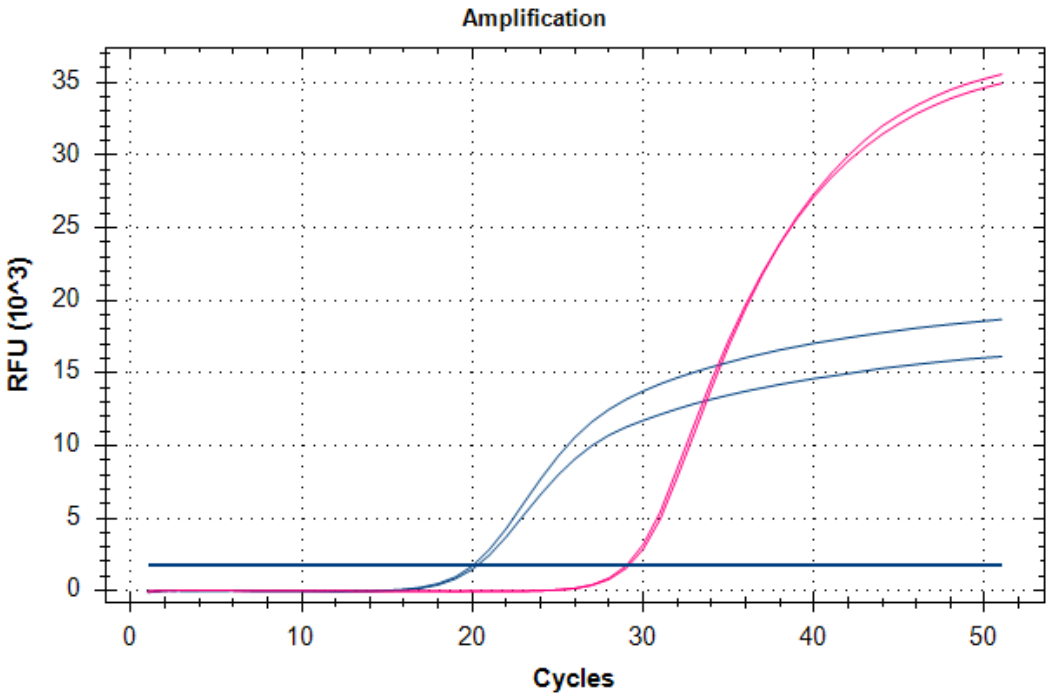

Sema3f (pink); ACTB (blue). Murine Lung results shown.

XII. Antibodies used in Lung Digest

Stain	Concentration	Supplier	Code
PE-CF594 Siglec F	0.00125	Biolegend	562757
BV450 CD11b	0.002	Biolegend	101239
FITC Ly6C	0.005	Biolegend	128005
PE Lys6G	0.0025	Biolegend	127607
PerCP Cy5.5 MHC 11	0.005	Biolegend	107625
PE Cy7 CD11c	0.005	Biolegend	117317
APC CD64	0.005	Biolegend	139305
AF700 CD45	0.005	Biolegend	AF700 CD45
BV450 CD11b	0.003	Thermofisher	48-0112-82

XIII. Antibodies used in Neuropilin 1 and 2 surface expression panel

Antibody	Concentration	Supplier	Code
Anti-NRP2	1/25	R&D Systems Inc, Oxford, UK	FAB22151A
Anti-NPR1(CD304)	1/50	Bio-legend, London, UK	354512
Anti-CD66b	1/100	BD Biosciences Oxford, UK,	562940
Anti-CD49d	1/250	BD Biosciences	563645
CD14	1/125	BD Biosciences	301835

XIV. Exclusion Criteria for healthy blood donors

Exclusions criteria:
Healthy donors were not eligible to be participate and be registered on the generic database if affected by any of the following:-

- Infection with any blood borne diseases (e.g. HIV, Hepatitis B or Hepatitis C)
- Previous or current intravenous drug abuse
- Current anaemia
- Blood clotting disorders
- Current anticoagulant (blood thinning) drug therapy
- Regular use of steroids
- Under the age of 16, or unable to give informed consent

For this piece of work further information was obtained by a trained physician to exclude the following:

- Recent use of anti-inflammatory medicines (including steroids, ibuprofen or similar)
- Active inflammatory conditions
- Known eosinophilia

- Current smoker
- Sex and age were anonymously recorded for each sample and used for matching purposes

XV. Matute-Bello lung scoring system

Parameter*	1	2	3
A. Neutrophils in the alveolar space	None	1–5	>5
B. Neutrophils in the interstitial space	None	1–5	>5
C. Hyaline membranes	None	1	>1
D. Proteinaceous debris filling the airspaces	None	1	>1
E. Alveolar septal thickening	<2×	2×–4×	>4×
F. Alveolar congestion	None	1–5	>5